

**THE PREPARATION AND NOVEL  
APPLICATION OF DIPHOSPHORUS XANTHENE FAMILY  
LIGANDS IN HOMOGENEOUS CATALYSIS**

by

THASHREE MARIMUTHU

Submitted in fulfilment of the academic  
requirements for the degree of Doctor of  
Philosophy in the School of Chemistry,  
University of KwaZulu-Natal, Durban

May 2011

As the candidate's supervisor I have approved this thesis for submission.

Signed: \_\_\_\_\_

Prof. Holger B. Friedrich (Supervisor)

Date: \_\_\_\_\_

## Abstract

Diphosphorus ligands containing a heterocyclic xanthene backbone are known to induce large chelation angles that have been correlated to favourable activity and selectivity in certain organic transformation reactions. In this work, a series of xanthene family ligands have been successfully prepared and applied to known homogeneous transition metal catalysed reactions where significant methodological improvements have been developed.

Twelve bidentate ligands have been prepared and selected ligands complexed to transition metal centres of interest, viz. Ir, Ru, Rh, and Os. All bidentate ligands and complexes were fully characterised by nuclear magnetic resonance analysis, infrared spectroscopy, mass spectrometry, and melting point determination. Selected metal complexes were analysed by differential scanning calorimetry. X-ray quality crystals were grown for eight bidentate ligands (six novel structures,  $R\% < 6$ ), and three metal complexes (three novel structures,  $R\% < 5$ ). The chelation angles of the prepared compounds were characterised by molecular mechanics calculations (for three novel ligands), and quantum chemical density functional theory calculations (for all prepared ligands and metal complex combinations). The calculated chelation angles were consistent with those reported in the literature.

The prepared bidentate compounds were applied to microwave mediated oxidation and transfer hydrogenation reactions. Benzylic and aliphatic alcohols substrates were efficiently oxidised to the corresponding aldehydes with a Ru xanthene based catalyst at 1 mol% loading in toluene. The aldehyde product yields range from 48 – 100% with facile oxidation of the electron rich substrates relative to the electron deficient substrates. The oxidation reactions were extended to solvent-free conditions and excellent yields of between 95 – 98% were obtained at different temperatures for the oxidation of benzyl alcohol.

Several ketone substrates were efficiently hydrogenated to the corresponding secondary alcohol under transfer hydrogenation conditions with a Ru xanthene based catalyst at 0.5 mol% loading in the presence of a 2-propanol hydrogen source and strong base. The secondary alcohol product yields range from 48 – > 99% with high observed turn-over frequencies of between  $\geq 1431 - 2982 \text{ h}^{-1}$ .

The chemoselective hydrogenation of  $\alpha,\beta$ -unsaturated aldehydes and ketones with a molecular hydrogen source was investigated in a mini reactor at high pressure (50 bar  $\text{H}_2$ ). A Rh xanthene based catalyst at 2 mol% loading in toluene demonstrated excellent activity and selectivity for the preferential hydrogenation of the alkene functionality over the carbonyl group.

The preparation of tridentate xanthene based ligands and metal complexes for possible C-H activation applications was investigated. Four tridentate ligands based on a N donor bidentate xanthene backbone were successfully prepared. Bidentate coordination of the tridentate ligands to an Ir metal centre was successful; however, the rigidity of the coordinated backbone disfavoured the positioning and coordination of the third

donor. The tridentate ligands were fully characterised and X-ray quality crystals were grown for two ligands (two novel structures,  $R\% < 4$ ).

## **Preface**

The experimental work described in this thesis was carried out in the School of Chemistry, University of KwaZulu-Natal, Durban, from January 2006 to December 2010, under the supervision of Professor H. B. Friedrich.

These studies represent original work by the author and have not otherwise been submitted in any form for any degree or diploma to any tertiary institution. Where use has been made of the work of others it is duly acknowledged in the text.

Signed: \_\_\_\_\_

Date: \_\_\_\_\_

Thashree Marimuthu

## Declaration 1

### PLAGIARISM

I, .....hereby declare that:

1. The research reported in this thesis, except where otherwise indicated, is my original research.
2. This thesis has not been submitted for any degree or examination at any other university.
3. This thesis does not contain other persons' data, pictures, graphs or other information, unless specifically acknowledged as being sourced from other persons.
4. This thesis does not contain other persons' writing, unless specifically acknowledged as being sourced from other researchers. Where other written sources have been quoted, then:
  - a. Their words have been re-written but the general information attributed to them has been referenced
  - b. Where their exact words have been used, then their writing has been placed in italics and inside quotation marks, and referenced.
5. This thesis does not contain text, graphics or tables copied and pasted from the Internet, unless specifically acknowledged, and the source being detailed in the thesis and in the References sections.

Signed: \_\_\_\_\_

Date: \_\_\_\_\_

Thashree Marimuthu

## Declaration 2

### PUBLICATIONS

- 1 Marimuthu, T.; Bala, M. D.; Friedrich, H. B. *Acta. Crystallogr., Sect. E: Struct. Rep. Online* **2008**, 64, O711-U1374.
- 2 Marimuthu, T.; Bala, M. D.; Friedrich, H. B. *Acta. Crystallogr., Sect. E: Struct. Rep. Online* **2008**, 64, O772-U1140.
- 3 Marimuthu, T.; Bala, M. D.; Friedrich, H. B. *Acta. Crystallogr., Sect. E: Struct. Rep. Online* **2008**, 64, O1984-U4311.
- 4 Marimuthu, T.; Bala, M. D.; Friedrich, H. B. *Acta. Crystallogr., Sect. E: Struct. Rep. Online* **2009**, 65, O828-U2615.
- 5 Marimuthu, T.; Bala, M.; Friedrich, H. B. *J. Coord. Chem.* **2009**, 62, 1407-1414.

### CONFERENCES

1. Poster titled "Synthesis and Characterisation of polyoxomolybdates clusters", Thashree Marimuthu and Holger B. Friedrich, presented at the International Symposium of Homogenous Catalysis, ISHC-XVI, Sun City, RSA, August, 2006.
2. Poster titled "Synthesis and Characterisation of polyoxomolybdates clusters", Thashree Marimuthu and Holger B. Friedrich, presented at the Catalysis Society of South Africa (CATSA) conference, Mossel Bay, RSA, November, 2006.
3. Poster titled "Synthesis of mixed-donor scorpionate ligands", Thashree Marimuthu and Holger B. Friedrich, presented at the International Symposium of Homogenous Catalysis, ISHC-XVI, Florence, Italy, July, 2008.
4. Poster titled "Synthesis of mixed-donor scorpionate ligands", Thashree Marimuthu and Holger B. Friedrich, presented at the SACI Postgraduate Symposium, Durban, South Africa, November 2008.
5. Poster titled "Synthesis and modelling of scorpionate ligands", Thashree Marimuthu and Holger B. Friedrich, presented at the Catalysis Society of South Africa (CATSA) conference, Parys, RSA, November, 2008.

6. Poster titled “Synthesis and modelling of scorpionate ligands”, Thashree Marimuthu and Holger B. Friedrich, presented at the 13<sup>th</sup> International conference on the applications of Density Functional Theory in Chemistry and Physics, DFT09, Lyon, France, September, 2009.
7. Oral titled “The preparation, characterisation, and novel application of diphosphine xanthene family ligands”, Thashree Marimuthu, and Holger B. Friedrich, presented at the SACI conference, Johannesburg, RSA, January, 2011.

Signed: \_\_\_\_\_

Thashree Marimuthu

Date: \_\_\_\_\_

## Table of Contents

<b>Chapter 1</b>	<b>Introduction.....</b>	<b>1</b>
1.1	Background and methodology .....	1
1.1.1	Solvent considerations .....	4
1.1.2	Energy considerations.....	4
1.2	Thesis scope and contents .....	5
1.3	References .....	8
<b>Chapter 2</b>	<b>Ligand design and diphosphorus ligands.....</b>	<b>10</b>
2.1	Introduction .....	10
2.2	Design parameters and considerations .....	10
2.2.1	Quantifying ligand design parameters – The bite angle.....	13
2.3	A brief review on selected diphosphorus ligands.....	16
2.4	References .....	25
<b>Chapter 3</b>	<b>The preparation of bidentate xanthene family ligands and catalysts.....</b>	<b>28</b>
3.1	Introduction and general strategy .....	28
3.2	Preparation of backbones .....	34
3.2.1	10-Isopropylidenexanthene (3.1) .....	34
3.2.2	10,10-Dimethylphenoxasilin (3.3).....	36
3.2.3	10-( <i>t</i> -butyldimethylsilyl) phenoxazine (3.4).....	37
3.2.4	10-Phenylphenoxaphosphine (3.5) .....	37
3.2.5	2,8-Dimethyl-10- <i>p</i> -tolyl-10H-phenoxaphosphine (3.6).....	38
3.2.6	2,8-Dimethylphenoxathiin (3.7).....	38
3.2.7	2,7-di- <i>n</i> -hexyl-9,9-dimethylxanthene (3.9).....	39
3.3	Preparation of ligands .....	40
3.3.1	Xanthene family ligands prepared with a common procedure.....	41
3.3.2	Xanthene family ligands prepared with separate procedures.....	45
3.3.3	Related xanthene family ligands.....	47
3.4	Preparation of metal complexes .....	49
3.4.1	Transition metal hydride precursors .....	49
3.4.2	Transition metal cod precursors.....	50
3.4.3	Complexation.....	51
3.5	X-ray crystal structures .....	54
3.5.1	Backbones and ligands.....	54
3.5.2	Metal Complexes .....	63
3.6	Bite angle characterisation .....	69
3.7	Experimental .....	74
3.7.1	General.....	74



3.7.2	Instrumentation .....	74
3.7.3	Experimental Methods .....	76
3.8	References .....	99
<b>Chapter 4</b>	<b>Microwave assisted oxidation of alcohols .....</b>	<b>102</b>
4.1	Introduction .....	102
4.2	Results and Discussion .....	104
4.3	Conclusions .....	114
4.4	Experimental .....	114
4.4.1	General .....	114
4.5	References .....	116
<b>Chapter 5</b>	<b>Microwave assisted transfer hydrogenation of ketones .....</b>	<b>118</b>
5.1	Introduction .....	118
5.2	Results and Discussion .....	120
5.3	Conclusions .....	128
5.4	Experimental .....	129
5.4.1	General .....	129
5.5	References .....	131
<b>Chapter 6</b>	<b>An investigation into the selective hydrogenation of <math>\alpha,\beta</math>-unsaturated carbonyls .....</b>	<b>132</b>
6.1	Introduction .....	132
6.2	Results and Discussion .....	133
6.3	Conclusions and Future Perspectives .....	138
6.4	Experimental .....	139
6.4.1	General .....	139
6.5	References .....	140
<b>Chapter 7</b>	<b>Towards the preparation of tridentate xanthene family ligands and catalysts .....</b>	<b>142</b>
7.1	Introduction .....	142
7.2	Results and Discussion .....	144
7.3	Conclusions .....	152
7.4	Experimental .....	153
7.4.1	General .....	153
7.4.2	Experimental Methods .....	153
7.5	References .....	160
	Summary and Future Perspectives .....	161

## List of Figures

Figure 1. 9,9-dimethylxanthene 1.1, and xantphos 1.2. ....	1
Figure 2. Generalised structure of the prepared ligands and metal complexes. ....	2
Figure 3. Ligand design parameters and considerations for a generalised bidentate diphosphorus complex. ....	12
Figure 4. Observed yield versus calculated bite angle for the Ni catalysed hydrocyanation of styrene [23]. ....	14
Figure 5. Selected bidentate diphosphorus ligands. ....	18
Figure 6. Selected coordination modes of ligand 2.8. ....	20
Figure 7. Hydroformylation of propene with diphosphorus ligands, adapted from [62]. n.d. =not determined. ....	21
Figure 8. (a) Generic structure of xanthene family ligands, and (b) selected xanthene family ligands. ....	23
Figure 9. Xantphos derivatives via modification of the phosphorus moieties. ....	25
Figure 10. Generalised structure of the prepared bidentate ligands and metal complexes. ....	28
Figure 11. Xanthene family ligands prepared with a common procedure. X, Y, and R refers to the ligand constituents in Figure 10. ....	42
Figure 12. Application of 3.15 in supported catalysis via functionalisation with suitable linker: (a) silica support [35], (b) polystyrene support [36], and (c) polyglycerol dendritic support [37]. ....	44
Figure 13. Preparation of 3.21 and 3.22, adapted from literature [10]. X, Y, and R refers to the ligand constituents in Figure 10. ....	48
Figure 14. Reported crystal structure of 3.10 [10] from different points of view: (a) front, and (b) bottom. ....	59
Figure 15. Crystal structure of 3.13 from from different points of view: (a) front, and (b) right. ....	60
Figure 16. Crystal structure comparison of 3.16: (a) Goertz et al. [28], and (b) this work. ....	61
Figure 17. Crystal structure of 3.17 from different points of view: (a) bottom, and (b) right. ....	62
Figure 18. The crystal structures of 3.23 with two crystallographically independent molecules in the asymmetric unit cell. ....	63
Figure 19. The crystal structures of 3.30 with two crystallographically independent molecules in the asymmetric unit cell. ....	64
Figure 20. Crystal structure of 3.30: (a) schematic representation, and (b) bottom view. ....	64
Figure 21. Crystal structure of 3.31 from different points of view: (a) schematic representation, (b) front, and (b) bottom. ....	67
Figure 22. Crystal structure of 3.32 from different points of view: (a) schematic representation, (b) front, and (c) bottom. ....	68
Figure 23. Geometry optimised structures for ligands 3.12, 3.17, and 3.19. ....	72
Figure 24. Metal preferred bite angle calculations for prepared bidentate ligands. ....	73
Figure 25. A comparison of the average metal preferred bite angle and natural bite angle. ....	73
Figure 26. General trend for the multiplets in the proton NMR spectrum of xantphos. ....	83
Figure 27. General trend for the multiplets in the carbon NMR spectrum of xantphos. ....	84
Figure 28. Validation and optimisation studies for the microwave assisted oxidation of benzyl alcohol. ....	105
Figure 29. Optimisation of ligands for the Ru catalysed oxidation of benzyl alcohol. Please refer to Chapter 2, Table 2a-b for ligand structures. ....	106
Figure 30a. Ru catalysed oxidation of primary alcohol substrates. ....	107

Figure 31. Investigation of ligand electronic and steric properties on benzylic alcohol substrates. ....	110
Figure 32. Solvent and temperature effects for the Ru catalysed oxidation of benzyl alcohol. ....	111
Figure 33a. Solvent-free oxidation of benzyl alcohol. ....	113
Figure 34. Ru catalysed hydrogenation of benzaldehyde, acetophenone, and benzophenone [7]. ....	119
Figure 35. Validation and metal optimisation studies for the microwave assisted hydrogenation of acetophenone. ....	121
Figure 36. Investigation of the alternative bases for the hydrogenation of acetophenone. ....	122
Figure 37. Optimisation of catalyst loading for the hydrogenation of acetophenone. ....	123
Figure 38. Optimisation of ligands for the Ru catalysed hydrogenation of acetophenone. Please refer to Chapter 2, Table 2a-b for ligand structures. ....	124
Figure 39. Comparison of reactivity at different reaction conditions for the Ru catalysed hydrogenation of acetophenone with different bidentate ligands. ....	125
Figure 40a. Ru catalysed hydrogenation of ketones. ....	126
Figure 41. Hydrogenation of cinnamaldehyde 6.1. ....	134
Figure 42. Product distribution as a function of time at 2 mol% loading and 50 bar H <sub>2</sub> , in toluene. ....	135
Figure 43. Hydrogenation of cinnamaldehyde 6.1 in different solvents. ....	136
Figure 44. Hydrogenation of cinnamaldehyde 6.1 at different catalyst loadings. ....	137
Figure 45. Hydrogenation of $\alpha,\beta$ -unsaturated carbonyls. ....	138
Figure 46. Generalised structure of an Ir PCP complex. ....	142
Figure 47. Generalised structure of the proposed tridentate ligands. ....	143
Figure 48. Crystal structure of tridentate ligand 7.3. ....	146
Figure 49. Crystal structure of tridentate precursor 7.6. ....	148
Figure 50. Crystal structure of complex 7.10. ....	149

## List of Tables

Table 1. Bite angle definitions and calculation methods. ....	15
Table 2a. Summary of prepared bidentate ligands and corresponding backbones. X, Y, and R refer to the ligand constituents in Figure 10.....	30
Table 3. Summary of employed characterisation methods. ....	32
Table 4a. X-ray crystal structures of backbones and bidentate ligands. ....	55
Table 5. Intramolecular P...P distances and dihedral angles for backbone and ligand crystal structures. ....	58
Table 6. Selected bond lengths and bond angles for backbone and bidentate ligand crystal structures. ....	58
Table 7. Selected bond lengths and bond angles for 3.30.....	65
Table 8. Selected bond lengths and bond angles for 3.31 and 3.32. ....	67
Table 9. Natural bite angle ( $\beta_n$ ) values for the bidentate ligands prepared in this study. ....	69
Table 10. Calculated metal preferred bite angles.....	72
Table 11. Summary of the prepared tridentate ligands and corresponding linker tails. ....	144

## List of Schemes

Scheme 1. Literature route [3] to 3.1.....	35
Scheme 2. Alternate synthesis for the preparation of 3.1. ....	35
Scheme 3. Optimisation of the acid source for the preparation of 3.1.....	35
Scheme 4. Preparation of 3.3.....	36
Scheme 5. Protection of phenoxazine for the preparation of 3.4. ....	37
Scheme 6. Preparation of 3.5 [14]. ....	37
Scheme 7. Preparation of 3.6 [16]. ....	38
Scheme 8. Preparation of 3.7 [17]. ....	38
Scheme 9. Preparation of precursor 3.8 [15]. ....	39
Scheme 10. Preparation of 3.9 via conventional heating [15]. ....	39
Scheme 11. Preparation of 3.9 via microwave assisted heating. ....	40
Scheme 12. Reported routes to 3.10: (a) Hillebrand et al. [24], and (b) van Leeuwen [10]. ....	41
Scheme 13. Deprotection of the precursor ligand 3.14 to 3.15.....	44
Scheme 14. Preparation of 3.18 adapted from literature [3]. ....	46
Scheme 15. Attempted synthesis of phosTolylxantphos. ....	46
Scheme 16. Preparation of 3.19 adapted from literature [42]. ....	47
Scheme 17. Preparation of 3.20 adapted from literature [43-44].....	47
Scheme 18. Preparation of 3.23 adapted from literature [10]. ....	49
Scheme 19. Synthesis of metal precursors: (a) 3.24, (b) 3.25, and (c) 3.26, adapted from literature [47].....	50
Scheme 20. Synthesis of metal precursors: (a) 3.27 [48-49], (b) 3.28 [50], adapted from literature. ....	51
Scheme 21. Preparation of 3.29. ....	52
Scheme 22. Preparation of 3.30. ....	52
Scheme 23. Preparation of 3.31 and 3.32. X, Y, and R refers to the ligand constituents in Figure 10.....	53
Scheme 24. Preparation of 3.33. ....	53
Scheme 25. Generalised borrowing hydrogen strategy, adapted from Seiple [4]. ....	102
Scheme 26. Generalised reaction for the oxidation of primary alcohols to methyl esters [5]. ....	103
Scheme 27. Reported oxidation of benzyl alcohol to benzaldehyde [5]. ....	103
Scheme 28. Ru xantphos catalysed asymmetric hydrogenation of 1-acetonaphthone [6]. ....	119
Scheme 29. Hydrogenation pathway of cinnamaldehyde 6.1 [6-9]. ....	132
Scheme 30. Preparation of tridentate ligands 7.3 and 7.4.....	145
Scheme 31. Preparation of tridentate precursor 7.6 and tridentate ligand 7.8. ....	147
Scheme 32. Complexation of tridentate ligands 7.3 and 7.4.....	148
Scheme 33. Attempted one step coupling of (a) salicylic acid, and (b) benzoyl chloride, to nixantphos. ....	150
Scheme 34. Proposed synthetic route to a tridentate xanthene ligand containing a kinked linker.....	151

## List of Abbreviations

API	-	Atmospheric pressure ionisation
bs	-	Broad signal
BDNA	-	1,8-bis(diphenylphosphinomethyl)naphthalene
$\beta$	-	Bite angle
$\beta\eta$	-	Natural bite angle
Bu	-	Butyl
CIF	-	Crystallographic information file
cod	-	1,5-cyclooctadiene
COSY	-	H-H correlation spectroscopy
d	-	Doublet
DBFphos	-	4,6-Bis(diphenylphosphino)dibenzofuran
DCM	-	Dichloromethane
dec	-	Decomposed
DFT	-	Density functional theory
DPEphos	-	Bis-(2-diphenylphosphino)phenyl) Ether
ESI	-	Electron spray ionisation
GC-MS	-	Gas chromatography mass - spectroscopy
Hexantphos	-	4,5-Bis(diphenylphosphino)-2,7-dihexyl-9,9-dimethylxanthene
HMBC	-	Homonuclear multiple - bond correlation
HRESIMS	-	High resolution electron spray ionisation mass spectroscopy
HSQC	-	Homonuclear single - quantum correlation
Hz	-	Hertz
<sup>i</sup> Pr	-	isopropyl
IR	-	Infrared
IsopropxantButylphos	-	4,5-Bis(di- <i>t</i> -butylphosphino)-9-isopropylidenexanthene
Isopropxantphos	-	4,5-Bis(diphenylphosphino)-9-isopropylidenexanthene
IsopropxantTolylphos	-	4,5-Bis(di- <i>p</i> -tolylphosphino)-9-isopropylidenexanthene
<i>J</i>	-	Coupling constant
L	-	Ligand
LCMS	-	Liquid chromatography mass - spectroscopy
M	-	Metal
m	-	Multiplet
mp	-	Melting point
mw	-	Microwave
<i>n</i> BuLi	-	<i>n</i> -Butyllithium
Nixantphos	-	4,6-Bis(diphenylphosphino)phenoxazine
NMR	-	Nuclear magnetic resonance
NR	-	No reaction
Ph	-	Phenyl
Phosxantphos	-	4,6-Bis(diphenylphosphino)-10-phenylphenoxaphosphine
PTEphos	-	Bis-(2-diphenylphosphino)- <i>p</i> -tolyl) Ether
<i>r</i> <sub>M-P</sub>	-	Metal phosphorus bond length
<i>r</i> <sub>P...P</sub>	-	Intramolecular P...P distance
Rf	-	Retention factor
rt	-	Room temperature

Sixantphos		4,6-Bis(diphenylphosphino)-10,10-dimethylphenoxasilin
t	-	Triplet
TBDMS	-	<i>tert</i> -Butyldimethylsilyl
TBDMSCl	-	<i>tert</i> -Butyldimethylsilylchloride
<sup>t</sup> Bu	-	<i>tert</i> -Butyl
THF	-	Tetrahydrofuran
Thixantphos		4,6-Bis(diphenylphosphino)-2,8-dimethylphenoxathiin
TMEDA	-	<i>N,N,N',N'</i> -tetramethylethylenediamine
TOF	-	Turn-over frequency
Xantphos		4,5-bis(diphenylphosphino)-9,9-dimethylxanthene
XPNphos		4,5-bis(diisopropylaminophosphino)- 9,9-dimethylxanthene

## Acknowledgements

- I gratefully acknowledge the financial support from SASOL, the National Research Foundation, and THRIP.
- I would like to thank my supervisor, Prof. H. B. Friedrich, for his advice and guidance, and the following academics for their assistance: Dr. M. D. Bala, Dr. T. Govender, Prof. H. C. M. Vosloo, Dr G. E. M. Maguire, and Prof. H. G. Kruger.
- Special thanks to Prof. Mike Green for his support and continued interest in the project.
- I am also grateful to Dr. M. Fernandes for the X-ray crystallographic data collection and refinement.
- Thanks to Prof. P. W. N. M. van Leeuwen for his helpful discussions and assistance with the natural bite angle calculations.
- I appreciate the contributions of the following technical staff at the School of Chemistry: Mrs. Anita Naidoo, Mr. Dilip Jagjivan, and Mr. Kishore Singh.
- Thanks to my irreplaceable laboratory friends Tricia, Byron, Evans, and Frans. Thanks for the help and encouragement.
- Thanks to my family and friends for their support and understanding.
- Finally, my North Star in times of despair, Shalen.



# Chapter 1

## Introduction

### 1.1 Background and methodology

The research presented in this thesis involves the synthesis, characterisation, and novel catalysis of a series of diphosphorus ligands and metal complexes. The unifying theme of the studied ligands is a xanthene backbone **1.1**, **Figure 1**, that imparts a measure of synthetic and catalytic versatility to the prepared compound. This versatile behaviour is best demonstrated by the ligand xantphos **1.2**, **Figure 1**, that has been successfully applied to a variety of homogeneous organic transformation reactions [1-4]. Due to the relative success of **1.2**, this ligand has been selected as the structural basis of this study. Xantphos is also used as a benchmark for comparison of the related xanthene ligands prepared in this work.

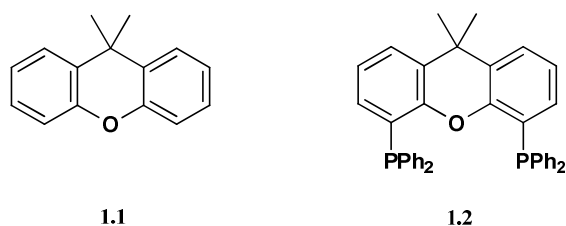


**Figure 1.** 9,9-dimethylxanthene **1.1**, and xantphos **1.2**.

The preparation of **1.2** was first reported in 1995 by Hillebrand et al. [5]. Working independently, van Leeuwen and co-workers [6] reported the synthesis, characterisation, and first catalytic application of **1.2** later that year. In the same work, the chemistry of a homologous series of related xanthene ligands, commonly referred to as xanthene or xantphos family ligands, was also reported [6]. The xanthene family ligands were prepared by varying the central atom opposite the ether bridge of the xanthene backbone, while keeping the diphenylphosphine donors unchanged.

The impetus for the historical development of the xanthene family ligands can be traced to the works of Casey and Whiteker. These researchers defined the natural bite angle of diphosphorus ligands as the P-M-P chelation angle imposed by backbone considerations only [7]. The natural bite angle ( $\beta_{\eta}$ ) was subsequently correlated to favourable regioselectivity in Rh catalysed hydroformylation reactions [8]. With the aim of developing ligands with wide chelation angles for similar applications, van Leeuwen and co-workers adopted  $\beta_{\eta}$  as an invaluable tool for ligand design [6,9-12]. Ligands based on a xanthene backbone **1.1** were found to induce a large intramolecular P...P distance that directly affected the P-M-P chelation angle. Xanthene family ligands with

wide natural bite angles (ca. 102 – 121°) have since been correlated to favourable activity and selectivity in other homogeneously catalysed reactions [13-14].

The parent ligand xantphos is readily available from commercial sources, a factor that contributes to its diverse and popular application in homogeneous studies. However, the remaining xanthene family ligands are either difficult to obtain from standard suppliers, or available at high cost from speciality chemical companies. The synthesis of xanthene family ligands is also not straightforward. As a result, homogeneous catalytic studies involving **1.2** are more frequently reported than studies involving the remaining family ligands. Catalytic studies involving the latter are usually scant and non-exhaustive [15-16], or limited to the research group of van Leeuwen [17-20] or to research groups working in collaboration with van Leeuwen [21]. Therefore, the preparation, characterisation, and homogeneous catalysis of the diphosphorus xanthene family ligands can be seen as a research area with significant potential for growth and diversification.

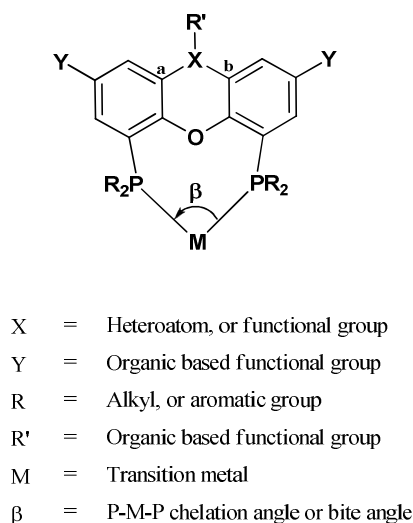


**Figure 2. Generalised structure of the prepared ligands and metal complexes.**

In this work, the prepared ligands and metal complexes can be described by the generalised structure in **Figure 2**. The ether bridge of the xanthene backbone is kept constant for all investigations, while position X can be modified with various non-chelating donor atoms. In some instances, the donor at position X is absent, with no bonding between the carbon atoms at position *a* and *b*. The backbone can be modified at position Y to improve solubility. Position X can be further functionalised with a linker unit, R', to investigate tridentate coordination or anchoring for supported catalysis applications. The backbone is functionalised with the chelating phosphorus donors where substituent R groups of varying steric and electronic properties can be investigated.

Most reported applications of **1.2** and derivatives involve early and late *d*-block transition metals. The chelating phosphorus donors are known to form stable metal complexes soluble in most organic solvents, and **1.2** has been successfully applied to homogeneous catalysis with Rh [22-23], Ru [21], Pd [2,24], and Ni [25-26] complexes. For this work, the chemistry of Ir, Rh, Ru, and Os metal complexes was of particular interest.

Ir and Os metal centres were identified on the basis of limited or no reported catalytic studies involving complexes with xanthene family ligands. Ir xantphos complexes have been reported by Fox et al. [27] for preliminary hydroformylation studies. However, to the best of our knowledge, there are no reports on the synthesis, characterisation, or application of the remaining family ligands with Ir. In recent work, Asensio et al. [28] have reported the preparation of novel Os xantphos complexes. However, the reported work was primarily a study on the coordination chemistry of such complexes with no catalytic applications investigated. To the best of our knowledge, there have been no reports on the preparation of Os complexes with xanthene family ligands.

Catalytic testing scenarios were devised and implemented to evaluate the performance and extend the catalytic scope of the diphosphorus ligands prepared in this work. A large number of transition metal catalysed transformations are applicable to the xanthene family ligands. Therefore, possible reaction types were filtered on the basis of those having previously involved the successful application of diphosphorus ligands or xantphos **1.2**. Reaction types were also limited to those involving only the transition metal centres of interest to this work. Suitable catalytic testing scenarios involved hydrogenation, oxidation, and C-H activation studies.

For studies of oxidation reactions, Rh, Ru, Ir, and Os xanthene complexes were investigated. The use of a Ru xantphos complex for the oxidation of benzyl alcohol has been previously reported [29]. However, no Ru xanthene family ligands, or Rh, Ir, or Os xanthene complexes have been applied to oxidation type reactions in literature. The use of an Os xantphos complex was of interest in this scenario since certain organometallic Os complexes are known to be efficient oxidation catalysts [30]. In the case of hydrogenation reactions, two catalytic testing scenarios were investigated, viz. transfer hydrogenation using Ru, Rh, and Ir complexes, and the hydrogenation of  $\alpha,\beta$ -unsaturated carbonyls with molecular hydrogen and Rh and Ir complexes. The use of a Ru xantphos complex has been previously reported for transfer hydrogenation reactions [31-32], however the remaining xanthene family ligands have not been previously investigated. In the case of C-H activation reactions, tridentate Ir PCP pincer complexes are known to be highly efficient, in particular for the upgrading of alkanes to alkenes [33-35]. As a result, an Ir metal centre was used for an investigation into the preparation of tridentate xanthene based ligands for similar applications.

After the identification of suitable reaction types, the catalytic testing scenario was implemented in the following manner. If the identified reaction was previously reported for the parent ligand **1.2**, then the reaction was first reproduced under literature conditions and modified, if necessary. If the identified reaction was initially reported for other diphosphorus ligands, then the reaction conditions were first adapted for ligand **1.2**, screened for activity, and modified, if necessary. In both instances, the resultant refined reaction was then optimised for **1.2** with respect to the following variables:

1. Transition metal centre
2. Catalyst loading
3. Time (Including in situ complexation time and total reaction time)
4. Solvent, base (if applicable), and hydrogen source (if applicable)

With the identified reaction optimised for the parent ligand **1.2**, the remaining xanthene family ligands were similarly screened for activity under the optimised conditions. The best or most effective xanthene ligand, in terms of activity, selectivity, and synthetic considerations, was then screened for a variety of related substrates to investigate ligand versatility and substrate scope.

### 1.1.1 Solvent considerations

Organic solvents are an inherent part of classical organometallic catalysis. However, most organic solvents are either highly toxic or adversely affect the environment, which complicates waste disposal and catalyst recovery. In keeping with modern environmental regulations and legislations, an increasing industrial and academic trend is the replacement of such solvents with environmentally friendly, benign alternatives. These new ‘greener’ solvents must possess the favourable properties of common organic solvents, and also satisfy or adhere to green chemistry concepts [36-37]. Green solvents that have been successfully applied in literature include room temperature ionic liquids, supercritical carbon dioxide, and water [38].

A further alternative to organic solvents that better embraces the principles of green chemistry [39-41] is the use of no reaction medium or solvent-free conditions. In homogeneous catalytic solvent-free applications, a liquid substrate usually acts as both a reactant and solvent that yields the homogeneous medium [42]. In this scenario the liquid substrate and solid catalyst are brought together and the addition of heat facilitates the formation of a single reaction medium. The distinct advantages of solvent-free reactions over organic or other reaction media have been discussed by Cave et al. [43], and can be summarised as follows:

1. No reaction medium to collect, purify, and cycle
2. Purification of prepared compounds via chromatography or recrystallisation is not required
3. Sequential solventless reactions are possible in high yielding systems
4. Reactions are substantially more rapid than for organic solvents
5. Lower energy usage
6. The need for pre-formed salts or complexes can be circumvented
7. Functional group protection/de-protection can be avoided
8. Considerable batch size reduction and processing costs

In terms of reducing waste, the greenest solvent is no solvent [42,44-45]. Solvent-free techniques have the added benefit of being economically attractive due to the reduction in solvent cost, resources, energy, waste disposal and time [46]. For this work, the use of solvent-free conditions, or rather the exclusion of harmful solvents, has been investigated in the catalytic testing scenarios.

### 1.1.2 Energy considerations

The consumption of energy accounts for a significant fraction of the operating costs in any chemical process. The minimisation of operating costs is a desirable economic goal, and the more efficient utilisation of resources

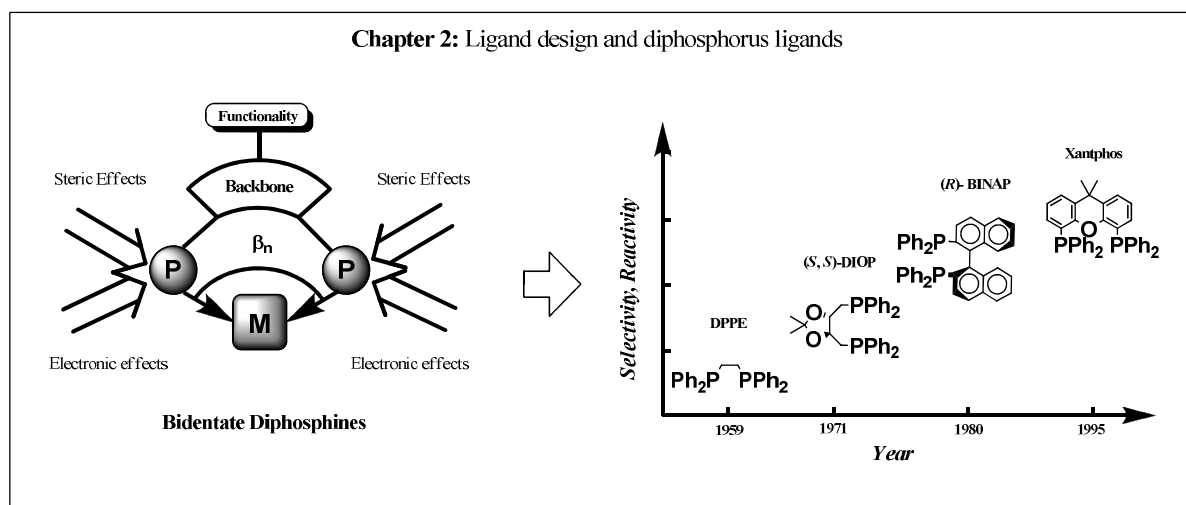
is desirable from a green chemistry point of view. In the case of homogeneous catalysis, significant energy is consumed in achieving and maintaining the correct operating conditions, in the recovery of reagents or solvents, and in waste disposal. By using highly active and selective organometallic catalysts and solvent-free techniques, the minimisation of energy consumption can be investigated by examining the operating conditions.

An important process parameter in catalysis is the reaction temperature. Most reactions are carried out at greater than ambient conditions that require the addition of energy. This energy is typically supplied as heat, usually in the form of conductive heating by oil baths, heating mantles, or heating jackets. However, this type of heating is not very efficient, since the reaction mixture is not in direct contact with the heat source. The heating rate is thus limited by heat transfer considerations, which can adversely affect the kinetics and thus reaction rate, and can result in increased reaction times [47].

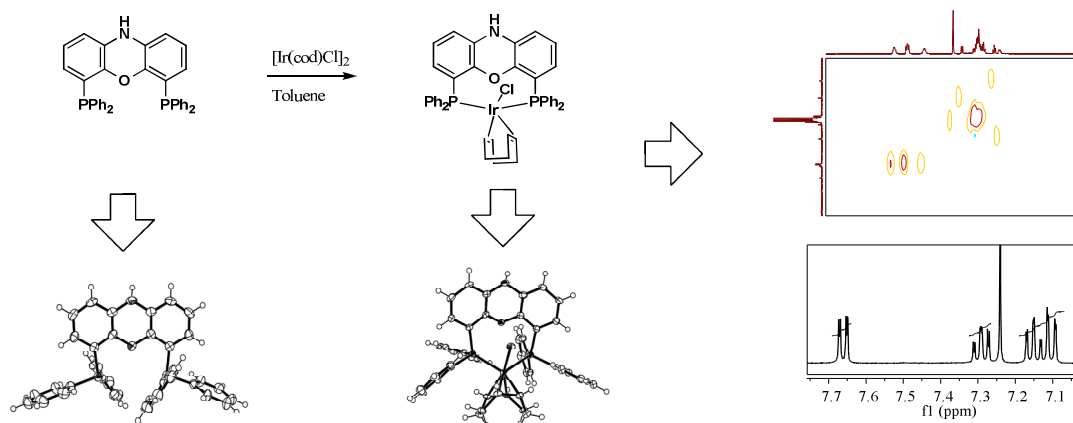
For this work, microwave irradiation was investigated as an alternate method of supplying heat to the catalytic reaction. The primary advantage of microwave energy over conventional heating methods is the dramatically reduced reaction times. Microwave energy facilitates flash heating, a condition where thermal energy required for the reaction is generated extremely rapidly [48]. This allows a high reaction temperature to be obtained in a short period of time, overcoming the heat transfer limitations of conventional heating. The accelerated heating rates can dramatically increase the reaction rate. For example, using the heuristic that for each 10 °C increase in temperature the reaction time halves, a reaction that takes 18 hours at 80 °C can be completed in 30 s at 200 °C in a microwave [49]. A further benefit is that competing side reactions can be minimised in such short reaction times, resulting in improved yields, increased product purity, and lower yields of decomposition products. Moreover, microwave mediated reactions can be readily extended to solvent-free conditions provided that the reagents are effective at coupling to microwave energy.

## 1.2 Thesis scope and contents

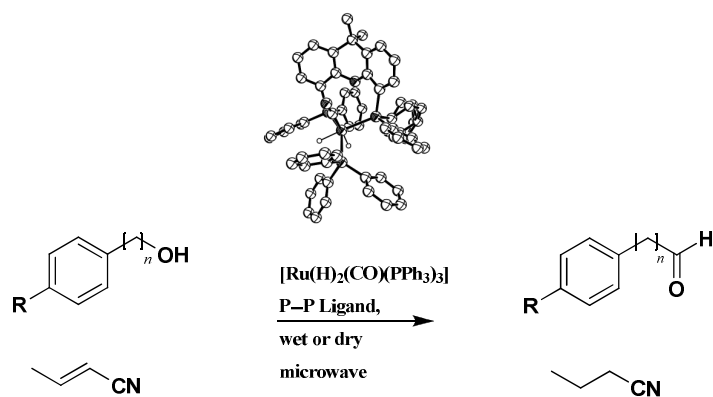
This thesis summarises and presents the research work involved in the preparation and application of xanthene family ligands. A graphical summary of the subsequent chapters of this thesis is given below.



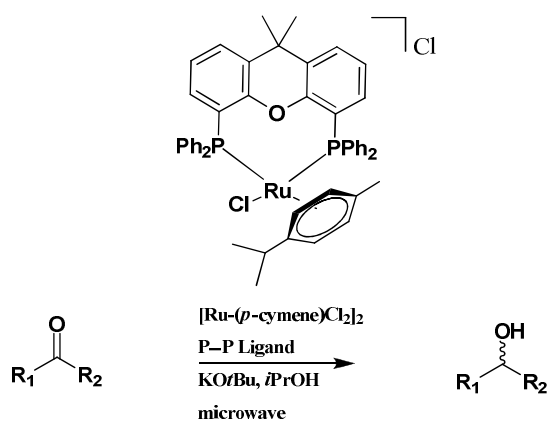
### Chapter 3: The preparation of bidentate xanthene family ligands and catalysts



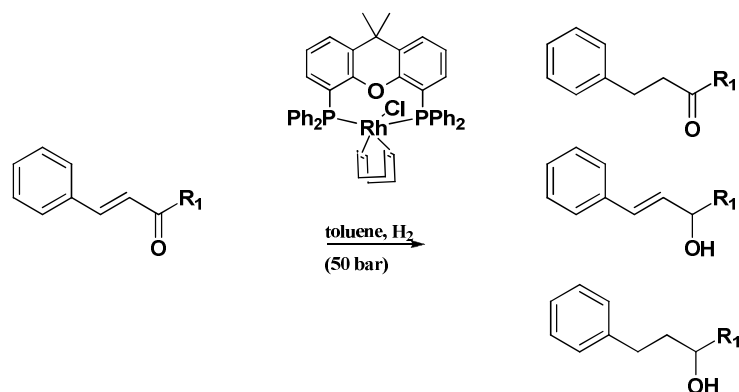
### Chapter 4: Microwave assisted oxidation of alcohols



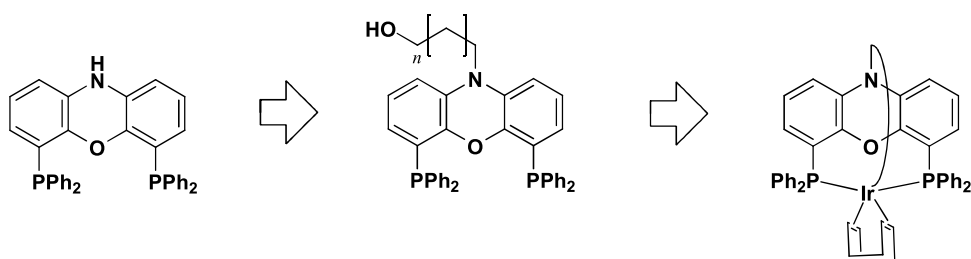
### Chapter 5: Microwave assisted transfer hydrogenation of ketones



**Chapter 6:** An investigation into the selective hydrogenation of  $\alpha,\beta$ -unsaturated carbonyls



**Chapter 7:** Towards the preparation of tridentate xanthene family ligands and catalysts



In Chapter 2 ligand design parameters are introduced and discussed with regard to diphosphorus ligands. These parameters include geometric, electronic and steric considerations. Among the different molecular descriptors the natural bite angle is defined, and methods of quantifying this parameter are discussed. Thereafter, significant developments in diphosphorus ligands have been identified and important milestones that range from early synthesis of long alkyl chain diphosphines to more complex trans-spanning ligands is presented. The chapter culminates with a review of xanthene based diphosphorus ligands with emphasis on ligand design, reactivity and the bite angle.

Chapter 3 is dedicated to the preparation and synthesis of xanthene based diphosphorus ligands and selected metal complexes. The synthetic steps and rationale are discussed together with yields obtained. All characterisation data is included at the end of the chapter. Crystal structure data is also presented for the ligands and metal complexes prepared in the study.

Chapter 4 describes the use of diphosphine ligands prepared in Chapter 3 for the oxidation of primary alcohols to aldehydes. A Ru hydride metal precursor is complexed in situ with the xanthene based diphosphorus ligand and the sacrificial hydrogen donor used is crotonitrile. Various benzyl alcohol derivatives and aliphatic alcohols

were also oxidised in good yields to respective aldehydes. Solvent free conditions were also investigated and these results are discussed in detail.

In Chapter 5, the ligands are applied to a second type of hydrogen transfer reaction involving the reduction of ketones to alcohols by the Ru(xantphos)arene catalyst. The hydrogen source is 2-propanol in the presence of a strong base. The substrate scope comprised of electron rich and electron deficient derivatives of acetophenone and some bulky ketones. Good TOF's were obtained and further optimisation of the reaction time and catalyst loading is presented.

In Chapter 6 the chemo-selective hydrogenation of  $\alpha,\beta$ -unsaturated carbonyl groups is carried out using an [Rh(xantphos)(cod)Cl] catalyst. Molecular hydrogen was used as the reducing agent at pressures of 50 bar. The substrate scope comprised of both  $\alpha,\beta$ -unsaturated aldehydes and ketones.

In Chapter 7 the preparation of tridentate ligands is presented. This involved functionalisation of the amine in the nixantphos ligand with a long alkyl tail containing the third donor. The resulting ligands were then complexed to Ir metal centres and X-ray crystallography was used to identify the mode of coordination. Based on these findings, alternative ligand design approaches are also discussed.

### 1.3 References

- 1 Gillespie, J. A.; Dodds, D. L.; Kamer, P. C. J. *Dalton Trans.* **2010**, 39, 2751-2764.
- 2 Gensow, M.-N. B.; Freixa, Z.; van Leeuwen, P. W. N. M. *Chem. Soc. Rev.* **2009**, 38, 1099-1118.
- 3 van Leeuwen, P. W. N. M. *Homogeneous Catalysis: Understanding the Art*; Kluwer Academic Publishers: Dordrecht, **2004**, p 155-156.
- 4 Kamer, P. C. J.; van Leeuwen, P. W. N. M.; Reek, J. N. H. *Acc. Chem. Res.* **2001**, 34, 895-904.
- 5 Hillebrand, S.; Bruckmann, J.; Kruger, C.; Haenel, M. W. *Tetrahedron Lett.* **1995**, 36, 75-78.
- 6 Kranenburg, M.; Vanderburgt, Y. E. M.; Kamer, P. C. J.; van Leeuwen, P. W. N. M.; Goubitz, K.; Fraanje, J. *Organometallics* **1995**, 14, 3081-3089.
- 7 Casey, C. P.; Whiteker, G. T. *Israel. J. Chem.* **1990**, 30, 299-304.
- 8 Casey, C. P.; Whiteker, G. T.; Melville, M. G.; Petrovich, L. M.; Gavney, J. A.; Powell, D. R. *J. Am. Chem. Soc.* **1992**, 114, 5535-5543.
- 9 van der Veen, L. A.; Keeven, P. H.; Schoemaker, G. C.; Reek, J. N. H.; Kamer, P. C. J.; van Leeuwen, P. W. N. M.; Lutz, M.; Spek, A. L. *Organometallics* **2000**, 19, 872-883.
- 10 van der Veen, L. A.; Kamer, P. C. J.; van Leeuwen, P. W. N. M. *Organometallics* **1999**, 18, 4765-4777.
- 11 van Leeuwen, P. W. N. M.; Kamer, P. C. J.; Reek, J. N. H.; Dierkes, P. *Chem. Rev.* **2000**, 100, 2741-2769.
- 12 Dierkes, P.; van Leeuwen, P. W. N. M. *J. Chem. Soc., Dalton Trans.* **1999**, 1519-1529.
- 13 Freixa, Z.; van Leeuwen, P. W. N. M. *Dalton Trans.* **2003**, 1890-1901.
- 14 van Leeuwen, P. W. N. M. *Homogeneous Catalysis: Understanding the Art*; Kluwer Academic Publishers: Dordrecht, **2004**, p 17-18.
- 15 Deprele, S.; Montchamp, J. L. *Org. Lett.* **2004**, 6, 3805-3808.
- 16 Ricken, S.; Osinski, P. W.; Eilbracht, P.; Haag, R. *J. Mol. Catal. A: Chem.* **2006**, 257, 78-88.
- 17 Kamer, P. C. J.; Kranenburg, M.; van Leeuwen, P. W. N. M.; de Vries, J. G., U.S. Patent, 5,817,848, Oct. 6, 1998.
- 18 Kranenburg, M.; Kamer, P. C. J.; van Leeuwen, P. W. N. M.; Vogt, D.; Keim, W. *J. Chem. Soc., Chem. Commun.* **1995**, 2177-2178.
- 19 Sandee, A. J.; Reek, J. N. H.; Kamer, P. C. J.; van Leeuwen, P. W. N. M. *J. Am. Chem. Soc.* **2001**, 123, 8468-8476.



- 20 Sandee, A. J.; van der Veen, L. A.; Reek, J. N. H.; Kamer, P. C. J.; Lutz, M.; Spek, A. L.; van Leeuwen, P. W. N. M. *Angew. Chem., Int. Ed.* **1999**, *38*, 3231.
- 21 Ledger, A. E. W.; Slatford, P. A.; Lowe, J. P.; Mahon, M. F.; Whittlesey, M. K.; Williams, J. M. J. *Dalton Trans.* **2009**, 716-722.
- 22 van Haaren, R. J.; Zuidema, E.; Fraanje, J.; Goubitz, K.; Kamer, P. C. J.; van Leeuwen, P. W. N. M.; van Strijdonck, G. P. F. *Cr Chim* **2002**, *5*, 431-440.
- 23 Claver, C.; van Leeuwen, P. W. N. M. *Rhodium Catalyzed Hydroformylation*; Kluwer Academic Publishers.: Dordrecht, **2000**, p 87.
- 24 van Haaren, R. J.; Keeven, P. H.; van der Veen, L. A.; Goubitz, K.; van Strijdonck, G. P. F.; Oevering, H.; Reek, J. N. H.; Kamer, P. C. J.; van Leeuwen, P. *Inorg. Chim. Acta* **2002**, *327*, 108-115.
- 25 Goertz, W.; Keim, W.; Vogt, D.; Englert, U.; Boele, M. D. K.; van der Veen, L. A.; Kamer, P. C. J.; van Leeuwen, P. W. N. M. *J. Chem. Soc., Dalton Trans.* **1998**, 2981-2988.
- 26 Kranenburg, M.; Kamer, P. C. J.; van Leeuwen, P. W. N. M.; Vogt, D.; Keim, W. *J. Chem. Soc. Chem. Commun.* **1995**, 2177-2178.
- 27 Fox, D. J.; Duckett, S. B.; Flaschenriem, C.; Brennessel, W. W.; Schneider, J.; Gunay, A.; Eisenberg, R. *Inorg. Chem.* **2006**, *45*, 7197-7209.
- 28 Asensio, G.; Cuenca, A. B.; Esteruelas, M. A.; Medio-Simón, M.; Oliván, M.; Valencia, M. *Inorg. Chem.* **2010**, *49*, 8665-8667.
- 29 Owston, N. A.; Parker, A. J.; Williams, J. M. J. *Chem. Commun.* **2008**, 624-625.
- 30 Griffith, W. P. *Transition Met. Chem.* **1990**, *15*, 251-256.
- 31 Deb, B.; Borah, B. J.; Sarmah, B. J.; Das, B.; Dutta, D. K. *Inorg. Chem. Commun.* **2009**, *12*, 868-871.
- 32 Subongkoj, S.; Lange, S.; Chen, W.; Xiao, J. *J. Mol. Catal. A: Chem.* **2003**, *196*, 125-129.
- 33 Goldman, A. S.; Goldberg, K. I. Organometallic C-H Bond Activation: An Introduction. In *Activation and Functionalisation of C-H Bonds, ACS Symposium Series 885*; Goldberg, K. I., Goldman, A. S., Eds.; American Chemical Society: **2004**, p 27.
- 34 Gupta, M.; Hagen, C.; Kaska, W. C.; Cramer, R. E.; Jensen, C. M. *J. Am. Chem. Soc.* **1997**, *119*, 840-841.
- 35 Rybitchinski, B.; Crabtree, R. H. Pincer systems as models for the activation of strong bonds: scope and mechanism. In *The Chemistry of Pincer Compounds*; Morales-Morales, D., Jensen, C. M., Eds.; Elsevier: Amsterdam, **2007**, p 87-103.
- 36 Anastas, P. T. *Tetrahedron* **2010**, *66*, 1026-1027.
- 37 Anastas, P. T.; Bartlett, L. B.; Kirchhoff, M. M.; Williamson, T. C. *Catal. Today* **2000**, *55*, 11-22.
- 38 Sheldon, R. A.; Arends, I.; Hanefeld, U. *Green Chemistry and Catalysis*; Wiley-VCH Verlag GmbH & Co. KGaA: Weinheim, **2007**, p 27-28.
- 39 Anastas, P. T.; Kirchhoff, M. M. *Acc. Chem. Res.* **2002**, *35*, 686-694.
- 40 Anastas, P. T.; Williamson, T. C. Green chemistry: An overview. In *Green Chem.* **1996**; Vol. 626, p 1-17.
- 41 Beach, E. S.; Cui, Z.; Anastas, P. T. *Energ. Environ. Sci.* **2009**, *2*, 1038-1049.
- 42 Kerton, F. M. *Alternative Solvents for Green Chemistry*; The Royal Society of Chemistry Cambridge, **2009**, p 23-24.
- 43 Cave, G. W. V.; Raston, C. L.; Scott, J. L. *Chem. Commun.* **2001**, 2159.
- 44 Tundo, P.; Perosa, A.; Zecchini, F. Green Chemistry: Catalysis and Waste Minimisation In *Methods and Reagents for Green Chemistry: An Introduction*; John Wiley & Sons: New Jersey, **2007**, p 195-197.
- 45 Rothenberg, G. *Catalysis Concepts and Green Applications*; Wiley-VCH Verlag GmbH & Co. KGaA: Weinheim, **2008**, p 11-13.
- 46 Braga, D.; Grepioni, F. *Angew. Chem., Int. Ed. Engl.* **2004**, *43*, 4002-4011.
- 47 Dallinger, D.; Kappe, C. O. *Chem. Rev.* **2007**, *107*, 2563-2591.
- 48 Tierney, J. P.; Lidstrom, P. *Microwave assisted organic synthesis*; Blackwell Publishing, CRC Press: Boca Raton, **2005**, p 14-15.
- 49 Roberts, B. A.; Strauss, C. R. *Acc. Chem. Res.* **2005**, *38*, 653-661.

# Chapter 2

## Ligand design and diphosphorus ligands

### 2.1 Introduction

Rational ligand design is a measured or considered approach towards the preparation of ligands and catalyst systems. Ligand design can also be thought of as a generational strategy that involves the analysis of previous successful ligands to afford a greater understanding that aids the development of novel or related compounds [1]. Ideally, design concepts should be considered early in the ligand development to aid the preparation of selective and active catalysts. However, this critical aspect is often overlooked. As suggested by Gillespie et al. [1], the current prevalent approach is a crude design philosophy followed by synthesis and catalytic testing that sometimes requires a significant redesign of the ligand system. In contrast, a well designed system that achieves the original goal can be used as a starting point for modifications, variations, or adaptations that not only optimise current systems, but also lead to new catalysts or applications. In this sense, xantphos can be considered well designed as it has been successfully applied to a variety of synthetic and catalytic reactions, and the associated derivatives and family of ligands exhibit similar catalytic efficacy and versatility.

The rational design of xantphos is based to a large extent on other successful bidentate diphosphorus ligands. The design parameters taken into consideration for this work are therefore discussed in the general context of bidentate diphosphorus ligands. To further aid this discussion, a brief review on the development of diphosphorus ligands, culminating in xantphos, is also presented.

### 2.2 Design parameters and considerations

The structure of a bidentate diphosphorus complex can be divided into discrete conceptual building blocks, viz. a backbone, two chelating phosphorus donors, metal centre, and in some cases a remote functionality attached to the backbone. Each building block contributes to the overall properties of the ligand and catalyst. The properties of the overall complex can therefore be tailored by taking into account the effect of each individual building block prior to synthesis. Such effects or considerations include [2-4]:

- **Steric effects:** These effects are related to size or bulkiness and occur as a result of non-bonding forces between parts of a molecule. Such parts could be the substituents on the phosphorus donor, or the atoms that make up the backbone. Each of these atoms within the ligand occupies a certain amount of space, and if the atoms are brought too close together then the overlapping electron clouds could affect the preferred shape and reactivity of the ligand. The steric bulk of phosphorus ligands has been defined by the Tolman's cone angle [5-6]. For phosphorus ligands the cone angle is defined as the apex angle of a cylindrical cone, originating from a metal centre at 2.28 Å from the P atom, which touches the

outermost atoms of the model[7]. However, this model is limited and cannot be accurately applied to diphosphine ligands as these ligands seldom form a cone around the metal centre. The backbone holds the diphosphines donors a distance apart, therefore any flexibility on the backbone can be induced onto the diphosphine donors. As a result instead of forming a cone, the substituent on these diphosphine donors can fold or overlap, to overcome steric hindrance when coordinated to a metal centre. In addition, if the X-ray crystal structure is unavailable, this parameter cannot be determined by molecular modelling. Nonetheless the pioneering work of Tolman has lead to the development of other techniques to help explain the properties of diphosphine ligands. Among the numerous parameters such as solid angle [8-10], repulsive energy [11]; pocket angle [12] and the accessible molecular surface [13] that have been reported, the bite angle is the simplest molecular descriptor that has been mostly used to understand the chelating properties of bidentate ligands. Therefore the bite angle was employed in this study.

- **Electronic effects:** These effects are a result of a ligand possessing donors with different levels of electronegativity [14]. Electronic effects are transmitted along chemical bonds, for example bonds formed between the metal and the phosphorus donor. This results in the donor either pushing electron density towards ( $\sigma$  donors) or withdrawing electron density from ( $\pi$  acceptors) the metal centre. In general,  $\sigma$  donors have high electronegativity, a lack of vacant orbitals, and a lone pair of electrons, whereas  $\pi$  acceptors have vacant orbitals and will accept electron density to make a complex more stable.
- **Geometric considerations:** This refers, in part, to the coordination geometry or geometrical pattern formed by the coordination of the ligand to the metal centre. Some types of coordination geometry can be determined by the repulsion of the ligands around the metal centre [15]. If the geometry of a compound is designed to mimic a transition state that is responsible for a desired product, then the route towards a more selective catalyst can be achieved. Geometric considerations also involve the blocking of active sites to prevent unwanted side reactions. It is therefore possible to influence the selectivity towards a desired product, or inhibit the formation of other products, by examining the way a ligand coordinates.
- **Structural considerations:** Structural effects are somewhat similar to geometric considerations. Both involve the shape of the compound, however structural considerations are more concerned with the chemical make-up of the molecule and how it affects properties such as the mechanical rigidity, flexibility, or topology. For example, aromatic rings can assist in making the backbone planar and more rigid, while alkyl substituents can result in an overly flexible ligand. Structural effects can also involve considerations of the mechanical stability or support of the complex as a whole. For example, in supported phase catalysis the complex is usually anchored onto a support via a linker tail that is attached to the backbone [16].

- **The bite angle effect:** A wide chelation angle (P-M-P angle,  $\beta$ ) accounts for both steric and electronic effects in a metal complex [17]. It is a somewhat cumulative or additive effect caused by other building blocks in the ligand. Although  $\beta$  is technically a property of the complex formed after chelation, the magnitude of  $\beta$  for a free ligand can be modelled prior to synthesis.

A generalised structure of a bidentate diphosphorus complex is presented in **Figure 3** where the effect of each building block to the overall properties is indicated, as well as the influence of the bite angle. It should be noted that at most times it is not easy to distinctly or conveniently separate the effect of each building block. These effects usually work in a concerted manner to affect overall catalyst properties. Nevertheless, in the context of conventional diphosphines the distinctions made in **Figure 3** serve as a good first approximation and are useful for the discussion of ligand design considerations.

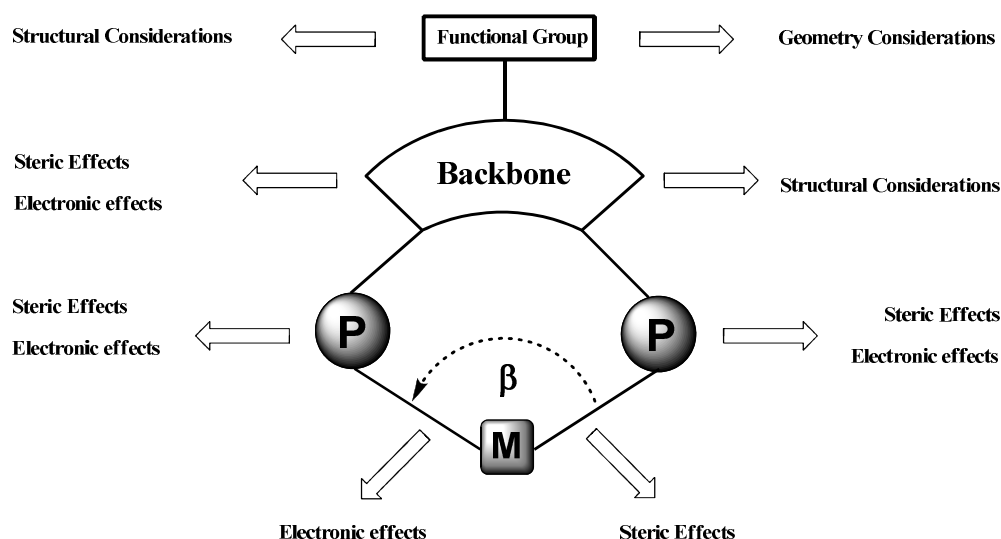


**Figure 3. Ligand design parameters and considerations for a generalised bidentate diphosphorus complex.**

The backbone can be considered the ‘core’ of a ligand, as it is the most important building block and starting point in ligand design. The relative size of the backbone is important as it serves as the bridge or scaffolding that holds the chelating phosphorus donors a distance apart. Flexibility of the backbone is also an important consideration. If a backbone is too rigid or constrained then the induced intramolecular P...P distance may be too large to support stable chelation. Conversely, an overly flexible backbone can result in significantly shortened intramolecular P...P distances that can adversely affect reactivity. Donor atoms in the backbone contribute to overall electronic effects of the ligand. Different donor atoms can be incorporated to tailor the electronic properties of the ligand for a particular reaction. The chemical makeup of the backbone and molecular size and bulkiness contribute to the overall steric hindrance. This can also be varied through judicious choice of donor atoms or substituents.

The remote functionality is not intrinsic of all diphosphorus ligands. The presence of such a functional group is usually dependant on the properties of the backbone, i.e. the backbone should have a pre-existing position

available for the functionality, and the position should not be hindered and should be able to undergo a functionalisation reaction. If these conditions are met, then a remote functionality, for example a linker unit with a third donor, can be successfully introduced. This allows the investigation of either tridentate coordination, mixed donor coordination, or anchoring onto a solid for supported catalysis applications.

Phosphorus donors are well known for their ability to effectively chelate to transition metal centres to form stable complexes. This strong chelation preference can be rationalised in terms of the back donating ability of the phosphorus atom. The electronegativity of the phosphorus atom can also be varied by changing the nature of the substituents. As a result, it is possible to tailor the electronic properties of the metal centre by manipulating the electronic environment of the phosphorus moieties. The size or bulkiness of the phosphorus moieties also contribute to the overall steric effects of the ligand. Bulky substituents can sterically hinder or block active sites, whereas less bulky groups, for example planar phenyl moieties, can twist or distort to accommodate chelation.

### **2.2.1 Quantifying ligand design parameters – The bite angle**

The ultimate aim of rational ligand design is to achieve active and selective catalysts. A possible route to this is by linking catalyst properties to catalytic results, for example with Quantitative Structure Activity Relationship (QSAR) models [18-19]. This allows the development of predictive models for the estimation of the catalytic performance of new complexes which can significantly aid in ligand design. Therefore, it is important to be able to describe catalyst properties with well defined molecular descriptors applicable to a wide range of catalysts.

Molecular descriptors for homogeneous catalysts are well known [18-20]. For this work, the preparation of bidentate diphosphorus ligands is of particular interest. Therefore, it is desirable to have a descriptor that is applicable to bidentate diphosphorus ligands, takes into account important ligand properties such as steric and electronic effects, can be correlated to experimental catalytic results, can be predicted prior to ligand synthesis, and is computationally inexpensive to calculate or easily determined.

A suitable parameter that fits the above description is the P-M-P chelation angle, or bite angle  $\beta$ . The bite angle is a well known descriptor of bidentate diphosphines that has been extensively used and popularised by the research group of van Leeuwen [7,17,21-25]. It was first proposed that the bite angle effect was primarily steric in nature, but this idea was later revised to include both electronic and steric effects [17,22]. As mentioned previously, these effects often work in a concerted manner dependant on the properties of the ligand. In order to viably use the bite angle as the primary molecular descriptor, it is preferable to have a homologous series of ligands where the core structure is relatively constant and subtle variations in the bite angle are induced by other means, for example variation of donor atoms in the backbone. As a result, the bite angle parameter has been successfully applied to the development and application of the xanthene family ligands that share a common or related backbone. Similarly, the influence of geometrical and electronic properties in a series of diphosphine ligands was investigated by Leitner et al. [26]. The phenyl rings of the phosphorus donors were functionalised

at the para positions with varying electron withdrawing and pushing substituents and this resulted in a corresponding variation of the bite angle. A systematic study of  $^{103}\text{Rh}$  chemical shift in the resulting complexes was then undertaken based on earlier work on  $^{59}\text{Co}$  shifts by Hofmann et al. [27]. It was shown by molecular modelling that the both the bite angle, metal-phosphine bond distance and the chelate ring size cannot be varied independently. These observations also agreed with experimental data and M-P bond distance obtained from X-ray crystal structures.

The bite angle has been successfully correlated to the selectivity of Rh catalysed hydroformylation reactions, Ni catalysed hydrocyanation reactions, and to the reactivity of various substrates in Pd catalysed C-N and C-C bond formation reactions [22,28-29]. Although wide bite angles are favourable in many applications, there is generally an upper limit to this range at which catalytic activity or selectivity decreases. In most cases there is an optimum value or range of the bite angle that is relatively wide when compared to most other diphosphorus ligands. A further increase or decrease in the chelation angle from the optimum range can result in a corresponding decrease in catalytic performance. This is illustrated in **Figure 4**, where the yield for the Ni catalysed hydrocyanation of styrene is compared for diphosphines of differing bite angles [23].

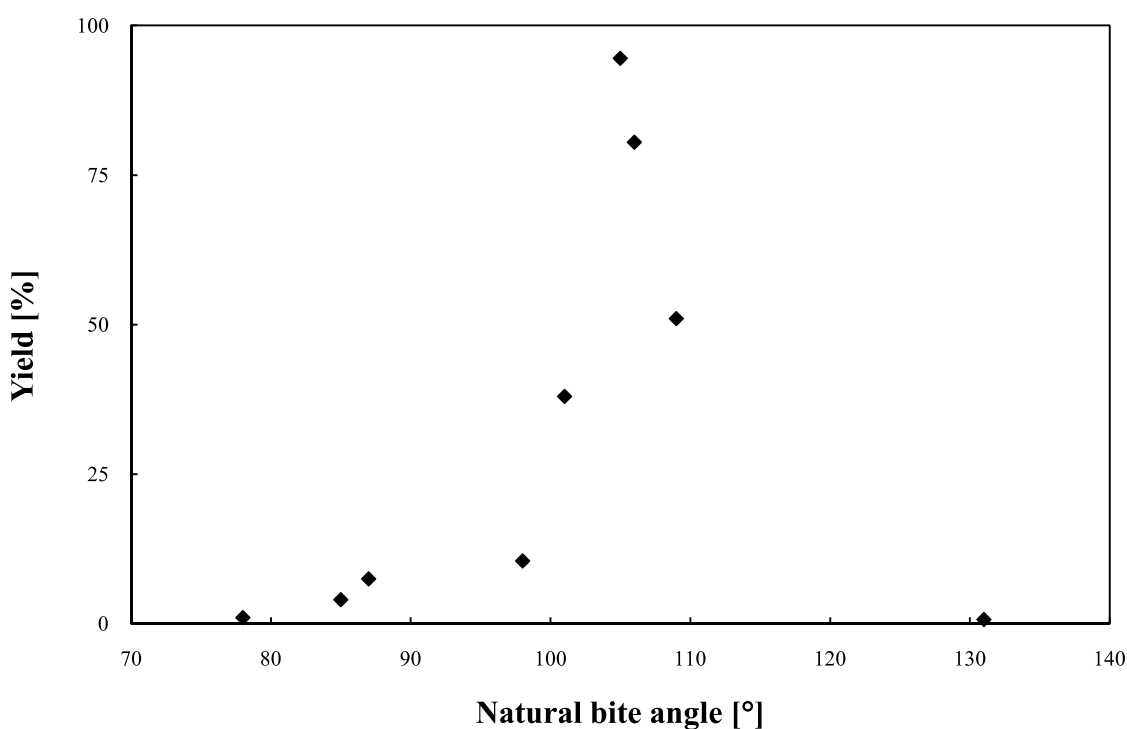


**Figure 4.** Observed yield versus calculated bite angle for the Ni catalysed hydrocyanation of styrene [23].

Entry	Nomenclature	Calculation Method	Ligand	Metal	M-P Bond [Å]
1	P-M-P bite angle ( $\beta$ )	X-ray crystal structure	X-ray	X-ray	X-ray
2	Natural bite angle ( $\beta_n$ )	Molecular mechanics	Modelled	Dummy atom	2.315
3	Ligand preferred bite angle	X-ray crystal structure	X-ray	X-ray	2.315
4	Metal preferred bite angle	Density functional theory	Modelled	Modelled	Optimised

**Table 1. Bite angle definitions and calculation methods.**

The bite angle can be further defined depending on the method of calculation, **Table 1**. The most rigorous determination of  $\beta$  is direct measurement of the P-M-P angle of an X-ray crystal structure of a metal complex, **Entry 1**. The bite angle measured in this manner takes into account the effects of the ligand and the metal, and can be seen as a compromise between the preferences of both [25]. This method presupposes the availability of the crystal structure of the required metal complex, and is therefore not very useful as a predictive ligand design tool. Nevertheless, bite angles measured in this manner can still be used for correlative and comparison purposes, as well as for the validation of predictive methods.

To evaluate  $\beta$  prior to synthesis, it is necessary to be able to accurately predict this value for either the free ligand or metal complex. The concept of the natural bite angle ( $\beta_n$ ) was therefore developed by Casey and Whiteker [30] using molecular mechanics calculations, **Entry 2**.  $\beta_n$  is defined as the preferred P-M-P chelation angle determined by ligand constraints only and not by metal valence angles. Any electronic preference imposed by the metal centre is therefore disregarded and the calculated P-M-P angle depends only on the properties of the ligand. However, the calculation of  $\beta_n$  cannot be performed without a metal atom as the substituents and lone pair of electrons on the P atoms need to be orientated in the correct direction [25]. Therefore, a dummy metal atom is used for this type of calculation, and the associated M-P bond lengths fixed to a suitable representative value. The P-M-P angle is related to the M-P bond lengths ( $r_{M-P}$ ) and intramolecular P...P distance ( $r_{P...P}$ ) by equation (1), where  $\beta$  is in degrees radians.

$$\beta = 2 \arcsin \left( \frac{r_{P...P}}{2r_{M-P}} \right) \quad (1)$$

By fixing the M-P bond length the bite angle is therefore determined by the intramolecular P...P distance which is strongly affected by the backbone. Casey and Whiteker developed  $\beta_n$  for application in Rh catalysed hydroformylation reactions. Therefore an M-P bond length of 2.30 Å, typical of most Rh-P bond lengths, was used in the original calculations [30]. However, to calculate a more generalised  $\beta_n$  applicable to any transition metal, van Leeuwen and co-workers [23,25,31] use a standardised M-P bond length of 2.315 Å that is typical of most M-P bond lengths for transition metal complexes found in the Cambridge Crystallographic Database. The values of  $\beta_n$  calculated for the free ligands compare favourably to P-M-P angles obtained from X-ray crystal structures [25]. The numerical value of  $\beta_n$  is also dependent on the software and molecular mechanics force field parameters used for the calculation. The comparison of various  $\beta_n$  values reported in literature should

therefore take this into account, and a comparison between trends rather than absolute values of  $\beta_n$  should be investigated.

The ligand preferred bite angle is calculated from analyses of X-ray crystal structures of transition metal complexes [25], **Entry 3, Table 1**. It is similar to direct measurement of the P-M-P angle ( $\beta$ ), with further assumptions. The M-P bond length obtained from the X-ray crystal structure is disregarded and instead fixed to 2.315 Å to mirror the assumption used for the calculation of  $\beta_n$ . The intramolecular P...P distance is also assumed to be determined by the backbone only, and is measured from the crystal structure of the complex of interest and used for the calculation of the ligand preferred bite angle, equation (2).

$$\text{Ligand preferred bite angle} = 2 \arcsin \left( \frac{r_{P \dots P}}{2(2.315)} \right) \quad (2)$$

Dierkes and van Leeuwen [25] suggest that the evaluation of the ligand preferred bite angle is a good starting point that enables greater insight into the ligand and metal preferences that contribute to  $\beta$ . In the same study, it was found that the calculated ligand preferred bite angles were in good agreement with calculated  $\beta_n$  values, which, to a certain extent, validates the natural bite angle method and calculations. The ligand preferred bite angle thus reinforces the importance or greater effect of the ligand on the bite angle and further highlights the importance of ligand design for fine tuning this parameter.

The metal preferred bite angle can be calculated to investigate the effect of metal preferences in combination with ligands preferences on  $\beta$ , **Entry 4, Table 1**. This calculation involves the modelling and optimisation of the complex with a real (i.e. non dummy) metal atom, and should take into account the nature of the counter ligands attached to the metal centre [25]. In order to accurately model the metal-ligand structure at the required level of complexity, density functional theory calculations are usually employed. Although this method gives a more realistic estimate of  $\beta$  when compared to  $\beta_n$ , the inherently higher computational cost of DFT calculations for somewhat similar accuracy renders the molecular mechanics calculations more attractive for ligand design purposes. However, the calculation of metal preferred bite angles is still useful for validation of  $\beta_n$  calculations, in particular for catalyst systems using complex or bulky counter ligands or ions. Moreover, the structures of crucial intermediates in a reaction cycle can also be modelled accurately via DFT to investigate the variation in the metal preferred bite angle during the cycle. Such calculations are beneficial since it allows the elucidation of bite angles required for the stabilisation of intermediates, which aids in the selection of the ligand for that particular application, therefore assisting in the design of more active and selective catalysts.

### 2.3 A brief review on selected diphosphorus ligands

A brief discussion on the historical development of wide bite angle diphosphorus ligands is presented in this section. Emphasis is placed on ligand design and the progression towards the xanthene backbone that led to the development of the xanthene family ligands. Owing to the large number of possible ligands, this discussion is restricted to selected representative diphosphines, **Figure 5**. These ligands were identified on the following



basis: (1) bidentate diphosphorus donors, (2) novel bridge or backbone, (c) reported complexes with transition metals, and (d) successful application in homogeneous transition metal catalysis. The common abbreviated names are given, and the ligands are arranged in order of the discussion, with the natural bite angle shown in brackets [23].

The earliest examples of diphosphorus ligands are the diphenylphosphino alkane family. The first diphosphine, 1,2-bisdiphenylphosphinoethane (dppe) **2.1**, was reported in 1959 [32]. The first derivatives of **2.1** were reported a year later [33-34], and involved modification of the phenyl substituents. The characteristic feature of this ligand family is the alkyl bridge that can be varied in length to alter the reactivity. For example, bisdiphenylphosphinomethane (dppm) **2.2** has only one bridging group that results in a small intramolecular distance between the phosphorous donors. This results in a constrained  $\beta_n$  and **2.2** therefore acts as a bridging ligand that prefers metal-metal interactions and forms dimetallic complexes. In contrast, bisdiphenylphosphinopropane (dppp) **2.3** and bisdiphenylphosphinobutane (dppb) **2.4** contain longer alkyl bridges that impart greater flexibility to the ligand. The larger  $\beta_n$  enables **2.3** and **2.4** to act as chelating ligands that can accommodate other donors as spectator ligands around the metal centre.

In the 1960's catalytic studies involving diphosphines were not extensively investigated [23]. Research at that time was focused on the application of monophosphines, for example the use of triphenylphosphine by Wilkinson in rhodium catalysed hydrogenation [35]. Diphosphines were of limited interest to researchers as catalytic screening of the archetypal diphosphine **2.1** often gave poor catalysis when compared to monophosphines in Wilkinsons reaction [36]. This poor catalysis was shown by Thorn and Hoffman [37] to be due to the 1,2-ethanediyl bridge and resulting rigid five membered ring that formed when **2.1** coordinated to the metal. The constrained P-M-P angle or small  $\beta_n$ , the effect of which was not fully understood or quantified then, significantly affected the catalysis. Unfortunately, this saddled diphosphines with a poor reputation for being slow, albeit somewhat selective catalysts. As a result, most research groups merely studied the use of diphosphines for the isolation of stable intermediates with various metals [33-34].

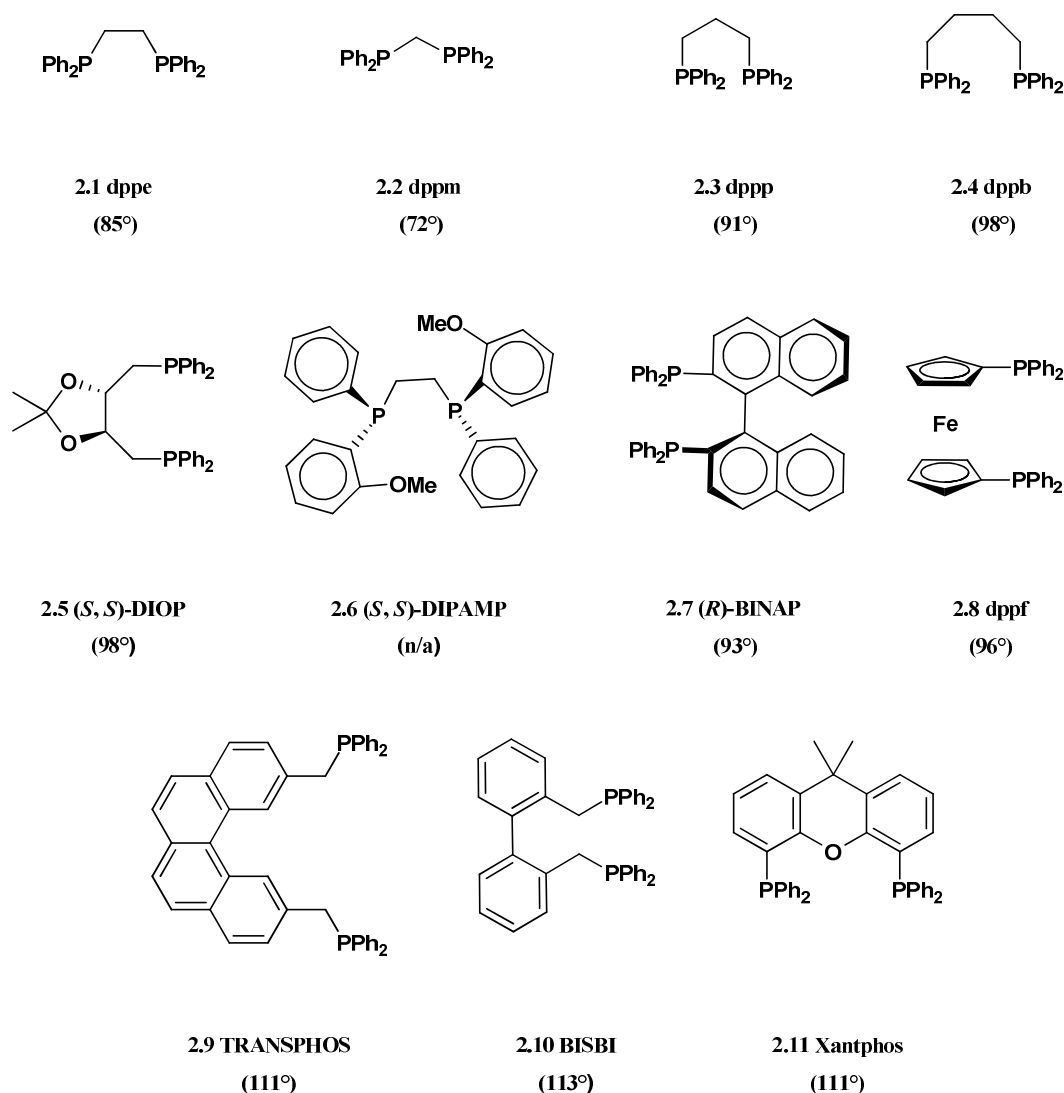


**Figure 5. Selected bidentate diphosphorus ligands.**

The first significant application of diphosphorus ligands in homogeneous catalysis was for the co-dimerisation of butadiene with ethylene for the synthesis of 1,4-hexadiene [38]. In the reported study the effect of the bridge length of selected diphosphines (e.g. **2.1**, **2.2**, and **2.3**) on the selectivity and activity was investigated. Although the reported study used different metal to ligand mole ratios for the catalytic testing, it was found that in general the catalysts exhibited increasing selectivity and reactivity in the order of increasing alkyl bridge length, i.e. **2.2** < **2.1** < **2.3**, behaviour that can now be correlated in terms of increasing  $\beta_n$ . The use of diphosphines in asymmetric catalysis did much to popularise and contribute to the catalytic development of diphosphines as a whole [39]. In 1971 Kagan and Dang [40] investigated the use of (-)-2,3-O-isopropylidene-2,3-dihydroxy-1,4-bis(diphenylphosphinobutane) (DIOP) **2.5**, in the Rh catalysed asymmetric hydrogenation of unsaturated acids. It was found that a ligand with a relatively rigid backbone was required to prevent different conformations and direct selectivity. Furthermore, the presence of a distinct ligand backbone became an important consideration since it could also introduce chirality onto the catalyst. The structure and properties of **2.5** were therefore beneficial for asymmetric catalysis, and it was found that **2.5** gave better enantioselectivity compared to

monodentate ligands [40]. In a later work, Kagan and co-workers [41] undertook a systematic study on diphosphines with bridge lengths varying from one to six carbon atoms for the Rh catalysed hydrogenation of styrene. It was found that the nature of the carbon chain linking the phosphorus donors, i.e. the backbone, greatly affected the selectivity of the catalyst.

Kagan and co-workers showed the first hint of the potential of diphosphorus ligands and paved the way for further significant studies. In particular, the work of Kagan highlighted the important role that ligand design would play in the future. The seminal work of Knowles et al. [42] involved the preparation of the  $C_2$  symmetric diphosphine DIPAMP **2.6** for the asymmetric hydrogenation of dehydroamino acids. Ligand **2.6** is considered a milestone work in the field of diphosphorus chiral ligands [39] due to the highly efficient nature of the catalyst and adoption by Monsanto for the industrial scale synthesis of the Levodopa precursor [43-44]. The author was subsequently awarded the Nobel Prize in 2001 for this research. A further significance of the reported work was that the phosphorus atoms could also be used for the enforcement of stereogenic chiral centres. This further highlights the importance of ligand design with respect to the nature of the substituents on the donor atoms.

Although Knowles and Kagan discovered practical and successful diphosphorus asymmetric hydrogenation, it was the discovery and application of 2,2'-bis(diphenylphosphino)-1,1'-binaphthyl (BINAP) **2.7** by Noyori [45-46] that significantly accelerated the development of diphosphorus ligands. Ligand **2.7** is an excellent example of a versatile, efficient, bidentate diphosphine. The starting point for the preparation of **2.7** is 1,1'-binaphthol (BINOL). The presence of the OH groups allows the possibility of different synthetic routes to **2.7**. The synthesis is therefore very versatile, evident by the more than 240 patents awarded for the preparation and application thereof [47]. Synthetic versatility is beneficial since it allows optimisation of the synthetic protocol. The synthesis of **2.7** is therefore very efficient, and is now one of the few chiral ligands produced on an industrial scale. Furthermore, synthetic versatility facilitates the investigation of modifications and alternative applications of a ligand system, evident by the numerous reported derivatives of **2.7** [47]. In comparison to ligand **2.6**, the chirality is induced by the disposition of phenyl rings of the backbone. Although first applied to Rh catalysed hydrogenation, **2.7** has proved to be a highly versatile catalyst, in particular for Ru catalysed hydrogenation of olefins and ketones [39]. Excellent catalytic results for the Ru-catalysed hydrogenation of  $\beta$ -keto esters were also reported by Noyori in 1987 [48]. The first significant industrial application of **2.7** was the commercial synthesis of menthol [49]. Derivatives of **2.7** are also used for the industrial scale synthesis of Naproxen [50], an anti-inflammatory drug. The high catalytic efficiency, excellent enantioselectivity, and versatility of ligand **2.7** earned Noyori the Nobel Prize in 2001.

The structural elucidation of ferrocene by Wilkinson [51] and working independently Fischer[52] led to the development of a new class of bidentate diphosphorus ligands containing metallocene backbones. The most significant is 1,1'-bis(diphenylphosphino)ferrocene (dppf) **2.8**, first synthesised in 1971. The cyclopentadienyl (Cp) rings of the metallocene backbone are functionalised with the diphosphorus donors. The rings are an important feature of the ligand backbone that allow different points of functionalisation. This can significantly affect the resulting geometry since the complex can assume different torsion angles to relieve the strain of coordination. As a result, **2.8** can act as either a chelating or bridging ligand, with numerous modes of

coordination reported [53], for example square planar, tetrahedral, or octahedral complexes with transition metals, **Figure 6**. This ligand family also demonstrates the importance of having a synthetically versatile backbone since it is possible to design a ligand with a specific coordination geometry to aid selectivity. Ligand **2.8** has a relatively wide bite angle ( $96^\circ$ ) that can be modified via ligand design by either changing the angle between the plane of the two Cp rings, or increasing the torsion angle along the axis of the two centroids of the Cp rings [25]. The reactivity of **2.8** is due to the ability of the flexible backbone to easily adapt to electronic or steric changes of the ligand environment during a reaction. The metallocene backbone of **2.8** is also fairly stable under most reaction conditions, and the ligand can further improve catalyst stability by also reacting to electronic environment changes. The stability and versatility of **2.8** has led to numerous reported catalytic applications [54], for example Suzuki, C-N coupling, and carbonylation reactions.

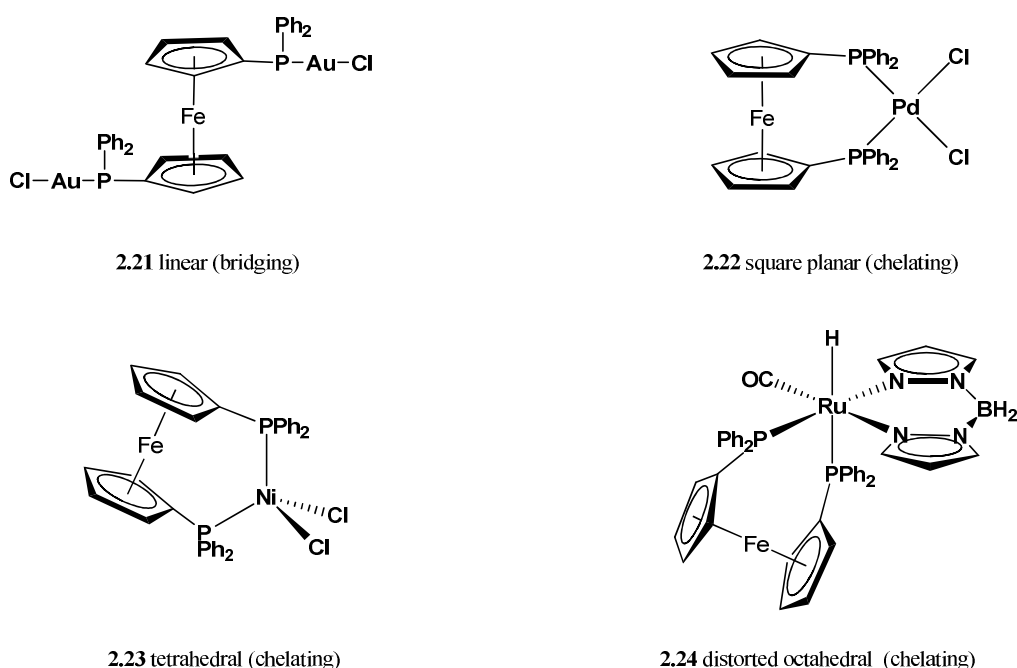


**Figure 6. Selected coordination modes of ligand 2.8.**

Bessel et al. [55] suggest that the historical development of bidentate ligands in coordination chemistry was initially for the investigation of *cis*-chelating ligands. However, *trans*-chelating ligands, although synthetically more challenging, have distinct beneficial properties, for example the enforcement of unusual metal geometries, the steric crowding or sheltering of certain ligand positions, ease of modification of the *trans*-spanning linkages or backbones, and large chelation angles [55-56]. The large chelation angles (ca  $180^\circ$ ) require a relatively large backbone to position the phosphorus donors a sufficient distance apart. Initial attempts at bidentate *trans*-spanning diphosphorus ligands involved long alkyl chain backbones that were unfortunately overly flexible and resulted in open chain polymeric structures [57-59]. In addition, the formation of *trans* complexes for these initial ligands were very dependent on reaction conditions and starting materials, with most initial attempts acting as bridging instead of chelating ligands [55,60]. Although the early *trans*-spanning complexes were able to support the formation of large chelation angles, they did not actively direct or enforce this formation. In the

mid 1970's, Venanzi et al. [61] reported the preparation of 2,11-bis(diphenylphosphinomethyl)benzo(c)phenanthrene **2.9**, the first ligand designed to successfully enforce trans coordination. It was also the first reported ligand with an unusually large bite angle (111°), and highlights the importance of a large backbone on the intramolecular P...P distance. Later named TRANSPHOS, this ligand also has a relatively rigid backbone with the aryl unit strategically functionalised with the phosphorus donors.

A comparison of catalytic results for the Rh catalysed hydroformylation of propene using some of the preceding diphosphines is presented in **Figure 7**, adapted from van Leeuwen [62]. The natural bite angle, turn over frequency (TOF), and linear to branched ratio are also presented. The diphenylphosphino alkane family ligands, in particular **2.1** and **2.3**, were reported to give poor activities and selectivities for the linear aldehyde product. In separate works, the chiral ligand **2.5** [63], and metallocene backbone ligand **2.8** [64], gave significantly greater activities (greater than an order of magnitude), yet only incrementally improved the selectivity for linear aldehyde formation.

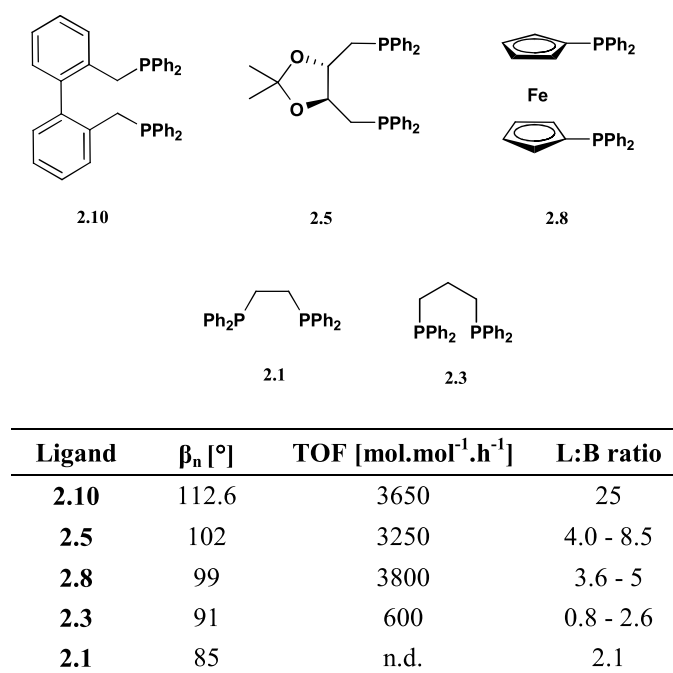


**Figure 7. Hydroformylation of propene with diphosphorus ligands, adapted from [62]. n.d. =not determined**

In 1987, Devon et al. [65] reported the use of 2,2'-bis-(diphenylphosphino)methyl-1,1'-biphenyl (BISBI) **2.10** for the same hydroformylation reaction. The application of the wide bite angle ligand **2.10** (112.6°), represented a major breakthrough in selective Rh catalysed hydroformylation. Although **2.10** gave similar reaction rates to ligands **2.5** and **2.8**, the linear to branched ratio was significantly improved (approximately three and five fold respectively), **Figure 7**.

To understand the efficacy of **2.10** and expand this success to other ligands, Casey and Whiteker developed the concept of the natural bite angle to predict chelation preferences [30]. It was postulated by Casey et al. [63] that the geometries of the intermediates in the catalytic cycle that favoured the formation of linear aldehydes possessed large bite angles. The number of possible intermediate structures could be reduced by using a chelating ligand with a known preferred bite angle in the same range, allowing the regioselectivity to be directed or manipulated. Prior to the preparation of ligands **2.8**, **2.9**, and **2.10**, most diphosphines had relatively short alkyl chain backbones that led to the formation of small chelate ring sizes and average P-M-P angles of 90° or smaller [63,66]. In the case of Rh catalysed hydroformylation, these small bite angle ligands cannot support the range of intermediate geometries which results in the observed poor regioselectivity, **Figure 7**. Casey and co-workers also correlated the increasing regioselectivity in the Rh catalysed hydroformylation of 1-hexene with a trend in increasing natural bite angle with ligands **2.1**, **2.5**, and **2.10** [63]. The trends for the hydroformylation of propene and 1-hexene are examples of a primarily steric bite angle effect where the substituents on the phosphorus donors are kept constant, and the backbone is changed, increasing the chelation angle that effectively increases the steric bulk of the ligand. Casey and co-workers had identified similar structural-activity relationships where increasing the steric bulk of monodentate ligands increased regioselectivity towards straight chain aldehydes [67], and applied this principle to the design of bidentate ligands enforcing large chelation angles near 120°.

van Leeuwen and co-workers recognised the importance of the bite angle effect on the catalytic cycle, and subsequently adopted the natural bite angle as a useful ligand design parameter [66,68-69]. At that point (ca. 1995), no detailed study on the effect of the variation of  $\beta_n$  in a series of wide bite angle ligands with similar steric size and electronic properties had been undertaken. This was due to the limitation that a homologous series of ligands, where such effects could be practically observed, did not exist [66]. van Leeuwen and co-workers therefore prepared a homologous family of ligands with the following characteristics [69]: (1) each ligand shared a similar backbone template or generic structure, (2) the identified backbone enforced wide chelation angles (ca. 109 – 120°), and (3) the identified backbone was amenable to slight alterations that would subtly alter the chelation angle without significantly affecting other properties of the ligand.

A common aromatic heterocyclic xanthene backbone was therefore investigated [69]. This ensured that all ligands in the series had negligible steric size differences. Furthermore, the xanthene backbone was relatively large in comparison to typical diphosphines. This induced a sufficiently large intramolecular P---P distance and ensured that the ligands were flexible yet still rigid, particularly in comparison to BISBI **2.10**. The generic structure of the xanthene family ligands of van Leeuwen and co-workers is presented in **Figure 8a**. Selected xanthene family ligands are presented **Figure 8b**. The parent ligand xantphos **2.11** is obtained when X = C(CH<sub>3</sub>)<sub>2</sub>, and Y = H. The remaining family ligands can be generated by altering the donor at the X position, and in the case of **2.14**, the Y position. It was shown via computational methods that modification of position X and Y did not significantly change the electronic properties of the phosphorus donors [66]. Due to the core xanthene structure, evident in all the ligands in **Figure 8b**, alteration of the backbone does not significantly alter the bite angle. The notable exception is ligand **2.19** which has a 5 membered central ring in the backbone that forces the phosphorus donors further apart. The ability to generate a homologous series of varying bite angle compounds

where the ligand steric and electronic effects are kept constant allowed the isolation and practical observation of the bite angle effect in catalytic experiments.

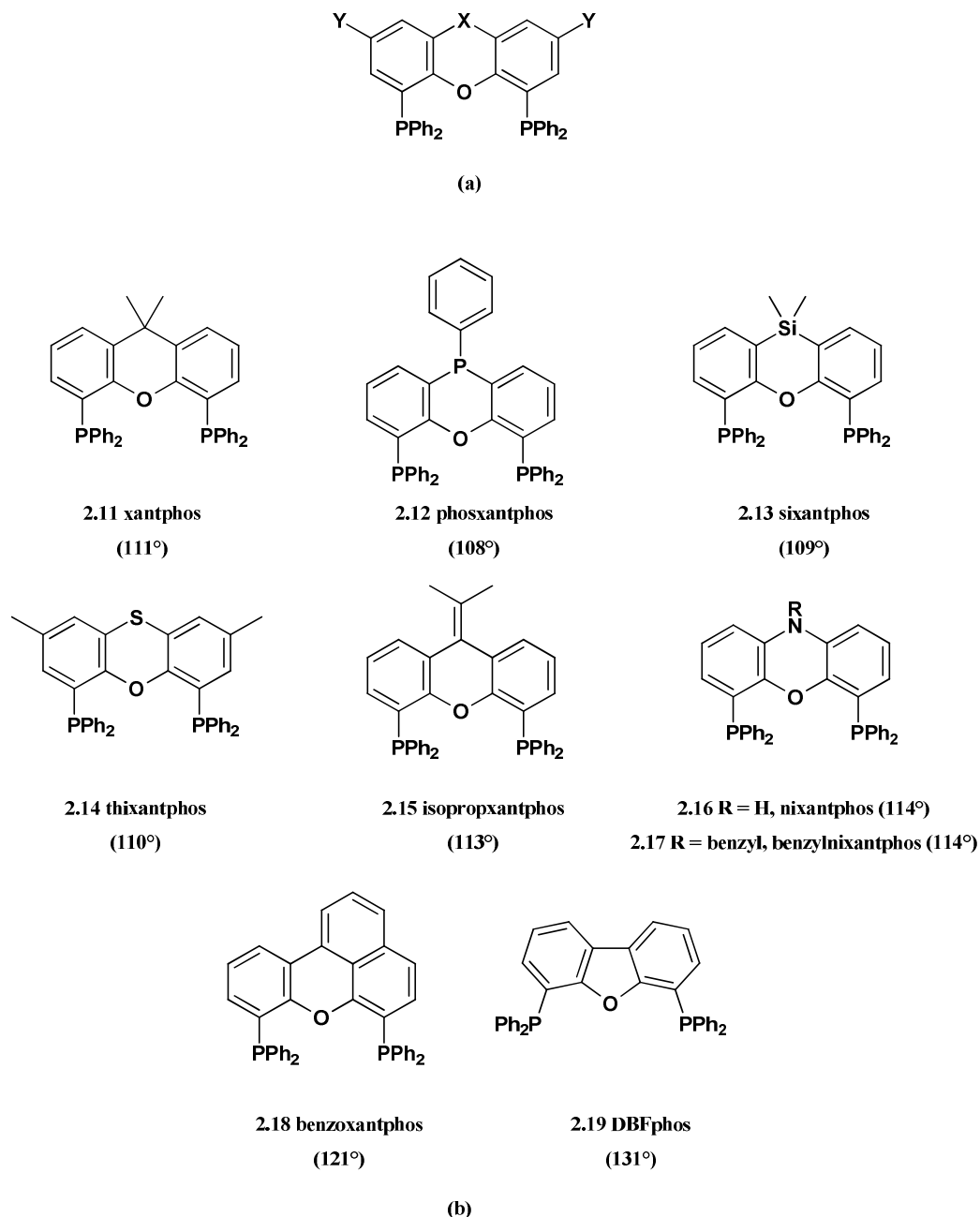


**Figure 8. (a) Generic structure of xanthene family ligands, and (b) selected xanthene family ligands.**

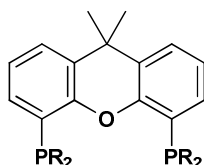
The xanthene family ligands were first applied to Rh catalysed hydroformylation reactions [69]. Initial experiments revealed that at low temperatures the xanthene family ligands, and ligand **2.11** in particular, were as effective as the previous benchmark ligand **2.10**. However, at higher temperatures the relatively more rigid xanthene backbone resulted in greater selectivity and decreased isomerisation for ligand **2.11** relative to **2.10**. Furthermore, a distinct increase in selectivity with an increasing bite angle was observed. A more extensive range of xanthene family ligands were also applied to Rh catalysed hydroformylation reactions by van Leeuwen

and co-workers [31]. For the hydroformylation of 1-octene and styrene, a correlation between increasing bite angle and selectivity was similarly observed. The bite angle was also found to effectively influence the catalytic activity for the hydroformylation of 1-octene, and to a lesser extent styrene. van Leeuwen and co-workers also applied the prepared family ligands to the Ni catalysed hydrocyanation of styrene [28]. Prior to xantphos, most diphosphorus catalysts were generally poorly activating for this reaction due to the small chelation angles (ca. 90°) which effectively retarded the rate determining step and favoured divalent species [28]. However, the application of the wide bite angle xanthene family ligands resulted in excellent conversion and regioselectivity, in particular for ligands with bite angles of ca. 110°.

Reported catalytic applications of the parent ligand **2.11** are abundant. Further examples include, but are not limited to, the Rh catalysed hydroaminomethylation of internal alkenes to linear amines [70], Pd catalysed cross-coupling of aryl thiols and aryl triflates [71], Ru catalysed C-C bond formation reactions [72], Ru catalysed alkylation of alcohols [73], and Cu catalysed conjugate reduction of  $\alpha,\beta$ -unsaturated nitriles [74]. The versatility of the xanthene backbone has also led to numerous reported derivatives of **2.11** via modification of the phosphorus moieties, **Figure 9**. However, **2.11** has also been modified at the Y position of backbone, **Figure 8a**, for example with *tert*-butyl [75], C<sub>6</sub>F<sub>13</sub>(CH<sub>2</sub>)<sub>3</sub> [76], and SO<sub>3</sub>H [77] functional groups. Derivatives of **2.11** with variation of both the phosphorus moieties and Y position of the backbone have also been reported [78]. The derivatives of **2.11** have, in turn, been applied to a variety of organic transformations for example the Pd catalysed arylation of ureas [79], Pd catalysed amine allylation [80], and the asymmetric Ni catalysed hydrocyanation of vinylarenes [81].

In comparison, catalytic studies involving the remaining family ligands and derivatives thereof are scarce. To the best of our knowledge, the only reported application of the remaining family ligands outside of the research group of van Leeuwen and co-workers involve modified nixantphos **2.16** derivatives for Pd catalysed phosphorus-carbon bond formation [82], and Rh catalysed hydroformylation [83] reactions. The work of Deprele and Montchamp [82] for the synthesis of H-phosphinic acids via P-C bond formation constitutes a novel application of a xanthene family ligand. However, the work of Ricken et al. [83] involves the preparation of a polymer supported nixantphos ligand to facilitate catalyst recovery in Rh catalysed hydroformylation – an organic transformation for which nixantphos has already been successfully applied [31]. Therefore, it can be concluded that great scope still exists for extending the range of catalytic application of the remaining family ligands and derivatives.





R	Ref.
<sup>t</sup> Bu	[71]
<i>p</i> -OMe C <sub>6</sub> H <sub>4</sub>	[79]
3,5-CF <sub>3</sub> C <sub>6</sub> H <sub>3</sub>	[79]
<i>o</i> -Me C <sub>6</sub> H <sub>4</sub>	[79]
C <sub>6</sub> F <sub>5</sub>	[79]
OE <sub>t</sub> <sub>2</sub>	[84]
3,5- <sup>t</sup> Bu-4-OMeC <sub>6</sub> H <sub>3</sub>	[84]
3,5-Me C <sub>6</sub> H <sub>3</sub>	[85]
NE <sub>t</sub> <sub>2</sub>	[86]
OAr	[86]
<i>p</i> -(CF <sub>2</sub> ) <sub>5</sub> CF <sub>3</sub> C <sub>6</sub> H <sub>4</sub>	[76]
<i>p</i> -CH <sub>2</sub> NE <sub>t</sub> <sub>2</sub> C <sub>6</sub> H <sub>4</sub>	[87]

**Figure 9. Xantphos derivatives via modification of the phosphorus moieties.**

## 2.4 References

- Gillespie, J. A.; Dodds, D. L.; Kamer, P. C. J. *Dalton Trans.* **2010**, 39, 2751-2764.
- McNaught, A. D.; Wilkinson, A. *IUPAC. Compendium of Chemical Terminology*; 2nd ed.; Blackwell Scientific Publications: Oxford, **1997**, p 1111-1112.
- McNaught, A. D.; Wilkinson, A. *IUPAC. Compendium of Chemical Terminology*; 2nd ed.; Blackwell Scientific Publications: Oxford, **1997**, p 1168-1169.
- Crabtree, R. H. *The organometallic chemistry of the transition metals*; John Wiley & Sons, Inc.: Hoboken, New Jersey, **2005**, p 41-43.
- Tolman, C. A. *J. Amer. Chem. Soc.* **1970**, 92, 2953-&.
- Tolman, C. A. *Chem. Rev.* **1977**, 77, 313-348.
- Kamer, P. C. J.; van Leeuwen, P. W. N. M.; Reek, J. N. H. *Acc. Chem. Res.* **2001**, 34, 895-904.
- Hirota, M.; Sakakibara, K.; Komatsuzaki, T.; Akai, I. *Comput. Chem.* **1991**, 15, 241-248.
- White, D.; Tavener, B. C.; Leach, P. G. L.; Coville, N. J. *J. Organomet. Chem.* **1994**, 478, 205-211.
- White, D.; Taverner, B. C.; Coville, N. J.; Wade, P. W. *J. Organomet. Chem.* **1995**, 495, 41-51.
- Brown, T. L.; Lee, K. J. *Coord. Chem. Rev.* **1993**, 128, 89-116.
- Koide, Y.; Bott, S. G.; Barron, A. R. *Organometallics* **1996**, 15, 2213-2226.
- Angermund, K.; Baumann, W.; Dinjus, E.; Fornika, R.; Görls, H.; Kessler, M.; Krüger, C.; Leitner, W.; Lutz, F. *Chem.--Eur. J.* **1997**, 3, 755-764.
- Morales-Morales, D.; Jensen, C. M. *The chemistry of pincer complexes*; Elsevier: Amsterdam, **2007**, p 2-3.
- Garnovskii, A. D.; Kharisov, B. I. *Synthetic Coordination and Organometallic Chemistry*; Marcel Dekker, Inc.: New York, **2003**, p 429.
- Reek, J. N. H.; van Leeuwen, P. W. N. M.; van der Ham, A. G. J.; de Haan, A. B. Supported catalysts: Immobilisation of Tailor-made Homogeneous Catalysis. In *Catalyst Separation, Recovery and Recycling*; Cole-Hamilton, D. J., Tooze, R. P., Eds.; Springer: Dordrecht, **2006**; Vol. 30, p 39-40.
- Freixa, Z.; van Leeuwen, P. W. N. M. *Dalton Trans.* **2003**, 1890-1901.
- Burello, E.; Rothenberg, G. *Int. J. Mol. Sci.* **2006**, 7, 375-404.
- Maldonado, A. G.; Rothenberg, G. *Chem. Soc. Rev.* **2010**, 39, 1891-1902.

- 20 van Leeuwen, P. W. N. M. *Homogeneous Catalysis: Understanding the Art*; Kluwer Academic Publishers: Dordrecht, **2004**, p 12-14.
- 21 Fey, N.; Harvey, J. N.; Lloyd-Jones, G. C.; Murray, P.; Orpen, A. G.; Osborne, R.; Purdie, M. *Organometallics* **2008**, *27*, 1372-1383.
- 22 Gensow, M.-N. B.; Freixa, Z.; van Leeuwen, P. W. N. M. *Chem. Soc. Rev.* **2009**, *38*, 1099-1118.
- 23 van Leeuwen, P. W. N. M.; Kamer, P. C. J.; Reek, J. N. H.; Dierkes, P. *Chem. Rev.* **2000**, *100*, 2741-2769.
- 24 van Leeuwen, P. W. N. M.; Kamer, P. C. J.; Reek, J. N. H. *Pure Appl. Chem.* **1999**, *71*, 1443-1452.
- 25 Dierkes, P.; van Leeuwen, P. W. N. M. *J. Chem. Soc., Dalton Trans.* **1999**, 1519-1529.
- 26 Leitner, W.; Bühl, M.; Fornika, R.; Six, C.; Baumann, W.; Dinjus, E.; Kessler, M.; Krüger, C.; Ruffinska, A. *Organometallics* **1999**, *18*, 1196-1206.
- 27 Benn, R.; Cibura, K.; Hofmann, P.; Jonas, K.; Rufinska, A. *Organometallics* **1985**, *4*, 2214-2221.
- 28 Kranenburg, M.; Kamer, P. C. J.; van Leeuwen, P. W. N. M.; Vogt, D.; Keim, W. *J. Chem. Soc. Chem. Commun.* **1995**, 2177-2178.
- 29 van Leeuwen, P. W. N. M. *Homogeneous Catalysis: Understanding the Art*; Kluwer Academic Publishers: Dordrecht, **2004**, p 139-174.
- 30 Casey, C. P.; Whiteker, G. T. *Israel. J. Chem.* **1990**, *30*, 299-304.
- 31 van der Veen, L. A.; Keeven, P. H.; Schoemaker, G. C.; Reek, J. N. H.; Kamer, P. C. J.; van Leeuwen, P. W. N. M.; Lutz, M.; Spek, A. L. *Organometallics* **2000**, *19*, 872-883.
- 32 Issleib, K.; Muller, D. W. *Chem. Ber.* **1959**, *92*, 3175.
- 33 Chatt, J.; Hart, F. A. *J. Chem. Soc.* **1960**, 1378-1389.
- 34 Hieber, W.; Freyer, W. *Chem. Ber.* **1960**, *93*, 462.
- 35 Young, J. F.; Osborn, J. A.; Jardine, F. A.; Wilkinson, G. J. *Chem. Commun.* **1965**, 131.
- 36 Cannel, L. G.; Slauch, L. H.; Mullineaux, R. D. *Chem. Abstr.* **1965**, *62*, 16054.
- 37 Thorn, D. L.; Hoffmann, R. *J. Am. Chem. Soc.* **1978**, *100*, 2079-2090.
- 38 Iwamoto, M.; Yuguchi, S. *J. Org. Chem.* **1966**, *31*, 4290-4291.
- 39 Tang, W.; Zhang, X. *Chem. Rev.* **2003**, *103*, 3029-3070.
- 40 Kagan, H. B.; Dang, T. P. *Chem. Commun.* **1971**, 481.
- 41 Poulin, J.-C.; Dang, T.-P.; Kagan, H. B. *J. Organomet. Chem.* **1975**, *84*, 87-92.
- 42 Vineyard, B. D.; Knowles, W. S.; Sabacky, M. J.; Bachman, G. L.; Weinkauff, O. J. *J. Am. Chem. Soc.* **1977**, *99*, 5946-5952.
- 43 Knowles, W. S. *J. Chem. Educ.* **1986**, *63*, 222.
- 44 Knowles, W. S.; Sabacky, M. J.; Vineyard, B. D., U.S. Patent 4,005,127, Jan. 25, 1977.
- 45 Noyori, R.; Hashiguchi, S. *Acc. Chem. Res.* **1997**, *30*, 97-102.
- 46 Knowles, W. S.; Noyori, R. *Acc. Chem. Res.* **2007**, *40*, 1238-1239.
- 47 Berthod, M.; Mignani, G.; Woodward, G.; Lemaire, M. *Chem. Rev.* **2005**, *105*, 1801-1836.
- 48 Noyori, R.; Ohkuma, T.; Kitamura, M.; Takaya, H.; Sayo, N.; Kumobayashi, H.; Akutagawa, S. *J. Am. Chem. Soc.* **1987**, *109*, 5856-5858.
- 49 Otsuka, S.; Tani, K.; Yamaga, T.; Akutagawa, S.; Kumobayashi, H.; Yagi, M., U.S. Patent 4,695,631, Sep. 22, 1987.
- 50 Harrington, P. J.; Lodewijk, E. *Org. Process Res. Dev.* **1997**, *1*, 72-76.
- 51 Wilkinson, G.; Rosenblum, M.; Whiting, M. C.; Woodward, R. B. *J. Am. Chem. Soc.* **1952**, *74*, 2125-2126.
- 52 Fischer, V. E. O.; Pfab, W. *Z. Naturforsch. B* **1952**, *7*, 377.
- 53 Togni, A.; Hayashi, T. *Ferrocenes*; VCH: New York, **1995**, p 18-26.
- 54 Stepnicka, P. *Ferrocenes : Ligands, Materials and Biomolecules*; John Wiley & Sons, Ltd: Chichester, **2008**, p 69-114.
- 55 Bessel, C. A.; Aggarwal, P.; Marschlok, A. C.; Takeuchi, K. *J. Chem. Rev.* **2001**, *101*, 1031-1066.
- 56 Freixa, Z.; van Leeuwen, P. W. N. M. *Coord. Chem. Rev.* **2008**, *252*, 1755-1786.
- 57 Issleib, K.; Hohlfield, G. Z. *Anorg. Allg. Chem.* **1961**, *312*, 169-179.
- 58 Shaw, B. L. *J. Organomet. Chem.* **1975**, *94*, 251-257.
- 59 March, F. C.; Mason, R.; Thomas, K. M.; Shaw, B. L. *J. Chem. Soc. Chem. Commun.* **1975**, 584-585.
- 60 Hill, W. E.; Minahan, D. M. A.; Taylor, J. G.; McAuliffe, C. A. *J. Am. Chem. Soc.* **1982**, *104*, 6001-6005.
- 61 Destefano, N. J.; Johnson, D. K.; Venanzi, L. M. *Angew. Chem.* **1974**, *86*, 133.
- 62 van Leeuwen, P. W. N. M. *Homogeneous Catalysis: Understanding the Art*; Kluwer Academic Publishers: Dordrecht, **2004**, p 154.
- 63 Casey, C. P.; Whiteker, G. T.; Melville, M. G.; Petrovich, L. M.; Gavney, J. A.; Powell, D. R. *J. Am. Chem. Soc.* **1992**, *114*, 5535-5543.
- 64 Unruh, J. D.; Christenson, J. R. *J. Mol. Catal.* **1982**, *14*, 19-34.

- 65 Devon, T. J.; Phillips, G. W.; Puckette, T. A.; Stavinoha, J. L.; Vanderbilt, J. J., U.S. Patent, 4,694,109, Sep. 15, 1987.
- 66 Kranenburg, M. Doctoral Dissertation, University of Amsterdam, **1995**.
- 67 Pruet, R. L.; Smith, J. A. *J. Org. Chem.* **1969**, *34*, 327-330.
- 68 Kranenburg, M.; Kamer, P. C. J.; van Leeuwen, P. W. N. M.; Vogt, D.; Keim, W. *J. Chem. Soc., Chem. Commun.* **1995**, 2177-2178.
- 69 Kranenburg, M.; Vanderburgt, Y. E. M.; Kamer, P. C. J.; van Leeuwen, P. W. N. M.; Goubitz, K.; Fraanje, J. *Organometallics* **1995**, *14*, 3081-3089.
- 70 Ahmed, M.; Bronger, R. P. J.; Jackstell, R.; Kamer, P. C. J.; van Leeuwen, P. W. N. M.; Beller, M. *Chem.--Eur. J.* **2006**, *12*, 8979-8988.
- 71 Mispelaere-Canivet, C.; Spindler, J.-F.; Perrio, S.; Beslin, P. *Tetrahedron* **2005**, *61*, 5253-5259.
- 72 Slatford, P. A.; Whittlesey, M. K.; Williams, J. M. J. *Tetrahedron Lett.* **2006**, *47*, 6787-6789.
- 73 Ledger, A. E. W.; Slatford, P. A.; Lowe, J. P.; Mahon, M. F.; Whittlesey, M. K.; Williams, J. M. J. *Dalton Trans.* **2009**, 716-722.
- 74 Kim, D.; Park, B. M.; Yun, J. S. *Chem. Commun.* **2005**, 1755-1757.
- 75 Johns, A. M.; Sakai, N.; Ridder, A.; Hartwig, J. F. *J. Am. Chem. Soc.* **2006**, *128*, 9306-9307.
- 76 Adams, D. J.; Cole-Hamilton, D. J.; Harding, D. A. J.; Hope, E. G.; Pogorzelec, P.; Stuart, A. M. *Tetrahedron* **2004**, *60*, 4079-4085.
- 77 Mul, W. P.; Ramkisoensing, K.; Kamer, P. C. J.; Reek, J. N. H.; van der Linden, A. J.; Marson, A.; Van Leeuwen, P. W. N. M. *Adv. Synth. Catal.* **2002**, *344*, 293-298.
- 78 Bronger, R. P. J.; Bermon, J. P.; Herwig, J.; Kamer, P. C. J.; van Leeuwen, P. W. N. M. *Adv. Synth. Catal.* **2004**, *346*, 789-799.
- 79 Sergeev, A. G.; Artamkina, G. A.; Beletskaya, I. P. *Tetrahedron Lett.* **2003**, *44*, 4719-4723.
- 80 Mora, G.; Deschamps, B.; van Zutphen, S.; Le Goff, X. F.; Ricard, L.; Le Floch, P. *Organometallics* **2007**, *26*, 1846-1855.
- 81 Goertz, W.; Kamer, P. C. J.; van Leeuwen, P. W. N. M.; Vogt, D. *Chem.--Eur. J.* **2001**, *7*, 1614-1618.
- 82 Deprele, S.; Montchamp, J. L. *Org. Lett.* **2004**, *6*, 3805-3808.
- 83 Ricken, S.; Osinski, P. W.; Eilbracht, P.; Haag, R. *J. Mol. Catal. A: Chem.* **2006**, *257*, 78-88.
- 84 Ito, H.; Watanabe, A.; Sawamura, M. *Org. Lett.* **2005**, *7*, 1869-1871.
- 85 Ito, H.; Saito, T.; Miyahara, T.; Zhong, C.; Sawamura, M. *Organometallics* **2009**, *28*, 4829-4840.
- 86 van der Vlugt, J.; Paulusse, J.; Zipp, E.; Tijmenssen, J.; Mills, A.; Spek, A.; Claver, C.; Vogt, D. *Eur. J. Inorg. Chem.* **2004**, *2004*, 4193-4201.
- 87 Buhling, A.; Kamer, P. C. J.; van Leeuwen, P. W. N. M.; Elgersma, J. W.; Goubitz, K.; Fraanje, J. *Organometallics* **1997**, *16*, 3027-3037.

# Chapter 3

## The preparation of bidentate xanthene family ligands and catalysts

### 3.1 Introduction and general strategy

This chapter details the synthetic strategy and protocols employed for the preparation of wide bite angle diphosphorus ligands and metal complexes. Xantphos was used as the prototype ligand to have a versatile, well designed ligand as the basis for further investigations.

The prepared bidentate compounds are well described by the generalised structure in **Figure 10**. The parent ligand xantphos is obtained when  $X = C(CH_3)_2$ ,  $Y = H$ , and  $R = Ph$ . Different donors of varying atomic size were introduced at the X position to investigate homologous ligands with subtle changes in the bite angle. The introduction of such donors contributes to electronic effects in the backbone, however the electronic environment around the phosphorus donors remains largely unaffected [1]. To minimise any adverse effects on the reactivity small variations in the bite angle was made possible by choosing donors of similar atomic size to C for example N, Si, P, or S, were investigated. For certain ligands, the C donor atom at the X position was maintained, however the functionality on the C atom was varied, for example with methyl groups.

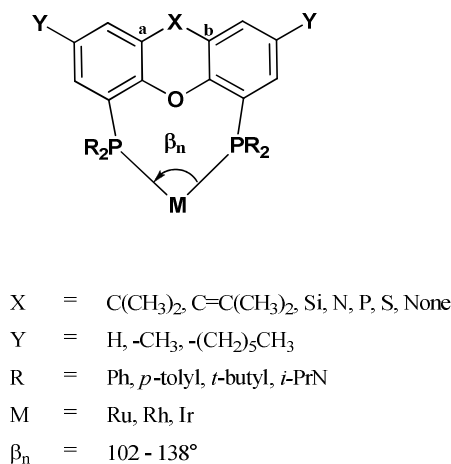


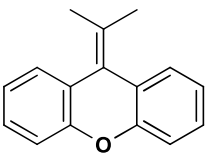
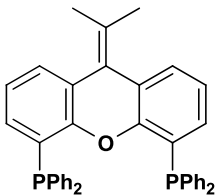
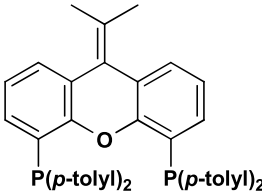
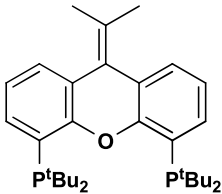
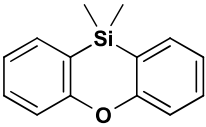
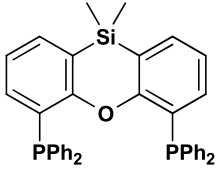
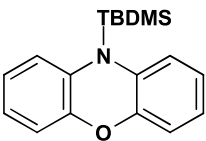
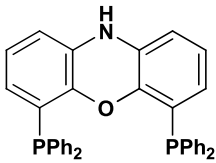
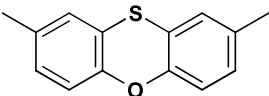
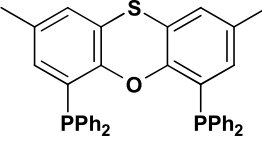
**Figure 10. Generalised structure of the prepared bidentate ligands and metal complexes.**

The substituents at the Y position were also varied to promote solubility of the ligand without significantly affecting the backbone and bite angle. However, in some cases modification of the substituent at the Y position was necessary from a synthetic point of view. For example, in the case of a sulphur donor the presence of two

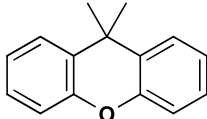
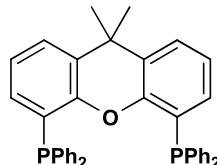
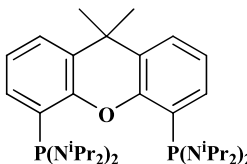
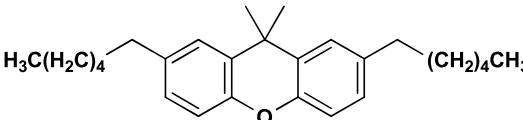
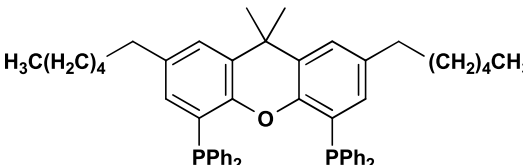
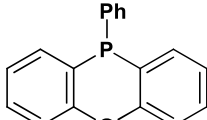
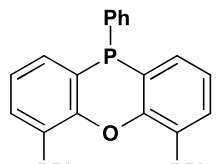
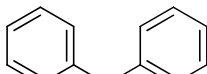
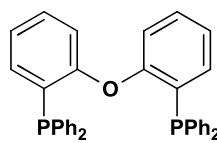
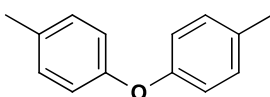
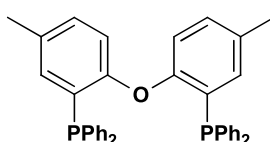
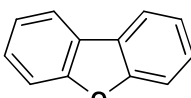
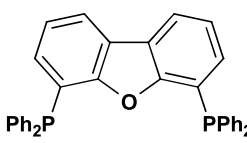
electronegative atoms, S at the X position in conjunction with the O atom of the ether linkage hinders the successful preparation of the backbone without the presence of a good electron donating group. For certain ligands, the environment around the chelating phosphorus donors was also varied to determine the effect on the bite angle and reactivity without modifying the backbone. For example, bulky *t*-butyl groups were employed to induce a steric effect at the phosphorus donors, whereas a strong electron *p*-tolyl group was used to induce an electronic effect. The general strategy for the preparation of the bidentate ligands and metal complexes involves: (1) preparation and characterisation of the backbone, (2) functionalisation of the backbone with the phosphorus moieties followed by characterisation of the ligand, (3) preparation and characterisation of the metal precursor, and (4) complexation of selected ligands followed by characterisation of the metal complex.

The preparation of xantphos and selected xanthene family ligands has been previously reported. However, literature methods were not used verbatim in this work. Reported synthetic protocols were first analysed and modified, if necessary, and in some cases new protocols were developed to facilitate good, efficient synthesis. In the context of this work, good synthesis refers to favourable yields, clean or uncontaminated products, and minimal synthetic steps. Possible modifications to reported literature methods include improved or extra purification steps, alternate heating methods, modification of reaction conditions with respect to reagents or solvents, and redesign and optimisation of the synthetic protocol with retro synthesis techniques. Suitable synthetic procedures were therefore established and attempted on a small scale, optimised on the small scale, and later extended to a larger scale. In certain instances, ancillary factors were also taken into account, for example lithiation type reactions where the extra ambient moisture or humidity on the east coast of South Africa necessitated the distillation of diphenylphosphine prior to immediate use. For this reason, TMEDA and solvents were also distilled prior to immediate use.

A summary of the prepared bidentate ligands and corresponding backbones is given in **Table 2a-b**. The constituents of the ligands, with respect to X, Y, and R from **Figure 10**, are also shown in the table. **Table 2a** and **Table 2b** serve to facilitate the presentation and discussion of the synthetic protocols in this chapter. For convenience and ease of reference, the ligands and backbones are given descriptive names in the tables that are used throughout this thesis.

Backbone	Ligand	
 <p>10-Isopropylidenexanthene</p>	 <p>Isopropxantphos</p>	<p>X = C=C(CH<sub>3</sub>)<sub>2</sub>  Y = H  R = Ph</p>
	 <p>IsopropxantTolylphos</p>	<p>X = C=C(CH<sub>3</sub>)<sub>2</sub>  Y = H  R = <i>p</i>-tolyl</p>
	 <p>IsopropxantButylphos</p>	<p>X = C=C(CH<sub>3</sub>)<sub>2</sub>  Y = H  R = <i>t</i>-butyl</p>
 <p>10,10-Dimethylphenoxasilin</p>	 <p>Sixantphos</p>	<p>X = Si  Y = H  R = Ph</p>
 <p>10-(<i>t</i>-butyltrimethylsilyl) phenoxazine</p>	 <p>Nixantphos</p>	<p>X = N  Y = H  R = Ph</p>
 <p>2,8-Dimethylphenoxathiin</p>	 <p>Thixantphos</p>	<p>X = S  Y = H  R = Ph</p>

**Table 2a.** Summary of prepared bidentate ligands and corresponding backbones. X, Y, and R refer to the ligand constituents in Figure 10.

Backbone	Ligand		
		X = C(CH <sub>3</sub> ) <sub>2</sub>	
9,9-dimethylxanthene <sup>a</sup>	Xantphos	Y = H	
		R = Ph	
		X = C(CH <sub>3</sub> ) <sub>2</sub>	
	XPNphos	Y = H	
		R = N <sup>i</sup> Pr	
		X = C(CH <sub>3</sub> ) <sub>2</sub>	
2,7-di- <i>n</i> -hexyl-9,9-dimethylxanthene	Hexantphos	Y = (CH <sub>2</sub> ) <sub>5</sub> CH <sub>3</sub>	
		R = Ph	
		X = P(Ph)	
10-phenylphenoxaphosphine	Phosxantphos	Y = H	
		R = Ph	
		X = none	
diphenyl ether <sup>a</sup>	DPEphos	Y = H	
		R = Ph	
		X = none	
di- <i>p</i> -tolyl ether <sup>a</sup>	PTEphos	Y = CH <sub>3</sub>	
		R = Ph	
		X = none	
dibenzofuran <sup>a</sup>	DBFphos	Y = H	
		R = Ph	

<sup>a</sup>Purchased from standard chemical suppliers

**Table 2b. Summary of prepared bidentate ligands and corresponding backbones. X, Y, and R refer to the ligand constituents in Figure 10.**

Characteristic	Characterisation Method/Variable
Synthetic protocol	Yield
	Number of steps
	Purification method
Appearance and properties	Colour
	Solubility
	Stability
	Differential scanning calorimetry (DSC)
Structural elucidation	NMR ( $^1\text{H}$ , $^{13}\text{C}$ , $^{13}\text{C}$ APT, $^{31}\text{P}$ , COSY, HSQC, HMBC)
	IR spectroscopy
	High resolution ESI mass spectroscopy (HRESIMS)
Purity	Melting point
	Elemental analysis (C, H, N, S)
Struture determination	X-ray crystallography
Bite angle	Natural bite angle ( $\beta_n$ )
	Metal preferred bite angle

**Table 3. Summary of employed characterisation methods.**

The prepared backbones, ligands, metal precursors, and metal complexes were characterised, where possible, by the methods in **Table 3**. Certain characterisation methods were necessarily restricted to certain compounds, for example  $^{31}\text{P}$  NMR analysis was specific to phosphorus containing backbones and ligands, and bite angle calculations were only applicable to the final ligands and metal complexes. The analysis of the synthetic protocols, as described previously, was of particular importance. The starting materials for the ligands and metal precursors (typically platinum group metals) are generally expensive, therefore highly efficient synthetic protocols are required to maximise their use. Purification methods for the reaction mixtures were also evaluated. For example, column chromatography is useful in most instances, however, the diphosphorus ligands were more easily purified by recrystallisation from suitable solvents.

The physical appearance of a reaction, viz. the colour change, was an important indicator, in particular for metal-ligand complexation reactions. Compounds were evaluated for stability by exposure to air at ambient conditions, followed by NMR analysis to determine decomposition. Solubility is especially important from a solution chemistry point of view, therefore the prepared ligands were tested for solubility in common organic solvents, and this solubility was also examined post complexation. The prepared compounds were soluble in deuterated chloroform and toluene, which facilitated both NMR analysis and variable temperature NMR studies, if required. Differential Scanning Calorimetry (DSC) has been used to study the thermal stability of selected metal complexes. The success of a particular synthesis was evaluated by structural elucidation techniques,



primarily via NMR analysis. This involved characterisation of the backbone, ligand, and metal complex with respect to certain key features.

The xanthene backbone is symmetric about the X-O axis, which results in the neighbouring aromatic protons being chemically equivalent in the NMR spectra. These chemical shifts and splitting patterns were used to elucidate the structure of the backbone. The respective aromatic carbons and fully substituted carbons were also assigned to the backbone from the  $^{13}\text{C}$  APT NMR spectra. Depending on the substituent at the X position, other indicative chemical signals were assigned in the  $^1\text{H}$  and  $^{13}\text{C}$  NMR spectra. For phosphorus containing backbones, i.e.  $\text{X} = \text{P}(\text{Ph})$  in the generalised structure in **Figure 10**, additional signals were present in the aromatic region and 2D NMR techniques were employed to correctly identify the peaks for structural analysis.  $^{31}\text{P}$  NMR analysis was also employed for the analysis of suitable backbones. In general, it was found that the  $^1\text{H}$  NMR analysis was very sensitive to the chemical environment and significant changes were observed with variation in the X donor of the backbone.

The diagnostic signals obtained for the prepared ligands were compared to those of the corresponding backbones where either an upward or downfield shift was diagnostic of successful functionalisation of the phosphorus donors. Additional coupling of the carbon atoms with the phosphorus nuclei was observed and the coupling constants were calculated and compared to literature where possible.  $^{31}\text{P}$  NMR analysis gave the chemical shift and number of different P nuclei in the sample. Both phosphorus donors were chemically equivalent in all ligands, therefore a single slightly broad signal was diagnostic of the prepared ligands. In the case of a ligand containing a third phosphorus donor in the backbone, two peaks of differing chemical shifts were present in the  $^{31}\text{P}$  NMR spectra that were assigned via comparison with the corresponding backbone. Variation of the ligand R groups affected the chemical environment of the phosphorus donors, which was also observed by  $^{31}\text{P}$  NMR analysis. Oxidation of the ligands and any phosphorus containing impurities were also detectable via  $^{31}\text{P}$  NMR analysis.

Complexation of the prepared ligands afforded the metal complexes and similar changes or additional signals were identified relative to the free ligand. 2D NMR techniques such as COSY, HSQC, and HMBC, were used to assign carbon atoms to corresponding hydrogens, as well as hydrogen-hydrogen coupling.  $^{31}\text{P}$  NMR analysis was also used to detect the presence of the free ligand to determine the success of the complexation reaction. The number, splitting, and chemical shift of the phosphorus nuclei depended on the metal precursor and the counter ligands. For example, when  $\text{M} = [\text{Ir}(\text{cod})(\text{Cl})]$  in **Figure 10**, the  $^{31}\text{P}$  NMR spectra revealed a single broad peak for the metal complex that was slightly shifted in comparison to the free ligand. For  $\text{M} = [\text{Ir}(\text{H})(\text{CO})(\text{PPh}_3)]$ , two signals were present in the  $^{31}\text{P}$  NMR spectra, assigned to the equivalent chelating phosphorus donors and triphenylphosphine counter ligand.

IR techniques were used as a complementary characteristic tool to support the NMR analysis. Strong bands, for example those of carbonyl, amine, and hydroxyl groups, were easily identifiable, and IR techniques were also used to detect oxidation of the phosphorus atoms via the strong  $\text{P}=\text{O}$  band between  $1100 - 1200\text{ cm}^{-1}$ .

The melting point determination of all compounds was undertaken and the results compared to literature where possible. Sharp melting points were indicative of a relatively clean compound, which is of particular importance for ligands and metal complexes. Elemental analysis was carried out for selected compounds and was found to be useful for detecting impurities such as solvent molecules or unreacted starting materials. Furthermore, HRESIMS analysis with an accuracy of up to 4 significant figures was performed for all novel backbones, all ligands, and all metal complexes. The isotopic patterns and molecular ion charges were compared to calculated values to give a good confirmation of compound identity.

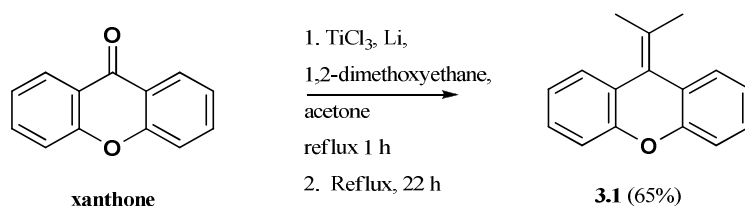
An unequivocal determination of the molecular structure can be obtained via X-ray crystallographic studies. However, the growth of single crystals suitable for X-ray analysis is often difficult and not always successful. Therefore, the analysis of *all* prepared ligands and metal complexes via this method was not possible. However, suitable single crystals were successfully grown for most prepared ligands and a limited number of metal complexes. X-ray crystallographic analysis is particularly important for determining bond lengths, bond angles, and other intramolecular information that cannot be inferred from NMR analysis. This information is useful for molecular modelling studies, for example the crystal structure coordinates of the free ligands can be used as a first approximation for the modelling of metal complexes for the calculation of metal preferred bite angles.

### 3.2 Preparation of backbones

The synthetic procedures for the preparation of the xanthene based backbones are presented in this section. The nomenclature or naming system used is based on the works of Patterson and Capell [2] that is generally used for cyclic compounds. The compounds are numbered in all presented schemes according to the first appearance in the discussion. Only compounds that have been synthesised, isolated, and characterised, are numbered. Compounds that were purchased and used as is are referred to by common names. Although this numbering system may lead to some compounds appearing in schemes out of order, the number of compounds presented in this section makes a sequential numbering system impractical. All spectral information is presented in **Appendix A**.

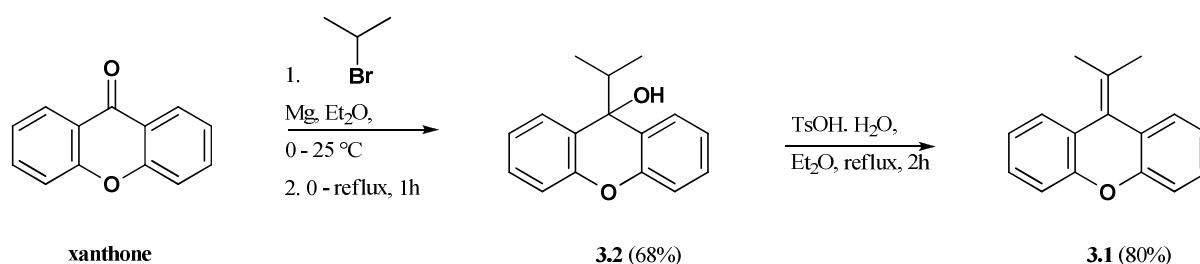
#### 3.2.1 10-Isopropylidenexanthene (3.1)

The backbone 10-isopropylidenexanthene **3.1** has the characteristic xanthene structure with an isopropylidene functionality introduced at position X of the generic structure in **Figure 10**. The reported synthesis of **3.1** involves the McMurry reaction, **Scheme 1** [3], a type of reductive coupling that occurs in two steps: (1) coupling of the ketone, and (2) dehydration to the alkene [4]. Lithium metal is usually added to reduce the titanium(III) chloride to the activated titanium(0) [5]. However, to avoid the use of titanium(III) chloride; which is expensive, required in stoichiometric amounts, usually added in large excess, hygroscopic, and reacts easily with oxygen; an alternate synthetic route was investigated.

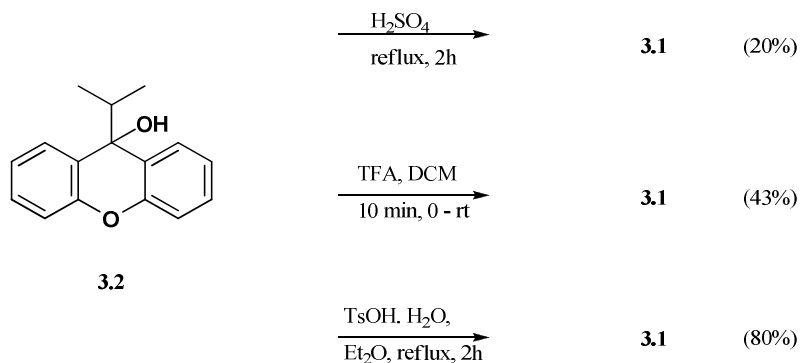


**Scheme 1. Literature route [3] to 3.1.**

The alternate synthesis for the preparation of **3.1** was adapted from literature [6-7] and involved the two step synthesis shown in **Scheme 2**. The first step involved the Grignard reaction of **3.1** followed by dehydration of **3.2**. Different dehydration agents for **3.2** were investigated, **Scheme 3**. The dehydration of **3.2** reported in Vogel's Textbook of Practical Organic Chemistry by Furniss et al. [6] uses  $\text{H}_2\text{SO}_4$  as the dehydrating agent, however poor yields were obtained due to limited solubility of the compound in the concentrated acid solution. The use of trifluoroacetic acid (TFA) was also investigated, as reported by Badejo et al. [7]. Although a two fold increase in the yield was obtained with TFA, the use of *p*-toluenesulfonic acid monohydrate ( $\text{TsOH} \cdot \text{H}_2\text{O}$ ) was also investigated, **Scheme 3**. Significantly improved yields were obtained with the latter. In addition, the latter reaction was easier to setup and work-up, and the reaction mixture was easily purified by column chromatography.



**Scheme 2. Alternate synthesis for the preparation of 3.1.**

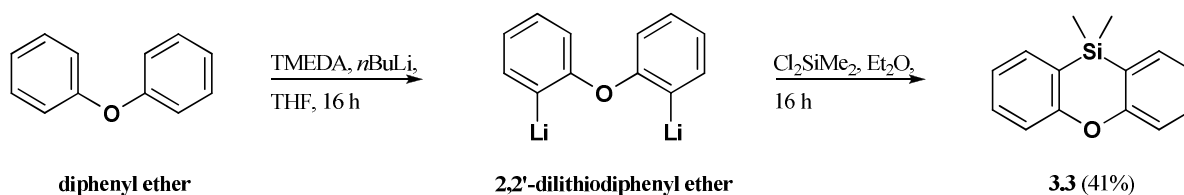


**Scheme 3. Optimisation of the acid source for the preparation of 3.1.**

### 3.2.2 10,10-Dimethylphenoxasilin (3.3)

The backbone 10,10-dimethylphenoxasilin **3.3** is analogous to 9,9-dimethylxanthene, with a Si atom replacing the C atom at the X position of the generic structure in **Figure 10**. Generally, 5-membered cyclic ring systems with a similar structure and a Si substituent are known to display ring strain tension that results in an unstable molecule, for example dibenzosiloles [8]. However, the structural properties of the ether linkage opposite the Si atom in **3.3** relieves this inherent ring strain which makes the backbone relatively more stable [9].

The synthesis of **3.3** was adapted from literature [10] with *n*-butyllithium (*n*-BuLi) substituted for *sec*-butyllithium (*sec*-BuLi) due to availability. The two step reaction is shown in **Scheme 4**. Diphenyl ether, co-evaporated with toluene to remove water, was lithiated for 16 hours under nitrogen to produce 2,2'-dilithiodiphenyl ether. The resultant solution was then reacted with a dichlorodimethylsilane solution in a separate reaction vessel for a further 16 hours to afford backbone **3.3**.

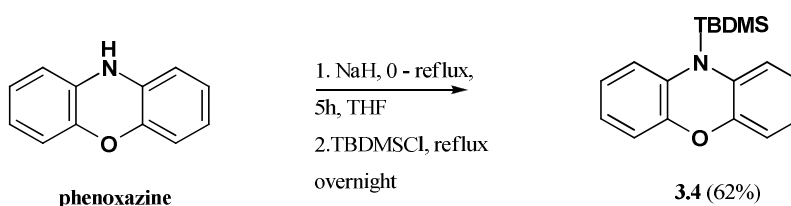


**Scheme 4. Preparation of 3.3**

The efficiency of the synthesis and yield of **3.3** depends on two main factors: (1) achieving and maintaining an inert nitrogen atmosphere throughout the synthesis, and (2) the concentrations of the reacting 2,2'-dilithiodiphenyl ether and dichlorodimethylsilane solutions. To ensure complete lithiation of the diphenyl ether backbone at room temperature the reaction was allowed to stir overnight in the presence of TMEDA. Both reactants have to be added simultaneously in dilute concentrations over a long period of time (typically 1 hour) to prevent the formation of dimeric phenoxasilin side products [8]. Care must be taken to ensure that no unwanted Si based impurities are present in the system, for example silicon grease commonly used for laboratory glassware. It is relatively difficult to meet the concentration requirements due to the solution volumes and tedious addition of each reaction mixture under the strict exclusion of oxygen and moisture. Furthermore, reported yields are generally low for this reaction (ca. 45%) [10]. The significant side products formed after hydrolysis are generally silanediols and silanols [8] that can be easily removed with activated charcoal.

### 3.2.3 10-(*t*-butyldimethylsilyl) phenoxazine (3.4)

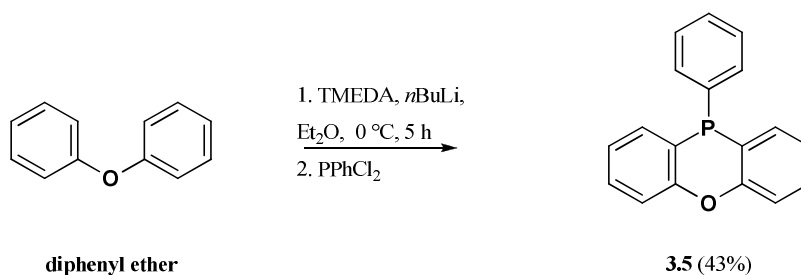
10-(*t*-butyldimethylsilyl) phenoxazine **3.4** was prepared from phenoxazine, purchased and used as is. The phenoxazine was protected following literature methods, **Scheme 5** [11], the success of which is dependent on the reaction being carried out under a strictly inert environment. The role of the protecting agent, *t*-butyldimethylsilylchloride (TBDMSCl) was to selectively protect the amine to prevent it from reacting during the lithiation of the backbone. The protection was carried out by sodium hydride induced alkylation of the amine in dry tetrahydrofuran (THF). This was followed by the addition of the TBDMSCl, using a cannula, and overnight reflux. A semi-solid oil that crystallised while standing was obtained in a 62% yield, as compared to the reported yield of 77% [11].



**Scheme 5. Protection of phenoxazine for the preparation of 3.4.**

### 3.2.4 10-Phenylphenoxaphosphine (3.5)

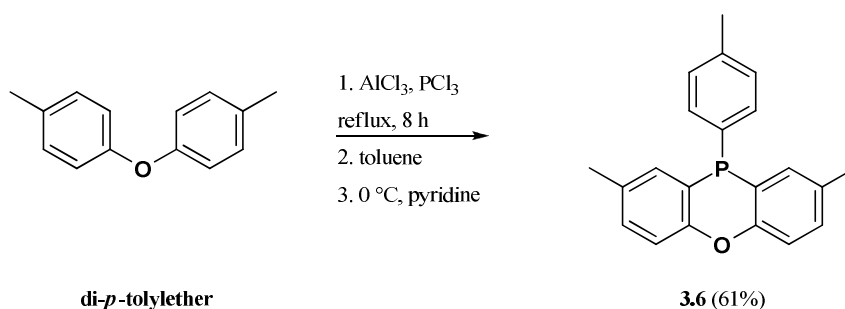
The preparation of 10-phenylphenoxaphosphine **3.5** was undertaken to investigate backbones with a non-chelating phosphorus donor. The synthesis of **3.5** was first reported in 1953 by Mann et al. [12] and involved the lithiation of 2,2'-dibromodiphenylether followed by the addition of phenyldichlorophosphine (PhPCl<sub>2</sub>) to give **3.5** in 63% yield. However, the reported multi-step synthesis is not very practical as it requires long reaction times, harsh reflux conditions, and the use of benzene as a solvent. A slightly simplified synthesis was reported in 1972 by Granoth et al. [13] and involved the lithiation of diphenyl ether, followed by the addition of PhPCl<sub>2</sub> under reflux conditions. Compared to the previous reported synthesis, significantly lower yields of 17% were reported. To the best of our knowledge, the most efficient synthesis of **3.5** was reported in 1987 in the patent literature [14] and employed *N, N, N', N'*-tetramethylethylenediamine (TMEDA) as a base, and did not require reflux. This method, **Scheme 6**, was used in this work and a yield of 43% **3.5** was obtained as compared to the reported yield of 56% [14].



**Scheme 6. Preparation of 3.5 [14].**

### 3.2.5 2,8-Dimethyl-10-*p*-tolyl-10H-phenoxaphosphine (3.6)

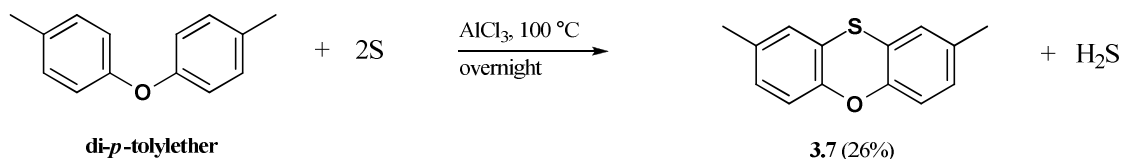
The novel compound 2,8-dimethyl-10-*p*-tolyl-10H-phenoxaphosphine **3.6** was prepared to obtain a further phosphorus containing backbone with improved yields relative to **3.5**. The synthetic procedure for **3.6** was modified from the synthesis of 2,8-dimethyl-10H-chlorophenoxaphosphine as reported by Bronger et al. [15]. Di-*p*-tolylether, aluminium chloride (AlCl<sub>3</sub>), and phosphorus trichloride (PCl<sub>3</sub>) were combined and refluxed, followed by the addition of excess toluene to the reaction mixture, **Scheme 7**. This resulted in the in situ alkylation of the intermediate phosphorus heterocycle with toluene. Compound **3.6** was obtained in 61% yield and X-ray quality crystals were grown from a 2-propanol/dichloromethane (1/1, v/v) solution [16].



**Scheme 7. Preparation of 3.6 [16].**

### 3.2.6 2,8-Dimethylphenoxathiin (3.7)

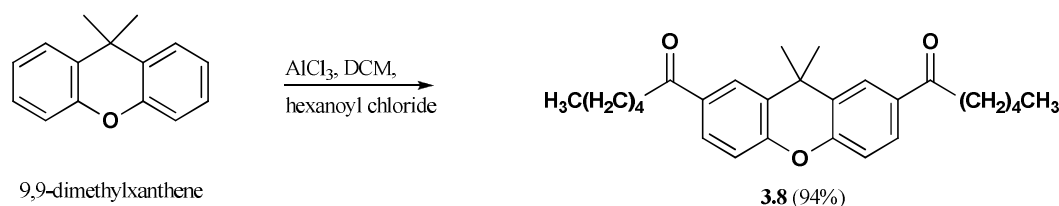
The synthesis of 2,8-dimethylphenoxathiin **3.7** was first reported by Al-Hiari et al. [17] and is commonly referred to as a Ferrario reaction [18]. This preparation involves the heating of excess di-*p*-tolylether in the presence of sulphur and AlCl<sub>3</sub> to give **3.7**, **Scheme 8**. Initially, the reaction was carried out on a relatively small scale (1 g di-*p*-tolylether) which proved unsuccessful and resulted in black tar-like reaction mixtures. It has been reported by Suter et al. [19] that Ferrario type reactions should be carried out on a relatively large scale with excess starting material to ensure good yields. This is a consequence of the neat or solvent free reaction where the excess starting material melts and forms the reaction medium [19]. Therefore, the synthesis of **3.7** was attempted on a larger scale (10 g di-*p*-tolylether) in a well vented fumehood as the reaction generates a considerable amount of heat with the evolution of hydrogen sulphide. A yield of 26% **3.7** was obtained, as compared to a reported yield of 35% obtained with 55 g starting material [17]. The product and unreacted di-*p*-tolyl ether could not be purified by column chromatography due to similar retention times and co-elution. The product was therefore purified by high vacuum distillation in a micro distillation apparatus.



**Scheme 8. Preparation of 3.7 [17].**

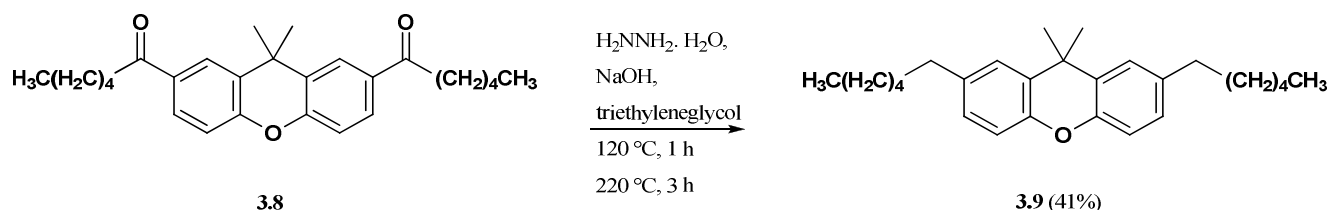
### 3.2.7 2,7-di-*n*-hexyl-9,9-dimethylxanthene (3.9)

The preparation of wide bite angle ligands similar to xantphos, but with improved solubility characteristics, was of interest to this work. The proposed synthetic strategy [20] involved functionalisation of 9,9-dimethylxanthene with a sufficiently long alkyl chain at the Y position of the backbone (with respect to the generalised structure in **Figure 10**) to improve solubility in organic and supercritical solvents. Bronger et al. [15] reported the preparation of similar phenoxaphosphino-modified xantphos type ligands with alkyl chains of six, eight, and ten carbon atoms in length. It was concluded that as the chain length increases, the solubility of these ligands increases, however, the increase in solubility plateaus, with the six carbon chain length ligand found to be optimum in terms of solubility and synthetic considerations, such as product yield and purification. The synthesis of 2,7-di-*n*-hexyl-9,9-dimethylxanthene **3.9** was therefore adapted from the work of Bronger et al. [15] with a modification to the heating method to further improve product yields. This synthesis involves the preparation of the precursor 2,7-di-*n*-hexanoyl-9,9-dimethylxanthene **3.8**, **Scheme 9**. The starting material 9,9-dimethylxanthene undergoes selective electrophilic aromatic substitution using hexanoyl chloride under standard Friedel-Crafts acylation reaction conditions. A yield of 94% **3.8** was obtained in the first step, which compared favourably to the literature value of 96 % [15].

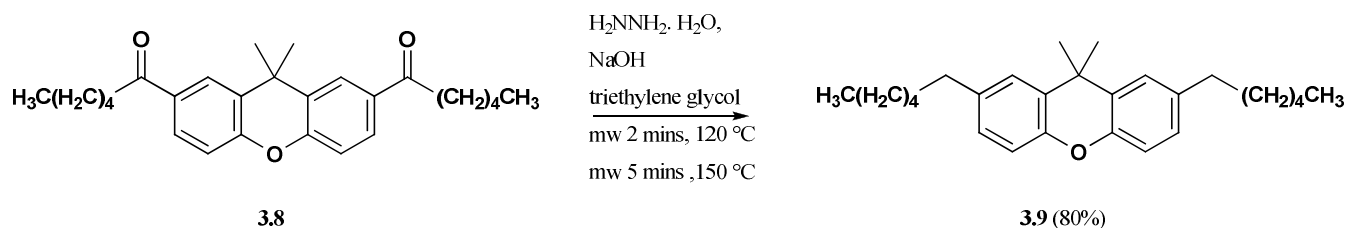


**Scheme 9. Preparation of precursor 3.8 [15].**

The ketone precursor **3.8** then undergoes the Huang-Minlon modified Wolf-Kischner reduction [21], **Scheme 10**. Following the method of Bronger et al. that employed conventional heating and ramping of the temperature to a maximum of 220 °C in an oil bath, a yield of 41% **3.9** was obtained that exactly matched literature. It was postulated that an alternate heating method that could supply large amounts of energy in a short period time, for example microwave irradiation, would suit the temperature requirements of the modified Wolf-Kischner reduction. The reduction was therefore carried out in a specialised laboratory microwave, **Scheme 11**, that resulted in significantly shorter reaction times and an almost two fold increase in yield.



**Scheme 10. Preparation of 3.9 via conventional heating [15].**



**Scheme 11. Preparation of 3.9 via microwave assisted heating.**

### 3.3 Preparation of ligands

The active sites of the prepared backbones underwent metalation reactions to facilitate the addition of the chelating phosphorus donors. These reactions generally work by the abstraction of the acidic protons at an active site, followed by selective lithiation. The prototype lithiation reaction was first reported by Schlenk and Holtz [22] who also developed and pioneered the use of Schlenk tube techniques for this application. Although most starting materials have more than one active site (acidic proton), regiospecific lithiation at the position *ortho* to the ether bridge has been previously reported for phenoxazine [9,23] and xanthene [24] backbones due to the directing effects of the oxygen. This selective lithiation directs the electrophilic attack by the phosphorus source which favours the functionalisation of the backbone with the phosphorus donors.

The success of the lithiation reaction is dependent on the solvent, temperature, and establishment and regulation of an inert atmosphere at all times. For this work, diethyl ether solvent was used since the organolithium sources, *n*-butyllithium and phenyllithium, are relatively stable in this solvent [25]. The reactivity of the organolithium compound can be dramatically improved by the addition of a Lewis base, in this work TMEDA. The Lewis base, and in some cases the solvent, affects the coordination sphere of the lithium and prevents the formation of oligomeric structures which can cause the organolithium structure to be highly compact and less reactive [22]. The TMEDA base promotes de-aggregation which yields smaller structures, for example dimers and monomers, that are known to increase the reactivity of the organolithium compounds [26].

An electrophilic  $\text{PR}_2\text{Cl}$  group was used to attack the dilithiated positions. The  $\text{PR}_2\text{Cl}$  solution was handled under the strict exclusion of air to prevent the rapid oxidation of the phosphorus source. The TMEDA base and  $\text{PR}_2\text{Cl}$  were freshly distilled and stored under argon. The required volumes were withdrawn via a syringe under a balloon of argon gas and the septum carefully sealed. Depending on the backbone and phosphorus source, low temperatures were maintained, or additional reflux was employed to increase the temperature to push the reaction to completion. Although long reaction times were generally required, the preparation of the ligand could be completed as a one pot synthesis with satisfactory yields. Furthermore, all ligands were stable in air which allowed reaction work up under non inert conditions. However, they are stored under Ar once dried under vacuum. The crude reaction mixtures were thereafter washed with hexane to remove any *n*-butyldiphenylphosphine impurities, and column chromatography was not required in most instances. The ligands were thereafter purified by recrystallisation with DCM/EtOH (1/1, v/v).

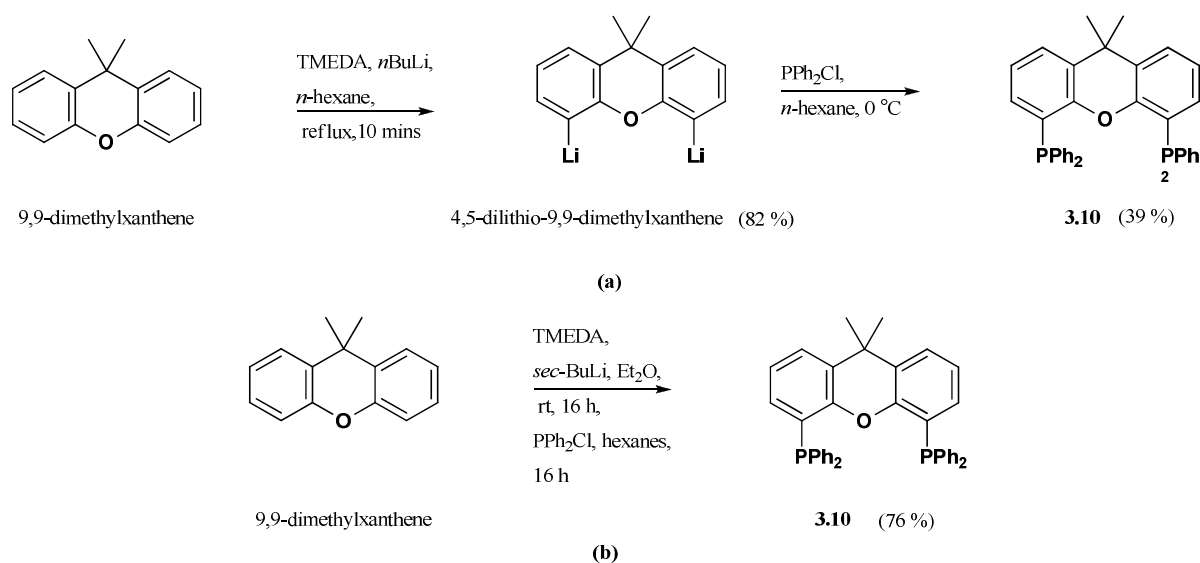


### 3.3.1 Xanthene family ligands prepared with a common procedure

The bidentate ligands in **Figure 11** were prepared from a common procedure adapted from literature [3,10]. The backbone, ligand numbering, and product yield are also indicated in **Figure 11**. The lithiation reaction was performed at 0 °C with 2.6 equivalents of *n*BuLi/TMEDA in ether. This synthesis requires the dropwise addition of *n*BuLi under a strict inert atmosphere to a chilled solution containing the backbone and TMEDA solution. The PR<sub>2</sub>Cl reagent (2.6 equivalents in hexane) was then added dropwise to the solution, during which time discolouration occurred, followed by precipitate formation.

#### 3.3.1.1 Xantphos (3.10)

The preparation of xantphos **3.10** was first reported by Hillebrand et al. [24], **Scheme 12a**. Following the synthesis of 1,8-bis(diphenylphosphino)anthracene [27], these researchers investigated analogous heteroarenes as rigid backbones for the preparation of novel diphosphorus ligands. The backbone was lithiated to give the intermediate 4,5-dilithio-9,9-dimethylxanthene, **Scheme 12a**, followed by functionalisation with the diphenylphosphine moiety to give **3.10** as colourless crystals in 39% yield. The intermediate compound was isolated and characterised by deuterium labelling to confirm regiospecific lithiation *ortho* to the ether linkage. Working concurrently, van Leeuwen and co-workers [10] developed the one pot synthesis of **3.10**, **Scheme 12b**. The backbone was added to the reaction vessel, followed by the addition of the relatively more reactive *sec*-BuLi and TMEDA, both in 3 mol equivalents at room temperature and thereafter 3 mol equivalents of the phosphorus source to afford **3.10** in 76% yield. *sec*-BuLi is more basic than *n*-BuLi and is therefore considered more reactive. Once the seal is pierced for a new bottle of *sec*-BuLi white LiOH precipitate formation occurs much sooner than for *n*-BuLi. In these instances *n*-BuLi is a more feasible to use in the laboratory. Both research groups independently reported the X-ray crystal structure of **3.10**. For this study, ligand **3.10** was prepared following the method of van Leeuwen and co-workers, with *n*-BuLi as the lithiation source, **Figure 11** [3].



**Scheme 12.** Reported routes to **3.10**: (a) Hillebrand et al. [24], and (b) van Leeuwen [10].

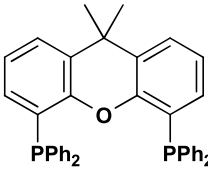
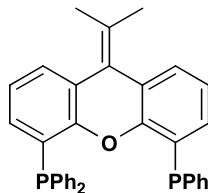
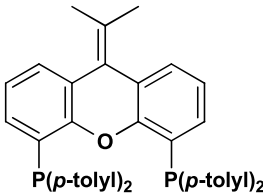
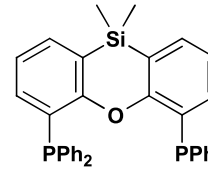
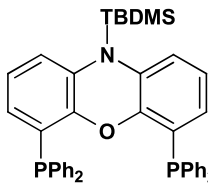
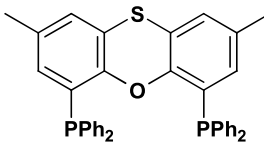
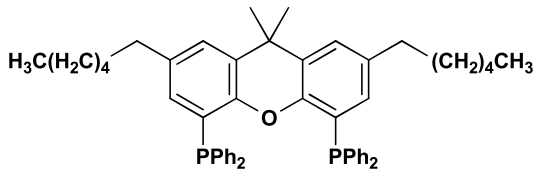
$  \begin{array}{c}  \text{Y} \text{---} \text{C}_6\text{H}_3 \text{---} \text{X} \text{---} \text{C}_6\text{H}_3 \text{---} \text{Y} \\  \text{O} \\  \text{1. TMEDA, } n\text{BuLi,} \\  \text{Et}_2\text{O, } 0^\circ\text{C, 16 h} \\  \text{2. PR}_2\text{Cl, hexane} \\  \text{-0}^\circ\text{C, 16 h}  \end{array}  \longrightarrow  \begin{array}{c}  \text{Y} \text{---} \text{C}_6\text{H}_3 \text{---} \text{X} \text{---} \text{C}_6\text{H}_3 \text{---} \text{Y} \\  \text{O} \\  \text{PR}_2 \quad \text{PR}_2  \end{array}  $		
Backbone	Ligand	Yield (%)
9,9-dimethylxanthene	 <p>           X = C(CH<sub>3</sub>)<sub>2</sub>            Y = H            R = Ph         </p>	58
3.1	 <p>           X = C=C(CH<sub>3</sub>)<sub>2</sub>            Y = H            R = Ph         </p>	52
3.1	 <p>           X = C=C(CH<sub>3</sub>)<sub>2</sub>            Y = H            R = <i>p</i>-tolyl         </p>	50
3.3	 <p>           X = Si            Y = H            R = Ph         </p>	43
3.4	 <p>           X = N            Y = H            R = Ph         </p>	70
3.7	 <p>           X = S            Y = H            R = Ph         </p>	62
3.9	 <p>           X = C(CH<sub>3</sub>)<sub>2</sub>            Y = (CH<sub>2</sub>)<sub>5</sub>CH<sub>3</sub>            R = Ph         </p>	56

Figure 11. Xanthene family ligands prepared with a common procedure. X, Y, and R refers to the ligand constituents in Figure 10.

### 3.3.1.2 Isopropxantphos (3.11)

Isopropxantphos **3.11** was prepared from backbone **3.1**, with  $X = C=C(CH_3)_2$ , and  $R = Ph$  with respect to the generalised structure in **Figure 10**. Ligand **3.11** has been previously applied to the hydroformylation of 1-octene and styrene with favourable selectivity and activities comparable to xantphos [3]. In 9,9-dimethylxanthene based ligands, inversion of the backbone around the C-O axis has been observed for the free ligand and metal complex [28-30]. Ligand **3.11** is of interest in a comparative study of xantphos type ligands as the isopropylidene linkage is postulated to promote backbone rigidity. This could possibly restrict or limit this inversion which can affect the selectivity and activity by preventing the formation of geometrical isomers, and also affect the catalyst stability. A yield of 52% of off-white crystals was obtained for **3.11**, as compared to the reported yield of 62% [3]. A good quality single crystal were grown by slow diffusion of EtOH into a dichloromethane solution of the ligand DCM/EtOH (1/1, v/v).

### 3.3.1.3 IsopropxantTolylphos (3.12)

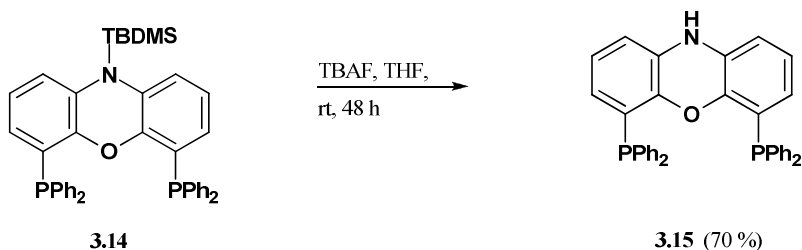
Backbone **3.1** was also used for the preparation of the novel compound isopropxantTolylphos **3.12**, an analogue of ligand **3.11** with the electronic environment of the phosphorus donors modified. Isopropxanthos type ligands with similar modifications on the phosphorus donors have previously shown good results for hydroformylation [31] and hydroaminomethylation applications [32]. A strong electron donating group ( $R = p$ -tolyl via a chlorodi- $p$ -tolylphosphine reagent) was employed, with the phenyl groups of the phosphorus atoms functionalised at the *para* position to minimise steric effects. Ligand **3.12** was obtained as yellow micro-crystals in 50% yield. **3.12** is a novel ligand, therefore no comparison with literature can be made, however yields for similar xantphos type ligands modified at the *para* position have been reported as ca. 46% [33]. A good quality single crystal were grown by slow diffusion of EtOH into a dichloromethane solution of the ligand DCM/EtOH (1/1, v/v).

### 3.3.1.4 Sixantphos (3.13)

Sixantphos **3.13** was prepared from backbone **3.3**, with a good  $\sigma$  donor at the X position of the backbone, i.e.  $X = Si$  with respect to the generalised structure in **Figure 10**. Relative to the parent ligand **3.10**, ligand **3.13** has a smaller natural bite angle of  $108.5^\circ$ , and is more effective at stabilising smaller bite angle geometries. For example, **3.13** has been reported to give significantly better yields and selectivities relative to **3.10** for the Ni catalysed hydrocyanation of styrene due to its ability to stabilise square planar Ni complexes [34]. **3.13** was obtained as white crystals in a low yield of 43% as compared to the literature yield of 68% [10]. A possible reason for the low yield could be the use of *n*-BuLi instead of the more reactive *sec*-BuLi as reported in literature. A good quality single crystal were grown by slow diffusion of EtOH into a dichloromethane solution of the ligand DCM/EtOH (1/1, v/v).

### 3.3.1.5 Nixantphos (3.15)

Nixantphos **3.15** was prepared from compound **3.4** in two steps. Backbone **3.4** was first functionalised with the phosphorus donors to give the precursor ligand **3.14**, **Figure 11**, with the N donor protected with the silyl moiety. The protecting group was removed by the addition of tetra-*n*-butylammonium fluoride (TBAF) to a solution of purified **3.14** in dry THF, **Scheme 13**, for a period of two days. Ligand **3.15** has been used with relative success for the regioselective hydroformylation of 1-octene to nonanal [3]. Moreover, ligand **3.15** has also been used in supported catalysis applications, **Figure 12**, where it has been anchored onto: (a) silica by functionalisation of the amine with a propyltrimethoxysilane linker [35], (b) polystyrene via an amide linker [36], and (c) a hyperbranched dendritic polyglycerol through various activated linkers [37]. The success of the modification of **3.15** with various linkers at the amine suggests that **3.15** is an interesting candidate for the investigation of tridentate ligands, (see Chapter 7). Ligand **3.15** was obtained as a pale yellow solid in 70% yield, which compared favourably to the literature value of 76% [3]. A good quality single crystal were grown by slow diffusion of EtOH into a dichloromethane solution of the ligand DCM/EtOH (1/1, v/v).



**Scheme 13.** Deprotection of the precursor ligand **3.14** to **3.15**.

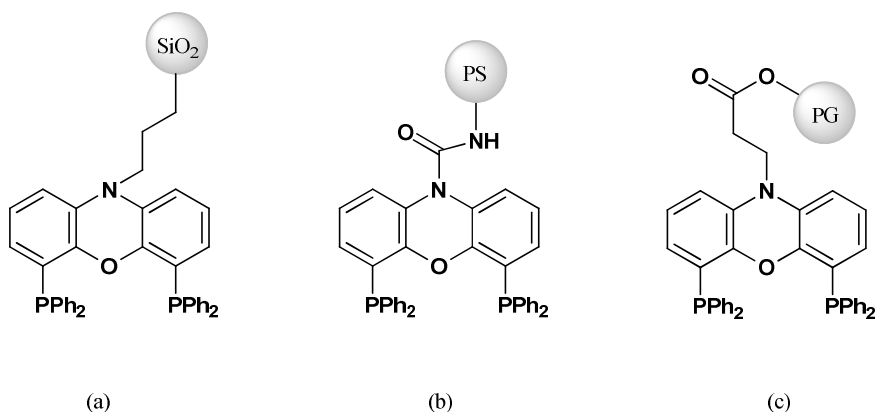


**Figure 12.** Application of **3.15** in supported catalysis via functionalisation with suitable linker: (a) silica support [35], (b) polystyrene support [36], and (c) polyglycerol dendritic support [37].

### 3.3.1.6 Thixantphos (3.16)

Thixantphos **3.16** was prepared from backbone **3.7**, with  $X = S$ , and  $Y = CH_3$  with respect to the generalised structure in **Figure 10**. To the best of our knowledge, there are no reports of S donor xantphos ligands without modification at the Y position of the backbone [1,3,28,38], however similar S donor ligands have been reported with modification of the  $PR_2$  groups [33,39]. It is postulated that the methyl group is required at the Y position to ensure selective dilithiation of the positions *ortho* to the ether linker as the presence of two strong electron withdrawing atoms (S, O) results in competing directing effects. Ligand **3.16** has been used for hydroformylation studies [10], asymmetric nickel catalysed hydrocyanation of vinyl arenes [28], and nickel catalysed hydrocyanation of styrene [28]. **3.16** was prepared as colourless fine crystals in 62% yield as compared to the reported yield of 71% [10]. A good quality single crystal were grown by slow diffusion of EtOH into a dichloromethane solution of the ligand DCM/EtOH (1/1, v/v).

### 3.3.1.7 Hexantphos (3.17)

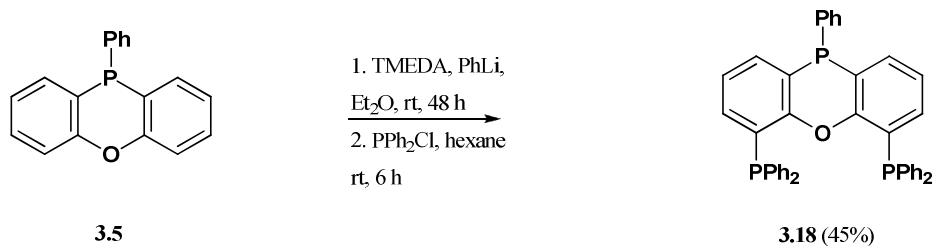
The novel ligand hexantphos **3.17** was prepared from backbone **3.9** as a xantphos analogue with enhanced solubility. The carbon donor at position X was retained to minimise changes in the bite angle, and  $R = PPh_2$  was also retained to prevent electronic and steric variations at the phosphorus donors. A flexible alkyl group was employed at the Y position of the backbone, i.e.  $Y = (CH_2)_5CH_3$ . Ligand **3.17** was obtained in 56% yield as white crystals. Bronger et al. [15] reported yields of ca. 54% for similar phenoxaphosphino-modified xantphos type ligands. A good quality single crystal were grown by slow diffusion of EtOH into a dichloromethane solution of the ligand DCM/EtOH (1/1, v/v).

## 3.3.2 Xanthene family ligands prepared with separate procedures

### 3.3.2.1 Phosxantphos (3.18)

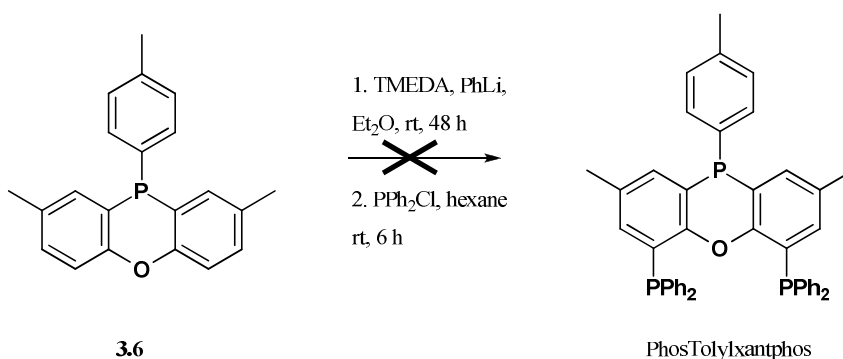
Phosxantphos **3.18** was prepared from compound **3.5** and incorporates a third non-chelating phosphorus donor in the xanthene backbone. The procedure for the functionalisation of the backbone was necessarily modified from the method discussed above. It has been previously reported [3,40] that *n*-BuLi attacks the phosphorus atom of the backbone resulting in an exchange of the phenyl and butyl groups. To negate this nucleophilic substitution, van Leeuwen and co-workers reported the use of phenyllithium [3],

**Scheme 14.** However, the use of this less reactive lithium source requires significantly longer reflux times for the lithiation reaction (48 hours). The phenyllithium was synthesised [41] prior to use to prevent oxidation, and the reaction was carried out under a strict inert atmosphere. Ligand **3.18** was obtained as off-white crystals in 45% yield as compared to the literature yield of 62% [3].



**Scheme 14. Preparation of 3.18 adapted from literature [3].**

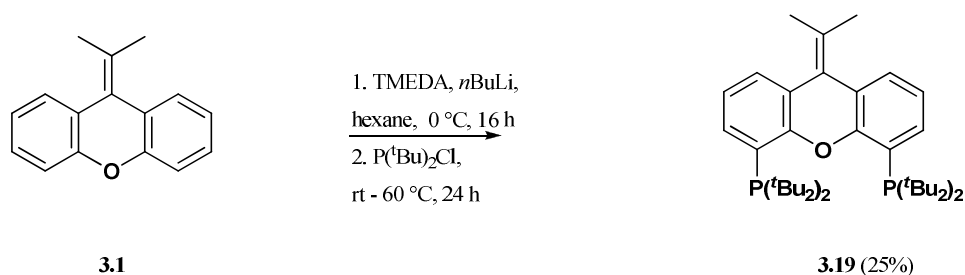
The preparation of a second ligand containing a third non-chelating phosphorus atom was unsuccessfully attempted, **Scheme 15**. The proposed ligand, phosTolylxantphos, is analogous to **3.18** with the electronic environment of the backbone (Y position), and the X donor functionality modified with electron donating methyl groups. The proposed ligand was synthesised from backbone **3.6**, however isolation of the crude product was not possible and analysis of the  $^{31}\text{P}$  NMR spectra revealed the presence of a mixture of different phosphorus containing molecules. Further analysis via LC-MS using both Electron Spray Ionisation (ESI) and API source gave no detectable mass corresponding to the desired compound. Attempts to recrystallise any material from the reaction mixture were also unsuccessful. It is postulated that the phenyllithium reagent was unable to activate the precursor compound **3.6**.



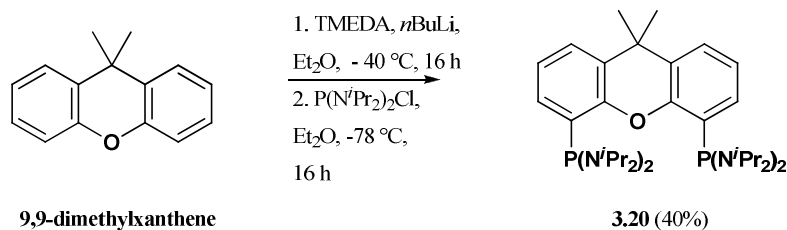
**Scheme 15. Attempted synthesis of phosTolylxantphos.**

### 3.3.2.2 IsopropxantButylphos (3.19)

The novel ligand isopropxantButylphos **3.19** is analogous to the previously prepared compounds **3.11** and **3.12**. The synthesis of **3.19** was adapted from literature [42], **Scheme 16**. The electronic environment of the phosphorus moieties of **3.12** were modified relative to **3.11**. As a contrasting study, the steric environment of the phosphorus moieties of **3.19** was modified by the addition of bulky *t*-butyl groups. Ligand **3.19** was obtained in 25% yield. In general, the preparation of xantphos type ligands that are similarly sterically bulky involve relatively low yields, for example the yield for the xantphos analogue of **3.19**, (bis-(*t*-butyl-phosphino)-9,9-dimethylxanthene has been reported as 38% [42].



**Scheme 16. Preparation of 3.19 adapted from literature [42].**



### 3.3.3.1 DPEphos (3.21)

DPEphos **3.21** was prepared from the readily available backbone diphenyl ether according to literature methods, **Figure 13** [10]. Ligand **3.21** has a calculated natural bite angle of 102°, larger than average bite angles for typical diphosphines (ca. 90°), but smaller than typical xantphos family ligands (108 – 114°). **3.21** has been extensively applied in homogeneous catalysis, for example in a variety of C-N, C-C, C-O, and C-S bond formation reactions [45]. The prepared compound was obtained as white air stable crystals in 69% yield, as compared to reported yields of 83% [10].

### 3.3.3.2 PTEphos (3.22)

PTEphos **3.22** was prepared as an analogue of **3.21** with modification of the electronic environment of the backbone by the introduction of a methyl group at the Y position. Ligand **3.22** was synthesized from the commercially available di-*p*-tolyl-ether backbone, **Figure 13**. To the best of our knowledge, a recent publication by Zuidema et al. [40] is the only instance where ligand **3.22** has been reported. However, only catalytic testing results for hydroformylation studies have been reported, and the synthesis and characterisation of **3.22** omitted. In this work, ligand **3.22** was obtained as white crystals in 67% yield. A good quality single crystal were grown by slow diffusion of EtOH into a dichloromethane solution of the ligand DCM/EtOH (1/1, v/v).

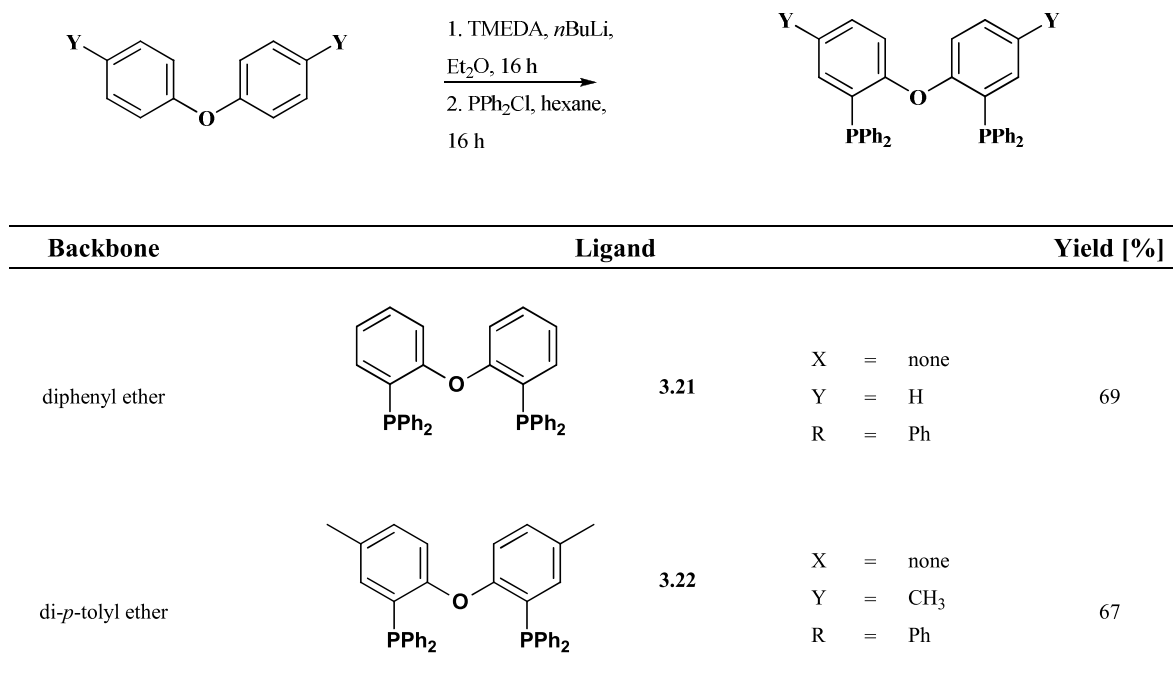
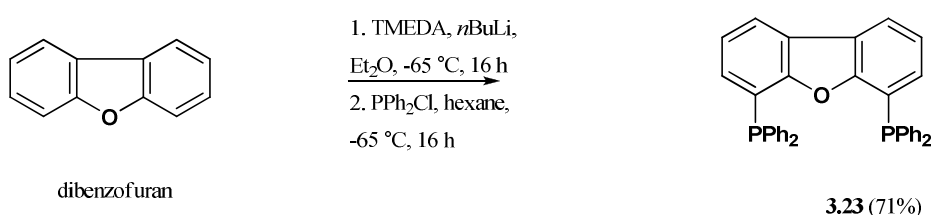


**Figure 13.** Preparation of **3.21** and **3.22**, adapted from literature [10]. X, Y, and R refers to the ligand constituents in Figure 10.



### 3.3.3.3 DBFphos (3.23)

The preparation of DBFphos **3.23** allows the investigation of a ligand with a natural bite angle ( $131.1^\circ$ ) larger than most xantphos family ligands. Ligand **3.23** contains a 5 membered central ring. However, the oxygen atom of the ether bridge possesses two lone pairs of electrons that could possibly result in weak orthometalation upon complexation. Ligand **3.23** was prepared from the commercially available dibenzofuran. The lithiation of dibenzofuran has been previously reported by Gilman and Gorsich [46], however functionalisation with the chelating phosphorus donors was first reported by Haenel et al. [27], with **3.23** obtained in 50% yield. A modified synthesis with improved yields was later reported by van Leeuwen and co-workers [10], and was adapted for this work, **Scheme 18**. Ligand **3.23** was obtained as white crystals in 71% yield as compared to the reported literature yield of 81%.



**Scheme 18.** Preparation of **3.23** adapted from literature [10].

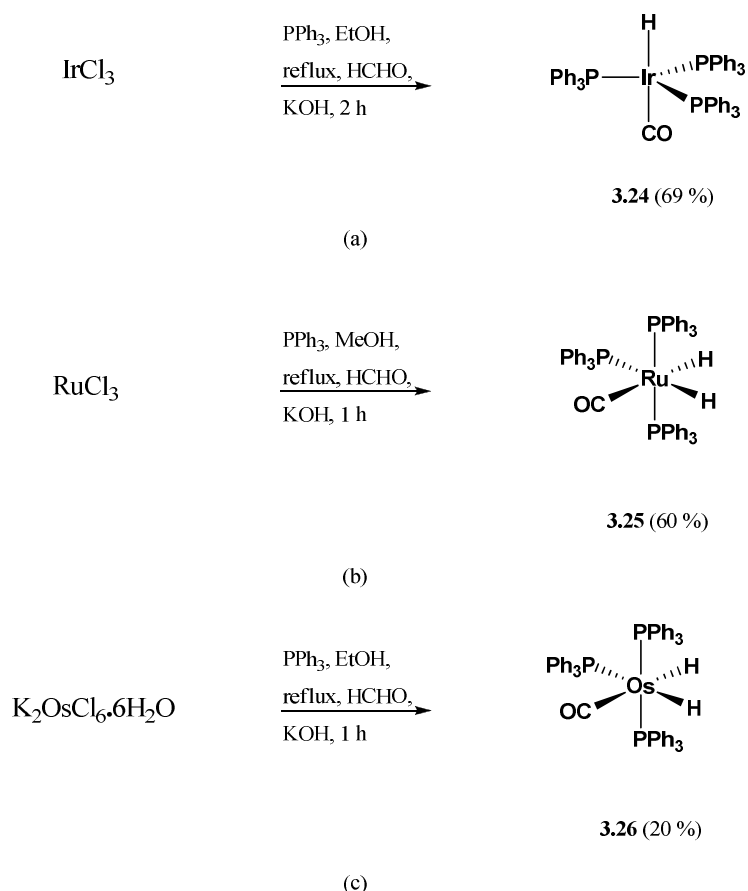
## 3.4 Preparation of metal complexes

The preparation of the metal complexes containing bidentate ligands involves the synthesis and characterisation of the metal precursor, complexation of the clean ligand, and characterisation of the resultant complexes. Certain metal precursors were synthesised, as donated salts of the PGMs were readily available. Such syntheses were beneficial from a financial point of view. Moreover, this preparation afforded the characterisation of the precursors which was useful for comparison and validation purposes. Two general types of metal precursors were prepared: (a) transition metal hydride, and (b) transition metal 1,5-cyclooctadiene (cod). A third type of precursor was also investigated, transition metal aromatic, and was purchased from local sources due to availability, time considerations, and tedious synthesis.

### 3.4.1 Transition metal hydride precursors

The preparation of the transition metal hydride precursors [Ir(H)(CO)(PPh<sub>3</sub>)<sub>3</sub>] **3.24**, [Ru(H)<sub>2</sub>(CO)(PPh<sub>3</sub>)<sub>3</sub>] **3.25**, and [Os(H)<sub>2</sub>(CO)(PPh<sub>3</sub>)<sub>3</sub>] **3.26** was adapted from literature, **Scheme 19** [47]. The general procedure is the same for all precursors, with the reaction carried out with the exclusion of air via standard Schlenk tube techniques. The platinum metal salt, formaldehyde, and KOH, were rapidly added in this order to a refluxing solution of triphenylphosphine in an alcohol solvent. The reaction was refluxed during which time deposition of a precipitate occurred. The products were collected by filtration, and the metal precursors purified by washing

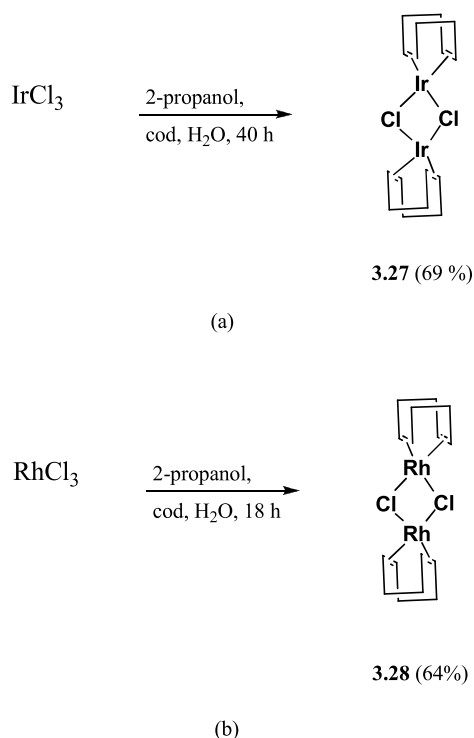
with water, ethanol, and *n*-hexane. Further purification was required for the Ru and Os precursors by filtering through a column of alumina, and recrystallisation from methanol. Complexes **3.24**, **3.25**, and **3.26** were obtained in yields of 69, 60, and 20% respectively which compared satisfactorily to literature [47].



**Scheme 19. Synthesis of metal precursors: (a) 3.24, (b) 3.25, and (c) 3.26, adapted from literature [47].**

### 3.4.2 Transition metal cod precursors

The preparation of the 1,5-cyclooctadiene (cod) transition metal precursors,  $[\text{Ir}(\text{cod})\text{Cl}]_2$  **3.27** [48-49], and  $[\text{Rh}(\text{cod})\text{Cl}]_2$  **3.28** [50], was adapted from literature, **Scheme 20**. In comparison to the transition metal hydrides, this preparation is fairly straightforward. A Schlenk tube was charged with the platinum metal salt, 2-propanol, cod, and water, and allowed to reflux for a set period of time. To improve product yields, the reaction temperature was strictly maintained and not allowed to cool to prevent precipitation of the metal. Chemically pure grade cod is required for the reaction, therefore a fresh bottle was used for each synthesis to avoid distillation of this noxious liquid. The products were collected by filtration and washed with cold methanol to remove any unreacted cod and organic solvents, with no further purification required. Complexes **3.27** and **3.28** were obtained in yields of 69 and 64% respectively, which compared favourably with literature.

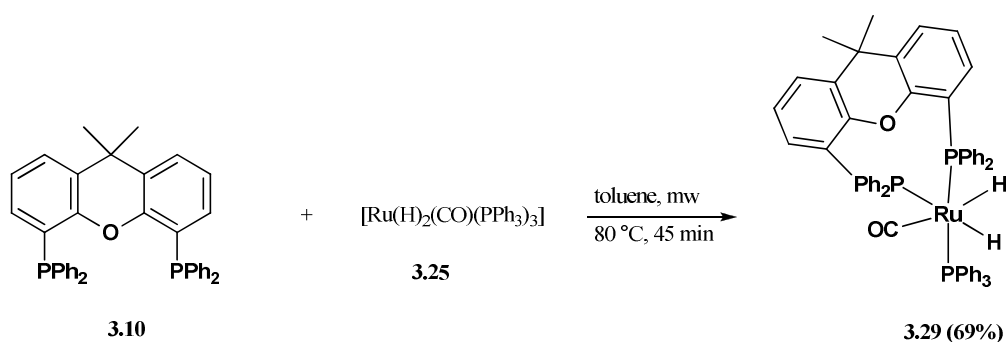


**Scheme 20.** Synthesis of metal precursors: (a) **3.27** [48-49], (b) **3.28** [50], adapted from literature.

### 3.4.3 Complexation

Two types of complexation protocols were investigated in this work: (a) microwave assisted in situ complexation for catalytic testing, and (b) complexation via conventional or microwave heating for isolation and characterisation of the metal complex.

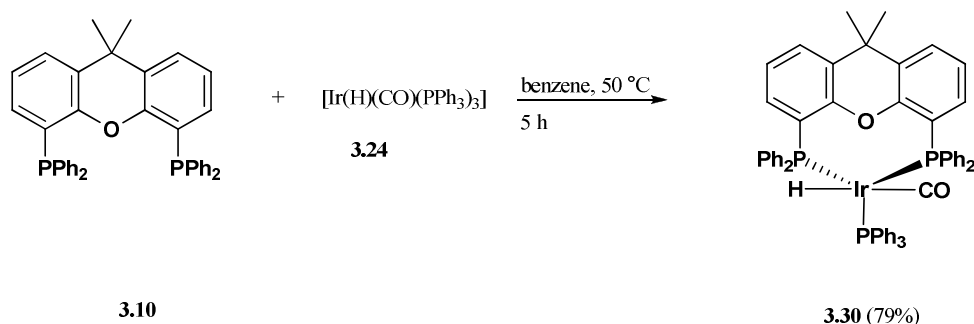
Microwave assisted in situ complexation afforded rapid and efficient complexation of all prepared ligands followed by addition of the substrate for catalytic testing studies. In some cases, in situ complexation methods were necessary, for example complexation with [Ru-*p*-cymene] and [RhCp\*] metal precursors that are prone to decomposition. A disadvantage of this method is that isolation and characterisation of the metal complexes is precluded as the prepared complex is immediately used for a catalytic reaction. To validate this in situ complexation method, a representative compound [Ru(xantphos)(H)<sub>2</sub>(CO)(PPh<sub>3</sub>)] **3.29** was prepared, isolated and characterised. The parent ligand xantphos was chosen as representative of the remaining prepared ligands. Furthermore, the preparation and X-ray crystal structure of **3.29** has only recently been reported by Williams and co-workers using conventional heating [51]. In this work, complex **3.29**, **Scheme 21**, was obtained in 69% yield after 45 minutes using microwave irradiation, as compared to a literature yield of 46% after 3 hours [51].



**Scheme 21. Preparation of 3.29.**

The application of selected prepared ligands to high pressure hydrogenation studies in a Parr reactor was also of interest to this work. The desired complexes were prepared, isolated, and characterised prior to the catalytic testing to avoid any difficulties associated with high pressure in situ complexation, as well as to maintain a closed system (with respect to loading and manipulation of the reaction vessel). Ir and Rh metal complexes were of interest for the intended application. The desired complexes were air stable and showed no decomposition in the solid state, which facilitated the preparation and storage for subsequent use.

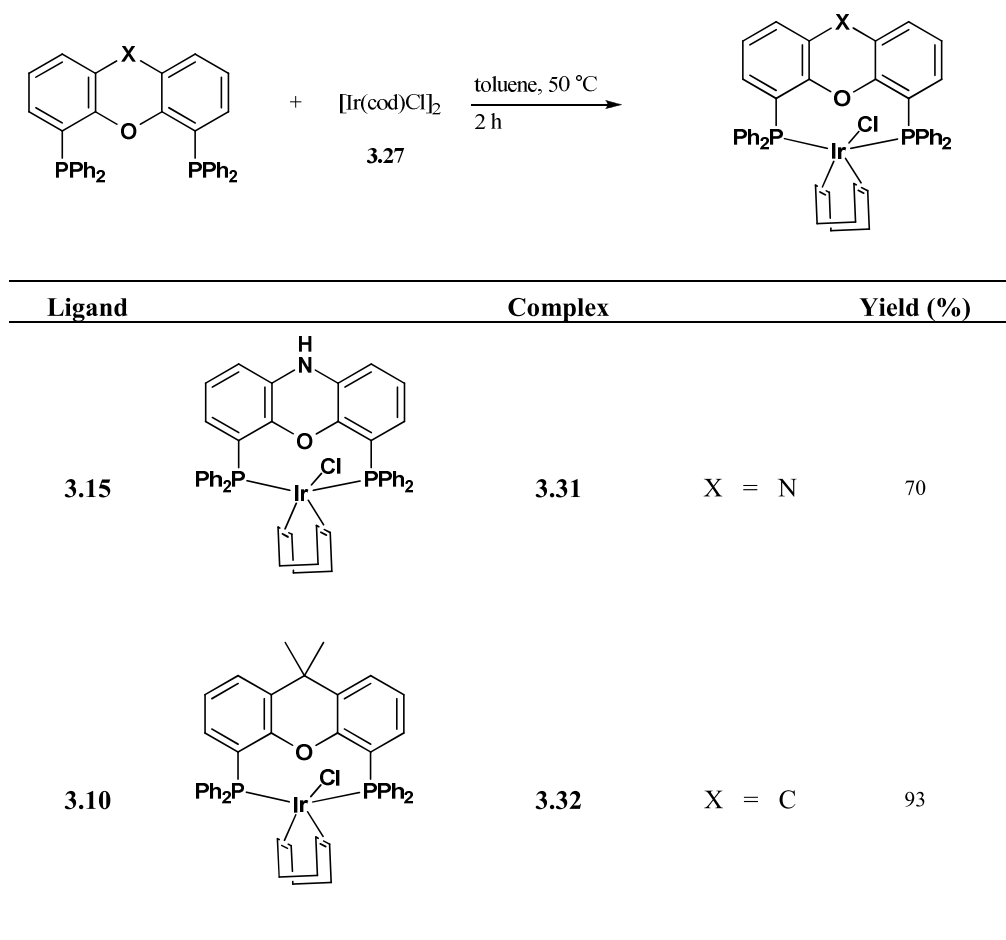
The novel metal complex  $[\text{Ir}(\text{xantphos})(\text{H})(\text{CO})(\text{PPh}_3)]$  **3.30** was prepared from the parent ligand **3.10**, **Scheme 22**. The ligand was combined with the metal precursor **3.24** and the contents stirred at 50 °C during which time **3.30** precipitated as a yellow solid in 79% yield. A single crystal was grown from a solution of DCM layered with hexane (1/1, v/v).



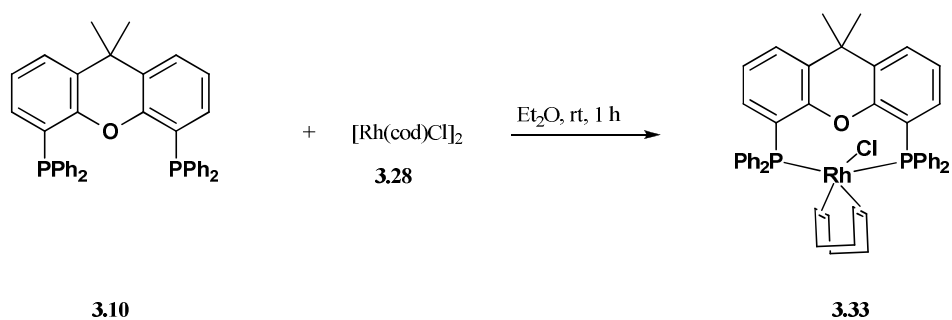
**Scheme 22. Preparation of 3.30.**

The general procedure for the preparation of the novel complexes  $[\text{Ir}(\text{nixantphos})(\text{cod})\text{Cl}]$  **3.31** and  $[\text{Ir}(\text{xantphos})(\text{cod})\text{Cl}]$  **3.32** is shown in **Scheme 23**. The ligand **3.15** (2 equivalents) was added to a solution of 1 equivalent of  $[\text{Ir}(\text{cod})\text{Cl}]_2$  dimer **3.27** to afford complex **3.31** in 70% yield. The DSC for complex **3.31** revealed no phase change up to the melting point observed as an endotherm at 198 °C. The DSC results indicate that the complex has good thermal stability with the onset of decomposition at temperatures greater than 400 °C. Similarly, ligand **3.10** was reacted with the precursor **3.27** to afford complex **3.32** in 93% yield. Single crystals

of complexes **3.31** and **3.32** were grown from a solution of DCM layered with absolute ethanol (1/1, v/v). The complex  $[\text{Rh}(\text{xantphos})(\text{cod})\text{Cl}]$  **3.33** was successfully prepared by the procedure shown in **Scheme 24** [52]. The preparation and X-ray crystal structure of **3.33** has been previously reported by van Haaren et al. [52]. Complex **3.33** was obtained as yellowish-orange crystals in 93% yield.



**Scheme 23.** Preparation of **3.31** and **3.32**. X, Y, and R refers to the ligand constituents in Figure 10



**Scheme 24.** Preparation of **3.33**.

### 3.5 X-ray crystal structures

Single crystals suitable for X-ray analysis were grown for various backbones, ligands, and metal complexes prepared in this work. The crystals were grown by slow vapour diffusion techniques at room temperature over several days (1/1 solvent ratio).

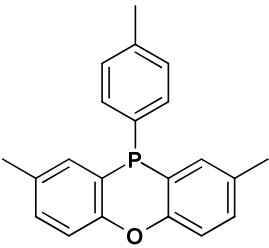
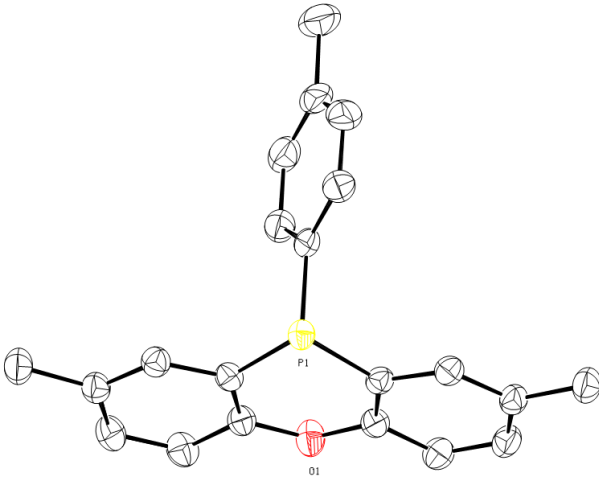
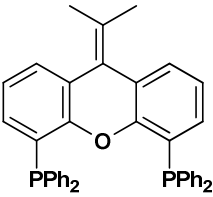
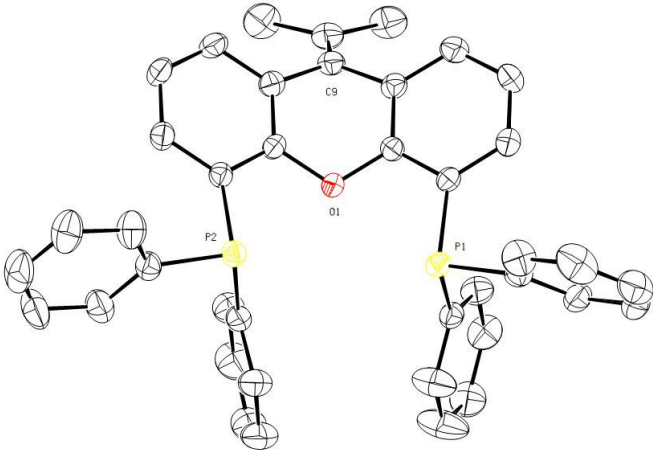
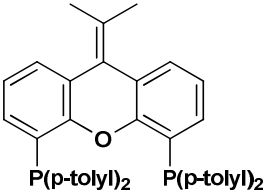
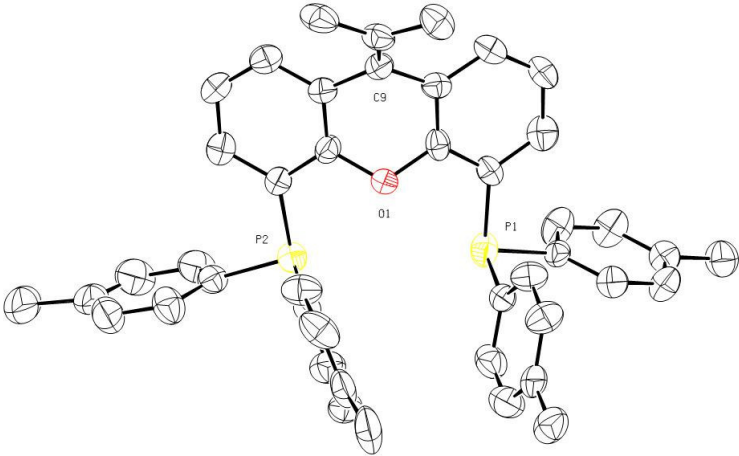
#### 3.5.1 Backbones and ligands

Crystal structures for a novel backbone and eight bidentate ligands were successfully grown, **Table 4a-c**. For all ORTEP representations, thermal ellipsoids are shown at 50% probability, with the hydrogen atoms omitted for clarity. A summary of key crystal features such as the intramolecular P...P distance and dihedral angle are presented in **Table 5**, and selected bond lengths and bond angles in **Table 6**.

All discussions are presented with reference to **Tables 4-6**. A full listing of crystal data and further supplementary information is presented in **Appendix B** of this thesis.

The novel backbone **3.6**, **Table 4a**, is closely related to backbone **3.5**, however the compounds were prepared by different synthetic routes. The successful in situ alkylation of the phosphorus atom with the tolyl moiety, as well as the success of the new synthetic protocol in general, was unequivocally confirmed by the single X-ray crystal structure of **3.6**. The *para* position of the phenyl groups of the xanthene skeleton and the phenyl group of the phosphorus donor at the X position are functionalised with methyl substituents. The tolyl ring lies nearly perpendicular to the mean plane through the phenoxaphosphine backbone, forming a dihedral angle of 83.26(3)°. The C-P bond length for the tolyl group bonded to P1 is 1.835(13) Å, and is longer than the C-P bond lengths found in the xanthene skeleton (1.805(13) – 1.809(13) Å). This is a result of the pyramidal geometry around atom P1 with the corresponding C-P-C bond angles ranging from 98.009(6) to 101.04(6)°. Similar bond lengths and bond angles involving the phosphorus atom are reported in the crystal structure of **3.5** by Mann et al. [53]. There is a significant difference in the planarity of the outer rings of the xanthene skeleton for crystals **3.5** and **3.6**. The outer rings of the phenoxaphosphine backbone of **3.6** are more planar, dihedral angle of 6.56(2)°, than the reported crystal structure of **3.5**, dihedral angle of 15° [53].

To facilitate meaningful discussion and comparison with the prepared ligands, the reported crystal structure of the parent ligand xantphos **3.10** [10] is presented in **Figure 14**. The backbone of **3.10** is bent by a dihedral angle of 23.75(2)°, evident by the roof-like structure in **Figure 14b**. The phosphorus atoms lie a distance of 4.059(2) Å apart, with selected bond lengths and bond angles reported in **Table 6**. The disposition of the diphenylphosphine moieties define the conformation of xantphos that has been described as pseudo-C<sub>s</sub> [3], with one mirror plane running through the central C-O axis.

Crystal Data	Crystal Structure
 <p><b>3.6</b></p> <p>Monoclinic, <math>P2_1/c</math> R factor (%) = 3.72 Novel</p>	
 <p><b>3.11</b></p> <p>Monoclinic, <math>P2_1/c</math> R factor (%) = 4.09 Novel</p>	
 <p><b>3.12</b></p> <p>Monoclinic, <math>P2_1/c</math> R factor (%) = 5.71 Novel</p>	

**Table 4a. X-ray crystal structures of backbones and bidentate ligands.**

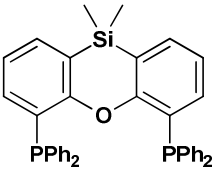
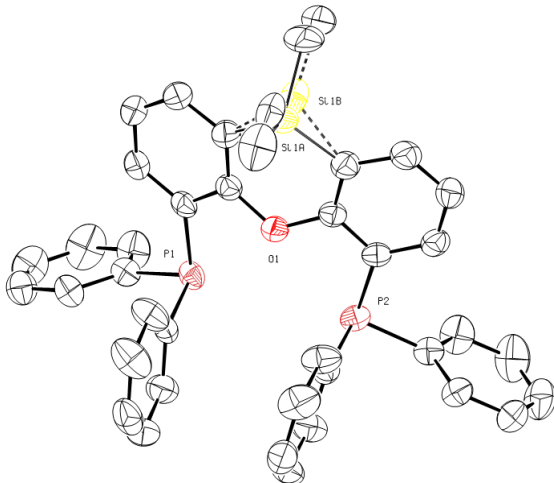
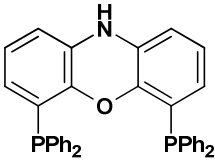
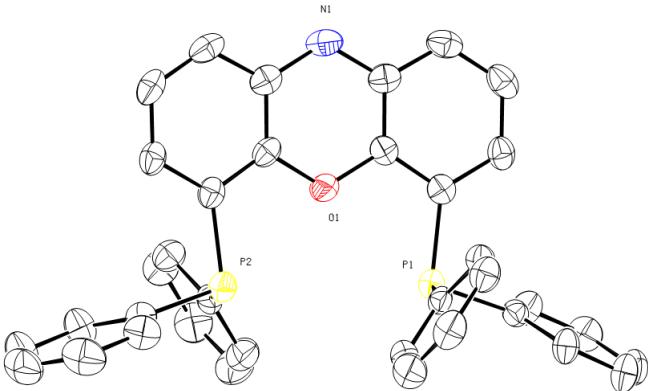
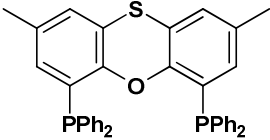
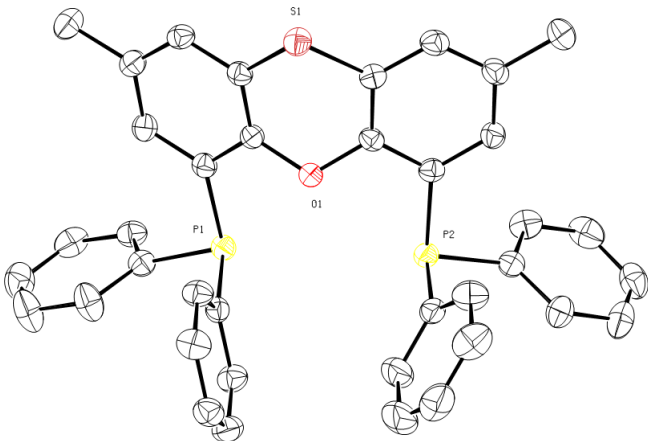
Crystal Data	Crystal Structure
 <p><b>3.13</b></p> <p>Orthorhombic, <math>P_{nma}</math>  R factor (%) = 4.86  Novel</p>	
 <p><b>3.15</b></p> <p>Triclinic, <math>P\bar{1}</math>  R factor (%) = 4.29  Novel</p>	
 <p><b>3.16</b></p> <p>Monoclinic, <math>P2_1/n</math>  R factor (%) = 3.61</p>	

Table 4b. X-ray crystal structures of bidentate ligands.



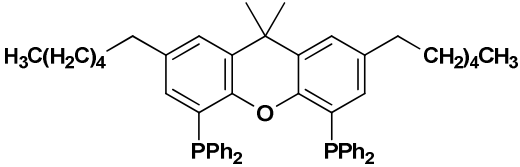
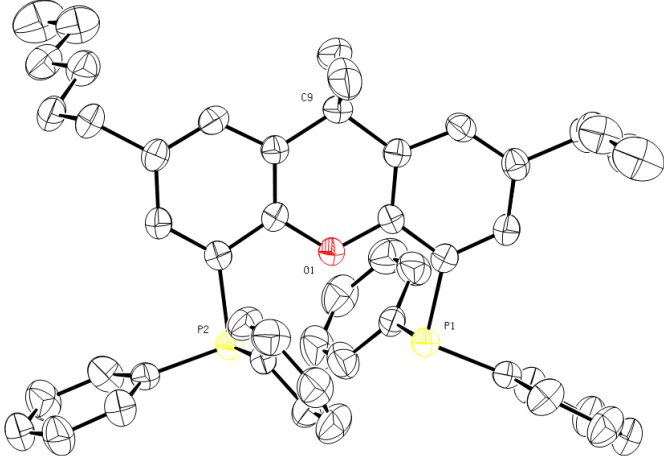
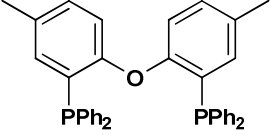
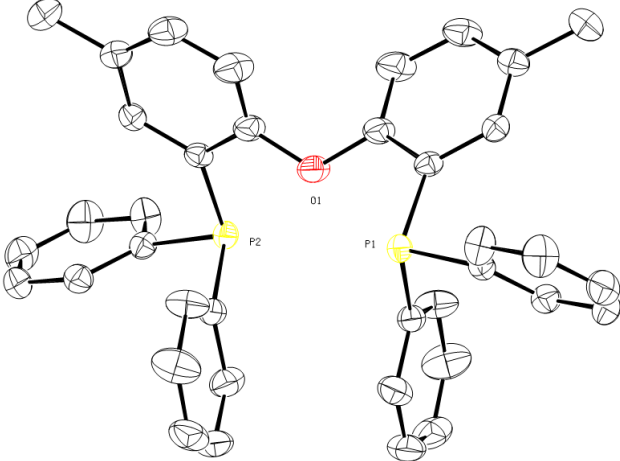
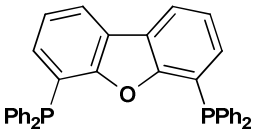
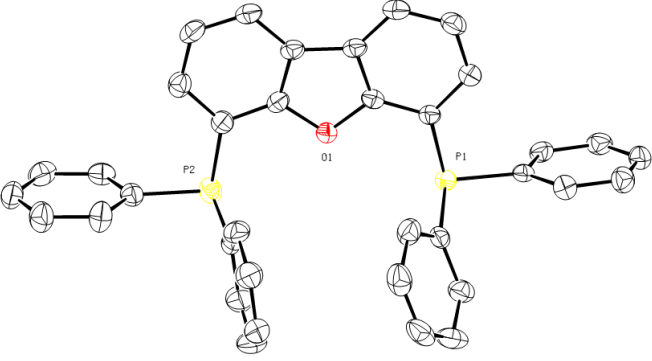
Crystal Data	Crystal Structure
 <p><b>3.17</b></p> <p>Monoclinic, <math>C_{2/c}</math> R factor (%) = 4.19 Novel</p>	
 <p><b>3.22</b></p> <p>Orthorhombic, <math>P_{bcn}</math> R factor (%) = 4.04 Novel</p>	
 <p><b>3.23 (a)</b></p> <p>Triclinic, <math>P-1</math> R factor (%) = 4.06</p>	

Table 4c. X-ray crystal structures of bidentate ligands.

Crystal	P---P [Å]	Dihedral Angle [°]
<b>Xantphos<sup>a</sup></b>	4.059(2)	23.75(2)
<b>3.6</b>	-	6.56(2)
<b>3.11</b>	4.104(2)	35.85(2)
<b>3.12 (a)</b>	4.18	34.55(2)
<b>3.12 (b)</b>	4.015	39.66(2)
<b>3.12 (c)</b>	4.116	35.64(2)
<b>3.13</b>	3.884(2)	24.14(2)
<b>3.15</b>	4.255(2)	4.76(2)
<b>3.16</b>	4.082(2)	32.88 (2)
<b>3.17</b>	4.181(2)	8.27(2)
<b>3.22</b>	5.151(2)	67.34(2)

**Table 5. Intramolecular P...P distances and dihedral angles for backbone and ligand crystal structures.**

Crystal	C-X [Å]	C-O [Å]	C-P [Å]	C-P-C [°]
<b>Xantphos<sup>a</sup></b>	1.529 (6)	1.397(5)	1.823(5) - 1.836(4)	101.0(2) - 101.7(2)
<b>3.6</b>	1.805(1) - 1.809(1)	1.378(2) - 1.379(2)	1.805(1) - 1.835(1)	98.01(6) - 101.04(6)
<b>3.11</b>	1.481(2) - 1.482(2)	1.387(2) - 1.396(2)	1.826(2) - 1.841(2)	99.36(7) - 104.36(7)
<b>3.12 (a)</b>	1.480(6) - 1.497(7)	1.387(5) - 1.385(6)	1.806(6) - 1.840(5)	100.1(3)-102.6(3)
<b>3.12 (b)</b>	1.501(7) - 1.475(7)	1.410(5) - 1.382(6)	1.185(6) - 1.828(5)	100.7(3) - 103.1(3)
<b>3.12 (c)</b>	1.465(7) - 1.493(7)	1.394(6)	1.830(5) - 1.843(6)	100.8(3) - 102.9(3)
<b>3.13</b>	1.859(2) A, 1.908(4) B	1.394(2)	1.834(2) - 1.841(2)	100.91(9) - 101.12(9)
<b>3.15</b>	1.398(3) - 1.403(3)	1.388(2) - 1.392(2)	1.825(2) - 1.836(2)	99.93(10) - 103.02(10)
<b>3.16</b>	1.760(2) - 1.761(2)	1.397(2) - 1.400(2)	1.835(2) - 1.849(1)	100.04(6) - 102.95(6)
<b>3.17</b>	1.527(2)	1.384(2)	1.839(2) -1.846(2)	98.37(7) - 102.40(8)
<b>3.22</b>	N/A	1.394(2)	1.834(1) -1.839(1)	100.16(7) - 102.17(7)
<b>3.23 (a)</b>	N/A	1.385(2) - 1.392(2)	1.831(2) -1.836(2)	100.66(9) - 103.80(8)
<b>3.23 (b)</b>	N/A	1.389(2) - 1.390(2)	1.826(2) -1.833(2)	100.40(9) - 103.45(9)

**Table 6. Selected bond lengths and bond angles for backbone and bidentate ligand crystal structures.**

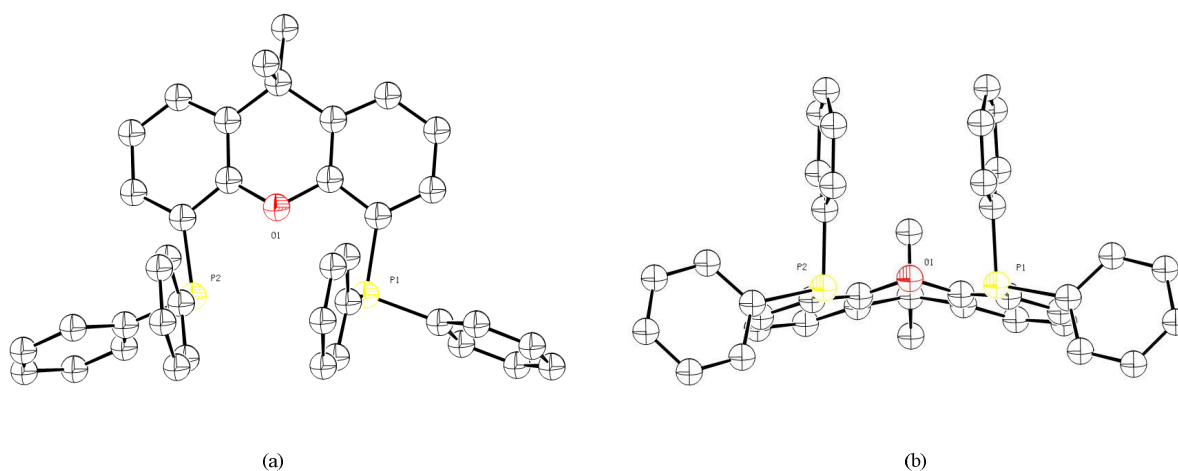


**Figure 14.** Reported crystal structure of **3.10** [10] from different points of view: (a) front, and (b) bottom.

In comparison to the parent ligand **3.10**, the outer phenyl rings of the novel crystal structure of compound **3.11**, **Table 4a**, shows a greater deviation from planarity, dihedral angle of  $35.85(2)^\circ$ , **Table 5**. The isopropylidene group of **3.11** is orientated in the same direction as the bending of backbone around the C-O axis, with an intramolecular P...P distance of  $4.104(2)$  Å. The C-P-C bond angles in **3.11** differ from the bond angles of **3.10**, **Table 6**. This is possibly due to the orientation of the phenyl rings to overcome the steric congestion caused by the greater bending of the backbone in **3.11**. This could also account for the larger intramolecular P...P distance of **3.11** relative to **3.10**. The crystal structure of **3.12** is structurally similar to the analogous ligand **3.11**. The structure of ligand **3.11** contains three molecules in the asymmetric unit and the results for each structure are presented in **Table 6**. The intramolecular P...P distances are essentially the same, **Table 5**, with both backbones exhibiting virtually identical deviations from planarity. The bond lengths and bond angles for ligands **3.11** and **3.12** compare favourably, **Table 6**.

The novel crystal structure of sixantphos **3.13**, **Table 4b**, exhibits positional disorder around the Si donor atom and methyl substituents. The disorder is represented in the crystal structures as SiA and SiB, **Figure 15**, with the corresponding bond lengths and angles indicated in **Table 6**. Ligand **3.13**, prepared as an analogue to **3.10**, displays similar backbone bending, dihedral angle of  $24.12(2)^\circ$ , with similarly matching C-P-C bond angles. The C-X (C-Si) bond length in **3.13** is elongated in comparison to **3.10** to accommodate the increase in donor atom size. However, the intramolecular P...P distance is significantly shorter for **3.13** relative to the parent ligand **3.10**.

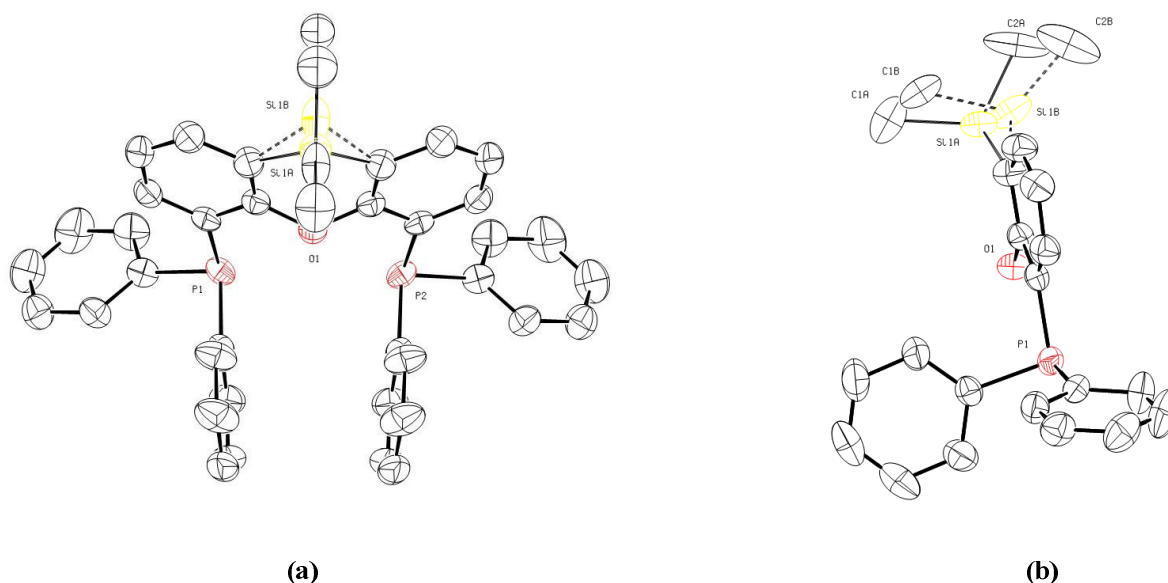


**Figure 15.** Crystal structure of **3.13** from from different points of view: (a) front, and (b) right.

The key feature of the novel crystal structure of **3.15**, **Table 4b**, is the significantly planar xanthene backbone, dihedral angle of  $4.76(2)^\circ$ , in comparison to the other xantphos family ligands, **Table 5**. The presence of the smaller nitrogen donor at the X position, relative to carbon in **3.10**, results in smaller C-X (X = N) bond lengths, with the bond angles involving the C-P-C atoms ranging from  $99.93(10) - 103.02(10)^\circ$ , **Table 6**. The intramolecular P...P distance of **3.15** is  $4.255(2) \text{ \AA}$  and compares favourably to other reported functionalised nixantphos type ligands [54-56]. This suggests that the functionality of the N donor has little influence on the natural bite angle, and further implies that tridentate derivatives or supported catalysts could be prepared without significantly altering the natural bite angle.

The crystal structure of thixantphos **3.16** was grown with a dichloromethane solvent molecule in the asymmetric unit cell. The solvent molecule has been omitted from all representations for clarity. The crystal structure of **3.16** has been previously reported by Goertz et al. [28]. However, the reported structure has an essentially planar backbone, dihedral angle of  $0.69(2)^\circ$ , **Figure 16a**, in contrast to the crystal structure obtained in this work, dihedral angle of  $32.88(2)^\circ$ , **Figure 16b**. Molecular modelling studies of xantphos family ligands [1] and the crystal structure of a metal complex of ligand **3.16** with Ni, dihedral angle of  $33.55(2)^\circ$  [28], suggest that the conformation of the backbone should be boat-like and similar to **3.10**, **Figure 14b**. Goertz et al. [28] suggest that the planarity of the reported crystal of the free ligand **3.16** is possibly due to crystal structure packing effects. The C-X (X = S) bond lengths, C-P bond lengths, and bond angles involving the C-P-C atoms of **3.16**, **Table 6**, compares favourably to the reported values. The intramolecular P...P distance and C-O bond lengths are, however, slightly elongated. It has been previously reported [24] that crystal structures of xantphos ligands obtained both with and without the presence of a solvent molecule have essentially identical molecular structures with only slight changes in C-P torsion angles. This could possibly account for the slight difference

in the observed intramolecular P...P distance of **3.16** for the crystal structure grown in this work with that reported in literature.

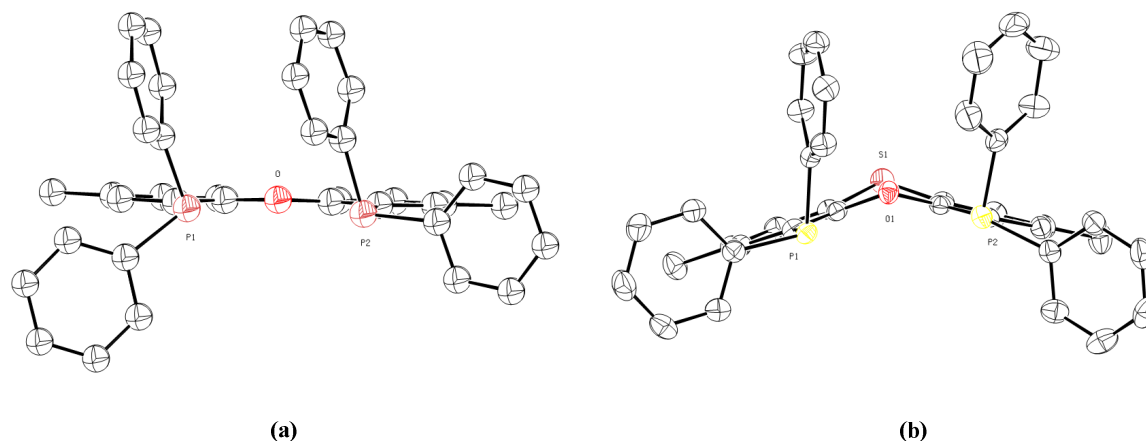


**Figure 16. Crystal structure comparison of 3.16: (a) Goertz et al. [28], and (b) this work.**

Hexantphos **3.17**, **Table 4c**, is the first example of a crystal structure of a xantphos family ligand with the backbone functionalised with linear alkyl chains at the Y position. In comparison to the parent ligand **3.10**, the backbone of **3.17** is nearly planar, dihedral angle of  $8.27(2)^\circ$ , **Figure 17a**. Furthermore, the diphenylphosphine rings are spatially positioned similar to other planar xantphos family structures, for example ligand **3.15** and the reported crystal structure of **3.16**, **Figure 16a** [28]. The *n*-hexyl chains are arranged as linear branches in opposing directions in the solid state crystal structure of **3.17**, **Figure 17a-b**. This arrangement is possibly due to crystal structure packing effects and symmetry considerations. A flexible alkyl linkage at the Y position could possibly adopt various conformations that may differ in the gas or liquid state, which could possibly affect the solubility of such compounds. The intramolecular P...P distance of **3.17** is larger than that of the benchmark ligand **3.10**, **Table 5**, with similar C-X bond distances. The C-O and C-P bond lengths compare favourably, with the bond angles involving the C-P-C atoms in **3.17** spanning a wider range, **Table 6**.



**Figure 17.** Crystal structure of **3.17** from different points of view: (a) bottom, and (b) right.

The novel crystal structure of PTEphos **3.22**, **Table 4c**, is an example of a related xanthene family ligand based on a di-*p*-tolyl ether backbone. The absence of a donor or chemical bond at the X position results in a flexible backbone with movement about the oxygen atom of the ether link. The backbone is significantly bent with a dihedral angle of  $67.34(2)^\circ$ , **Table 5**. Reported crystal structures for the analogous ligand, DPEphos **3.21**, exhibit similar dihedral angles of  $68(2)^\circ$  [57] and  $67(2)^\circ$  [58]. The intramolecular P...P distance of **3.22** is significantly larger ( $5.151(2)$  Å) than both the related ligand **3.21** ( $4.881$  [57] and  $4.875$  Å [58]), and the xantphos family ligands, **Table 5**. The C-O bond lengths, C-P bond lengths, and C-P-C bond angles for **3.22** compared favourably to benchmark ligand **3.10** and related ligand **3.21**.

The crystal structure of **3.23**, DBFphos, **Table 4c**, was obtained as two crystallographically independent molecules (A and B) in the asymmetric unit cell, **Figure 18**. Both molecules are essentially planar, dihedral angles of  $3.20(2)$  and  $1.86(2)^\circ$ , **Table 5**, with comparative bond lengths and bond angles, **Table 6**. However, molecule A exhibits a larger intramolecular P...P distance of  $5.574(2)$  Å, as compared to  $5.485(2)$  Å for molecule B. A single crystal of **3.23** was previously reported by Vogl et al. [59] with a slightly larger intramolecular P...P distance of  $5.741(1)$  Å and different orientation of the diphenylphosphine rings. The bond lengths and bond angles for molecule A and B compare favourable to the those reported by Vogl et al. [59].

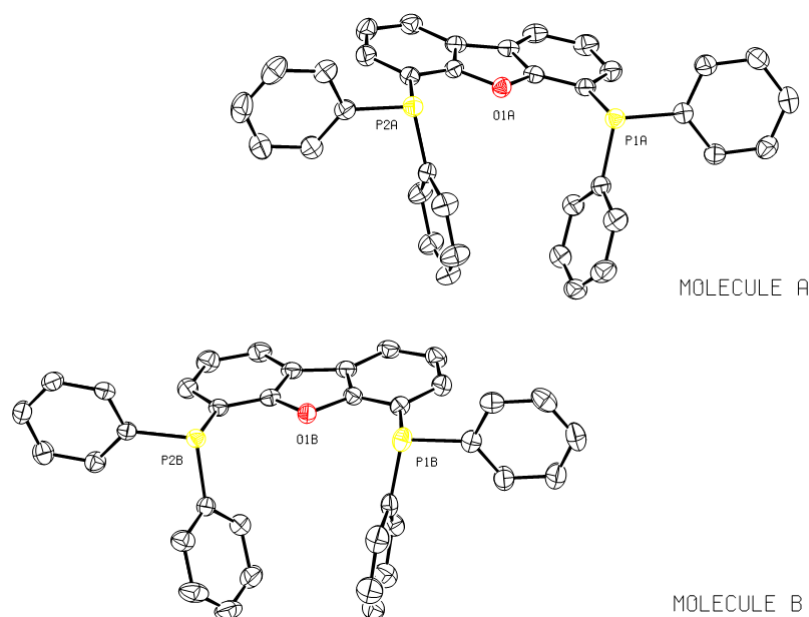


**Figure 18.** The crystal structures of **3.23** with two crystallographically independent molecules in the asymmetric unit cell.

A comparison of the selected bond lengths and bond angles in **Table 6** reveals expected patterns. Average values for the C-P and C-O bond lengths fall within the same range for all ligands. The average bond angles involving the C-P-C atoms also fall within the same range, except for those structures that have significantly planar backbones relative to xantphos, and where the diphenylphosphine moieties adopt different conformations. The C-X bond lengths vary with a change in donor atom, i.e. as the size of the donor atom increases, the C-X bond lengths also increase to accommodate the increasing size of the atomic radii, and vice versa. In some cases the decrease or increase in donor atom size can be linked to an increase or decrease in the intramolecular P---P distance and, by extension, the natural bite angle, for example ligands **3.11**, **3.13**, and **3.15**. However, this generalisation is not always true. For ligands **3.16** and **3.17** this situation is reversed, most likely through electronic effects such as the strong  $\sigma$  donating ability of sulphur, or geometric effects due to the flexible alkyl chain.

### 3.5.2 Metal Complexes

The crystal structure of  $[\text{Ir}(\text{xantphos})(\text{H})(\text{CO})(\text{PPh}_3)]$  **3.30** was obtained as two crystallographically independent molecules (A and B) in the asymmetric unit cell, **Figure 19**. A solvent molecule for each molecule was also present in the asymmetric unit cell, and is omitted from all representations for clarity. Selected bond lengths and bond angles for molecules A and B are presented in **Table 7**. The molecular framework of A and B are essentially identical. The discussion of the crystal structure of **3.30** will be presented with reference to the bond lengths and angles of molecule A only.

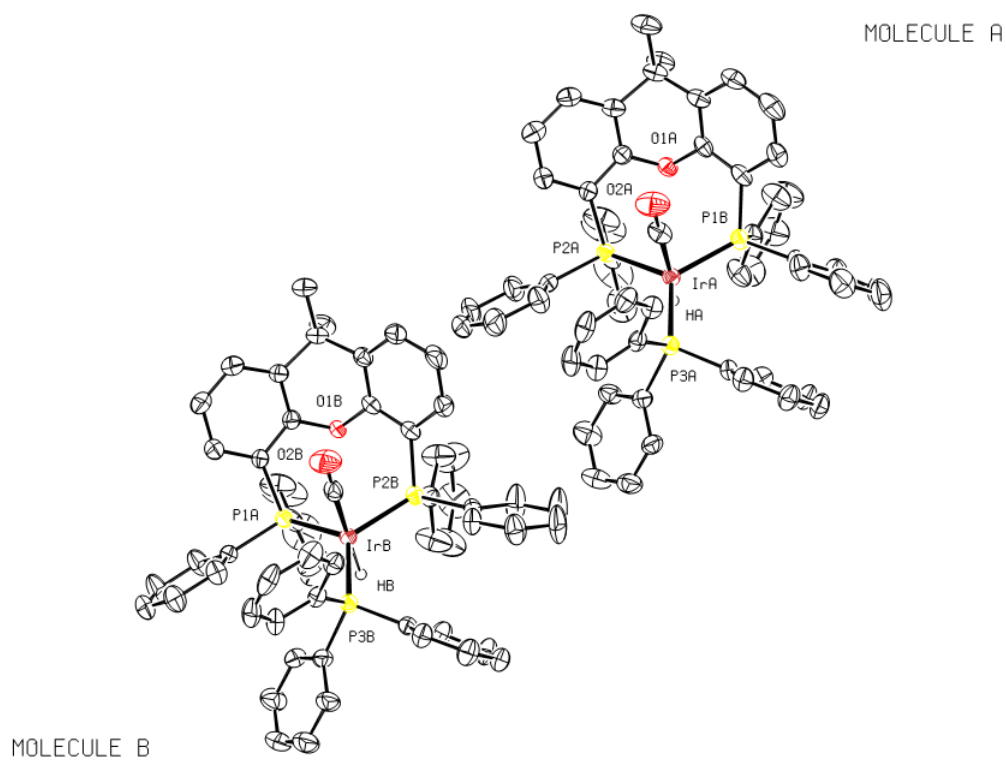


**Figure 19.** The crystal structures of 3.30 with two crystallographically independent molecules in the asymmetric unit cell.

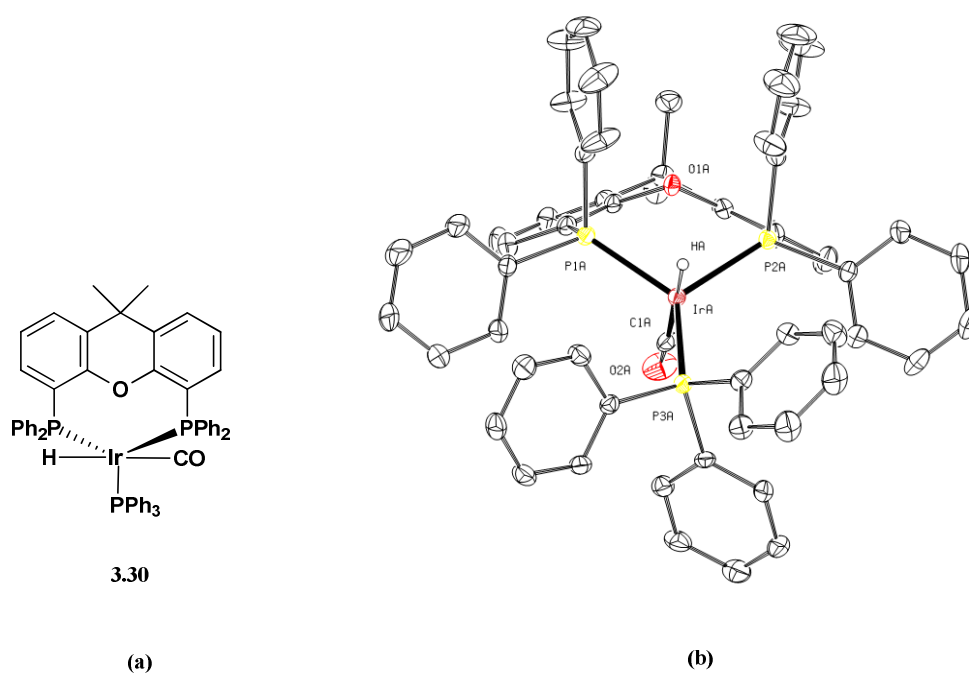


**Figure 20.** Crystal structure of 3.30: (a) schematic representation, and (b) bottom view.



Bond lengths [Å]	Molecule A	Molecule B
Ir-P1	2.304(1)	2.299(1)
Ir-P2	2.315(1)	2.302(1)
Ir-P3	2.287(1)	2.287(1)
Ir-CO	1.888(6)	1.870(6)
Ir-H	1.49(5)	1.12(4)
P---P	3.763(2)	3.781(2)

Bond Angles [°]	Molecule A	Molecule B
P1-Ir-P2	109.13(5)	110.50(5)
P1-Ir-P3	125.47(5)	121.75(5)
P2-Ir-P3	122.31(4)	124.52(5)
CO- Ir -P1	92.76(16)	94.09(18)
CO- Ir -P2	95.77(17)	94.77(18)
CO- Ir -P3	98.57(17)	98.67(17)
Dihedral	47.98(2)	48.09(1)

**Table 7. Selected bond lengths and bond angles for 3.30.**

The Ir metal centre of the novel crystal structure of **3.30** is bonded to 3 phosphorus donors that occupy equatorial positions, and a carbonyl ligand and metal hydride that occupy axial positions. This results in a trigonal bipyramidal geometry that is slightly distorted due to the wide bond angles involving the P-Ir-P atoms, **Table 7**. The position of the Ir atom is found to be slightly above the plane (0.233(2) Å) formed by the three phosphorus atoms. Due to weak scattering factors of hydrogen versus iridium, the hydride position cannot be exactly located [60-61]. Therefore, the approximate position of the hydride hydrogen is shown to be *trans* to the carbonyl ligand, **Figure 19** and **Figure 20b**, with an Ir-H bond length of 1.49(5) Å. This *trans* conformation is supported by the IR and NMR spectroscopy data for complex **3.33** (**Section 3.7**). The IR spectrum shows a broad band at 1923 cm<sup>-1</sup> for  $\nu_{\text{CO}}$  stretching, indicating a weak C-O bond. This suggests that the hydrogen and not phosphorus is *trans* in the apical position to the carbonyl, since a *trans* phosphine would contribute to back donation to the metal thereby weakening the Ir-C bond and strengthening the C-O bond. For the <sup>1</sup>H NMR spectrum, the hydride shift is assigned to a pseudo doublet of triplets, which implies that the hydride is coupling to two chemically equivalent P1 and P2 nuclei, and then further split by the P3 nucleus. This is further confirmed by the small coupling constants (26.2 and 19.6 Hz) usually indicative of hydrides *cis* to the phosphine [3].

Fox et al. [62] have previously reported crystal structures for Ir xantphos complexes with different counter ligands of the general formula [Ir(X)(CO)<sub>2</sub>(xantphos)] and [Ir(H)<sub>2</sub>(Cl)(CO)(xantphos)], where X = Cl, Br, I, and COEt. The range of reported intramolecular P...P distances (3.692(2) – 3.781(2) Å) compares favourably to the distance measured for **3.30** (3.763(2) Å). However, the backbone of **3.30** is more bent and roof-like, dihedral angle of 47.98(2)° **Figure 20b**, as compared to the reported complexes, dihedral angle range of 27.27(2) – 38.84(2)°. The Ir-P bond distances for the chelating phosphorus donors in **3.30** are 2.304(1) and 2.314(1) Å,

which are shorter than those reported by Fox and co-workers, 2.387(4) – 2.4250(8) Å. The combination of the greater backbone bending and shorter Ir-P bond lengths in **3.30**, results in a significantly larger P-M-P chelation angle, 109.13(5)°, than those reported by Fox and co-workers, 100.01 (1) – 103.03(2)°. This further highlights the flexibility of the xanthene backbone and demonstrates the ability of the ligand and bite angle to accommodate different counter ligands. The effect of the counter ligand can also be seen by comparing the crystal structure of **3.30** to related xantphos family crystals with the same counter ligands, for example [Rh(nixantphos)(H)(CO)(PPh<sub>3</sub>)] [3]. An intramolecular P...P distance of 3.830(2) Å, and P-M-P chelation angle of 110.21(3)° have been reported for the Rh nixaphos complex [3] which is closer to the crystal structure of **3.30**, **Table 7**, than the Ir xantphos complexes of Fox et al. [62]. In comparison to the free ligand **3.10**, the intramolecular P...P distance in **3.30** has decreased by 0.296 Å on chelation. The phosphorus atoms are brought together by an increase in the bending of the flexible backbone from 23.75(2)° in the free ligand, to 47.98(2)° for the metal complex. Furthermore, the orientation of the diphenylphosphine moieties is similar for both compounds, which indicates that very little adjustment of the free ligand is necessary to form a chelate complex.

To the best of our knowledge, the crystal structure of [Ir(nixantphos)(cod)(Cl)] **3.31**, **Figure 21**, is the first example of a xantphos family crystal with the 1,5-cyclooctadiene (cod) counter ligand. Considering the cod ligand, Cl atom, and chelated ligand **3.15**, the coordination around the Ir metal centre can be described as approximately trigonal bipyramidal. The equatorial plane contains the two *cis* chelating phosphorus donors and the midpoint of the C65=C66 cod double bond, whereas the 2 axial positions include the chloro ligand and the midpoint of the C61=C62 cod double bond. The observed bis-equatorial coordination is similar to that of the crystal structure of complex **3.30**. Selected bond lengths and bond angles are presented in **Table 8**.

In comparison to the essentially planar free ligand **3.15**, complex **3.31** is significantly bent, dihedral angle of 25.04(2)°, and assumes the characteristic roof-like conformation, **Figure 21c**. Considering a mean plane of planarity involving the 14 ring atoms of the backbone, complex **3.31** is bent about the N-O axis to accommodate added strain due to the Ir metal coordination. The maximum deviations from planarity for the N and O atoms in **3.31** are 0.408(2) and 0.618(2)° respectively, and is significantly larger than in the free ligand, 0.079(2) and 0.095(2)°. The intramolecular P...P distance has decreased by 0.364 Å relative to **3.15**, with a P-M-P chelation angle of 106.49(3)°, **Table 8**. The Ir M-P bond lengths range from 2.3802(9) – 2.4761(2) Å, which compare favourably to the M-P bond lengths in the Ir xantphos complexes of Fox et al. [62]. The M-P lengths in **3.31** are slightly longer than those of **3.31**, possibly due to the third chelating P donor in the PPh<sub>3</sub> counter ligand. The bond length of the equatorial Ir-cod (C65=C66) is 1.443(5) Å, and the axial (C61=C62) is 1.412(5) Å, significantly longer than the 1.38(2) Å reported for [Ir(cod)(PPh<sub>3</sub>)<sub>2</sub>][PF<sub>6</sub>] [63] and [Ir(C<sub>5</sub>H<sub>4</sub>NOS)(cod)] [64] complexes that contain non-chelating monodentate ligands.

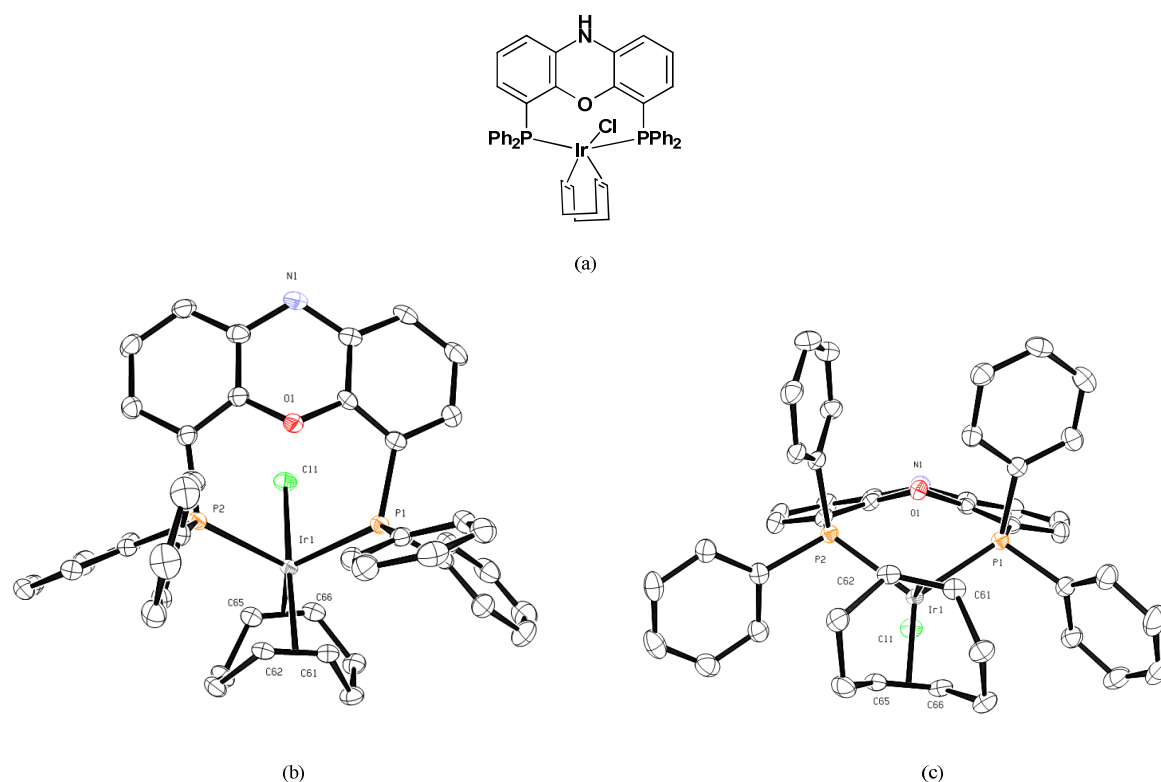


**Figure 21.** Crystal structure of **3.31** from different points of view: (a) schematic representation, (b) front, and (b) bottom.

Bond lengths [Å]	<b>3.31</b>	<b>3.32</b>
Ir-P1	2.3802(9)	2.4714(5)
Ir-P2	2.4761 (2)	2.3703(6)
(C=C) <sub>cod</sub>	1.412 (5) - 1.443(5)	1.414(3) - 1.437(3)
Ir-Cl	2.4227(8)	2.3941(6)
P---P	3.891(2)	3.794

Bond angles [°]	<b>3.31</b>	<b>3.32</b>
P1-Ir-P2	106.49(3)	103.15(2)
P1-Ir-Cl	89.16(3)	85.79(2)
P2-Ir-Cl	86.37(3)	84.49(7)
P-Ir-C <sub>cod</sub>	81.34(10) - 148.85(10)	83.43(7) - 151.24(7)
Dihedral	25.04(2)	36.78(2)

**Table 8.** Selected bond lengths and bond angles for **3.31** and **3.32**.

A second cod containing xanthene family crystal, [Ir(xantphos)(cod)Cl] **3.32**, was successfully grown and characterised by X-ray crystallography. The novel crystal structure of **3.32**, **Figure 22b-c**, displays the similar distorted trigonal bipyramidal geometry of complexes **3.30** and **3.31**. The xanthene backbone is similarly bent, dihedral angle of 36.78(2)°, with the characteristic roof-like structure **Figure 22c**. Considering a mean plane involving the 14 atoms of the xanthene backbone, complex **3.32** is bent around the C-O axis with maximum

deviations from planarity of 0.7421 (2) and 0.645(2) Å for the C and O atoms respectively. In comparison, the backbone of the free ligand **3.10** is bent by a dihedral angle of 23.75(2)°, with deviations of 0.498(2) and 0.456(2) Å for the C and O atoms respectively.

The Ir M-P bond lengths range from 2.3703(6) – 2.4714(5) Å, which compares favourably to the crystal structure of complex **3.31**, and by extension the Ir xantphos complexes of Fox et al. [62]. The axial and equatorial Ir-cod C=C bond lengths, Ir-Cl bond lengths, P-Ir-C, and P-Ir-Cl bond angles all compare favourably to complex **3.31**, **Table 8**. The intramolecular P...P distance is similar to that of **3.30** and the reported Ir xantphos complexes [62], however complex **3.30** with the PPh<sub>3</sub> counter ligand has the shortest Ir M-P bond lengths and therefore largest P-M-P chelation angle of the compared Ir complexes.

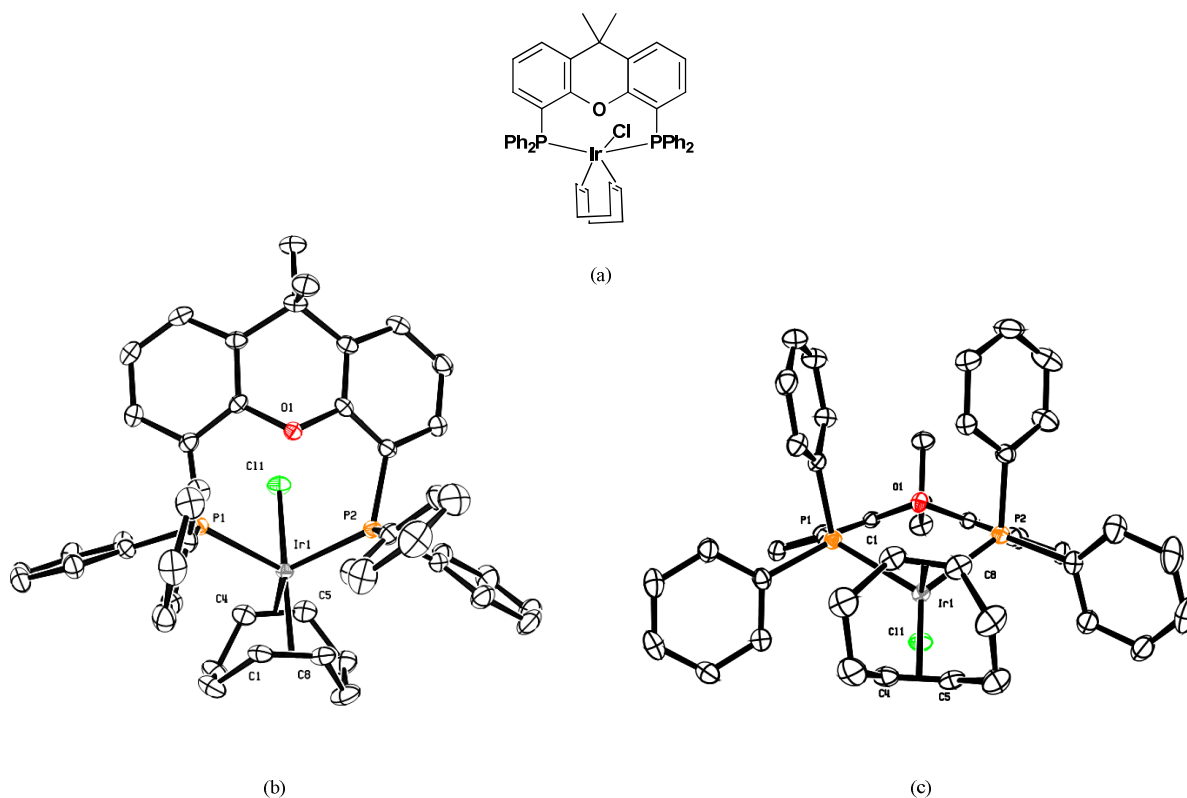


**Figure 22.** Crystal structure of **3.32** from different points of view: (a) schematic representation, (b) front, and (c) bottom.

### 3.6 Bite angle characterisation

The bite angle is a useful molecular descriptor that can be conveniently linked to a figure of merit in catalysis, (see Chapter 2). Natural bite angle ( $\beta_{\eta}$ ) values are presented in **Table 9** for the bidentate ligands prepared in this work. The ligands are arranged in ascending order according to  $\beta_{\eta}$ . Values for various xantphos family ligands have been previously reported in literature. For a valid comparison, only those values calculated using the same software, force field parameter set, and methodology have been collated in the table below for the ligands of interest.

Ligand	Natural Bite Angle $\beta_{\eta}$ [°]
DPEphos <b>3.21</b>	102.2 <sup>a</sup>
Phosxantphos <b>3.18</b>	107.9 <sup>b</sup>
PTEphos <b>3.22</b>	108.0 <sup>c</sup>
Sixantphos <b>3.13</b>	108.5 <sup>b</sup>
Thixantphos <b>3.16</b>	109.6 <sup>b</sup>
Xantphos <b>3.10</b>	111.4 <sup>b</sup>
IsopropxantTolylphos <b>3.12</b>	113.1 <sup>d</sup>
Isopropxantphos <b>3.11</b>	113.2 <sup>b</sup>
Nixantphos <b>3.15</b>	114.2 <sup>b</sup>
Hexantphos <b>3.17</b>	116.0 <sup>d</sup>
DBFphos <b>3.23</b>	131.1 <sup>e</sup>
IsopropxantButylphos <b>3.19</b>	137.9 <sup>d</sup>

<sup>a</sup> Dierkes and van Leeuwen [65], <sup>b</sup> van der Veen et al. [3]  
<sup>c</sup> Zuidema et al. [40], <sup>d</sup> Calculated in this work, <sup>e</sup> Kranenburg et al. [10]

**Table 9. Natural bite angle ( $\beta_{\eta}$ ) values for the bidentate ligands prepared in this study.**

Values for  $\beta_{\eta}$  were calculated for three novel ligands prepared in this work, isopropxantTolylphos **3.12**, hexantphos **3.17**, and isopropxantButylphos **3.19**. These values were calculated according to the method of Casey and Whiteker [66], and involved geometry optimisations using molecular mechanics force field methods. The Tripos force field [67], as implemented in the Sybyl programme package [68], was used along with additional force field parameters reported in literature [1,10]. A systematic conformer search was performed in Sybyl in order to ensure that the lowest energy conformation was used for the subsequent bite angle calculations [69]. The minimised or optimised geometry structures for the three ligands are presented in **Figure 23**. The backbones for all three ligands are bent with the characteristic roof-like structure and the diphenylphosphine moieties of **3.12** and **3.17** assume the typical xantphos family conformation.

The calculated  $\beta_{\eta}$  value for ligand **3.12** is similar to the reported value for ligand **3.11**. This is expected as only the electronic properties on the phosphorus donors of **3.12** were modified relative to **3.11**, which should not significantly alter the bite angle. The calculated  $\beta_{\eta}$  of ligand **3.17** was also expected to be similar to the

analogous ligand **3.10**. The calculated larger value is possibly due to the long *n*-hexyl chains that prevent the backbone from bending to the same extent as ligand **3.10**, resulting in a larger intramolecular P...P distance and natural bite angle. This is supported by the crystal structures of the respective ligands, where **3.17** is significantly more planar than **3.10**, dihedral angles of 8.27(2)° and 23.75(2)° respectively. Although the backbone of **3.19** is closely related to **3.11** and **3.12**, the bite angle is expected to differ due to the presence of the *t*-butyl substituents on the phosphorus donor atoms. The arrangement of the bulky *t*-butyl groups to overcome steric interactions and collisions results in a significantly larger intramolecular P...P distance than the other xanthene family ligands that is reflected in the large natural bite angle.

The ligands prepared in this work were further characterised by the calculation of the metal preferred bite angle to more precisely determine the effect of the metal centre and counter ligand. In order to accurately model and optimise the transition metal structures at the required level of complexity, quantum chemical density functional theory (DFT) [70] calculations were undertaken. All calculations were performed with the DMol<sup>3</sup> DFT code [71-72] as implemented in Accelrys Materials Studio 5.0 [73]. Further details on the calculation method and procedure are presented in **Section 3.7**. The calculations involved the molecular modelling of each prepared ligand with a transition metal/counter ligand combination. The optimised or minimised geometry for each complex was found and the chelation angle measured. In total, five sets of calculations were performed for each of the twelve prepared ligands with the following metal/counter ligand combinations, (where L = prepared bidentate ligand):

1. [Ir(L)(H)(CO)(PPh<sub>3</sub>)]
2. [Ir(L)(cod)Cl]
3. [Ru(L)(H)<sub>2</sub>(CO)(PPh<sub>3</sub>)]
4. [Rh(L)(H)(CO)(PPh<sub>3</sub>)]
5. [Rh(L)(cod)Cl]

The above metal/counter ligand pairings were chosen since crystal structures of at least one xanthene family ligand was available for each combination, either from literature or determined in this work. The availability of ‘reference’ crystal structures was important as the results obtained from the calculations were very sensitive to the input geometry of the molecules. It was therefore important to have good estimates of the molecular structures of each complex. The starting geometries for each complex were estimated by either:

1. Importing the coordinates of a crystal structure of a metal complex, and then optimising the structure
2. Importing the coordinates of a crystal structure of a free ligand, optimising the structure of the free ligand, building the complex, and then optimising the structure of the complex
3. Building the free ligand, optimising the geometry of the free ligand, building the metal complex, optimising geometry of the metal complex

The choice of the estimation method depended on how close the properties of a modelled ligand or metal complex matched the reference crystal structures. In some instances, a combination of the above estimation

methods was used to obtain a good starting geometry. Not all calculations were successful. For example, those involving the large bite angle ligands DBFphos and isoproxantButylphos with the bulky cod counter ligands were problematic, and meaningful results were not obtained, i.e. unrealistic M-P bond lengths and bond angles were obtained. Therefore, these results have been omitted.

The successful geometry optimisation calculations yielded meaningful structures for each transition metal/counter ligand set. The P-M-P chelation angle was measured, and an average value calculated. The numerical results are presented in **Table 10**. The results are also presented graphically in **Figure 24**, with the *x* and *y* ordinates referring to the data from **Table 10**. From an analysis of the data in **Table 10** and **Figure 24**, the metal complexes with the cod counter ligands have calculated chelation angles in approximately the same range, and follow the same general trend or distribution. However, for the structures involving hydride counter ligands, only Ir and Rh complexes have similar trends. The Ru-H complexes display chelation angles similar to those of the cod containing complexes. A possible reason is that the geometry of the Ru-H complexes is dissimilar to the other transition metal hydrides and results in relatively lower chelation angles. From all calculations, the transition metal hydride complexes exhibited consistently higher chelation angles than the cod complexes. This is consistent with the bite angles characterised in the X-ray crystal structures discussed previously.

A graphical comparison of the average metal preferred bite angle and natural bite angle is presented in **Figure 25**. Qualitative analysis reveals that both sets of data follow the same general trend. This supports the assumptions of Casey and Whiteker regarding the natural bite angle calculations as the molecular mechanics method yields similar trends to the computationally more complex quantum chemical calculations. An interesting trend is that as the bite angles increase, the difference between the average calculated metal preferred and natural bite angle also increases, albeit slightly. If the metal preferred values are assumed to be a more realistic representation of the chelation angle, then this can be seen as a shortcoming of the molecular mechanics method which tends to overestimate bite angles for ligands with bulky alkyl substituents or co-planar phenyls by overestimating the repulsive interactions of alkyl groups or  $\pi$ -stacking interactions of aromatic groups [65].

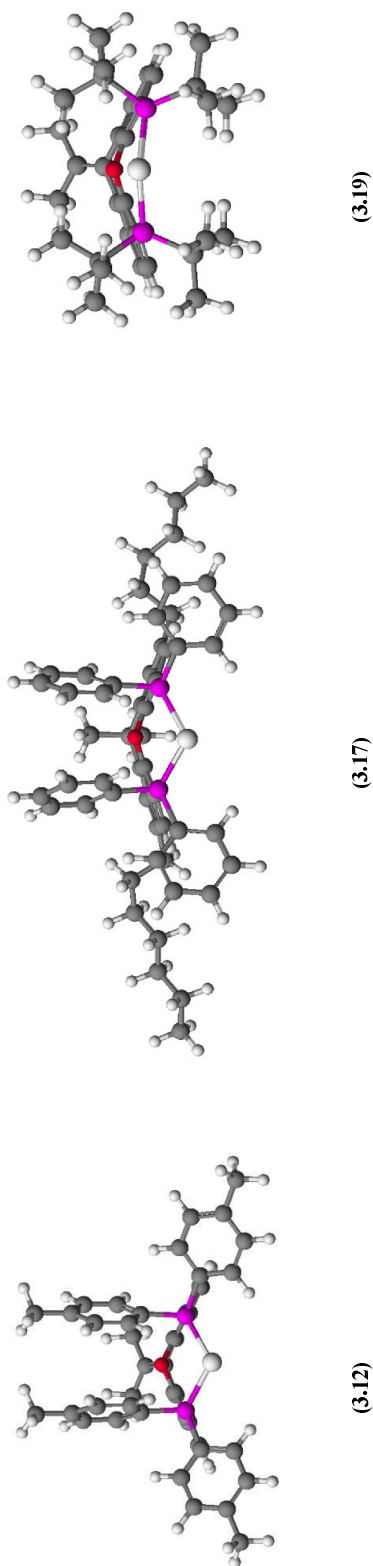


Figure 23. Geometry optimised structures for ligands 3.12, 3.17, and 3.19.

Entry	Ligand	Ir(L)HCO(PPh <sub>3</sub> ) [°]	Ir(L)codCl [°]	Ru(L)(H) <sub>2</sub> CO(PPh <sub>3</sub> ) [°]	Rh(L)HCO(PPh <sub>3</sub> ) [°]	Rh(L)codCl [°]	Average [°]
1	DPEphos <b>3.21</b>	102.5	93.7	96.5	103.9	94.9	98.3
2	Phosxantphos <b>3.18</b>	107.9	101.0	101.0	108.2	98.7	103.3
3	PTEphos <b>3.22</b>	106.3	102.4	100.0	107.9	102.0	103.7
4	Sixantphos <b>3.13</b>	107.3	101.3	101.0	107.9	101.9	103.9
5	Thixantphos <b>3.16</b>	108.4	102.1	101.2	108.7	103.0	104.7
6	Xantphos <b>3.10</b>	108.8	102.3	102.3	110.2	103.3	105.4
7	IsopropxantTolylphos <b>3.12</b>	108.7	102.4	103.9	109.6	103.3	105.6
8	Isopropxantphos <b>3.11</b>	108.6	102.3	102.8	109.5	103.1	105.3
9	Nixantphos <b>3.15</b>	109.8	103.6	102.8	110.6	104.2	106.2
10	Hexantphos <b>3.17</b>	113.2	106.4	106.3	114.5	107.8	109.6
11	DBFphos <b>3.23</b>	116.0	-	109.9	116.2	-	114.1
12	IsopropxantButylphos <b>3.19</b>	123.5	-	118.3	119.7	-	120.5

Table 10. Calculated metal preferred bite angles.



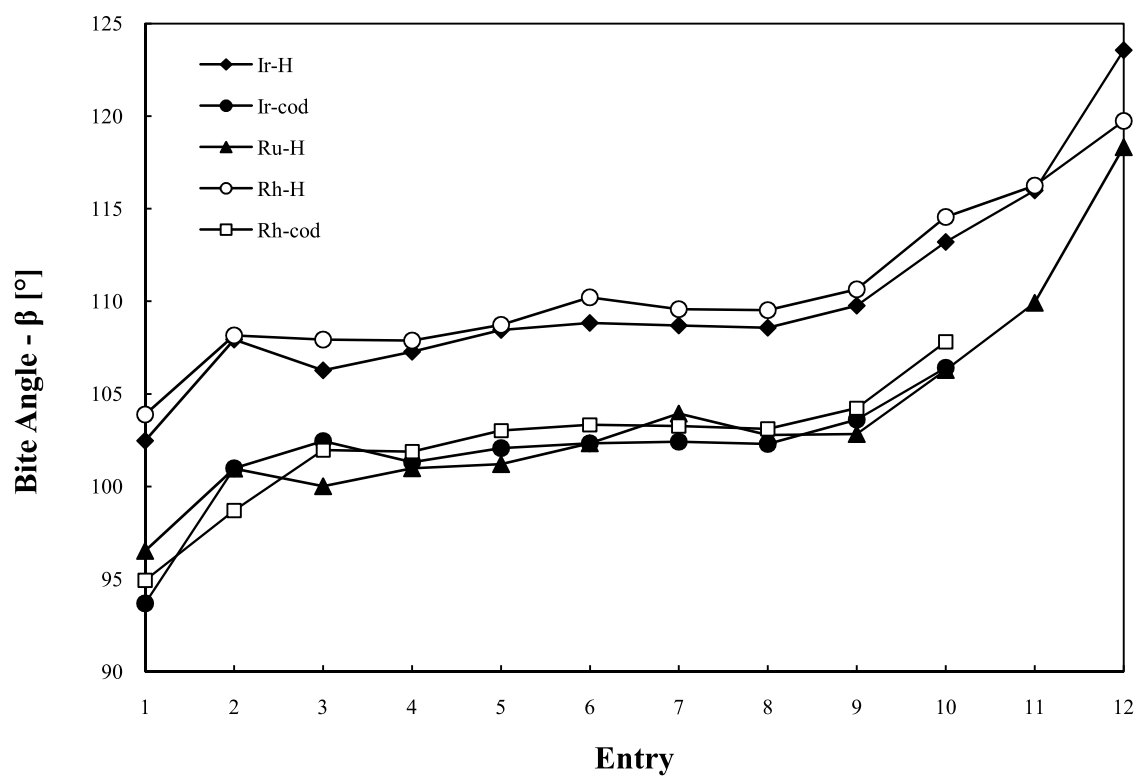


Figure 24. Metal preferred bite angle calculations for prepared bidentate ligands.

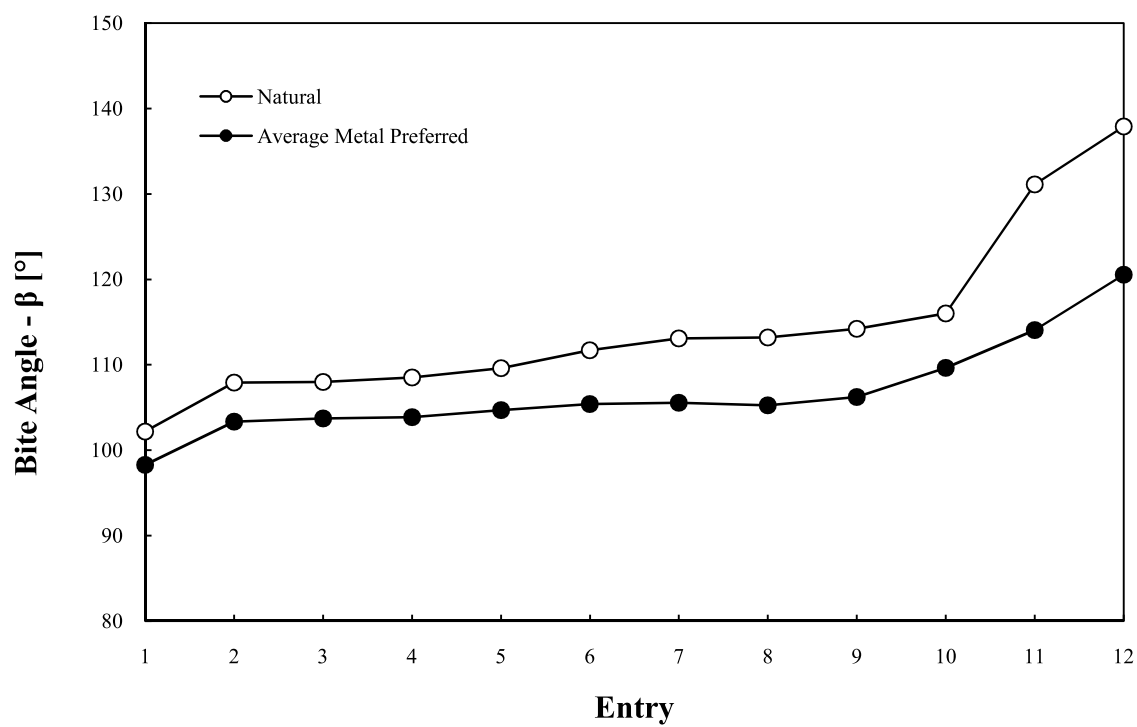


Figure 25. A comparison of the average metal preferred bite angle and natural bite angle.

## 3.7 Experimental

### 3.7.1 General

All reactions were performed under an inert atmosphere containing (UHP) grade gases nitrogen or argon. All solvents were distilled from an appropriate drying agent according to standard procedures. Hexane, THF, diethyl ether (Et<sub>2</sub>O), toluene, and benzene, were dried over sodium wire. Dichloromethane (DCM) was dried over phosphorous pentoxide, and ethanol (EtOH) and methanol (MeOH) were dried over magnesium turnings/iodine. Dried solvents were stored over 3 Å and 4 Å molecular sieves.

Triphenylphosphine (99%), *p*-toluenesulfonic acid monohydrate (98%), *tert*-butyldimethylsilylchloride (97%), tetra-*n*-butylammonium fluoride trihydrate (TBAF, 98%), 1.6M solution in hexanes of *n*-Butyllithium (*n*BuLi), phenoxazine (97%), imidazole (99%), sodium hydride (NaH, 60% dispersed in mineral oil), 9,9-dimethylxanthene (96%), di-*p*-tolylether, diphenyl ether (99%), xanthone (97%), hydrazine monohydrate (98%), and di-*tert*-butylchlorophosphine (96%) were sourced from Sigma-Aldrich. *N,N,N',N'*-tetramethylethylenediamine (TMEDA, 99%) was purchased from Sigma Aldrich, distilled over lithium aluminium hydride, and stored under Ar. Dibenzofuran (97%), phosphorus trichloride (PCl<sub>3</sub>, 99%), hexanoyl chloride (98%), and dichlorophenylphosphine (PPhCl<sub>2</sub>, 98%) were purchased from Merck and used as received. Chlorodiphenylphosphine (97%) was purchased from Sigma Aldrich, distilled under vacuum, and stored under Ar. Chloro-di(*p*-tolyl)phosphine (95%) and chlorodiaminoisopropyldiphosphine (95%) were purchased from Alfa Aesar and used as obtained. For column chromatography, Silica gel 60 and F<sub>254</sub> thin layer chromatography (TLC) silica gel plates were purchased from Merck. Hydrated iridium chloride, ruthenium chloride, rhodium chloride, and osmium tetroxide were donated by Johnson and Matthey.

### 3.7.2 Instrumentation

NMR spectra were recorded on Varian Gemini 300 MHz, and Varian Inova 400 MHz spectrometers, as well as the Bruker AVANCE 600 MHz, and 400 MHz NMR spectrometers. The <sup>1</sup>H NMR are presented as: chemical shift (δ, reported in ppm and referenced to the respective solvent peak CDCl<sub>3</sub> [7.24 ppm], [d<sup>6</sup>]-DMSO [2.49 ppm], [d<sup>6</sup>]-benzene [7.15 ppm], multiplicity, number of protons, coupling constants (<sup>3</sup>J or ortho coupling ~ 7-8, and <sup>4</sup>J or meta coupling ~ 2 Hz for aromatic protons in the ring). The proton decoupled <sup>13</sup>C NMR listed as: chemical shift (δ, reported in ppm and referenced to the respective solvent peak CDCl<sub>3</sub> [77.0 ppm], [d<sup>6</sup>]-DMSO [39.5 ppm], [d<sup>6</sup>]-benzene- [128.0 ppm], [d<sup>8</sup>]-toluene [20.4 ppm], multiplicity (due to C-P spin coupling), number of carbons, coupling constants.

Infrared spectra were recorded on a Perkin Elmer Attenuated Total Reflectance (ATR) spectrometer. Only the significant wavenumbers in cm<sup>-1</sup> are reported, where m = medium, w = weak, s = strong, b = broad, vs = very strong.

Elemental analyses were performed on a LECO CHNS elemental analyser. The analyses were performed for the carbon, nitrogen, sulphur, and hydrogen channels only. Melting points were recorded using a Stuart Scientific melting point apparatus and are uncorrected. Differential scanning calorimetry (DSC) measurements ( $\text{Al}_2\text{O}_3$  reference standard) were performed on a Shimadzu DSC-60 at a heating rate of  $10\text{ }^\circ\text{C min}^{-1}$ .

High resolution mass spectrometry was carried out on a LCMS Waters LCT Premier TOF (Time of Flight) mass spectrometer using direct infusion. High resolution mass spectrometric data were also obtained using a Bruker micrOTOF-Q II instrument operating at ambient temperatures, under electron spray ionisation conditions (ESI), using a sample concentration of approximately 1 ppm.

All microwave mediated reactions were conducted using a CEM Discover microwave. Temperature measurements were conducted using an infrared temperature sensor situated below the reaction vessel. Reaction times refer to the total hold time at the indicated temperature with the ramp times ranging from 1 to 2 minutes. The microwave was calibrated for power and temperature by the supplier prior to laboratory experiments.

Single-crystal structure determination by X-ray diffraction was performed on a Bruker APEXII CCD area-detector diffractometer with graphite monochromated  $\text{Mo } K_\alpha$  radiation (50kV, 30mA) using the APEX 2 [74] data collection software. Data reduction was carried out using the *SAINT+* [75] software. The crystal structure was solved by direct methods using *SHELXTL* [76].

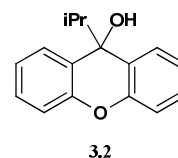
All geometry optimisation calculations were performed with the DMol<sup>3</sup> DFT code [71-72,77] as implemented in Accelrys Material Studio 5.0 on 3GHz Intel Pentium IV computers with 1GB RAM. The non-local generalized gradient approximation (GGA) functional by Perdew and Wang (PW91) [78] was used for all geometry optimisations. The convergence criteria for these optimisations consisted of threshold values of  $2\times 10^{-5}$  Ha, 0.004Ha/Å and 0.005Å for energy, gradient and displacement convergence, respectively, while a self-consistent field (SCF) density convergence threshold value of  $1\times 10^{-5}$  Ha was specified. DMol<sup>3</sup> utilizes a basis set of numeric atomic functions, which are exact solutions to the Kohn–Sham equations for the atom. In this study a polarized split valence basis set, termed double numeric polarized (DNP) basis set has been used.

The specifications of the cluster were as follows: 52 CPU cluster (HP Proliant CP4000 Linux Beowulf with Procurve Gb/E Interconnect on compute nodes. 1× Master node: HP DL385 – 2×2.8 MHz AMD Opteron 64, 2 GB RAM, 2×72 GB HDD. 12× Compute nodes: HP DL145G2 – 2×2.8 MHz, AMD Opteron 64, 2 GB RAM, 2×36 GB HDD. Operating system on compute nodes: Redhat Enterprise Linux 4, Cluster operating system: HPC CMU v3.0 cluster.

### 3.7.3 Experimental Methods

#### 9-isopropyl-9H-xanthen-9-ol (3.2)

The synthesis was adapted from literature [7]. To 25 mL of freshly distilled Et<sub>2</sub>O, 2-bromopropane (8.4 mL, 89.2 mmol) was added, and the solution cooled to 0 °C under positive Ar pressure. To this solution, Mg turnings (2.2 g, 89.2 mmol) were added in small portions as a safety measure. After 30 min the solution turned murky white, and once all Mg turnings were added the reaction was left to stir under positive pressure of Ar for 30 min while the temperature was maintained at 0 °C. Thereafter a solution of xanthone (3.5 g, 17.8 mmol) in 25 mL of dry Et<sub>2</sub>O was added portion wise to the chilled Grignard reagent solution. Xanthone is not completely soluble in Et<sub>2</sub>O, therefore dropwise addition was not possible. After the addition of xanthone (30 min), the reaction was allowed to warm to room temperature and the solution refluxed for 1 h. The reaction was left to cool to room temperature, diluted with Et<sub>2</sub>O (40 mL), and the solution cooled to 0 °C. The reaction was quenched by dropwise addition of a saturated ammonium chloride solution. The solution was filtered, washed with Et<sub>2</sub>O and the organic layer extracted thrice with Et<sub>2</sub>O. The combined fractions were dried over anhydrous magnesium sulphate. After removal of solvent, the yellow viscous oil was passed through a short silica column and the product obtained via hexane/ Et<sub>2</sub>O (90/10) solvent elution. The product was dried under vacuum to give compound **3.2** that was used without further purification.



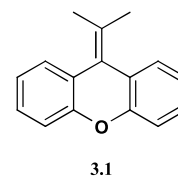
Yield:	68 % (3.5 g white crystals)
mp:	69–70 °C
TLC:	<i>R<sub>f</sub></i> 0.5 (hexane/EtOAc 90/10).
<sup>1</sup> H NMR (400 MHz, CDCl <sub>3</sub> , δ):	7.66 (dd, <sup>3</sup> <i>J</i> (H,H) = 7.8, <sup>4</sup> <i>J</i> (H,H) = 1.6 Hz, 2H), 7.29 (ddd, <sup>3</sup> <i>J</i> (H,H) = 8.1, 7.3, <sup>4</sup> <i>J</i> (H,H) = 1.7 Hz, 2H), 7.18 – 7.07 (m, 4H), 2.22 (s, 1H; OH), 2.10 (m, 1H; –CH(CH <sub>3</sub> ) <sub>2</sub> ), 0.71 (d, <i>J</i> = 6.8 Hz, 6H; –CH(CH <sub>3</sub> ) <sub>2</sub> ).
<sup>13</sup> C NMR (101 MHz, CDCl <sub>3</sub> , δ):	151.0 (CO), 128.6 (C), 126.9 (CH), 126.7 (CH), 123.0 (CH), 115.8 (CH), 72.1 (C), 42.6 (–CH(CH <sub>3</sub> ) <sub>2</sub> ), 16.8 (–CH(CH <sub>3</sub> ) <sub>2</sub> ).
IR ν <sub>max</sub> (cm <sup>–1</sup> ):	3331 (s), 2981 (w), 2960 (m), 2932 (m), 2874 (m), 1601 (m), 1575 (m), 1473 (m), 1447 (s), 1020 (s), 1285 (s), 743 (s).
HRESIMS (m/z):	[M – OH] <sup>+</sup> calcd for C <sub>16</sub> H <sub>15</sub> O, 223.1117; found, 223.1117.

#### 10-Isopropylidenexanthene (3.1)

##### Method A

To 30 mL of dry DCM, compound **3.2** (3.0 g, 12.5 mmol) was added, and once dissolved two equivalents of anhydrous *p*-toluenesulfonic acid monohydrate (4.8 g, 25.0 mmol) were added. The reaction was refluxed for 2 h and monitored by TLC. The reaction was left to cool to room temperature, 10 mL of deionised water added,

and 15 mL of 10% sodium hydroxide solution added slowly. The organic layers were extracted with DCM (3 x 15 mL), combined fractions dried over anhydrous magnesium sulphate, and the solid concentrated by rotary evaporation. The product was chromatographed on silica with 100% hexane.



Yield: 81% (2.2 g yellow solid)  
mp: 78 °C (lit.[ref] mp 78–80 °C)  
TLC:  $R_f$  0.6 (hexane)  
 $^1\text{H}$  NMR (400 MHz,  $\text{CDCl}_3$ ,  $\delta$ ): 7.38 (dd,  $^3J(\text{H,H}) = 7.6$ ,  $^4J(\text{H,H}) = 1.3$  Hz, 2H), 7.17 (m, 4H),  $\delta$  7.09 (td,  $^3J(\text{H,H}) = 7.6$ ,  $^4J(\text{H,H}) = 1.5$  Hz, 2H), 2.09 (s, 6H;  $\text{C}=\text{C}(\text{CH}_3)_2$ ).  
 $^{13}\text{C}$  NMR (101 MHz,  $\text{CDCl}_3$ ,  $\delta$ ): 154.2 (CO), 130.7 (C), 128.4 (CH), 127.1 (CH), 126.9 (C), 122.4 (– $\text{C}=\text{C}(\text{CH}_3)_2$ ), 122.4 (CH), 116.2 (CH), 23.2 (– $\text{C}=\text{C}(\text{CH}_3)_2$ ).  
IR  $\nu_{\text{max}}$  ( $\text{cm}^{-1}$ ): 3067 (w), 3035 (w), 2938 (m), 2905 (m), 2852 (m), 1595 (w), 1471 (w), 1441 (m), 1250 (m), 1211 (2), 1195 (w), 744 (vs).

#### Method B [6]

The Grignard reaction as for **3.2** was done on a smaller scale using (0.5 g, 2.5 mmol) xanthone. The reaction was cooled to room temperature, 2.5 g ice added, followed by the slow addition of 6.3 mL of chilled 0.5 M  $\text{H}_2\text{SO}_4$ . The resulting green-yellow syrup solution was transferred to a separating funnel, and the bottom layer removed and extracted with ether. Thereafter, the ether was evaporated and a further 2.5 mL of acid added to the mixture. The reaction was left to boil rapidly for 4 hours.

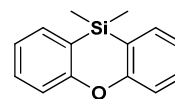
Thereafter the reaction was cooled and the organic layer extracted into ether. The combined fractions were filtered and dried over anhydrous magnesium sulphate. Evaporation of the solvent yielded a thick oil. The product was purified by column chromatography (silica).

#### Method C [7]

To 12 mL of DCM, compound **3.2** (0.5g, 2.2 mmol) was added, and the solution cooled to 0 °C. Thereafter, trifluoroacetic acid (1.7 mL, 22.4 mmol) was added over 5 min. When the solution reached room temperature trifluoroacetic acid (1.7 mL, 22.4 mmol) was further added dropwise over 10 min. The reaction was quenched with solid anhydrous potassium carbonate, the mixture diluted with DCM (15 mL), and washed with water. The aqueous layer was extracted once more with DCM before all fractions were combined and dried over anhydrous magnesium sulphate. The solvents were removed under reduced pressure to give a yellow residue. This was filtered through a short silica column and eluted with 100% hexane to give 0.1 g of **3.1**.

### 10,10-Dimethylphenoxasilin (3.3)

The synthesis was adapted from literature [10]. To a dry argon filled Schlenk tube, diphenyl ether (4.0 g, 23.5 mmol) was added and co-evaporated with toluene. After drying under high vacuum for 3 h, 16 mL of degassed dry THF was added via a cannula. The resulting solution was then added dropwise to a second solution containing *n*-butyllithium (1.6 M, 32 mL, 51.7 mmol) in hexanes and TMEDA (1.9 mL, 51.7 mmol). Once all of the diphenyl ether was added, the reaction was allowed to stir for 16 h under positive Ar pressure. Thereafter, the resulting solution and a third solution of dimethyldichlorosilane (2.8 mL, 23.5 mmol) in 60 mL of dry degassed Et<sub>2</sub>O were added simultaneously dropwise to a further solution of Et<sub>2</sub>O (20 mL) over a period of 1 h. The resulting reaction mixture was left to stir for a further 16 h. The reaction was hydrolysed with 15 mL of deionised water and left to stir for 2 h. Thereafter, the organic layer was separated, and the aqueous layer extracted with ether (3 x 15 mL). All organic layers were combined, treated with activated charcoal, filtered, dried over anhydrous magnesium sulphate, and filtered again. The filtrate was washed and concentrated to give dark brown grassy-odour oil. The crude product was filtered over a short plug of silica and recrystallised from methanol (-20 °C) to afford a white solid, that upon standing at room temperature melted to an oil.

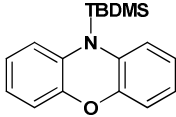


3.3

Yield:	41% (1.9 g white semi solid)
TLC:	$R_f$ 0.6 (hexane).
<sup>1</sup> H NMR (400 MHz, CDCl <sub>3</sub> , δ):	7.51 (d, <sup>3</sup> <i>J</i> (H,H) = 7.1 Hz, 2H), 7.43 – 7.37 (m, 2H), 7.17 (d, <sup>3</sup> <i>J</i> (H,H) = 8.1 Hz, 2H), 7.13 (t, <sup>3</sup> <i>J</i> (H,H) = 6.7 Hz, 2H), 0.47 (s, 6H).
<sup>13</sup> C NMR (101 MHz, CDCl <sub>3</sub> , δ):	159.6 (CO), 133.8 (CH), 131.1 (CH), 122.5 (CH), 119.1 (C–Si), 117.9 (CH), 0.45 (–(CH <sub>3</sub> ) <sub>2</sub> Si).
IR $\nu_{\max}$ (cm <sup>-1</sup> ):	3065 (m), 3002 (m), 2952 (m), 1591 (m), 1264 (s), 1573 (m), 1460 (s), 1420 (s), 1297 (s), 1216 (s), 1129 (s), 780 (s), 751 (s).

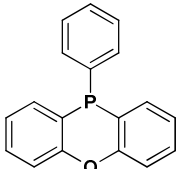
### 10-(*t*-butyldimethylsilyl) phenoxazine (3.4)

The preparation of **3.4** was adapted from Petrassi et al. [11]. A solution of phenoxazine (5.0 g, 27.3 mmol) in degassed freshly distilled THF (250 mL) was cooled to 0 °C in an ice/H<sub>2</sub>O bath. Under a positive flow of nitrogen the Schlenk tube was charged with NaH (1.6 g, 40.9 mmol). The reaction mixture was allowed to slowly warm to room temperature and the solution refluxed for 2 hrs. The reaction mixture was thereafter allowed to cool to room temperature. A solution of *t*-butyldimethylsilylchloride (6.2 g, 40.5 mmol) in 40 mL of degassed THF was added and the reaction mixture allowed to reflux overnight. The reaction mixture was cooled and poured into an ice/H<sub>2</sub>O slurry (250 mL). The organic layer was extracted with ethyl acetate (4 x 100 mL). The combined fractions were dried over anhydrous magnesium sulphate, filtered, and the solvent removed in vacuo to afford a light brown residue. The crude product was chromatographed on silica gel and the colourless oil recrystallised from hexane.

Yield:	62% (1.9 g white semi solid)	 3.4
mp:	55–56°C (lit. [11] mp 55–56 °C)	
TLC:	$R_f$ 0.9 (hexane/EtOAc 95/5).	
$^1\text{H}$ NMR (400 MHz, $\text{CDCl}_3$ , $\delta$ ):	6.90 – 6.84 (m, 8H), 0.94 (s, 9H, –(CH <sub>3</sub> ) <sub>3</sub> C-Si), 0.24 (s, 6H, –(CH <sub>3</sub> ) <sub>2</sub> Si).	
$^{13}\text{C}$ NMR (101 MHz, $\text{CDCl}_3$ , $\delta$ ):	151.5 (CO), 134.0 (CN), 123.2 (CH), 123.1 (CH), 122.0 (C), 116.0 (CH), 27.3 –C(CH <sub>3</sub> ) <sub>3</sub> , 20.2 –(CH <sub>3</sub> ) <sub>3</sub> C-Si, -2.57 –(CH <sub>3</sub> ) <sub>2</sub> Si.	
IR $\nu_{\text{max}}$ (cm <sup>-1</sup> ):	3062 (w), 2952 (m), 2937 (m), 1495 (m), 1466 (vs), 1452 (m), 1285 (m), 1259 (vs), 1230 (s), 1284 (m), 837 (s), 813 (s), 740 (s).	

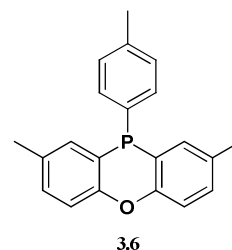
### 10-phenylphenoxaphosphine (3.5)

The synthesis was adapted from literature [14]. Diphenyl ether was co-evaporated three times with toluene in a dry argon filled Schlenk tube and left to dry under vacuum for 3 h. Thereafter, degassed Et<sub>2</sub>O (50 mL) was cannulated into the reaction tube and TMEDA (5.3 mL, 35.3 mmol) added. Under a positive Ar atmosphere, *n*-butyllithium (22 mL, 35.3 mmol) was added dropwise. After 5 h of stirring, phenylphosphorus dichloride (3.2 mL, 16.6 mmol) was added dropwise over 1 h. The yellow solution turned bright yellow and was left to stir for 1 h at room temperature. Degassed water (15 ml) was added dropwise to slowly quench the reaction mixture. The organic layer was separated, the aqueous layer extracted once more, and the combined organic fractions dried over anhydrous magnesium sulphate and filtered. The filtrate was evaporated under reduced pressure and afforded an orange viscous oil, that was purified by column chromatography (silica) using 0-5% ethyl acetate in hexane as the eluent. Compound **3.5** was obtained as white crystals after recrystallisation from absolute ethanol.

Yield:	43% (2.1 g white crystals)	 3.5
mp:	95°C (lit.[53] mp 95 °C)	
TLC:	$R_f$ = 0.5 (hexane/EtOAc 95/5)	
$^1\text{H}$ NMR (400 MHz, $\text{C}_6\text{D}_6$ , $\delta$ ):	$\delta$ 7.13 (ddd, $^2J(\text{P,H}) = 10.2$ , $^3J(\text{H,H}) = 7.5$ , $^4J(\text{H,H}) = 1.7$ Hz, 2H), 7.06 – 6.98 (m, 2H), 6.80 (d, $^3J(\text{H,H}) = 8.2$ Hz, 2H), 6.69 (ddd, $^2J(\text{P,H}) = 8.3$ , $^3J(\text{H,H}) = 7.3$ , $^3J(\text{H,H}) = 1.7$ Hz, 2H), 6.63 – 6.54 (m, 3H), 6.50 (tt, $J = 7.4$ , 1.4 Hz, 2H).	
$^{13}\text{C}$ NMR (101 MHz, $\text{C}_6\text{D}_6$ , $\delta$ ):	154.3 (C), 139.7 (d, $J(\text{P,C}) = 22.3$ Hz, C), 134.0 (CH), 133.7 (CH), 130.9 (CH), 130.7 (CH), 129.8 (CH), 127.7 – 127.0 (m, CH), 117.8 (d, $J(\text{P,C}) = 4.7$ Hz, C), 116.7 (CH).	
$^{31}\text{P}$ NMR (162 MHz, $\text{C}_6\text{D}_6$ ) $\delta$	-54.4	
IR $\nu_{\text{max}}$ (cm <sup>-1</sup> ):	3058 (m), 2923 (m), 2853 (w), 1562 (w), 1582 (m), 1460 (s), 1425 (s), 1299 (s), 1262 (vs), 1129 (m), 1074 (m), 883 (s), 743 (s).	

### 2,8-dimethyl-10-*p*-tolyl-10H-phenoxaphosphine (3.6)

The synthesis of **3.6** was modified from literature [15]. Under an inert nitrogen atmosphere  $\text{AlCl}_3$  (2.5 g, 18.9 mmol) was added to di-*p*-tolylether (2.5 g, 12.6 mmol) in 9 mL  $\text{PCl}_3$ . The reaction mixture was refluxed for 8 h at 85 °C and thereafter the excess  $\text{PCl}_3$  distilled off at 90 °C. At this temperature, excess anhydrous toluene was added to the reaction mixture. The remaining  $\text{PCl}_3$  and toluene was distilled off at 110 °C to afford an orange-red residue. The residue was again diluted with 15 mL of toluene and cooled to 0 °C, followed by the dropwise addition of 3.6 mL pyridine to the mixture while stirring. After an hour, the resulting salts were filtered off and the yellow residue extracted with toluene. The solvent was removed in vacuo, and the crude product purified by filtration through a short plug of silica gel to yield **3.6** as an oil that solidified at room temperature.



Yield: 61% (2.5 g white crystals)

mp: 64-65 °C

TLC:  $R_f$  0.5 (hexane/EtOAc 70/30).

$^1\text{H}$  NMR (400 MHz,  $\text{C}_6\text{D}_6$ , 323 K)  $\delta$  7.44 – 7.36 (m, 2H, tolyl-CCHCH), 7.31 (dd,  $^2J(\text{P},\text{H}) = 10.6$ ,  $^3J(\text{H},\text{H}) = 2.2$  Hz, 2H, tolyl-CCHCH), 7.09 (d,  $^4J(\text{H},\text{H}) = 8.2$  Hz, 2H, CHCCH), 6.85 (ddd,  $^2J(\text{P},\text{H}) = 8.3$ ,  $^4J(\text{H},\text{H}) = 2.3$ ,  $^4J(\text{H},\text{H}) = 0.6$  Hz, 2H, CHCCH), 6.80 – 6.72 (m, 2H, CCHCH), 1.98 (s, 6H,  $\text{CH}_3$ ), 1.93 – 1.83 (m, 3H,  $\text{CH}_3$ ).

$^{13}\text{C}$  NMR (101 MHz,  $\text{C}_6\text{D}_6$ , 323 K)  $\delta$  153.9 (C), 138.9 (C), 138.5 - 138.3 (C), 135.5 - 135.2 (CH), 133.1 - 133.0 (C), 132.9 - 132.7 (CH), 131.8 (d,  $J(\text{P},\text{C}) = 0.5$  Hz, CH), 129.7 (d,  $J(\text{P},\text{C}) = 7.2$  Hz, CH), 119.5 (d,  $J(\text{P},\text{C}) = 4.3$  Hz, CCH $_3$ ), 117.9 (m, CH), 21.0 (s,  $\text{CH}_3$ ), 20.4 (s,  $\text{CH}_3$ ).

$^{31}\text{P}$  NMR (162 MHz,  $\text{CDCl}_3$ )  $\delta$  -53.2

IR  $\nu_{\text{max}}$  ( $\text{cm}^{-1}$ ): 3009(w), 2920(m), 1585(m), 1489(s), 1466(w), 1385(w), 1295(m), 1265(w), 1231(w), 1215(w), 810(vs), 715(m).

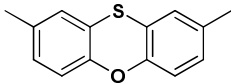
HRESIMS (m/z):  $[\text{M} + \text{O}]^+$  calcd for  $\text{C}_{21}\text{H}_{20}\text{O}_2\text{P}$ , 335.1195; found, 335.1198

### 2,8-Dimethylphenoxathiin (3.7)

The synthesis of **3.7** was adapted from literature [17]. A dry Schlenk tube was charged with di-*p*-tolyl ether (10 g, 50.4 mmol) and heated until all the solid had melted. Anhydrous aluminium chloride (70.6 mmol, 9.3 g), and sulphur (1.6 g, 50.4 mmol), were added to the Schlenk tube and the mixture heated to 100 °C for 17 h while stirring under argon. Thereafter, the slightly thickened reaction mixture was cooled and 18 mL of chilled 10% HCl solution added slowly. The resulting green solution was left to stir for 2 h at room temperature, diluted with  $\text{Et}_2\text{O}$  (30 mL), and the organic layer extracted with  $\text{Et}_2\text{O}$  (3 x 40 mL). The organic layer fractions were dried over anhydrous magnesium sulphate, filtered, and the solvent removed in vacuo. The resulting green oil

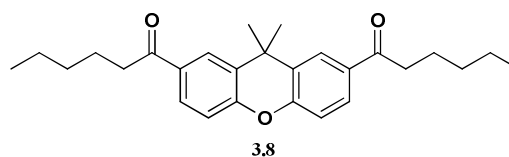


was filtered over a short plug of silica with 100% hexane elution. Two spots co-eluted, the product and the unreacted *p*-tolylether with  $R_f$  of 0.6 and 0.5 respectively. Thereafter, the fractions were concentrated and the di-*p*-tolyl ether distilled off (110 to 115 °C) using high vacuum distillation and a 3 way pig collector until only the product remained. The collected distillate was monitored by  $^1\text{H}$  NMR.

Yield:	26% (1.8 g white solid)	 3.7
mp:	69°C (lit [17] mp 69 - 71 °C)	
TLC:	$R_f$ 0.6 (hexane).	
$^1\text{H}$ NMR (400 MHz, $\text{CDCl}_3$ , $\delta$ ):	7.11 – 6.77 (m, 6H), 2.24 (s, 6H).	
$^{13}\text{C}$ NMR (101 MHz, $\text{CDCl}_3$ , $\delta$ ):	150.1 (CO), 133.9 (C), 128.1 (CH), 127.0 (CH), 119.6 (CS), 117.3 (CH), 20.5 ( $\text{CH}_3$ ).	
IR $\nu_{\text{max}}$ ( $\text{cm}^{-1}$ ):	3065 (m), 3002 (m), 2952 (m), 1592 (m), 1574 (m), 1461 (m), 1420 (vs) 1297 (m), 1264 (m), 1216 (m), 1129 (s), 780 (m), 751 (s).	

### 2,7-di-*n*-hexanoyl-9,9-dimethylxanthene (3.8)

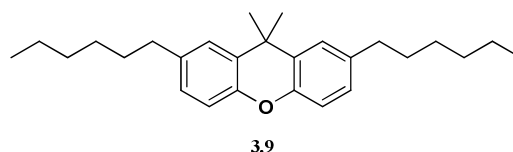
Compound **3.8** was prepared according to literature methods [15]. A solution of 9,9-dimethylxanthene (1.0 g, 4.8 mmol) and hexanoyl chloride (1.6 mL, 11.4 mmol) in DCM (20 mL) was cooled to 0 °C. In a well ventilated fumehood,  $\text{AlCl}_3$  (1.5 g, 11.4 mmol) was slowly added while the solution stirred under nitrogen atmosphere. The reaction was allowed to warm to room temperature and left to stir for 5 h. Thereafter, the solution was poured into chilled water (20 mL) and the organic fraction extracted with DCM (3 x 20 mL). The fractions were combined and dried over anhydrous magnesium sulphate. The filtrate was concentrated under reduced pressure to give a yellow residue. The crude product was chromatographed on silica gel with 0-10% ethyl acetate in hexane to afford a yellow solid.



Yield:	94% (1.8 g yellow crystals)
mp:	85 °C
TLC:	$R_f$ 0.6 (hexane/EtOAc 95/5)
$^1\text{H}$ NMR (400 MHz, $\text{CDCl}_3$ , $\delta$ ):	8.09 (d, $^4J(\text{H,H}) = 2.0$ Hz, 2H), 7.82 (dd, $^3J(\text{H,H}) = 8.5$ , $^4J(\text{H,H}) = 2.0$ Hz, 2H), 7.09 (d, $^3J(\text{H,H}) = 8.5$ Hz, 2H), 2.93 (t, $J = 7.4$ Hz, 4H), 1.85 – 1.68 (m, 5H), 1.68 (s, 3H), 1.42 – 1.21 (m, 8H), 0.90 (t, $J = 7.1$ Hz, 6H).
$^{13}\text{C}$ NMR (101 MHz, $\text{CDCl}_3$ , $\delta$ ):	199.2 (C=O), 153.2 (CO), 133.0 (C), 129.9 (C), 128.2 (CH), 127.1 (CH), 116.6 (CH), 38.4 (C), 34.2 ( $\text{CH}_2$ ), 32.9 ( $\text{CH}_2$ ), 31.6 ( $\text{CH}_3$ ), 24.2 ( $\text{CH}_2$ ), 22.6 ( $\text{CH}_2$ ), 14.0 ( $\text{CH}_3$ ).
IR $\nu_{\text{max}}$ ( $\text{cm}^{-1}$ ):	3060 (w), 2958 (m), 2958 (m), 2933 (s), 2868 (m), 1681 (vs), 1595 (s), 1483 (m), 1467 (m), 1360 (m), 1266 (m), 1249 (m), 809 (vs), 725 (s).

### 2,7-di-*n*-hexyl-9,9-dimethylxanthene (3.9)

Compound **3.9** was prepared according to literature methods [15]. Triethyleneglycol (15 mL) and compound **3.8** (1.7 g, 4.2 mmol) were added to a dry Schlenk tube fitted with a condenser. To this stirred suspension, NaOH (1.0 g, 25.1 mmol) and hydrazine monohydrate (1.6 mL, 33.2 mmol) were added and the reaction mixture heated using an oil bath with high temperature silicon oil. Compound **3.8** dissolved at 110 °C under gentle reflux for 1 h. The reflux condenser was removed and the reaction heated to 196 °C. At this temperature the condenser was reattached and the mixture refluxed for 3 h at 220 °C. The reaction colour varied from bright yellow to orange and after 3 h a yellow solution was present. The reaction mixture was cooled to room temperature, diluted with DCM (20 mL), and washed with 10% aqueous HCl solution (3 x 10 mL). The product was purified on a silica gel column with 100% hexane elution.



Yield:	41% (0.65 g white crystals)
mp:	136 °C
TLC:	$R_f$ 0.5 (hexane)
$^1\text{H}$ NMR (400 MHz, $\text{CDCl}_3$ , $\delta$ ):	7.18 (d, $^4J(\text{H,H}) = 1.5$ Hz, 2H), 6.99 (dd, $^3J(\text{H,H}) = 8.3$ , $^4J(\text{H,H}) = 1.8$ Hz, 2H), 6.93 (d, $^3J(\text{H,H}) = 8.2$ Hz, 2H), 2.57 (t, $J = 7.5$ Hz, 4H), 1.77 – 1.53 (m, 10H), 1.42 – 1.15 (m, 12H), 0.88 (t, $J = 6.6$ Hz, 6H).
$^{13}\text{C}$ NMR (101 MHz, $\text{CDCl}_3$ , $\delta$ ):	$\delta$ 148.6 (CO), 137.2 (C), 129.7 (C), 127.2 (CH), 125.8 (CH), 116.0 (CH), 35.6 ( $\text{CH}_2$ ), 34.0 (C), 32.4 ( $\text{CH}_2$ ), 31.8 ( $\text{CH}_3$ ), 31.7 ( $\text{CH}_2$ ), 29.0 ( $\text{CH}_2$ ), 22.7 ( $\text{CH}_2$ ), 14.1 ( $\text{CH}_3$ ).
IR $\nu_{\text{max}}$ ( $\text{cm}^{-1}$ ):	3070 (w), 3054 (w), 2957 (m), 2922 (m), 2852 (m), 1585 (m), 1569 (m), 1432 (m), 1419 (s), 1240 (m), 737 (s), 692 (vs).

### A note on the NMR of xanthene family ligands

The NMR data for the xanthphos family ligands are presented in the following sections. Due to the large P-P coupling, certain general trends were observed. Considering the illustrative structure of the parent ligand xanthphos, **Figure 26a**, in the aromatic region of the  $^1\text{H}$  NMR the three neighbouring protons  $\text{H}^{1,8}$ ,  $\text{H}^{2,7}$  and  $\text{H}^{3,6}$  show a doublet of doublets **Figure 26b**, a triplet **Figure 26c**, and one ABCXX" system (X and X" =  $^{31}\text{P}$ ) of twofold intensity **Figure 26d**. Similar trends were observed for all xanthphos family ligands and are reported as such.

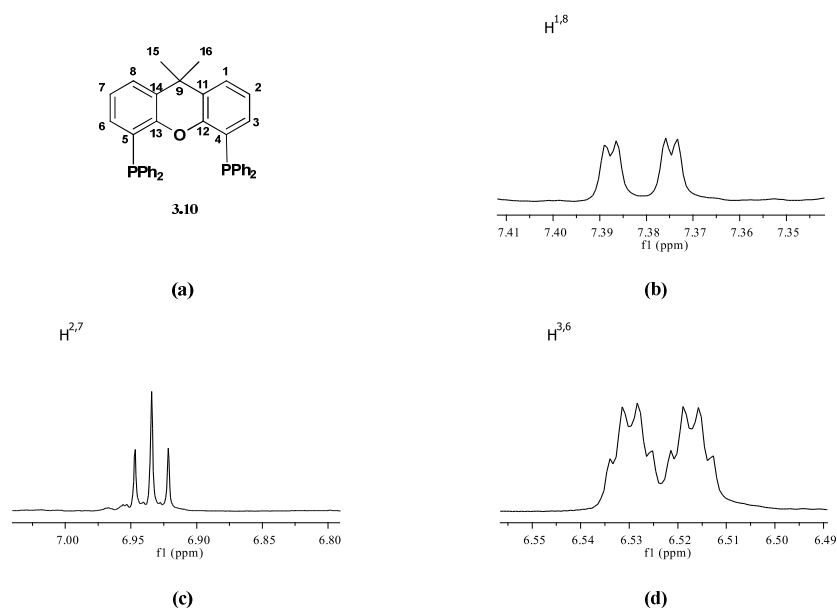


**Figure 26. General trend for the multiplets in the proton NMR spectrum of xantphos.**

Considering the expanded illustrative structure of the parent ligand xantphos in **Figure 27a**, multiplets in the  $^{13}\text{C}$  NMR spectrum were observed for the xanthene  $\text{C}^{12,13}$  **Figure 27b**, the phenyl  $\text{C}^{20}$  **Figure 27c**, the phenyl  $\text{C}^{21,25}$  **Figure 27d**, and the xanthene  $\text{C}^{4,-5}$  **Figure 27e**. These were analysed as AA'X-systems ( $A = A' = ^{31}\text{P}$ ,  $X = ^{13}\text{C}$ ) by Hillebrand et al. [24] and Kranenburg et al. [10], who suggested that the resonance is the result of a through-space coupling of the two phosphorus atoms. The orientation of the lone pairs of the two phosphorus atoms is such that it causes degeneracy of the magnetic resonances of the P nuclei. This results in some of the carbon atoms coupling to two equivalent P atoms giving rise to a virtual triplet. In certain ligands a doublet of doublets was also observed as the phosphorus nuclei are sensitive to other donors or atoms in the ligand. The virtual coupling behaviour was not observed for DPEphos and PTEphos due to the less rigid backbone, and also not observed for DBFphos due to the large bite angle.

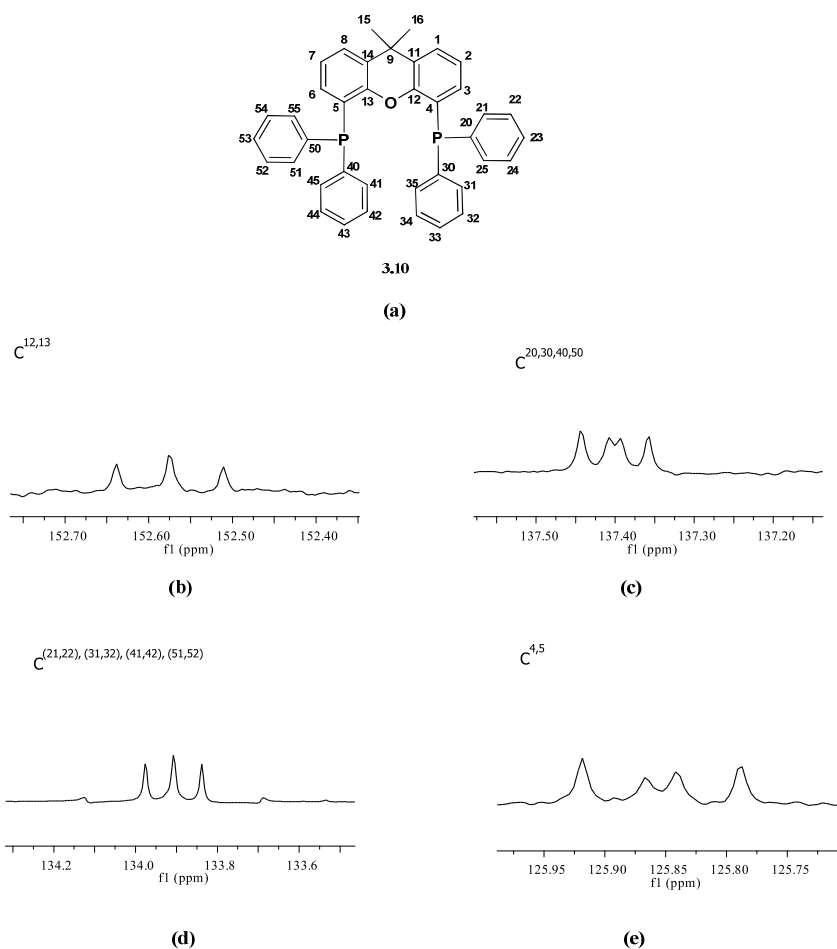
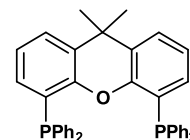


**Figure 27. General trend for the multiplets in the carbon NMR spectrum of xantphos.**

#### 4,5-bis(diphenylphosphino)-9,9-dimethylxanthene (**3.10**)

The synthesis of **3.10** was adapted from literature [3,10]. A solution of 9,9-dimethylxanthene (1.0 g, 4.8 mmol) and TMEDA (1.6 mL, 10.5 mmol) in 30 mL of dry degassed Et<sub>2</sub>O was cooled to 0 °C. To the chilled solution, *n*BuLi (6.6 mL, 10.5 mmol) was added dropwise.

The reaction mixture was allowed to warm to room temperature and left to stir for 16 h. The resulting dark orange reaction mixture was cooled to 0 °C and PPh<sub>2</sub>Cl (1.94 mL, 10.5 mmol) in 4 mL of dry hexane added dropwise. The reaction mixture slowly decolourised and a fine precipitate formed. The reaction was allowed to stir for a further 16 h. Thereafter, the reaction was slowly hydrolysed with 35 mL of 10% HCl/brine mixture (1/1). The organic layer was removed, and the aqueous layer extracted with DCM. The combined fractions were dried over anhydrous magnesium sulphate, filtered, and the volume reduced to give a yellow oil. The crude product was washed with hexane (3 x 15 mL), the oil dissolved in DCM, and an equal volume of ethanol added slowly. The solution was left to recrystallise at room temperature and the crystals filtered and dried under vacuum.

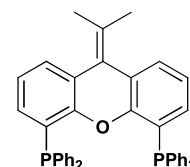


3.10

Yield:	58% (1.6 g white crystals).
mp:	221 °C (lit. [10] mp 221-222 °C dec)
$^1\text{H}$ NMR (400 MHz, $\text{CDCl}_3$ ) $\delta$ :	7.38 (dd, $^3J(\text{H,H}) = 7.8$ , $^4J(\text{H,H}) = 1.4$ Hz, 2H; CCHCH), 7.16-7.23 (m, 20H), 6.93 (t, $^3J(\text{H,H}) = 7.6$ Hz, 2H; CHCHCH), 6.52 (dq, $^3J(\text{H,H}) = 7.5$ , $^4J(\text{H,H}) = 1.6$ , $^2J(\text{P,H}) = 1.6$ Hz, 2H; CPCHCH), 1.63 (s, 6H).
$^{13}\text{C}$ NMR (151 MHz, $\text{CDCl}_3$ ) $\delta$ :	152.6 (t, $J(\text{P,C}) = 19.3$ Hz, CO), 137.4 (dd, $J(\text{P,C}) = 7.1$ , 5.7 Hz, phenyl C- <i>ipso</i> , PC), 133.9 (t, $J(\text{P,C}) = 10.4$ Hz, phenyl CH, PCCH), 132.1 (CH), 129.9 (C), 128.2 (CH), 128.1 (t, $J(\text{P,C}) = 6.8$ Hz, phenyl CH, PCCHCH), 126.3 (CH), 125.9 (dd, $J = 11.7$ , 7.9 Hz, CHCHC-P), 123.3 (CH), 34.4 (C), 31.8 ( $\text{CH}_3$ ).
$^{31}\text{P}$ NMR (162 MHz, $\text{CDCl}_3$ ) $\delta$ :	-18.0
IR $\nu_{\text{max}}$ ( $\text{cm}^{-1}$ ):	3056 (w), 2975 (w), 2951 (w), 1432 (s), 1399 (s), 1232 (s), 737 (m), 744 (s), 688 (s), 504 (s), 497 (s).
HRESIMS (m/z):	$[\text{M} + \text{H}]^+$ calcd for $\text{C}_{39}\text{H}_{33}\text{OP}_2$ , 579.2001; found, 579.2001

#### 4,5-Bis(diphenylphosphino)-9-isopropylidenexanthene (3.11)

Ligand **3.11** was prepared analogously to **3.10** using **3.1** (1.5g, 6.75 mmol), TMEDA (2.55 mL, 17.2 mmol), 1.6 M *n*BuLi (10.8 mL, 17.2 mmol), and  $\text{PPh}_2\text{Cl}$  (3.18 mL, 17.2 mmol) in 7.5 mL of dry hexane.

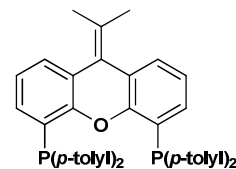


3.11

Yield:	52% (2.1 g yellow crystals)
mp:	214 °C (lit.[3] mp 214 °C dec)
$^1\text{H}$ NMR (400 MHz, $\text{CDCl}_3$ ) $\delta$ :	7.33 (dd, $^3J(\text{H,H}) = 7.6$ , $^4J(\text{H,H}) = 1.5$ Hz, 2H), 7.25 – 7.11 (m, 20H), 6.96 (t, $^3J(\text{H,H}) = 7.6$ Hz, 2H), 6.54 (dq, $^3J(\text{H,H}) = 7.6$ , $^4J(\text{H,H}) = 1.7$ , $^2J(\text{P,H}) = 1.7$ Hz, 2H), 2.07 (s, 6H).
$^{13}\text{C}$ NMR (101 MHz, $\text{CDCl}_3$ ) $\delta$ :	156.0 (t, $J(\text{P,C}) = 20$ Hz, CO), 137.2 (dd, $J(\text{P,C}) = 6.5$ , 6.0 Hz, phenyl C- <i>ipso</i> , PC), 134.0 (t, $J(\text{P,C}) = 21$ Hz, phenyl CH), 131.5 (CH), 131.3 (C), 128.2 (CH), 128.2 (t, $J(\text{P,C}) = 6.8$ Hz, phenyl CH), 126.3 (CH), 125.7 (dd, $J(\text{P,C}) = 1.9$ , 11 Hz, CHCHC-P), 122.8 (C), 122.7 (CH), 23.2 ( $\text{CH}_3$ ).
$^{31}\text{P}$ NMR (162 MHz, $\text{CDCl}_3$ ) $\delta$ :	-17.9
IR $\nu_{\text{max}}$ ( $\text{cm}^{-1}$ ):	3058 (m), 2931 (m), 1433 (s), 1477 (m), 1393 (s), 1221 (s), 1178 (s), 801 (m), 739 (m), 692 (m), 504 (s).
HRESIMS (m/z):	$[\text{M} + \text{H}]^+$ calcd for $\text{C}_{40}\text{H}_{33}\text{OP}_2$ , 591.2001; found, 591.2002.

#### 4,5-Bis(di-*p*-tolylphosphino)-9-isopropylidenexanthene (3.12)

Ligand **3.12** was prepared analogously to compound **3.10** using **3.1** (0.7g, 3.2 mmol), TMEDA (1.2 mL, 7.9 mmol), 1.6 M *n*BuLi (5.0 mL, 7.9 mmol) and chloro-di(*p*-tolyl)phosphine (1.8 mL, 7.9 mmol) in hexane (5 mL).

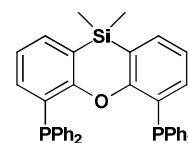


3.12

Yield:	50% (1.0 g yellow crystals)
mp:	182 °C
TLC:	$R_f$ 0.5 (hexane/EtOAc 95/5)
$^1\text{H}$ NMR (400 MHz, $\text{CDCl}_3$ , $\delta$ ):	7.38 (dd, $^3J(\text{H,H}) = 7.6$ , $^4J(\text{H,H}) = 1.3$ Hz, 2H), 7.17 (m, 4H), 7.09 (dquar, $^3J(\text{H,H}) = 7.6$ , $^4J(\text{H,H}) = 1.7$ , $^2J(\text{P,H}) = 1.6$ Hz 2H), 2.35 (s, 12H, $\text{CH}_3$ - $\text{C}_6\text{H}_4\text{P}$ ), 2.09 (s, 6H, $-\text{CCH}_3$ ).
$^{13}\text{C}$ NMR (101 MHz, $\text{CDCl}_3$ , $\delta$ ):	156.0 (t, $J(\text{P,C}) = 19.6$ Hz, CO), 137.9 (phenyl C- <i>ipso</i> , PC), 134.0 (m, phenyl CH), 133.9 (C- $\text{CH}_3$ ), 131.3 (CH), 131.0 (C), 129.0 (t, $J(\text{P,C}) = 7$ Hz, phenyl CH), 128.7 (CH), 126.4-126.2 (m, CHCHC-P), 126.1 (C) 123.0 C( $\text{CH}_3$ ) $_2$ , 122.5 (CH), 23.3 C( $\text{CH}_3$ ) $_2$ , 21.3 (phenyl- $\text{CH}_3$ ).
$^{31}\text{P}$ NMR (162 MHz, $\text{CDCl}_3$ ) $\delta$	-19.3
IR $\nu_{\text{max}}$ ( $\text{cm}^{-1}$ ):	3062 (w), 2966 (w), 2917 (w), 2860 (m), 1495 (m), 1420 (s), 1395 (s), 1222 (s), 1183 (m) 1199 (m), 798 (s), 756 (s), 504 (s)..
HRESIMS (m/z):	$[\text{M} + \text{H}]^+$ calcd for $\text{C}_{44}\text{H}_{41}\text{OP}_2$ , 511.3253; found, 511.3257.

#### 4,6-Bis(diphenylphosphino)-10,10-dimethylphenoxasilin (3.13)

Ligand **3.13** was prepared analogously to **3.10** using **3.3** (1.5 g, 6.6 mmol), TMEDA (2.6 mL, 16.9 mmol), *n*BuLi (11 mL, 16.9 mmol) and chlorodiphenylphosphine (3.1 mL, 16.9 mmol).



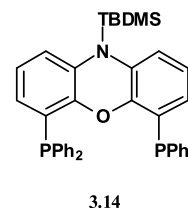
3.13

Yield:	43% (1.7 g white crystals)
mp:	245°C (lit. [10] mp 246 °C)
TLC:	$R_f$ 0.6 (hexane/EtOAc 95/5)
$^1\text{H}$ NMR (400 MHz, $\text{CDCl}_3$ , $\delta$ ):	7.40 (dd, $^3J(\text{H,H}) = 7.2$ , $^4J(\text{H,H}) = 1.7$ Hz, 2H), 7.21 – 7.07 (m, 20H), 6.91 (t, $^3J(\text{H,H}) = 7.3$ Hz, 2H), 6.70 (dquar, $^3J(\text{H,H}) = 7.6$ , $^4J(\text{H,H}) = 1.7$ , $^2J(\text{P,H}) = 1.8$ Hz, 2H), 0.41 (s, 6H).
$^{13}\text{C}$ NMR (101 MHz, $\text{CDCl}_3$ , $\delta$ ):	161.3 (t, $J(\text{P,C}) = 18.4$ Hz, CO), 138.1 (dd, $J(\text{P,C}) = 7.6$ , 6.2 Hz, phenyl C- <i>ipso</i> , PC), 136.5 (CH), 134.6 (CH), 134.0 (t, $J(\text{P,C}) = 10.6$ Hz, phenyl CH), 128.1 (m, phenyl CH), 128.0 (CH), 127.5 (dd, $J(\text{P,C}) = 12.3$ Hz, 10 Hz, CHCHC-P), 122.9 (CH), 118.7 (–CSi.), -0.23 (– $\text{CH}_3$ ) $_2$ Si.).
$^{31}\text{P}$ NMR (243 MHz, $\text{CDCl}_3$ ) $\delta$	-19.1

IR  $\nu_{\max}$  (cm<sup>-1</sup>): 3065 (w), 2891 (m), 2934 (m), 2856 (m), 1473 (m), 1456 (m), 1390 (s), 1360 (s), 1219 (s), 1176 (m), 797 (m), 758 (s).  
 HRESIMS (m/z): [M + H]<sup>+</sup> calcd for C<sub>38</sub>H<sub>33</sub>OP<sub>2</sub>Si, 595.1770; found, 595.1766.

#### 10-(*t*-butyldimethylsilyl)-4,6-bis(diphenylphosphino)phenoxazine (3.14)

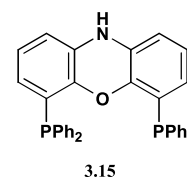
Compound **3.14** was prepared analogously to **3.10** using **3.4** (5.1 g, 17.0 mmol), TMEDA (6.2 mL, 40.7 mmol), *n*BuLi (25 mL of 1.6 M in hexane, 40.7 mmol), and chlorodiphenylphosphine (7.5 mL, 40.7 mmol) in hexane.



Yield: 63% (7.1 g white microcrystals)  
 mp: 157 °C (lit. [54] mp 159-160 °C)  
<sup>1</sup>H NMR (400 MHz, CDCl<sub>3</sub>, δ): 7.29 – 6.85 (m, 20H), 6.78 (d, <sup>3</sup>J(H,H) = 7.8 Hz, 2H), 6.70 (t, <sup>3</sup>J(H,H) = 7.7 Hz, 2H), 6.13 (d, <sup>3</sup>J(H,H) = 7.4 Hz, 2H), 0.76 (s, 9H), 0.20 (d, *J* = 13.5 Hz, 6H).  
<sup>13</sup>C NMR (101 MHz, CDCl<sub>3</sub>, δ): 153.8 (t, *J*(P,C) = 20.0 Hz, CO), 136.8 (t, *J*(P,C) = 6.0 Hz, phenyl *C-ipso*, PC), 136.6 (C), 133.9 (t, *J*(P,C) = 10.3 Hz, CH-phenyl), 128.2 (CH), 128.1 (t, *J*(P,C) = 3.4 Hz, CHCHC–P), 127.5 (CH), 126.1 – 125.2 (CH), 123.0 (CH), 122.7 (CH), 27.3 (s, CH<sub>3</sub>), 20.3 (C), -2.2 (CH<sub>3</sub>).  
<sup>31</sup>P NMR (243 MHz, CDCl<sub>3</sub>) δ -17.7  
 IR  $\nu_{\max}$  (cm<sup>-1</sup>): 2952 (m), 2936 (m), 2880 (m), 2855 (m), 1452 (m), 1284 (m), 1230 (m), 1284 (m).  
 HRESIMS (m/z): [M + H]<sup>+</sup> calcd for C<sub>42</sub>H<sub>41</sub>NOP<sub>2</sub>Si, 666.2511; found, 666.2511

#### 4,6-Bis(diphenylphosphino)phenoxazine (3.15)

To dry THF (200 mL), compound **3.14** (7.1 g, 10.7 mmol) and TBAF (6.8 g, 17.9 mmol) were added and the solution left to stir at room temperature for 2 days. After this time, brine (50 mL) and benzene (100 mL), were added to the reaction mixture and the solution transferred to a separating funnel. The organic layer was removed, washed with brine, and dried over anhydrous magnesium sulphate. The solvent was removed in vacuo and the crude extract chromatographed with hexane/EtOAc (70/30) to yield the pure ligand **3.15**.



Yield: 70% (4.1 yellow crystals).  
 mp: 250 °C (lit. [3] mp 251 °C dec)

TLC:  $R_f$  0.5 (hexane/EtOAc 70/30).

$^1\text{H}$  NMR (600 MHz,  $[\text{d}^6]$ -DMSO)  $\delta$ : 8.36 (s, 1H), 7.32 (m, 12H), 7.11 (m, 8H), 6.65 (t,  $^3J(\text{H,H}) = 7.8$  Hz, 2H), 6.46 (dd,  $^3J(\text{H,H}) = 7.7$ , 1.2 Hz, 2H), 5.80 (dquar,  $^3J(\text{H,H}) = 7.7$ ,  $^4J(\text{H,H}) = 1.6$  Hz,  $^2J(\text{P,H}) = 1.6$  2H).

$^{13}\text{C}$  NMR (101 MHz,  $\text{CDCl}_3$ )  $\delta$ : 145.6 (t,  $J(\text{P,C}) = 20.7$  Hz, CO), 136.8 (m, phenyl *C-ipso*, PC), 134.0 (t,  $J(\text{P,C}) = 20.6$  Hz, CH phenyl), 131.5 (CN), 128.1 (t,  $J(\text{P,C}) = 3.4$  Hz, CH phenyl), 125.7 (CH), 125.7 (CH), 125.3 (dd,  $J(\text{P,C}) = 11.9$ , 7.1 Hz, CHCHC-P), 123.7 (CH), 113.8 (CH).

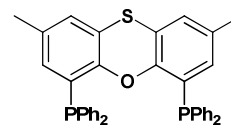
$^{31}\text{P}$  NMR (243 MHz,  $[\text{d}^6]$ -DMSO)  $\delta$  20.2

IR  $\nu_{\text{max}}$  ( $\text{cm}^{-1}$ ): 3408 (w), 1565 (s), 1452 (s), 1398 (s), 1286 (s), 1256 (m), 1206 (m), 1090 (m), 766 (m), 739 (m), 723 (m), 690 (s).

HRESIMS (m/z):  $[\text{M} + \text{H}]^+$  calcd for  $\text{C}_{36}\text{H}_{27}\text{NOP}_2$ , 552.1633; found, 552.1648

#### 4,6-Bis(diphenylphosphino)-2,8-dimethylphenoxathiin (3.16)

Ligand **3.16** was prepared analogously to **3.10** using **3.7** (1.5 g, 6.6 mmol), TMEDA (2.5 mL, 16.8 mmol), *n*BuLi (10.3 mL, 16.8 mmol), and  $\text{PPh}_2\text{Cl}$  (3.1 mL, 16.8 mmol).



Yield: 62% (2.2 g yellow crystals)

mp: 184 °C (lit. [10] mp 180 °C)

$^1\text{H}$  NMR (400 MHz,  $\text{CDCl}_3$ ,  $\delta$ ): 7.29 – 7.12 (m, 20H), 6.86 (apparent d,  $^4J(\text{H,H}) = 1.0$  Hz, 2H), 6.22 (bs, 2H), 2.05 (s, 6H).

$^{13}\text{C}$  NMR (101 MHz,  $\text{CDCl}_3$ ,  $\delta$ ): 152.2 (t,  $J(\text{P,C}) = 24.4$  Hz, CO), 137.2 (t,  $J(\text{P,C}) = 13.1$  Hz phenyl *C-ipso*, PC), 133.9 (t,  $J(\text{P,C}) = 21$  Hz, CH phenyl), 133.5 (C), 132.7 (CH), 128.2 (CH phenyl), 128.1 (t,  $J(\text{P,C}) = 3.5$  Hz, CH phenyl), 127.6 (CH), 127.3 (dd,  $J(\text{P,C}) = 12.6$ , 11 Hz, CHCHC-P), 119.5 (CS), 20.6 ( $\text{CH}_3$ ).

$^{31}\text{P}$  NMR (162 MHz,  $\text{CDCl}_3$ )  $\delta$  -17.9

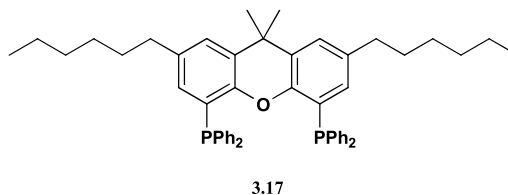
IR  $\nu_{\text{max}}$  ( $\text{cm}^{-1}$ ): 3050 (w), 2961 (w), 2921 (w), 1556 (m), 1476 (m), 1432 (m), 1402 (s), 1238 (m), 1221 (m), 1199 (m), 742 (s), 692 (s).

HRESIMS (m/z):  $[\text{M} + \text{H}]^+$  calcd for  $\text{C}_{38}\text{H}_{31}\text{OP}_2\text{S}$ , 597.1565; found, 597.1559.

#### 4,5-Bis(diphenylphosphino)-2,7-dihexyl-9,9-dimethylxanthene (3.17)

Ligand **3.17** was prepared analogously to **3.10** using **3.9** (1 g, 2.6 mmol), TMEDA (1.0 mL, 6.7 mmol), *n*BuLi (4.2 mL, 6.7 mmol), and  $\text{PPh}_2\text{Cl}$  (1.3 mL, 6.8 mmol) in 4 mL of hexane.

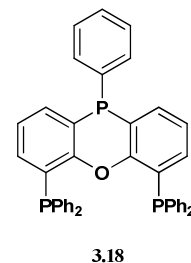




Yield:	56% (1.1 g white crystals)
mp:	166 °C
<sup>1</sup> H NMR (400 MHz, CDCl <sub>3</sub> , δ):	7.59 – 6.96 (m, 20 H, P(C <sub>6</sub> H <sub>5</sub> ) <sub>2</sub> and 2H xanthene ring), 6.32 (bs, 2H), 2.38 (t, <i>J</i> = 7.5 Hz, 4H), 1.62 (s, 6H), 1.48 – 0.98 (m, 16H), 0.84 (t, <i>J</i> = 6.9 Hz, 6H).
<sup>13</sup> C NMR (101 MHz, CDCl <sub>3</sub> , δ):	150.9 (t, <i>J</i> (P,C) = 19.6 Hz, CO), 137.7 (dd, <i>J</i> (P,C) = 7.2, 5.9 Hz, phenyl C- <i>ipso</i> , PC), 137.1 (C), 133.9 (t, <i>J</i> (P,C) = 10.4 Hz, CH phenyl), 131.9 (CH), 129.5 (C), 128.0 – 128.5 (m, CH phenyl), 126.2 (CH), 125.1 (dd, <i>J</i> = 10.6, 2.4 Hz, CHCHC–P), 35.3 (CH <sub>2</sub> ), 31.9 (CH <sub>3</sub> ), 31.6 (CH <sub>2</sub> ), 31.2 (CH <sub>2</sub> ), 28.6 (CH <sub>2</sub> ), 22.6 (CH <sub>2</sub> ), 14.1 (CH <sub>3</sub> ).
<sup>31</sup> P NMR (162 MHz, CDCl <sub>3</sub> ) δ	-17.8 (s).
IR ν <sub>max</sub> (cm <sup>-1</sup> ):	3069(w), 3054(w), 2955(m), 2921(m), 2831(m), 1585(m), 1569(m), 1419(vs), 1252(m), 1240(m), 737(s), 692(vs).

#### 4,6-Bis(diphenylphosphino)-10-phenylphenoxaphosphine (3.18)

The synthesis of **3.18** was adapted from literature [3]. To a solution of **3.5** (1.0 g, 3.6 mmol) and TMEDA (4.1 mL, 27 mmol) in Et<sub>2</sub>O (30 mL) at room temperature, phenyllithium (34 mL, 27 mmol) was added dropwise. The brown reaction mixture was refluxed for 48 h. The reaction was cooled to room temperature and a solution of PPh<sub>2</sub>Cl (1.4 mL, 7.5 mmol) in hexane (4 mL) was added dropwise. The reaction was stirred for 6 h at room temperature, and hydrolysed with 1/1 mixture of 10% HCl and brine solution. The organic layer was extracted with DCM and fractions combined, dried over anhydrous magnesium sulphate, and filtered. The solvent was removed to afford a brown-yellow oil. The crude product was washed with hexane. Attempts to recrystallise the product were unsuccessful. The crude product was chromatographed on a short silica column with hexane/EtOAc (95/5) elution to afford **3.18**.



Yield:	45% (0.94 g white powder)
mp:	202 °C (lit. [3] mp 204-207 °C )
TLC:	<i>R<sub>f</sub></i> 0.5 (hexane/EtOAc 95/5).
<sup>1</sup> H NMR (400 MHz, C <sub>6</sub> D <sub>6</sub> , δ):	7.52 (ddd, <sup>2</sup> <i>J</i> (P,H) = 10.6, <sup>3</sup> <i>J</i> (H,H) = 7.5, <sup>4</sup> <i>J</i> (H,H) = 1.6 Hz, 2H, CHCHCH), 7.47 (m, 4H), 7.43 (m, 2H), 7.20 – 7.14 (m, 6H), 7.12 – 7.00 (m, 9H), 6.97 (dquar, <sup>3</sup> <i>J</i> (H,H) = 7.5, <sup>4</sup> <i>J</i> (H,H, PCCHCH) = 1.6, <sup>2</sup> <i>J</i> (P,H) = 1.6 Hz, 2H), 6.77 (dt, <sup>3</sup> <i>J</i> (H,H) = 7.5, <sup>2</sup> <i>J</i> (P,H) = 1.5 Hz, 2H, CHCHCH).

$^{13}\text{C}$ NMR (101 MHz, $\text{C}_6\text{D}_6$ , $\delta$ ):	157.8 (t, $J(\text{P,C}) = 9.7$ Hz, CO), 141.0 (d, $J = 21.4$ Hz, PC benzyl), 138.2 ("t", $J(\text{P,C}) = 12.6$ Hz, phenyl C- <i>ipso</i> , PC), 137.7 ("t", $J(\text{P,C}) = 14.3$ Hz, PC), 136.1 (CH), 135.7 (CH), 135.0 (t, $J(\text{P,C}) = 21.8$ Hz, PCCH), 134.2 (t, $J(\text{P,C}) = 20.8$ Hz, PCCH), 132.3 (d, $J(\text{P,C}) = 19.6$ Hz, PCCH), 128.8 (CH), 128.7 (t, $J(\text{P,C}) = 3.4$ Hz, CH), 128.5 (t, $J(\text{P,C}) = 3.3$ Hz, CH), 124.6 (d, $J(\text{P,C}) = 11.8$ Hz, CH), 119.6 (d, $J(\text{P,C}) = 5.4$ Hz, C xanthene).
$^{31}\text{P}$ NMR (162 MHz, $\text{C}_6\text{D}_6$ ) $\delta$	-16.4, -55.0
IR $\nu_{\text{max}}$ ( $\text{cm}^{-1}$ ):	3067(w), 1478(m), 1432(m), 1411(m), 1376(s), 1226(s), 1198(m), 1182(m), 735(s), 689(s).
HRESIMS (m/z):	$[\text{M} + \text{H}]^+$ calcd for $\text{C}_{42}\text{H}_{33}\text{OP}_3$ , 645.1661; found, 645.1662

### Phenyllithium

The preparation was carried out under an atmosphere of argon. Cut pieces of lithium metal (0.84 g, 120 mmol) were added to degassed dry  $\text{Et}_2\text{O}$  (25 mL) in a 3-neck flask fitted with a condenser and pressure-equalizing funnel. The funnel was charged with a solution of bromobenzene (16.5 mL, 100 mmol), and 40 drops were slowly added to the stirring solution. After a short initiation period, the solution warmed up and the rate of reflux was maintained by careful dropwise addition of the bromobenzene solution. The reaction was kept at reflux and not allowed to cool. For the small scale synthesis the use of cooling was not necessary. After 1 hour the addition of bromobenzene was complete, and the reaction was left to stir for a further hour until the solution reached room temperature. Thereafter the reaction solution was transferred by cannula into a Schlenk apparatus and filtered through a short plug of glass wool.

A light yellow solution was obtained and the PhLi content was found to be 0.95 M by the Gilman double titration method (see below). The prepared PhLi was stored at  $-20^\circ\text{C}$  and used the same day.

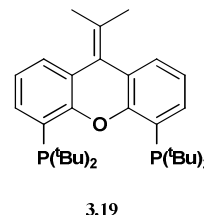
### Gilman Double titration

**Total base content of the organometallic solution:** A 0.50 mL aliquot of PhLi was carefully quenched with water (20 mL) and 2 drops of phenolphthalein solution added. The solution was titrated with standardised 0.1034 N HCl solution until the endpoint was reached. Total base content 1.0 M.

**Total non-organometallic base content:** A further 0.5 mL aliquot of PhLi was added to 0.2 mL of dry 1,2-dibromoethane in 3 mL of dry  $\text{Et}_2\text{O}$ . The reaction mixture was stirred vigorously for 5 min. Water (20 mL) was added and the solution titrated. The differences in the concentration obtained via the 2 methods was used to calculate the final concentration.

#### 4,5-Bis(di-*t*-butylphosphino)-9-isopropylidenexanthene (**3.19**)

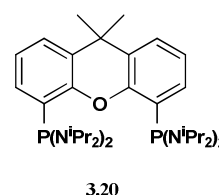
The preparation of **3.19** was adapted from literature [79]. To a solution of **3.1** (0.6 g, 2.6 mmol) and TMEDA (1 mL, 6.6 mmol) in hexane (15 mL) at 0 °C, *n*BuLi (5 mL, 7.8 mmol) was added dropwise. The red solution was left to stir overnight. At room temperature, *t*-butyldiphosphine chloride (1.5 mL, 7.8 mmol) was slowly added. The resulting yellow solution was warmed to 60 °C and left to stir for 24 h. Thereafter, the solvent was removed in vacuo and the residue dissolved in dichloromethane, washed with water, dried over anhydrous magnesium sulphate, filtered, and the solvent removed to dryness. The oil was washed with petroleum ether and chromatographed on a short plug of silica gel.



Yield:	20% (0.3 g yellow crystals)
mp:	199 °C
TLC:	$R_f$ 0.4 (hexane/EtOAc 95/5)
$^1\text{H}$ NMR (400 MHz, $\text{CDCl}_3$ , $\delta$ ):	7.58 (d, $^3J(\text{H,H}) = 7.6$ Hz, 2H), 7.32 (dd, $^3J(\text{H,H}) = 7.5$ , $^4J(\text{H,H}) = 1.4$ Hz, 2H), 7.03 (t, $^3J(\text{H,H}) = 7.6$ Hz, 2H), 2.06 (s, 6H), 1.21 - 1.24 (m, 36H).
$^{13}\text{C}$ NMR (101 MHz, $\text{CDCl}_3$ , $\delta$ ):	158.7 (t, $J(\text{P,C}) = 24.4$ Hz, CO), 133.4 (CH), 129.9 (C), 128.6 (CH), 126.6 (t, C), 126.0 (dd, $J(\text{P,C}) = 8.2, 4.6$ Hz, C), 124.1 (C), 120.7 (CH), 32.6 (dd, $J = 15.4, 12.9$ Hz, C), 30.8 (t, $J = 9.1$ Hz, $\text{PC}(\text{CH}_3)_3$ ), 23.3 ( $\text{CH}_3$ ).
$^{31}\text{P}$ NMR (162 MHz, $\text{CDCl}_3$ ) $\delta$	10.7
IR $\nu_{\text{max}}$ ( $\text{cm}^{-1}$ ):	3065 (w), 2891 (m), 2934 (m), 2856 (m), 1473 (m), 1456 (m), 1390 (s), 1360 (s), 1219 (s), 1176 (m), 797 (m), 758 (s).
HRESIMS (m/z):	$[\text{M} + \text{H}]^+$ calcd for $\text{C}_{32}\text{H}_{49}\text{OP}_2$ , 223.1117; found, 223.1117.

#### 4,5-bis(diisopropylaminophosphino)-9,9-dimethylxanthene (**3.20**)

The synthesis of **3.20** was adapted from literature [44]. A mixture of 9,9-dimethylxanthene (1.5 g, 5.2 mmol) and TMEDA (1.6 mL, 10.9 mmol) in 30 mL of degassed  $\text{Et}_2\text{O}$  was cooled to -40 °C. Thereafter, *n*BuLi (7 mL, 10.9 mmol) was added dropwise, while maintaining an inert argon atmosphere. The reaction was left to slowly warm to room temperature, and stirred overnight. Thereafter, the reaction mixture was cooled to -70 °C and chlorodiaminoisopropylidiphosphine (1.9 g, 7.3 mmol) in 15 mL of  $\text{Et}_2\text{O}$  added dropwise. The reaction was once again left to stir overnight. The solvent was removed and hexane (20 mL) was added to the residue. Thereafter, the solids were filtered off and the hexane removed under vacuum. Excess TMEDA was removed by co-evaporation with toluene (3x 10 mL). The resulting yellow residue was dissolved in 10 mL of dry hexane and left to recrystallise overnight at -25 °C. The crystals were filtered to afford the compound **3.20**.

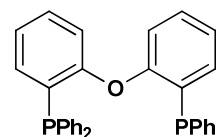


Yield:	40% (1.4 g yellow crystals)
mp:	187 °C

$^1\text{H}$ NMR (400 MHz, $\text{CDCl}_3$ , $\delta$ ):	7.58 (dt, $^3J(\text{H,H}) = 7.4$ Hz, 1.9 2H), 7.26 (m, 2H), 6.98 (t, $^3J(\text{H,H}) = 7.5$ Hz, 2H), 3.38 – 3.14 (m, 4H), 1.56 (s, 6H), 1.18 (dd, $J = 42.4$ , 6.6 Hz, 48H).
$^{13}\text{C}$ NMR (101 MHz, $\text{CDCl}_3$ , $\delta$ ):	150.2 – 148.6 (m, C), 132.7 (d, $J = 31.5$ Hz, C), 131.1 (CH), 128.6 (C), 126.5 (CH), 121.2 (CH), 48.1 – 47.0 (m, $(\text{CH}_2)_2\text{CH}$ ), 34.7 ( $\text{CH}_3$ ), 33.9 (C), 25.2 (t, $J = 5.0$ Hz, $(\text{CH}_2)_2\text{CH}$ ), 24.0 – 23.40 (m, $(\text{CH}_2)_2\text{CH}$ ).
$^{31}\text{P}$ NMR (162 MHz, $\text{CDCl}_3$ ) $\delta$	57.1
IR $\nu_{\text{max}}$ ( $\text{cm}^{-1}$ ):	3061(w), 2966(m), 2928(m), 2867(m), 1393(s), 1386(s), 1295(m), 1217(s), 1116(s), 947(s), 783(s), 743(s), 509(s), 499(s).
EA	Calculated for $\text{C}_{39}\text{H}_{68}\text{N}_4\text{OP}_2$ C, 69.8; H, 10.2; N, 8.4 found C, 69.4, H, 10.3, N, 8.6

### Bis-(2-diphenylphosphino)phenyl Ether (3.21)

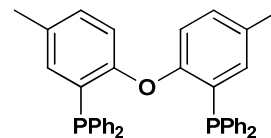
The preparation of ligand **3.21** was adapted from literature [10]. At room temperature, diphenyl ether (2.0 g, 11.8 mmol) in 8 mL of THF was added dropwise to a stirred solution of n-BuLi (16 mL, 25.9 mmol) and TMEDA (4.1 mL, 25.9 mmol). The reaction mixture was allowed to stir for 16 h. At room temperature, under a positive flow of argon, chlorodiphenylphosphine (4.7 mL, 25.9 mmol) in 8 mL of hexanes was added dropwise. The beige solution turned yellow and a white precipitate formed. The reaction mixture was left to stir for a further 16 h. Thereafter dichloromethane (15 mL) and water (15 mL) were added and the reaction mixture stirred rapidly. The two layers were separated, and the aqueous layer further extracted with dichloromethane (2 x 10 mL) and the combined fractions dried over anhydrous magnesium sulphate, filtered, and the solvent removed under vacuum to give a viscous green-yellow residue. The crude product was washed with acetone, dried, and recrystallised from dichloromethane/EtOH.



Yield:	69% (4.4 g white powder).	
mp:	175 °C (lit. [10] mp 175-176 °C )	<b>3.21</b>
$^1\text{H}$ NMR (400 MHz, $\text{CDCl}_3$ ) $\delta$ :	7.35 – 7.03 (m, $\text{P}(\text{C}_6\text{H}_5)_2$ and H xanthene, 22H), 6.89 (td, $^3J(\text{H,H}) = 7.5$ , $^2J(\text{H,H}) = 0.9$ Hz, 2H), 6.75 (ddd, $^3J(\text{H,H}) = 7.6$ , $^3J(\text{H,H}) = 4.2$ , $^3J(\text{H,H}) = 1.6$ Hz, 2H), 6.68 – 6.53 (m, 2H).	
$^{13}\text{C}$ NMR (101 MHz, $\text{CDCl}_3$ ) $\delta$ :	159.2 (d, $J(\text{P,C}) = 17.8$ Hz, CO), 136.6 (d, $J(\text{P,C}) = 11.6$ Hz, phenyl C- <i>ipso</i> , PC), 133.4 (CH phenyl), 133.8 (CH), 130.2 (CH), 129.0 (d, $J(\text{P,C}) = 16.1$ Hz, P-CCHCH), 128.4 (CH), 128.4 – 128.2 (m, CH phenyl), 123.6 (CH), 118.1 (CH).	
$^{31}\text{P}$ NMR (162 MHz, $\text{CDCl}_3$ ) $\delta$	-16.9	
IR $\nu_{\text{max}}$ ( $\text{cm}^{-1}$ ):	3056 (w), 3002 (w), 1458 (m), 1432 (s), 1221 (s), 1179 (m), 733 (s), 744 (m), 692 (s), 501 (s).	
HRESIMS (m/z):	$[\text{M} + \text{H}]^+$ calcd for $\text{C}_{36}\text{H}_{29}\text{OP}_2$ , 539.1688; found, 539.1689	

### Bis-(2-diphenylphosphino)-*p*-tolyl Ether (3.22)

Ligand **3.22** was prepared analogously to **3.21**. At room temperature, *p*-tolylether (1.0 g, 5.0 mmol) in 8 mL of THF, was added dropwise to a stirred solution of *n*-BuLi (7.0 mL, 11.1 mmol), TMEDA (1.7 mL, 11.1 mmol), and chlorodiphenylphosphine (2.4 mL, 11.1 mmol) in 4 mL hexane.



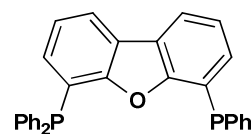
**3.22**

Yield:	67% (1.9 g white powder).
mp:	184 °C
<sup>1</sup> H NMR (400 MHz, CDCl <sub>3</sub> ) δ:	7.31 – 7.14 (m, 20H), 6.98 (dd, <sup>3</sup> <i>J</i> (H,H) = 8.3, <sup>4</sup> <i>J</i> (H,H) = 2.0 Hz, 2H), 6.59 (dd, <sup>4</sup> <i>J</i> (H,H) = 4.5, <sup>3</sup> <i>J</i> (H,H) = 2.0 Hz, 2H), 6.56 (m, 2H), 2.14 (s, 6H).
<sup>13</sup> C NMR (101 MHz, CDCl <sub>3</sub> ) δ:	157.4 (d, <i>J</i> (P,C) = 17.5 Hz, CO), 136.8 (d, <i>J</i> (P,C) = 11.7 Hz, phenyl C- <i>ipso</i> , PC), 134.2 (CH), 133.8 (d, <i>J</i> (P,C) = 20.6 Hz, CH phenyl), 132.7 (C), 130.8 (CH), 128.3 (CH), 128.2 (dd, <i>J</i> (P,C) = 8.8, 5.3 Hz, CCHC-P), 117.9 (CH), 20.8 (CH <sub>3</sub> ).
<sup>31</sup> P NMR (162 MHz, CDCl <sub>3</sub> ) δ	-16.4
IR ν <sub>max</sub> (cm <sup>-1</sup> ):	3068 (w), 3016 (w), 2918 (w), 1468 (s), 1433 (m), 1232 (s), 1212 (m), 747 (m), 736 (m), 689 (s).
HRESIMS (m/z):	[M + H] <sup>+</sup> calcd for C <sub>38</sub> H <sub>33</sub> OP <sub>2</sub> , 567.2001; found, 567.2000

### 4,6-Bis(diphenylphosphino)dibenzofuran (3.23)

The preparation of **3.23** was adapted from literature [10]. A solution of dibenzofuran (1.5 g, 8.9 mmol) in 60 mL of dry ether was cooled to -65°C, using a dry ice/acetone ice bath in a Dewar vessel. Thereafter, TMEDA (3.8 mL, 25 mmol) was added and the solution stirred. Under argon positive pressure, *n*BuLi (15.6 mL, 25 mmol) was added dropwise and the reaction left to stir for 16 h. Thereafter the stirred reaction mixture was cooled to -65°C and chlorodiphenylphosphine (4.6 mL, 25 mmol) in hexane (13 ml) added dropwise.

The reaction was once again left to stir overnight. A (1/1) mixture of dichloromethane/water (25 mL) was added. After allowing sufficient time to stir, the organic layer was removed, and the aqueous layer extracted with dichloromethane (2 x 15 mL). The combined organic fractions were dried over anhydrous magnesium sulphate, filtered, and the solvent removed to dryness. The resulting oil was washed with hexane and recrystallised from dichloromethane/EtOH.



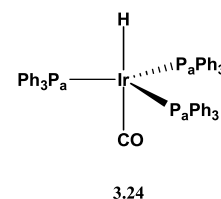
**3.23**

Yield:	71% (3.4 g off white crystals).
mp:	212 °C (lit. [10] mp 211-214 °C )

$^1\text{H}$ NMR (400 MHz, $\text{CDCl}_3$ ) $\delta$ :	7.91 (dd, $^3J(\text{H,H}) = 7.7$ , $^4J(\text{H,H}) = 1.2$ Hz, 2H), 7.44 – 7.09 (m, $\text{P}(\text{C}_6\text{H}_5)_2$ and H xanthene, 22H), 7.03 (td, $^3J(\text{H,H}) = 7.4$ , $^4J(\text{H,H}) = 1.2$ Hz, 2H).
$^{13}\text{C}$ NMR (101 MHz, $\text{CDCl}_3$ ) $\delta$ :	157.9 (d, $J(\text{P,C}) = 13.7$ Hz, CO), 135.8 (d, $J(\text{P,C}) = 10.7$ Hz, phenyl C- <i>ipso</i> , PC), 133.8 (d, $J(\text{P,C}) = 20.3$ Hz, CH), 132.0 (d, $J = 8.6$ Hz, CH), 128.7 (s, CH), 128.3 (d, $J(\text{P,C}) = 7.1$ Hz, CH), 123.5 (bs, C), 123.1 (d, $J(\text{P,C}) = 3.0$ Hz, CH), 121.2 (d, $J(\text{P,C}) = 19.5$ Hz, C), 121.5 (CH).
$^{31}\text{P}$ NMR (162 MHz, $\text{CDCl}_3$ ) $\delta$	-16.9
IR $\nu_{\text{max}}$ ( $\text{cm}^{-1}$ ):	3046 (w), 3006 (w), 1476 (m), 1433 (s), 1408 (s), 1387 (m), 1173 (s), 772 (m), 739 (s), 691 (s).
HRESIMS (m/z):	$[\text{M} + \text{H}]^+$ calcd for $\text{C}_{36}\text{H}_{27}\text{OP}_2$ , 537.1532; found, 537.1531

### Tris(phenylphosphine)hydridocarbonyl iridium(I) (3.24)

The synthesis of the precursor **3.24** was adapted from literature [47,80]. A round bottom flask was charged with  $\text{PPh}_3$  (2.6 g, 10 mmol), and absolute ethanol (100 ml). The solution was allowed to reflux rapidly. To this mixture, a solution of iridium trichloride hydrate (0.32 g, 1 mmol) dissolved in warm ethanol (10 mL), potassium hydroxide (0.8 g, 14.3 mmol) dissolved in warm ethanol (10 mL), and formaldehyde (10 mL, 40% w/v solution), were then added in quick succession. The solution turned yellow and was allowed to reflux for 2 hours, during which time a yellow precipitate formed. The crude product was filtered in air, washed with ethanol, water, ethanol, and hexane.

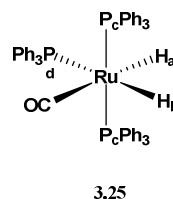


Yield:	79% (0.8 g yellow powder)
mp:	168 °C (lit. [80] mp 166-167 °C )
$^1\text{H}$ NMR (600 MHz, $\text{CDCl}_3$ ) $\delta$ :	7.41 – 6.62 (m, 45H), -10.77 (q, $^2J(\text{P,H}) = 21.5$ Hz, 1H)
$^{31}\text{P}$ NMR (243 MHz, $\text{CDCl}_3$ ) $\delta$	14.4 (bs).
IR $\nu_{\text{max}}$ ( $\text{cm}^{-1}$ ):	2120(w, $\nu_{\text{Ir-H}}$ ), 2096(w, $\nu_{\text{Ir-H}}$ ), 2074(m, $\nu_{\text{Ir-H}}$ ), 1917(s, $\nu_{\text{CO}}$ ).
EA:	Calculated for $\text{C}_{55}\text{H}_{46}\text{P}_3\text{Ir}$ : C, 65.5; H, 4.6. Found: C, 65.7; H, 4.6

### Tris(phenylphosphine)dihydridocarbonyl ruthenium(II) (3.25)

The preparation of **3.25** was adapted from literature [47,81]. A 3-necked round bottom flask, equipped with a condenser, was purged with nitrogen and charged with  $\text{PPh}_3$  (3.2 g, 12 mmol) and 100 mL of degassed MeOH. The mixture was heated for 10 min at a rapid reflux. In quick succession, a solution of ruthenium trichloride hydrate (0.5 g, 2 mmol) in 40 mL of MeOH, aqueous formaldehyde (37% w/v, 20 mL) and potassium hydroxide (0.6 g, 10.7 mmol) in MeOH (20 mL), were added to the mixture. The reaction mixture was refluxed for 1 h during which time a grey precipitate formed. The reaction was cooled with an ice bath and left to stir for 30 min. Thereafter, the resulting precipitate was filtered under vacuum and washed with absolute EtOH (25 mL), water (25 mL), absolute EtOH (25 mL), and hexane (25 mL). After drying under vacuum, the grey coloured

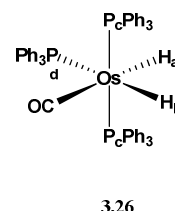
crude product was dissolved in toluene and filtered through a short column packed with neutral alumina. Careful loading of the column was essential to ensure the adequate purification of the product. The column was washed with toluene and the solvent concentrated, under vacuum. The product precipitated by the addition of MeOH. Thereafter, the solvent was removed via a cannula and the product dried under vacuum.



Yield: 60% (1.1 g white powder)  
 mp: 161 °C (lit. [47] mp 160-162 (air) )  
<sup>1</sup>H NMR (600 MHz, CDCl<sub>3</sub>) δ 7.69 – 6.78 (m, 45H), -6.90 (ddt,  $J(\text{P}_c\text{-H}_a) = 30.5$ ,  $^2J \text{P}_d\text{-H}_a = 15.2$ ,  $^2J \text{H}_a\text{-H}_b = 6.0$  Hz, 1H), -8.86 (ddt,  $^2J(\text{P}_d\text{-H}_b) = 74.3$ ,  $J(\text{P}_c\text{-H}_b) = 28.3$ ,  $J(\text{H}_b\text{-H}_a) = 6.1$  Hz, 1H)  
<sup>31</sup>P NMR (243 MHz, C<sub>6</sub>D<sub>6</sub>, proton decoupled) δ 57.6 (d,  $J(\text{P}_c\text{-P}_d) = 17.4$  Hz), 45.5 (dt,  $J(\text{P}_d\text{-P}_c) = 17.6$  Hz, 4.6)  
 IR  $\nu_{\text{max}}$  (cm<sup>-1</sup>): 1938(s,  $\nu_{\text{CO}}$ ).

### Tris(phenylphosphine)dihydridocarbonyl osmium(II) (3.26)

The metal precursor **3.26** was prepared analogously to precursor **3.24** using PPh<sub>3</sub> (3.1 g, 12 mmol) in ethanol (18 mL), potassium hexachloroosmate(IV) hexahydrate (0.5 g, 1 mmol) in EtOH (7 mL), aqueous formaldehyde (7.5 mL, 37% w/v solution), and potassium hydroxide (0.56 g, 10 mmol) in absolute EtOH (9mL).

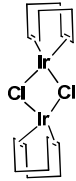


Yield: 20% (0.2 g white powder)  
 mp: 181 °C (lit. [47] mp 179-183 °C (air) )  
<sup>1</sup>H NMR (400 MHz, CDCl<sub>3</sub>, δ): -7.72 (m, 1H), -9.44 (dtd,  $J(\text{P}_d\text{-H}_b) = 57.1$ ,  $J(\text{P}_c\text{-H}_b) = 28.9$ ,  $J(\text{H}_b\text{-H}_a) = 4.1$  Hz, 1H).  
<sup>31</sup>P NMR (162 MHz, CDCl<sub>3</sub>, proton decoupled) δ 18.8 (dd,  $J(\text{P}_c\text{-P}_d) = 11.0, 8.0$  Hz), 14.3 (dt,  $J(\text{P}_d\text{-P}_c) = 17.8, 11.2$  Hz).  
 IR  $\nu_{\text{max}}$  (cm<sup>-1</sup>): 2045(m,  $\nu_{\text{Os-H}}$ ), 1945(vs,  $\nu_{\text{CO}}$ ), 1850(s,  $\nu_{\text{CO}}$ ).

### Di-μ-chlorobis(η<sup>4</sup>-1,5-cyclooctadiene)diiridium (3.27)

The synthesis of precursor **3.27** was adapted from literature [48-49]. A Schlenk tube was charged with iridium trichloride hydrate (0.8 g, 2.3 mmol), 2-propanol (4 mL), 1,5-cyclooctadiene (1.2 mL, 9.8 mmol), and degassed distilled water (5.5 mL, 0.31 mol). The solution was allowed to reflux under inert nitrogen atmosphere for 40 h, during which time the product precipitated as an orange solid. The reaction was allowed to cool to room

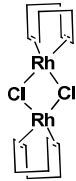
temperature and the precipitate filtered, washed with cold methanol to remove any unreacted 1,5-cyclooctadiene, and dried in vacuo.

Yield:	69% (1.0 g bright orange-red crystals)	
mp:	174°C dec (lit. [49] mp > 200 °C dec)	
<sup>1</sup> H NMR (400 MHz, CDCl <sub>3</sub> , δ):	4.21 (m, 4H), 2.56 – 2.04 (m, 4H), 1.51 (q, <i>J</i> (H,H) = 7.8 Hz, 4H).	
IR ν <sub>max</sub> (cm <sup>-1</sup> ):	2964(w), 2978(w), 2933(m), 2878(m), 2828(m), 978(s), 968(m), 903(s), 869(m), 831(s).	

3.27

### [Di-μ-chlorobis(η<sup>4</sup>-1,5-cyclooctadiene)dirhodium (3.28)

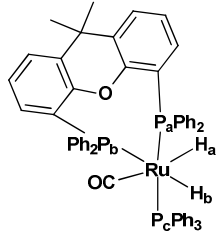
The preparation of **3.28** was adapted from literature [50]. A Schlenk tube was charged with rhodium trichloride hydrate (1 g, 3.8 mmol), a (1/5) mixture of water/ethanol (10 mL), and 1,5-cyclooctadiene (1.5 mL, 12.2 mmol). The reaction was heated at reflux for 18 h during which time the product precipitated as a yellow solid. Thereafter the solution was allowed to cool to room temperature, and the precipitate filtered and washed with cold methanol and pentane, and the product dried under high vacuum.

Yield:	64% (1.2 g yellow powder)	
mp:	250 °C (lit. [82] mp > 256 °C )	
<sup>1</sup> H NMR (400 MHz, CDCl <sub>3</sub> , δ):	4.21 (s, 4H), 3.38 – 2.25 (m, 4H), 1.73 (q, <i>J</i> (H,H) = 7.2 Hz, 4H).	
IR ν <sub>max</sub> (cm <sup>-1</sup> ):	2964(w), 2934(w), 2873(m), 2827(m), 994(m), 960(s), 866(s), 816(s), 775(m).	

3.28

### [Ru(xantphos)(H<sub>2</sub>)(CO)(PPh<sub>3</sub>)] (3.29)

A microwave vial was charged with [Ru(H)<sub>2</sub>CO(PPh<sub>3</sub>)<sub>3</sub>] (50 mg, 0.05 mmol) and toluene (1 mL). To this solution **3.10** (38 mg, 0.14 mmol) was added, and the mixture heated for 45 min at 80 °C in the microwave. Thereafter, the toluene was removed in vacuo and the solid washed with absolute EtOH (2 x 1 mL) and hexane (2 x 1 mL). The product was then dried under high vacuum to afford complex **3.29** as an orange solid.

Yield:	69% (36.5 mg orange solid)	
mp:	135 – 138 °C	
<sup>1</sup> H NMR (400 MHz, C <sub>6</sub> D <sub>6</sub> ,)		
( <i>J</i> calculated from g-NMR) δ:	-6.42 (dddd, <i>J</i> (P,H) = 39 Hz, <i>J</i> (P,H) = 24 Hz, <sup>2</sup> <i>J</i> (P,H) = 15 Hz, <sup>2</sup> <i>J</i> (H,H) = 6Hz), -8.50 (ddd, <i>J</i> (P,H) = 86 Hz, <i>J</i> (P,H) = 42 Hz, <i>J</i> (P,H) = 27 Hz, <sup>2</sup> <i>J</i> (H,H) = 6Hz)	

3.29



$^{31}\text{P}$  NMR (243 MHz,  $[\text{d}^8]$ -toluene)

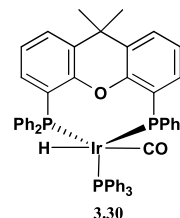
(333 K, proton decoupled)  $\delta$ : 58.7 (dd,  $J(\text{P},\text{P}) = 239.3, 16.4$  Hz), 47.5 (dd,  $J(\text{P},\text{P}) = 239.1, 16.2$  Hz), 30.8 (t,  $J(\text{P},\text{P}) = 14.8$  Hz).

IR  $\nu_{\text{max}}$  ( $\text{cm}^{-1}$ ): 1938(s), 2920(m), 1585(m), 1489(s).

HRESIMS ( $m/z$ ):  $[\text{M}+\text{H}-\text{H}_2]^+$  calcd for  $\text{C}_{58}\text{H}_{48}\text{RuO}_2\text{P}_3$ , 971.1911; found, 971.1921

### [Ir(xantphos)(H)(CO)(PPh<sub>3</sub>)] (3.30)

To 20 mL of dry benzene,  $[\text{Ir}(\text{H})(\text{CO})(\text{PPh}_3)_3]$  (0.1 g, 0.22 mmol) and xantphos **3.10** (0.1 g, 0.17 mmol) were added. The resulting yellow solution was left to stir at 50 °C for 5 h. Thereafter the solvent was removed to half its volume in vacuo and the remaining precipitate was washed with methanol, and then hexane. Complex **3.30** was recrystallised from dichloromethane/Hexane (1/1) to give a bright yellow powder.



Yield: 79% (0.8 g bright yellow powder)

mp: 190 – 192 °C

$^1\text{H}$  NMR (600 MHz,  $\text{C}_6\text{D}_6$ )  $\delta$ : 7.74 (m, 4H), 7.66 – 7.57 (m, 6H), 7.45 (m, 4H), 7.07 (dd,  $^3J(\text{H},\text{H}) = 7.6$ ,  $^2J(\text{P},\text{H}) = 1.1$  Hz, 2H, CHCHCC), 6.99 – 6.80 (m, 20H), 6.75 (t,  $^3J(\text{H},\text{H}) = 7.7$  Hz, 2H), 6.73 – 6.66 (m, 2H), 1.48 – 1.38 (m, 3H,  $\text{CH}_3$ ), 1.35 (3H,  $\text{CH}_3$ ), -10.5 (dt,  $J(\text{P},\text{H}) = 26.2, 19.6$  Hz, 1H).

$^{13}\text{C}$  NMR (151 MHz,  $\text{C}_6\text{D}_6$ )  $\delta$ : 189.9 (bs, Ir-CO), 156.3 (t,  $J(\text{P},\text{C}) = 4.5$  Hz), 141.3 (dt,  $J(\text{P},\text{C}) = 41.6, 4.1$  Hz), 139.5 (t,  $J(\text{P},\text{C}) = 24.6$  Hz), 136.8 (td,  $J(\text{P},\text{C}) = 22.1, 2.8$  Hz), 135.2 (C), 133.7 (t,  $J(\text{P},\text{C}) = 6.4$  Hz), 133.5 (CH), 133.4 (CH), 130.2 (CH), 128.4 (CH), 128.1 (CH), 127.4 (d,  $J(\text{P},\text{C}) = 9.7$  Hz), 122.9 (CH), 36.1 (C), 29.0 ( $\text{CH}_3$ ), 24.3 ( $\text{CH}_3$ ).

$^{31}\text{P}$  NMR (243 MHz,  $\text{C}_6\text{D}_6$ )  $\delta$ : 16.52 (t,  $J_{\text{PbPa}} = 137.1$  Hz), -1.50 (d,  $J_{\text{PaPb}} = 138.7$  Hz)

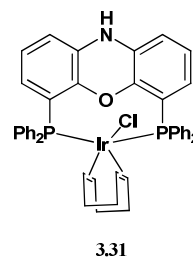
IR  $\nu_{\text{max}}$  ( $\text{cm}^{-1}$ ): 3056(w), 2057(m,  $\nu_{\text{Ir-H}}$ ), 1923(s,  $\nu_{\text{CO}}$ ), 1585(w), 2860(w), 1478(m), 1433(s), 1401(s), 1218(s), 1088(s), 741(s), 692(s), 505(s).

HRESIMS ( $m/z$ ):  $[\text{M}]^+$  calcd for  $\text{C}_{58}\text{H}_{49}\text{IrO}_2\text{P}_3$ , 1063.2569; found, 1063.2569

EA: Calculated for  $\text{C}_{58}\text{H}_{48}\text{IrO}_2\text{P}_3$ : C, 65.6; H, 4.6. Found: C, 65.7; H, 4.6

### [Ir(nixantphos)(cod)Cl] (3.31)

A dry Schlenk tube was charged with  $[\text{Ir}(\text{cod})\text{Cl}]_2$  (30 mg, 0.05 mmol) in 5 mL of degassed toluene. Nixantphos **3.15** (50 mg, 0.09 mmol) was added to the stirring mixture and warmed to 50 °C. The solution was left to stir for 2 h over which time a yellow solid precipitated out of solution. The solvent was removed via a cannula and the precipitate was washed with dry methanol and hexane. Complex **3.31** was thereafter recrystallised from an EtOH/dichloromethane solution (1/1).



Yield: 70% (62 mg yellow powder)

mp: 196 °C

$^1\text{H}$  NMR (600 MHz,  $[\text{d}^6]$ -DMSO)  $\delta$  8.40 (s, 1H), 7.51 (m, 12H), 7.37 (m, 8H), 7.15 (t,  $^3J(\text{H,H}) = 7.8$  Hz, 2H), 7.05 (dd,  $^3J(\text{H,H}) = 7.7$ ,  $^2J(\text{P,H}) = 1.1$  Hz, 2H), 6.14 (t,  $J = 6.6$  Hz, 2H), 3.29 (bs, 4H, olefinic protons cod), 1.33 (m, 4H, aliphatic protons cod), 1.18 (m, 4H, aliphatic protons cod).

$^{13}\text{C}$  NMR (101 MHz,  $[\text{d}^6]$ -DMSO)  $\delta$  145.4 (t,  $J(\text{P,C}) = 4.9$  Hz, CO), 134.2 (d,  $J(\text{P,C}) = 2.8$  Hz, *Cipso* phenyl, PC), 133.5 – 133.3 (t,  $J(\text{P,C}) = 5.6$  Hz), 131.7 (C), 129.3 (d,  $J(\text{P,C}) = 4.3$  Hz, PC), 128.7 – 128.2 (m, CH), 128.9 (CH), 127.8 (m, CH), 124.0 (CH), 123.8 (CH), 114.6 (CH), 79.0 (t,  $J = 33.3$  Hz), 62.3 (CH), 48.6 (CH<sub>2</sub>).

$^{31}\text{P}$  NMR (162 MHz,  $[\text{d}^6]$ -DMSO)  $\delta$  -19.36 (s).

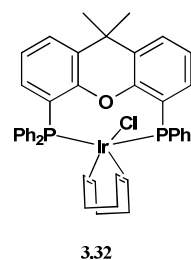
IR  $\nu_{\text{max}}$  (cm<sup>-1</sup>): 3329(w), 2053(w), 2931(w), 2829(w), 1574(m), 1452(s), 1400(s), 1325(w), 1263(m), 1293(s), 1263(m), 1210(m), 1091(s), 693(s).

HRESIMS (m/z):  $[\text{M}]^+ - \text{Cl}$  calcd for C<sub>44</sub>H<sub>39</sub>IrOP<sub>2</sub>, 879.2136; found, 852.2156

EA: Calculated for C<sub>44</sub>H<sub>49</sub>ClIrOP<sub>2</sub>: C, 59.6; H, 4.43; N, 1.58. Found: C, 59.0; H, 4.14; N, 1.46.

### [Ir(xantphos)(cod)Cl] (**3.32**)

Complex **3.32** was prepared analogously to complex **3.31** using [Ir(cod)Cl]<sub>2</sub> (30 mg, 0.05 mmol) and **3.10** (54.3 mg, 0.10 mmol).



Yield: 93% (90 mg yellow powder)

mp: 231 °C

$^1\text{H}$  NMR (600 MHz, CD<sub>2</sub>Cl<sub>2</sub>)  $\delta$  6.72 – 7.41 (m, 26H), 3.42 (m, 4H, olefinic protons cod), 1.85 (m, 4H, aliphatic protons cod), 1.45 (bs, 4H, aliphatic protons cod), 1.27 (6H)

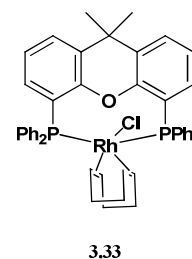
$^{13}\text{C}$  NMR (151 MHz, CD<sub>2</sub>Cl<sub>2</sub>)  $\delta$  156.8 – 154.9 (m, C), 140.3 – 137.3 (m), 134.4 – 134.1 (m), 133.5 (dd,  $J(\text{P,C}) = 23.2$ , 10.1 Hz), 133.2 – 133.0 (m), 132.0, 129.5 (d,  $J(\text{P,C}) = 31.5$  Hz), 129.1 – 128.1 (m), 126.5 (CH), 124.0 (CH), 122.0 (dt,  $J(\text{P,C}) = 20.1$ , 6.6 Hz), 63.8 (CH), 36.3 (C), 33.0 (CH<sub>2</sub>), 23.8 (CH<sub>3</sub>).

$^{31}\text{P}$  NMR (243 MHz, CD<sub>2</sub>Cl<sub>2</sub>)  $\delta$  -16.8 (s)

IR $\nu_{\max}$ (cm <sup>-1</sup> ):	3059(w), 3022(w), 2974(w), 2932(w), 2860(m), 1478(m), 1435(s), 1409(s), 1236(s), 1090(m), 789(m), 741(s), 694(s).
HRESIMS (m/z):	[M] <sup>+</sup> - Cl calcd for C <sub>47</sub> H <sub>44</sub> IrOP <sub>2</sub> , 879.2491; found, 879.2491
EA:	Calculated for C <sub>47</sub> H <sub>44</sub> ClIrOP <sub>2</sub> : C, 61.7; H, 4.9. Found: C, 60.5; H, 4.7

### [Rh(xantphos)(cod)Cl] (3.33)

The preparation of complex **3.33** was adapted from literature [52]. **3.10** (116 mg, 0.20 mmol) was added to a solution of [Rh(cod)Cl]<sub>2</sub> (50 mg, 0.10 mmol) in dry Et<sub>2</sub>O (10 mL), and the reaction left to stir for 1 h. The orange precipitate was filtered and washed with Et<sub>2</sub>O (3 x 20 mL). The product was dried under vacuum for 4 h to afford **3.33** as an orange powder.



Yield:	93% (153 mg orange powder)
mp:	225 °C dec
<sup>1</sup> H NMR (400 MHz, C <sub>6</sub> D <sub>6</sub> ) $\delta$	881 – 7.12 (m, 14H), 7.18 – 5.83 (m, 12H), 4.11 (bs, 4H, olefinic protons cod), 1.96 – 1.63 (m, 6H), 1.58 – 1.40 (4H, aliphatic protons cod).
<sup>31</sup> P NMR (162 MHz, C <sub>6</sub> D <sub>6</sub> ) $\delta$	2.05 (d, <i>J</i> (Rh,P) = 89.5 Hz)
IR $\nu_{\max}$ (cm <sup>-1</sup> ):	1938(s), 2920(m), 1585(m), 1489(s).
HRESIMS (m/z):	[M] <sup>+</sup> - Cl calcd for C <sub>47</sub> H <sub>44</sub> RhOP <sub>2</sub> , 789.1917; found, 789.1917
EA:	Calculated for C <sub>47</sub> H <sub>44</sub> ClRhOP <sub>2</sub> : C, 68.4; H, 5.4. Found: C, 68.0; H, 5.1

## 3.8 References

- Kranenburg, M. Doctoral Dissertation, University of Amsterdam, **1995**.
- Patterson, A. M.; Capell, L. *The Ring Index*; Reinhold Publishing Corporation: New York, **1940**.
- van der Veen, L. A.; Keeven, P. H.; Schoemaker, G. C.; Reek, J. N. H.; Kamer, P. C. J.; van Leeuwen, P. W. N. M.; Lutz, M.; Spek, A. L. *Organometallics* **2000**, *19*, 872-883.
- Ephritikhine, M. *Chem. Commun.* **1998**, 2549-2554.
- McMurry, J. E.; Krepski, L. R. *J. Org. Chem.* **1976**, *41*, 3929-3930.
- Furniss, B. S.; Hannaford, A. J.; Smith, P. W. G.; Tatchell, A. R. *Vogel's Textbook of Practical Organic Chemistry*; Longman Scientific & Technical: Essex, **1989**, p 846.
- Badejo, I. T.; Karaman, R.; Fry, J. L. *J. Org. Chem.* **1989**, *54*, 4591-4596.
- Oita, K.; Gilman, H. *J. Am. Chem. Soc.* **1957**, *79*, 339-342.
- Mallan, J. M.; Bebb, R. L. *Chem. Rev.* **1969**, *69*, 693-755.
- Kranenburg, M.; Vanderburgt, Y. E. M.; Kamer, P. C. J.; van Leeuwen, P. W. N. M.; Goubitz, K.; Fraanje, J. *Organometallics* **1995**, *14*, 3081-3089.
- Petrassi, H. M.; Klabunde, T.; Sacchetti, J.; Kelly, J. W. *J. Am. Chem. Soc.* **2000**, *122*, 2178-2192.
- Mann, F. G.; Millar, I. T. *J. Chem. Soc.* **1953**, 3746-3750.
- Granoth, I.; Levy, J. B.; Symmes, C. J. *J. Chem. Soc. Perkin II* **1972**, 697-700.
- Blum, D. M., U.S. Patent, 4698447, Oct. 6, 1987.
- Bronger, R. P. J.; Bermon, J. P.; Herwig, J.; Kamer, P. C. J.; van Leeuwen, P. W. N. M. *Adv. Synth. Catal.* **2004**, *346*, 789-799.

- 16 Marimuthu, T.; Bala, M. D.; Friedrich, H. B. *Acta. Crystallogr., Sect. E: Struct. Rep. Online* **2009**, *65*, O828-U2615.
- 17 Al-Hiari, Y. M.; Bennett, S. J.; Cox, B.; Davies, R. J.; Khalaf, A. I.; Waigh, R. D.; Worsley, A. J. *J. Heterocycl. Chem.* **2005**, *42*, 647-659.
- 18 Suter, C. M.; Green, F. O. *J. Am. Chem. Soc.* **1937**, *59*, 2578-2580.
- 19 Suter, C. M.; McKenzie, J. P.; Maxwell, C. E. *J. Am. Chem. Soc.* **1936**, *58*, 717-720.
- 20 Cole-Hamilton, D. J., University of St. Andrews, Fife, Personal Communication **2008**.
- 21 Huang, M. *J. Am. Chem. Soc.* **1946**, *68*, 2487-2488.
- 22 Gessner, V. H.; Däschlein, C.; Strohmman, C. *Chem.--Eur. J.* **2009**, *15*, 3320-3334.
- 23 Antonio, Y.; Barrera, P.; Contreras, O.; Franco, F.; Galeazzi, E.; Garcia, J.; Greenhouse, R.; Guzman, A.; Velarde, E.; Muchowski, J. M. *J. Org. Chem.* **1989**, *54*, 2159-2165.
- 24 Hillebrand, S.; Bruckmann, J.; Kruger, C.; Haenel, M. W. *Tetrahedron Lett.* **1995**, *36*, 75-78.
- 25 Stanetty, P.; Mihovilovic, M. D. *J. Org. Chem.* **1997**, *62*, 1514-1515.
- 26 Schlosser, M. *Organoalkali Reagents. In Organometallics in Synthesis, A Manual*; Schlosser, M., Ed.; Wiley: Chichester, **1994**, p 11.
- 27 Haenel, M. W.; Jakubik, D.; Krüger, C.; Betz, P. *Chem. Ber.* **1991**, *124*, 333-336.
- 28 Goertel, W.; Keim, W.; Vogt, D.; Englert, U.; Boele, M. D. K.; van der Veen, L. A.; Kamer, P. C. J.; van Leeuwen, P. W. N. M. *J. Chem. Soc., Dalton Trans.* **1998**, 2981-2988.
- 29 Goertz, W.; Kamer, P. C. J.; van Leeuwen, P. W. N. M.; Vogt, D. *Chem.--Eur. J.* **2001**, *7*, 1614-1618.
- 30 Minglana, J. J. G.; Okazaki, M.; Hasegawa, K.; Luh, L.-S.; Yamahira, N.; Komuro, T.; Ogino, H.; Tobita, H. *Organometallics* **2007**, *26*, 5859-5866.
- 31 Bronger, R. P. J.; Kamer, P. C. J.; van Leeuwen, P. W. N. M. *Organometallics* **2003**, *22*, 5358-5369.
- 32 Ahmed, M.; Bronger, R. P. J.; Jackstell, R.; Kamer, P. C. J.; van Leeuwen, P. W. N. M.; Beller, M. *Chem.--Eur. J.* **2006**, *12*, 8979-8988.
- 33 van der Veen, L. A.; Boele, M. D. K.; Bregman, F. R.; Kamer, P. C. J.; van Leeuwen, P. W. N. M.; Goubitz, K.; Fraanje, J.; Schenk, H.; Bo, C. *J. Am. Chem. Soc.* **1998**, *120*, 11616-11626.
- 34 Kranenburg, M.; Kamer, P. C. J.; van Leeuwen, P. W. N. M.; Vogt, D.; Keim, W. *J. Chem. Soc. Chem. Commun.* **1995**, 2177-2178.
- 35 Sandee, A. J.; Reek, J. N. H.; Kamer, P. C. J.; van Leeuwen, P. W. N. M. *J. Am. Chem. Soc.* **2001**, *123*, 8468-8476.
- 36 Deprele, S.; Montchamp, J. L. *Org. Lett.* **2004**, *6*, 3805-3808.
- 37 Ricken, S.; Osinski, P. W.; Eilbracht, P.; Haag, R. *J. Mol. Catal. A: Chem.* **2006**, *257*, 78-88.
- 38 Kranenburg, M.; G. P. Delis, J.; C. J. Kamer, P.; W. N. M. van Leeuwen, P.; Vrieze, K.; Veldman, N.; L. Spek, A.; Goubitz, K.; Fraanje, J. *J. Chem. Soc., Dalton Trans.* **1997**, 1839-1850.
- 39 Lenero, K. A.; Kranenburg, M.; Guari, Y.; Kamer, P. C. J.; van Leeuwen, P. W. N. M.; Sabo-Etienne, S.; Chaudret, B. *Inorg. Chem.* **2003**, *42*, 2859-2866.
- 40 Zuidema, E.; Goudriaan, P. E.; Swennenhuis, B. H. G.; Kamer, P. C. J.; van Leeuwen, P. W. N. M.; Lutz, M.; Spek, A. L. *Organometallics* **2010**, *29*, 1210-1221.
- 41 Gilman, H.; Zoellner, E. A.; Selby, W. M. *J. Am. Chem. Soc.* **1932**, *54*, 1957-1962.
- 42 Mispelaere-Canivet, C.; Spindler, J.-F.; Perrio, S.; Beslin, P. *Tetrahedron* **2005**, *61*, 5253-5259.
- 43 Adams, D. J.; Cole-Hamilton, D. J.; Harding, D. A. J.; Hope, E. G.; Pogorzelec, P.; Stuart, A. M. *Tetrahedron* **2004**, *60*, 4079-4085.
- 44 van der Vlugt, J.; Paulusse, J.; Zipp, E.; Tijmenssen, J.; Mills, A.; Spek, A.; Claver, C.; Vogt, D. *Eur. J. Inorg. Chem.* **2004**, *2004*, 4193-4201.
- 45 Gensow, M.-N. B.; Freixa, Z.; van Leeuwen, P. W. N. M. *Chem. Soc. Rev.* **2009**, *38*, 1099-1118.
- 46 Gilman, H.; Gorsich, R. *J. Org. Chem.* **1957**, *22*, 687-689.
- 47 Ahmad, N.; Levison, J. J.; Robinson, S. D.; Uttley, M. F. Complexes of ruthenium, osmium, rhodium, and iridium containing hydridecarbonyl, or nitrosyl ligands. In *Inorg. Syn.*; Parshall, G. W., Ed.; McGraw-Hill: New York, **1974**; Vol. 15, p 45-64.
- 48 Cotton, F. A.; Lahuerta, P.; Sanau, M.; Schwotzer, W. *Inorg. Chim. Acta* **1986**, *120*, 153-157.
- 49 Herde, J. L.; Lambert, J. C.; Senoff, C. V. *Inorg. Syn.* **1974**, *15*, 14-20.
- 50 Giordano, G.; Crabtree, R. H. *Inorg. Syn.* **1990**, *28*, 88-90.
- 51 Ledger, A. E. W.; Slatford, P. A.; Lowe, J. P.; Mahon, M. F.; Whittlesey, M. K.; Williams, J. M. J. *Dalton Trans.* **2009**, 716-722.
- 52 van Haaren, R. J.; Zuidema, E.; Fraanje, J.; Goubitz, K.; Kamer, P. C. J.; van Leeuwen, P. W. N. M.; van Strijdonck, G. P. F. *C. R. Chimie* **2002**, *5*, 431-440.
- 53 Mann, F. G.; Millar, I. T.; Powell, M.; Watkin, D. J. *J. Chem. Soc., Perkin II* **1976**, 1383-1384.
- 54 Osinski, P. W.; Schurmann, M.; Preut, H.; Haag, R.; Eilbracht, P. *Acta. Crystallogr., Sect. E: Struct. Rep. Online* **2005**, *61*, O3115-O3116.

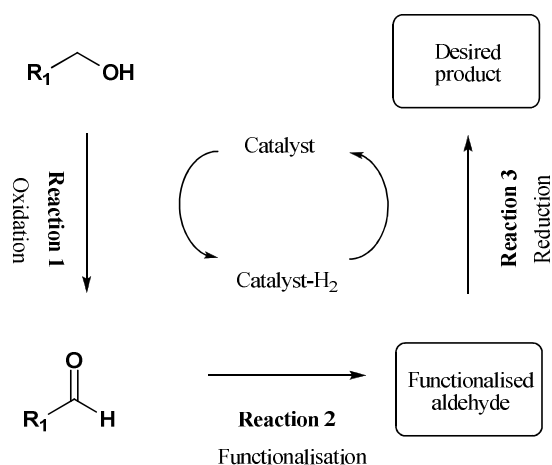
- 55 Ricken, S.; Osinski, P. W.; Schurmann, M.; Preut, H.; Eilbracht, P. *Acta. Crystallogr., Sect. E: Struct. Rep. Online* **2006**, 62, O1807-O1808.
- 56 Ricken, S.; Schurmann, M.; Preut, H.; Eilbracht, P. *Acta. Crystallogr., Sect. E: Struct. Rep. Online* **2006**, 62, O2637-O2638.
- 57 Deb, B.; Sarmah, P. P.; Dutta, D. K. *Eur. J. Inorg. Chem.* **2010**, 1710-1716.
- 58 Pintado-Alba, A.; de la Riva, H.; Nieuwhuyzen, M.; Bautista, D.; Raithby, P. R.; Sparkes, H. A.; Teat, S. J.; Lopez-de-Luzuriaga, J. M.; Lagunas, M. C. *Dalton Trans.* **2004**, 3459-3467.
- 59 Vogl, E. M.; Bruckmann, J.; Krüger, C.; Haenel, M. W. *J. Organomet. Chem.* **1996**, 520, 249-252.
- 60 Chiu, Y.-C.; Lin, C.-H.; Hung, J.-Y.; Chi, Y.; Cheng, Y.-M.; Wang, K.-W.; Chung, M.-W.; Lee, G.-H.; Chou, P.-T. *Inorg. Chem.* **2009**, 48, 8164-8172.
- 61 Ionkin, A. S.; Marshall, W. J. *Organometallics* **2004**, 23, 6031-6041.
- 62 Fox, D. J.; Duckett, S. B.; Flaschenriem, C.; Brennessel, W. W.; Schneider, J.; Gunay, A.; Eisenberg, R. *Inorg. Chem.* **2006**, 45, 7197-7209.
- 63 Chaloner, P. A.; Hitchcock, P. B.; Reisinger, M. *Acta. Crystallogr., Sect. E: Crystal Structure Commun.* **1992**, C46, 735-737.
- 64 Theron, M.; Purcell, W.; Basson, S. S. *Acta. Crystallogr., Sect. E: Crystal Structure Commun.* **1996**, C52, 336-338.
- 65 Dierkes, P.; van Leeuwen, P. W. N. M. *J. Chem. Soc., Dalton Trans.* **1999**, 1519-1529.
- 66 Casey, C. P.; Whiteker, G. T. *Israel. J. Chem.* **1990**, 30, 299-304.
- 67 Clark, M.; Cramer, R. D.; van Opdenbosch, N. *J. Comp. Chem.* **1989**, 10, 982-1012.
- 68 Sybyl 6.03, Tripos Associates, 1699 S. Hanley Road, Suite 303, St. Louis, MO 63144, **1995**.
- 69 van Leeuwen, P. W. N. M.; Kamer, P. C. J.; Reek, J. N. H.; Dierkes, P. *Chem. Rev.* **2000**, 100, 2741-2769.
- 70 Marx, F.; Jordaan, J.; Vosloo, H. *J. Mol. Model.* **2009**, 15, 1371-1381.
- 71 Delley, B. *J. Phys. Chem.* **1996**, 100, 6107-6110.
- 72 Delley, B. *J. Chem. Phys.* **2000**, 113, 7756-7764.
- 73 Materials Studio 5.0, Accelrys Software Inc., 10188 Telesis Court, Suite 100, San Diego, CA 92121, **2010**.
- 74 Bruker APEX2 Version 2.0-1, Bruker AXS Inc., Madison, Wisconsin, USA., **2005**.
- 75 Bruker SAINT-NT Version 6.0., Bruker AXS Inc., Madison, Wisconsin, USA., **2005**.
- 76 Bruker SHELXTL Version 5.1., Bruker AXS Inc., Madison, Wisconsin, USA., **1999**.
- 77 Delley, B. *J. Chem. Phys.* **1990**, 92, 508.
- 78 Perdew, J. P.; Wang, Y. *Phys. Rev. B* **1992**, 45, 13244.
- 79 Mispelaere-Canivet, C.; Jean-Francis, S.; Perrio, S.; Beslin, P. *Tetrahedron* **2005**, 61, 5253-5259.
- 80 Ahmad, N.; Robinson, S. D.; Uttley, M. F. *J. Chem. Soc., Dalton Trans.* **1972**, 7, 843-847.
- 81 Owston, N. A.; Parker, A. J.; Williams, J. M. J. *Chem. Commun.* **2008**, 624-625.
- 82 Chatt, J.; Venanzi, L. M. *J. Chem. Soc.* **1957**, 4735-4741.

# Chapter 4

## Microwave assisted oxidation of alcohols

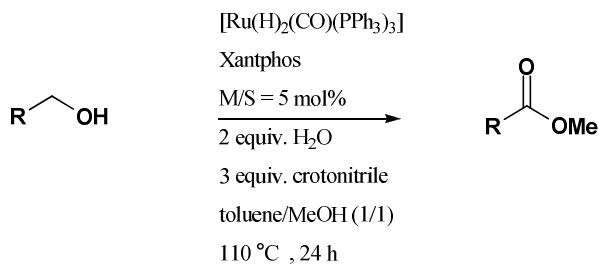
### 4.1 Introduction

The prepared bidentate ligands were applied to the microwave mediated oxidation of primary alcohols to aldehydes. Aldehydes, as a result of the increased electrophilic nature, are more reactive in a wider range of transformations than the precursor alcohols [1]. These carbonyl compounds are the building blocks in the manufacture of many high value commodities. Therefore, the development of improved catalytic protocols is of interest in this work. Moreover, the oxidation of primary alcohols to aldehydes is a key step in the activation of alcohols via the borrowing hydrogen strategy, **Scheme 25** [1-3]. In this approach, an alcohol is temporarily converted into an aldehyde that is functionalised and then reduced in situ to a higher value or more reactive product. The preparation of compounds by this approach is an area of significant interest due to the ‘green’ advantages over typical reaction pathways [4]. The development and improvement of protocols for this key oxidation step can be used to further develop or optimise borrowing hydrogen strategies.



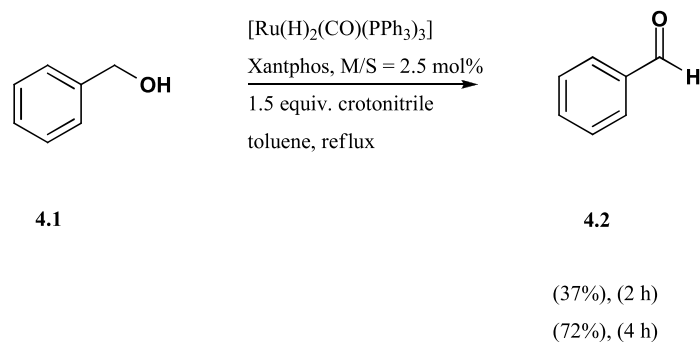
**Scheme 25. Generalised borrowing hydrogen strategy, adapted from Seiple [4].**

To the best of our knowledge, there have been no reported applications on the use of xanthene family ligands solely for the oxidation of alcohols to aldehydes. A communication by Owston et al. [5] reported the conversion of primary alcohols to methyl esters via an aldehyde intermediate with a  $[Ru(xantphos)(PPh_3)_3(CO)H_2]$  catalyst. The generalised reaction for the reported one pot procedure is shown in **Scheme 26**. The catalyst is formed in-situ (1:1 metal to ligand ratio) and the substrate, either an aliphatic or benzylic alcohol, is reacted with methanol in the presence of a sacrificial hydrogen acceptor. The yields for the desired methyl ester products were reported to be between 70 – 74% for the benzylic alcohols, and 76 – 87% for the aliphatic substrates.



**Scheme 26.** Generalised reaction for the oxidation of primary alcohols to methyl esters [5].

The reported catalytic testing was done as a one pot protocol, therefore the eleven primary alcohol substrates investigated were not isolated in the aldehyde form. However, the conversion of benzyl alcohol to benzaldehyde was quantified during a preliminary optimisation study for the sacrificial hydrogen acceptor crotonitrile. For the reported preliminary study, a similar protocol to **Scheme 26** was used where a 1:1 ratio of metal to ligand was allowed to complex prior to the addition of the reagents. Benzyl alcohol **4.1** was oxidised in the presence of crotonitrile, toluene, and the catalyst, to give benzaldehyde **4.2** in the reported yields, **Scheme 27**.



**Scheme 27.** Reported oxidation of benzyl alcohol to benzaldehyde [5].

This preliminary experiment is the only related work that has been identified in literature. However, as mentioned previously, only the use of a Ru xantphos complex was reported and no comparative study on xanthene family ligands presented. Moreover, all reported reactions involved conventional heating methods and long reaction times. Nevertheless, the reaction presented in **Scheme 27** has been identified as the starting point for this catalytic testing study. To optimise this reaction and extend it to the xanthene family ligands prepared in **Chapter 3**, the general catalytic testing strategy outlined in Chapter 1 was followed.

## 4.2 Results and Discussion

*All catalytic results are presented as an average of 2 or more runs. All products were quantified by  $^1\text{H}$  NMR using an internal standard (1,4-dimethoxybenzene, or 2,6-lutidine) and normal interpolation techniques [6]. Further details on the experimental conditions and procedures are presented at the end of this chapter.*

The identified literature reaction, **Scheme 27**, was first reproduced at the reported conditions [5]. A similar yield of 71% benzaldehyde was obtained after 4 hours under reflux. The literature conditions used relatively small volumes of solvent (0.5 mL toluene) which could possibly result in non uniform, inefficient heating under reflux conditions. The use of more efficient microwave irradiation was therefore investigated, which had the concomitant advantages of improved product yield, shortened reaction times, and more uniform heating. This also allowed the heating of smaller volumes of the reaction mixture in a closed system above the boiling point of toluene without incurring significant solvent losses. In general, there are very few literature examples of microwave assisted reactions involving xantphos ligands [7]. To the best of our knowledge, the only reported studies are for Pd catalysed C-N bond formations [8], Rh catalysed hydroaminomethylation of alkenes [9], and Rh catalysed hydroformylation in a laboratory microwave modified for moderate pressures [10]. This study represents the first reported application of xantphos, and xanthene family ligands, in microwave assisted oxidation reactions.

The identified literature reaction was attempted in a specialised laboratory microwave, with the reported catalyst loading and solvent concentrations maintained. The microwave adapted conditions involved in situ complexation for 15 minutes at 80 °C, and the reaction was allowed to proceed for 10 minutes at 110 °C. A yield of 72% benzaldehyde was obtained at a catalyst loading of 2.5 mol%. In a preliminary optimisation, the catalyst loading was decreased to 1 mol%, and the aldehyde obtained in yields of 30% after 10 mins, and 75% after 30 mins. A compromise between catalyst loading, yield, and reaction time was made, and a loading of 1 mol% used for further investigations. The successful adaptation of this reaction to the microwave assisted conditions prompted the further investigation of the scope of this reaction with respect to related benzylic and aliphatic alcohols.

Additional validation and optimisation studies were performed on the catalyst system, **Figure 28**. All results presented in **Figure 28** were obtained at 120 °C, 10 °C above the normal boiling point of the solvent, and the reaction limited to 25 mins. This reaction time was considered sufficient as microwave heating is known to reduce conventional reaction times by 2-3 orders of magnitude [11]. At 120 °C and 1 mol% loading, an 83% yield of benzaldehyde was obtained for the Ru xantphos catalyst, **Entry 1**. The transition metal centre was varied to screen for activity, **Entries 2 – 4**. It was found that changing the metal centre to Ir, Rh, or Os gave complexes that showed minimal or no activity towards the aldehyde. A recent publication by Asensio et al. [12] reported the single X-ray crystal of an Os xantphos complex where ortho-metallation to the ether bridge has occurred. In addition, soft Os(II) species tend to bond to soft functional groups [13], for example the C=C alkene in crotonitrile. The preference of Os complexes for coordination or metal-carbon bond formation could possibly account for the lack of activity in this catalytic cycle. Ir and Rh complexes are well known for their



application in reduction or hydrogenation type reactions [14-15]. A decrease in activity relative to the Ru complexes for this ‘inverse’ reaction was anticipated; however the extent of the inactivity was unexpected. Ru was subsequently used for all further oxidation studies. Two blank runs were performed to determine the validity of the organometallic catalysis, **Entries 5-6**. The observed lack of reaction (NR) and minimal conversion eliminates the possibility of benzyl alcohol decomposition or metal precursor activity as sole factors for the conversion to benzaldehyde. In **Entry 7**, the catalyst loading was further decreased to 0.5 mol% with a corresponding aldehyde yield of 63%. As a result of this decreased yield, a loading of 1 mol% was used for all further studies.

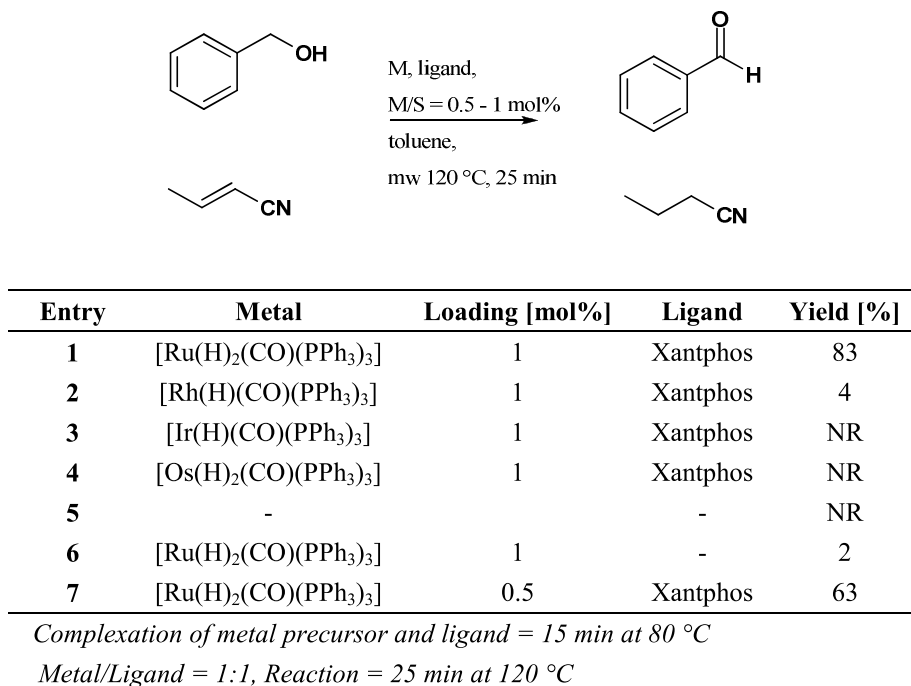


**Figure 28. Validation and optimisation studies for the microwave assisted oxidation of benzyl alcohol.**

The bidentate ligands prepared in Chapter 3 were applied to the Ru catalysed oxidation of benzyl alcohol, **Figure 29**. The ligands are arranged in order of increasing natural bite angle. The xanthene related ligands, **Entries 1, 3**, and **10**, displayed poor activity towards the aldehyde as compared to the xanthene family ligands, **Entries 2, 4-7**, and **9**. The low yields for DPEphos, **Entry 1**, and related ligand PTEphos, **Entry 3**, is possibly due to the relatively more flexible diphenyl ether backbone. The low yields were not unexpected as similar inactivity for Ru DPEphos complexes has been reported by Ledger et al. [16] for the formation of an in situ aldehyde intermediate from benzyl alcohol in C-C bond formation reactions. The low activity of DBFphos, **Entry 10**, was also not unexpected due to the large chelation angle which makes the formation of stable complexes difficult [17].

In comparison to most catalytic results of xanthene family ligands reported by van Leeuwen and co-workers [17-21], there is no obvious correlation between the observed reactivity and natural bite angle, **Figure 29**. However, most xanthene family ligands were active for this reaction. The N donor ligand, nixantphos **Entry 8**,

gave the lowest yields for the family ligands (14%), significantly below the parent ligand, **Entry 6**. The poor reactivity is possibly due to weak interactions between the amine in the phenoxazone ring and the metal centre. Similar poor results for nixantphos relative to other xanthene family ligands have been reported in C-C bond formation reactions [16]. **Entries 4-6** exhibited similar activity, suggesting that electronic changes in the backbone do not significantly affect the reactivity for this particular reaction. Phosxantphos, **Entry 2**, and isopropxantphos, **Entry 7**, gave improved reactivity relative to the benchmark ligand, **Entry 6**. The effect of the xanthene backbone is apparent from the results for phosxantphos and PTEphos, **Entry 3**. Both ligands have essentially identical bite angles yet remarkably different activity was observed. Although phosxantphos and isopropxantphos showed similar activity, the latter was chosen for further investigations due to the relative ease of synthesis, higher yields, and greater potential for modification or derivatisation.

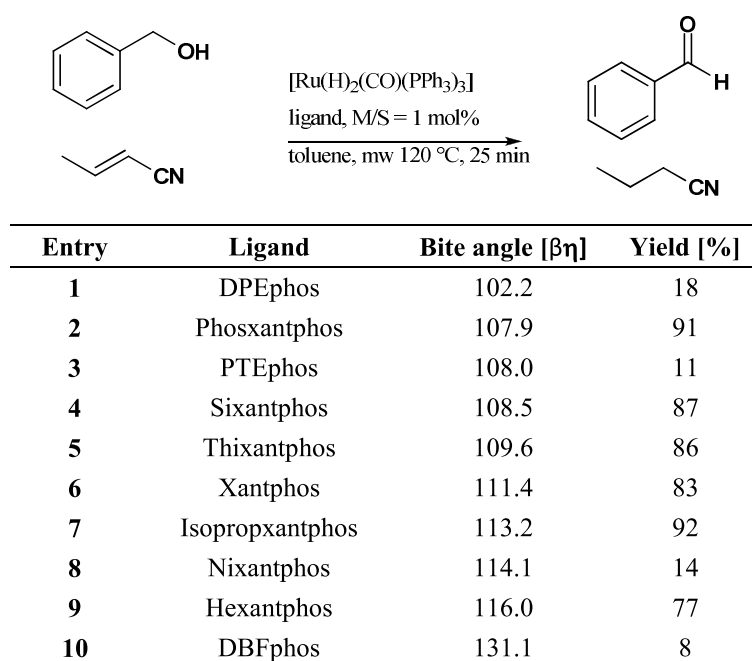


**Figure 29. Optimisation of ligands for the Ru catalysed oxidation of benzyl alcohol. Please refer to Chapter 2, Table 2a-b for ligand structures.**

The substrate activation scope for isopropxantphos was investigated to demonstrate the versatility of the identified ligand. The oxidation of benzylic alcohols and derivatives was of particular interest as aromatic aldehydes are important raw materials in the manufacture of products for the perfumery and pharmaceutical industries [22]. To diversify the range of applicable substrates, aliphatic alcohols were also investigated. The primary alcohols were therefore screened for activity with a Ru isopropxantphos catalyst, and the results presented in **Figure 30**.

<div style="display: flex; align-items: center; justify-content: space-around;"> <div style="text-align: center;"> </div> <div style="text-align: center;"> <math>[\text{Ru}(\text{H})_2(\text{CO})(\text{PPh}_3)_3]</math>              Isopropanthos              M/S = 1 mol%              toluene,              mw 120 °C, 25 min           </div> <div style="text-align: center;"> </div> </div>			
Entry	Alcohol	Aldehyde	Yield [%]
1			92
2			79
3			100
4			60
5			58
6			50
7			60
8			93

Complexation of metal precursor and ligand = 15 min at 80 °C  
 Metal/Ligand = 1:1, Reaction = 25 min at 120 °C

**Figure 30a. Ru catalysed oxidation of primary alcohol substrates.**

<div style="display: flex; align-items: center; justify-content: space-around;"> <div style="text-align: center;"> </div> <div style="text-align: center;"> <math>[Ru(H)_2(CO)(PPh_3)_3]</math>              Isopropoxantphos              M/S = 1 mol%              toluene,              mw 120 °C, 25 min           </div> <div style="text-align: center;"> </div> </div>			
Entry	Alcohol	Aldehyde	Yield [%]
9			43
10			NR
11			74
12			58
13			48
14			72
15			55
16	1-decanol	decanal	67

*Complexation of metal precursor and ligand = 15 min at 80 °C*  
*Metal/Ligand = 1:1, Reaction = 25 min at 120 °C*

**Figure 30b. Ru catalysed oxidation of primary alcohol substrates.**

Owston et al. [5] studied the conversion of similar substrates to methyl esters via an in situ aldehyde intermediate. It was suggested that the conversion of aliphatic alcohols (to the aldehyde intermediate and then the ester) was favoured over benzylic alcohols due to steric hindrance, however no definitive reason was given. The aldehyde intermediate for only one of eleven substrates was isolated in the work of Owston and co-workers, therefore no definite comparison can be made with the reported work regarding the oxidation reaction. However, it is speculated that the simultaneous addition of methanol, rather than steric hindrance, caused competitive aldehyde and hemiacetal formation, which would be more pronounced for the benzylic rather than aliphatic substrates. In this work it was therefore expected that in the absence of methanol, the benzylic alcohols would be relatively more reactive than the aliphatic counterparts. This is supported by the observed catalytic results, **Figure 30**, where the Ru catalyst showed greater activity for the oxidation of the benzylic alcohols, **Entries 1-8, 10**, than the aliphatics, **Entries 11-16**.

The aldehyde yield for the benzylic alcohol substrates, **Figure 30a-b**, range from 50–100%. These observed results can be rationalised in terms of the electron donating or withdrawing nature of the substrates relative to benzyl alcohol, **Entry 1**. For this discussion, benzyl alcohol is used as the reference compound and is considered 'neutral'. **Entry 2, Figure 30a**, can also be considered neutral, and would be expected to have a similar or increased product yield due to extra conjugation relative to **Entry 1**. However, the observed yield was slightly lower than that for benzyl alcohol (79% and 92%), possibly due to an increase in the bulkiness of the substrate. **Entries 3-6** represent electron deficient substrates of varying strengths. The strongest electron deficient substrate, **Entry 6**, underwent partial oxidation with an observed yield of 50%. This was expected as the nitrogen has a lone pair of electrons and can take electron density away from the ring, thus retarding the oxidation of the 4-nitrobenzyl alcohol. Similar mediocre oxidation results for the strong electron withdrawing substrates have been reported by Slatford et al. [23] for aldehyde intermediates in C-C bond formation reactions. This suggests that the extent of the electron withdrawing nature strongly affects the reactivity towards the aldehyde. The relatively weaker, or moderately electron withdrawing substrates, **Entries 4-5**, have correspondingly higher yields than **Entry 6**, (60 and 58% respectively). However, this is still significantly lower than the neutral benzyl alcohol, **Entry 1**. Compared to **Entry 4**, 4-chlorobenzyl alcohol **Entry 3**, is less electron withdrawing as the Cl atom is less electronegative than F. Therefore, it was expected that the oxidation of 4-chlorobenzyl alcohol would be relatively easier than 4-fluorobenzyl alcohol. However, the extent of the observed oxidation was unexpected. 4-Chlorobenzaldehyde was obtained in 100% yield, suggesting that the electronic environment of this substrate was ideally suited for this catalytic system.

**Entries 7-8** account for substrates that are electron donating relative to benzyl alcohol. A yield of 93% 4-methoxybenzaldehyde was obtained for **Entry 8** due to the strong electron donating methoxy group. The relatively weaker, or moderately electron rich substrate 4-methylbenzyl alcohol gave a lower yield of 60%. Cyclohexylmethanol, **Entry 9, Figure 30b**, was investigated as a structurally similar, less activated analogue of **Entry 1**. The aldehyde product was obtained in 43% yield, showing the effect of the lack of aromaticity on the oxidation reaction. No observable aldehyde yield was obtained for **Entry 10**, possibly due to chelation of the nitrogen donor in the pyridine ring. Slatford et al. [23] have reported similar inactivity for a furfuryl alcohol substrate due to chelation of the O donor in the furyl ring.

The aldehyde yield for the aliphatic alcohol substrates, **Entries 11-13**, and **16**, **Figure 30b**, range from 48 to 74%. **Entry 11** shows a decreased yield of 74% compared to **Entry 1**, possibly due to the loss of 'benzylic' nature caused by an increase in the chain length of the alkyl linker. A further increase in this alkyl linker length leads to a corresponding decrease in product yield for **Entry 12**. The addition of an electron donating methyl group, **Entry 13**, further decreases the yield of desired product. A similar yield reduction was observed in the case of the benzylic alcohols for **Entry 7** relative to **Entry 1**. **Entries 14-15** represent  $\alpha,\beta$ -unsaturated alcohols. In **Entry 14**, a yield of 72% was obtained, with no observable alkene isomerisation. The results obtained suggest that the redox properties of the metal centre are very sensitive to the electronic properties of the substrate. Alteration of the electronic environment by the introduction of an  $sp^2$  carbon in the alkene bond could possibly account for the increased product yield for **Entry 14** relative to the related substrate in **Entry 12**. In comparison to the parent molecule in **Entry 14**, a decreased aldehyde yield is observed in **Entry 15**. This is possibly due to the methoxy group donating electron density and initiating a 'push-pull' effect involving the alkene bond, which renders the aliphatic tail less activated. The oxidation of 1-decanol was also investigated, **Entry 16**. Although straight chain aliphatic alcohols are generally difficult to oxidise, a yield of 67% decanal was observed. This yield could possibly be improved by increasing the microwave reaction time or catalyst loading, however in order to have a comparative study, these variables were kept constant for all substrates.

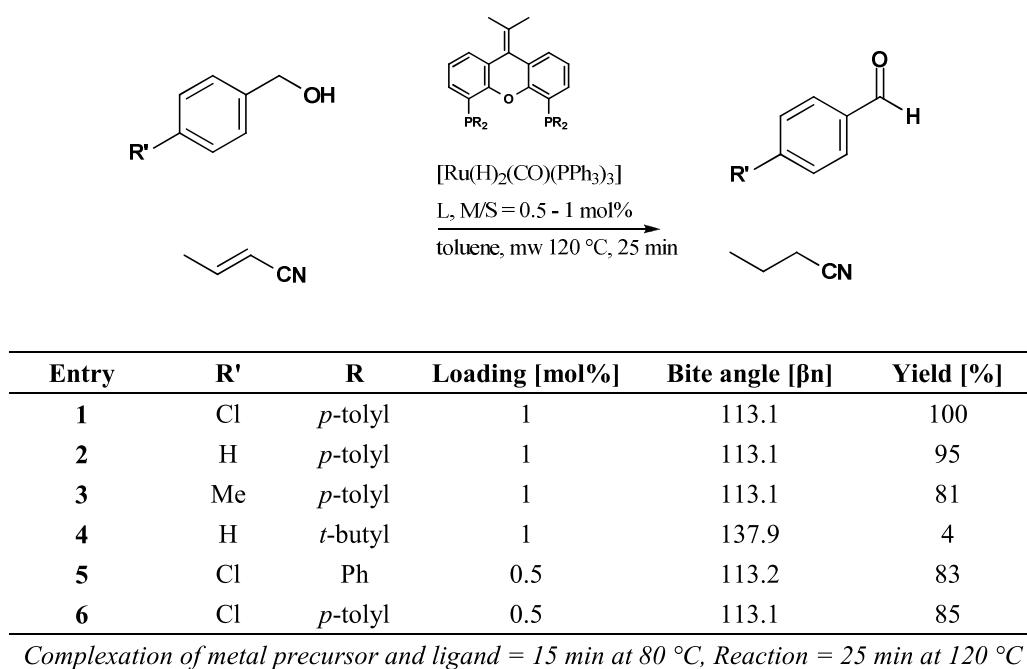


**Figure 31. Investigation of ligand electronic and steric properties on benzylic alcohol substrates.**

The observed reactivity towards the aldehyde for the Ru isopropxantphos complex was found to be very sensitive to the electronic environment of the substrates, **Figure 30**. To determine the effect of other electronic and steric variations, the environment around the chelating phosphorus donors was varied. Isopropxantphos was first modified at the R position (with respect to the generalised structure in **Figure 10**) with a good electron withdrawing group to give the corresponding isopropxantTolylphos complex, **Entry 1**, **Figure 31**. Using the

electron deficient substrate 4-chlorobenzyl alcohol **Entry 1**, a quantitative yield of 4-chlorobenzaldehyde was observed, as in the previous catalytic study, **Figure 30a**. Encouraged by this result, the Ru isopropxantTolylphos catalyst was then applied to an electron rich substrate 4-methylbenzyl alcohol **Entry 3**. A significantly improved aldehyde yield of 81% was obtained, as compared to 60% in the previous study, **Entry 7, Figure 30a**. The bis-(*t*-butyl-phosphino) derivatised ligand was found to be poorly activating, giving a yield of 4% towards benzaldehyde, **Entry 4**. The low yield is possibly due to the significantly larger natural bite angle preventing the formation of stable chelates. Poor catalytic activity has also been observed for Pd catalysed cross coupling reactions involving similar wide bite angled ligands with bis-(*t*-butyl-phosphino) substituents on xantphos [24]. Isopropxantphos and isopropxantTolylphos were also found to be active at a lower catalyst loading of 0.5 mol%, **Entries 5-6**. Due to the favourable catalytic results observed for isopropxantTolylphos for benzyl alcohol, as well as electron deficient and electron rich derivatives, this ligand was used for all further investigations.

With the increasing academic and industrial trend of embracing green chemistry principles, solvent-free techniques are an attractive option. It is well known that the choice of solvent can significantly affect the reactivity in microwave reactions, even more so than reactions under conventional heating [25]. Certain low absorbance solvents, for example toluene, can in some instances be unaffected or negate the benefits of accelerated microwave heating by inefficient coupling with microwave irradiation. Although the reagents absorb microwave energy and undergo molecular heating, the toluene can sometimes act as a heat sink and absorb the heat produced by the reagents [25]. Although the reaction is still receiving the required activation energy, the internal energy will be effectively lower than if a more efficient microwave solvent were present, or if solvent-free conditions were used. To investigate solvent and temperature effects, the conversion of benzyl alcohol with Ru isopropxantTolylphos was investigated under different conditions, **Figure 32**.

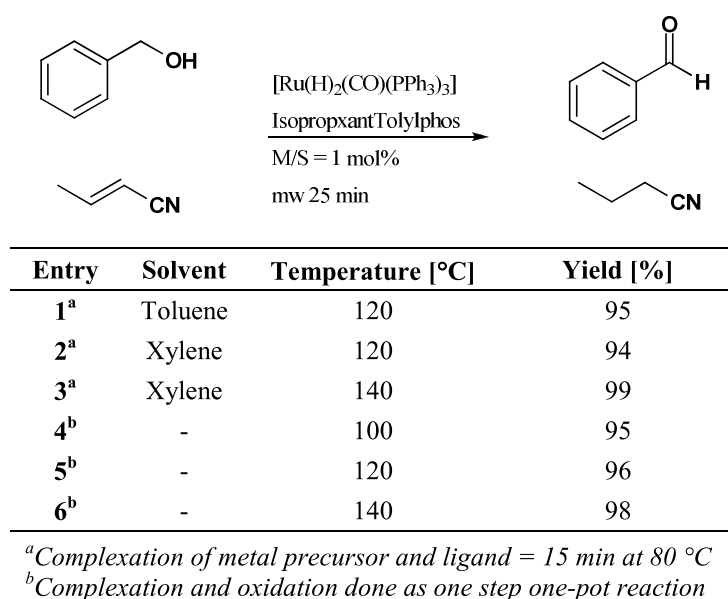


**Figure 32. Solvent and temperature effects for the Ru catalysed oxidation of benzyl alcohol.**

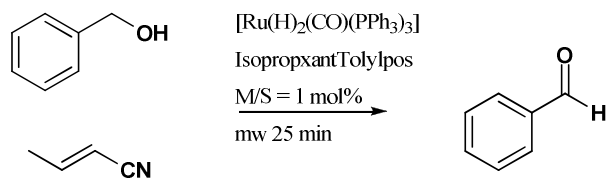
The catalytic results for **Entry 1, Figure 32**, have been previously discussed and are collated to facilitate discussion. **Entries 2-3** were performed using xylene as an analogue to toluene. In the context of microwave assisted reactions, xylene behaves similarly to toluene as these solvents possess similar dielectric parameters [26]. The use of the less volatile xylene allows the reaction temperature to be increased to 140 °C to investigate the effect of temperature. An average conversion of 94% over three runs was obtained with xylene at 120 °C, **Entry 2**. This compares favourably to the 95% obtained using toluene, **Entry 1**. At 140 °C, a corresponding higher yield of 99% aldehyde was obtained, **Entry 3**. This suggests that despite the inefficient coupling of xylene and toluene with the energy source, the net effect of the increased reaction temperature and microwave irradiation is so significant that an increase in reaction rate and yield is still observable. This further suggests that the reaction could be successfully adapted to solvent-free conditions.

Two approaches were investigated for the development of solvent-free protocols. The first method involved melting of the ligand and metal precursor to induce complexation. However, all attempts to melt the Ru precursor and isopropylantTolylphos ligand at various temperatures (100–140 °C) were unsuccessful. The second approach involved a one pot preparation where the metal precursor, ligand, substrate, and crotonitrile were added to a microwave vial and heated for 25 minutes. Analysis of the resultant mixture revealed successful complexation, as well as oxidation of the substrate. The success of this one step, one pot synthesis is due to the liquid substrate acting as both a reactant and the homogeneous medium [27].

The solvent-free oxidation was carried out at three temperatures, **Entries 4–6, Figure 32**. Excellent results were obtained at all solvent-free conditions that were comparable to, if not better than, the results obtained using xylene and toluene. However, the green advantages of solvent-free conditions outweigh the minimal differences in yield. These results suggest that, with the substrate able to act as both the reagent and homogeneous medium, the solvent has minimal or no effect on the reactivity. Therefore the catalytic results presented and discussed previously can in most cases be interpreted in a solvent-free context, depending on the melting point of the substrate. Furthermore, the one step solvent-free testing protocol also precludes the 15 mins microwave complexation previously employed. This further aids the rapid and efficient screening of ligands and substrates, and facilitates high throughput experiments.

In an extended study of the catalytic activity as a function of time, the yield of benzaldehyde was examined under different solvent-free conditions. The results are presented numerically in **Figure 33a**, and graphically in **Figure 33b**. As the temperature increases, an expected increase in the aldehyde product yield is observed, with the reaction approaching maximum yields after 30-35 mins at all temperatures. The difference in yield between the data at 100 °C and 120 °C is greater than for 120 °C and 140 °C. This suggests that a further increase in temperature from 140 °C will not significantly increase the aldehyde yield or shorten the reaction time.





Time [mins]	T = 100 °C	T = 120 °C	T = 140 °C
	Yield [%]	Yield [%]	Yield [%]
0	0	0	0
5	29	45	51
10	52	67	70
15	69	78	81
20	82	88	90
25	95	96	98
30	98	98	98
35	99	99	99

Figure 33a. Solvent-free oxidation of benzyl alcohol.

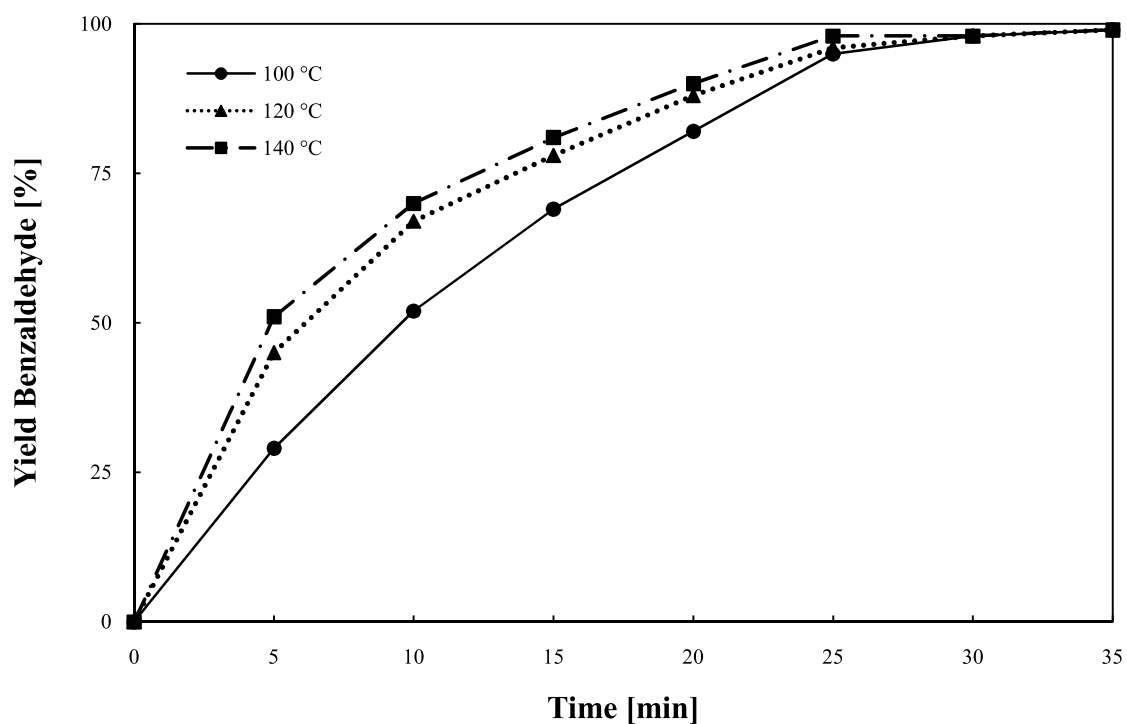


Figure 33b. Catalytic activity as a function of time for the solvent-free oxidation of benzyl alcohol.

### 4.3 Conclusions

The transition metal catalysed dehydrogenative oxidation of primary alcohols to aldehydes has been investigated. Catalytic testing protocols have been developed, implemented and optimised, and green considerations such as alternative heating methods and solvent-free techniques examined. The protocols developed here can be used for the preparation of aldehydes or implemented in a borrowing hydrogen scheme for the activation of alcohols. In comparison to Rh, Os, and Ir metal centres, Ru xantphos complexes were found active for the oxidation of benzyl alcohol in toluene at 1 mol% catalytic loading. The xanthene family ligands were applied to the oxidation of benzyl alcohol. In general, no correlation between the natural bite angle and reactivity could be observed for this reaction. However, most xanthene family ligands were found active giving good yields of the desired aldehyde product. The best performing ligand was isopropoxantphos, and was used for further oxidation reactions. A total of sixteen primary alcohol substrates were oxidised and the yields for benzylic alcohols range from 50–100%, and from 48–74% for aliphatic alcohols. The reactivity of the transition metal catalyst was found to be sensitive to the electronic nature of the substrate. The isopropylxantphos derivatives, isopropoxantTolylphos and isopropoxantButylphos, were tested for the oxidation of benzylic alcohols. IsopropoxantTolylphos showed improved reactivity for both electron withdrawing and donating substrates. The wide bite angle ligand isopropoxantButylphos showed no activity towards the oxidation reaction. Solvent effects were investigated, and solvent-free conditions gave excellent yields and activity comparable to the reactions using toluene and xylene solvents.

### 4.4 Experimental

#### 4.4.1 General

Toluene was distilled over sodium wire and stored under an inert atmosphere. Xylene was used as purchased. Benzyl alcohol (99.8%) and crotonitrile (99%, mixture of *cis* and *trans*) were purchased from Sigma-Aldrich and used without further purification. The internal standard 1,4-dimethoxybenzene (Aldrich, 99%) was dried under vacuum and stored under an inert atmosphere. For substrates containing a methoxy group, 2,6-lutidine (Aldrich, 99%) was used as the internal standard. All alcohol substrates and aldehydes (for calibration purposes) were purchased from Aldrich, Merck, and Fluka unless stated otherwise. All metal precursors, (except  $[\text{Rh}(\text{H})(\text{CO})(\text{PPh}_3)_3]$ , Aldrich, 97%) were prepared as described in Chapter 3.

A calibration curve for each substrate-product combination was generated. This involved the  $^1\text{H}$  NMR analysis of a mixture of varying concentrations of a primary alcohol and its respective oxidised product in  $\text{CDCl}_3$  (250  $\mu\text{L}$ ). An internal standard was used for each run at constant concentration (2.5 mg) and set as the reference peak (integration value of 1). Relevant proton peaks of the substrate and product were integrated at the current concentration and a curve of integration area versus concentration (minimum 4 points) was generated. Least squares regression yielded the calibration equation which was used for all catalytic testing, with normal interpolation techniques used when necessary. For further details see Bekiroglu et al. [6]. In some cases GC-MS was used as a supplementary analysis tool.

## **Microwave Instrument/Methods**

All microwave mediated reactions were conducted using a CEM Discover microwave. Temperature measurements were conducted using an infrared temperature sensor situated below the reaction vessel. Reaction times refer to the total hold time at the indicated temperature with the ramp times ranging from one to two minutes. While there was some variation in the ramp time for each experiment, all reported examples were reproducible using the indicated hold time/temperature. The microwave was calibrated for power and temperature by the distributor prior to all experiments.

### **Procedure for the oxidation of benzyl alcohol to benzaldehyde using conventional heating**

The catalytic testing protocol using conventional heating was reproduced from literature [5]. To an oven-dried argon purged Schlenk tube containing  $[\text{Ru}(\text{H}_2)(\text{CO})(\text{PPh}_3)_3]$  (11.5 mg, 0.0125 mmol, 2.5 mol%) and xantphos (7.25 mg, 0.0125 mmol, 2.5 mol%), degassed anhydrous toluene (0.5 mL) was added, and the mixture heated at reflux for 1 hour, then allowed to cool to room temperature. To the resultant deep-red solution was added benzyl alcohol (54 mg, 0.5 mmol), alkene (61.1 mL, 0.75 mmol), and the mixture heated at 110 °C for 2 hours. On completion, the reaction was allowed to cool to room temperature, diluted with dichloromethane, and the solvent removed in vacuo. The conversion and yield were determined by  $^1\text{H}$  NMR.

### **Representative procedure for the microwave mediated oxidation of benzyl alcohol to benzaldehyde with xantphos**

A dry microwave vial under Ar gas was charged with the metal precursor (0.0025 mmol, 1 mol%), xantphos (1.45 mg, 0.0025 mmol, 1 mol%), and toluene (250  $\mu\text{L}$ ) added. The vial was sealed and the reaction mixture microwaved for 15 min at 80 °C for complexation. There was an immediate colour change that varied from dark red to orange. Under an inert Ar atmosphere, benzyl alcohol (26  $\mu\text{L}$ , 0.25 mmol) was added, followed by crotonitrile (31  $\mu\text{L}$ , 0.375 mmol). The reaction mixture was microwave irradiated for a further 25 mins at 120 °C. The resultant yellow mixture was cooled, diluted with dichloromethane and both solvents removed in vacuo, and the sample analysed by  $^1\text{H}$  NMR using an internal standard.

### **Representative procedure for the microwave mediated oxidation of primary alcohols to aldehydes in toluene**

A dry microwave vial under Ar gas was charged with  $[\text{Ru}(\text{H}_2)(\text{CO})(\text{PPh}_3)_3]$  (2.3 mg, 0.0025 mmol, 1 mol%), ligand (0.0025 mmol, 1 mol%), and toluene (250  $\mu\text{L}$ ) added. The vial was sealed and the reaction mixture microwave irradiated for 15 min at 80 °C for complexation. Under an inert Ar atmosphere, the primary alcohol substrate (0.25 mmol) was added, followed by crotonitrile (31  $\mu\text{L}$ , 0.375 mmol). The reaction mixture was microwave irradiated for a further 25 mins at 120 °C. The resultant yellow mixture was cooled, diluted with dichloromethane and both solvents evaporated, and the sample analysed by  $^1\text{H}$  NMR using an internal standard.

### Representative procedure for the microwave mediated oxidation of benzyl alcohol to benzaldehyde in xylene

A dry microwave vial under Ar gas was charged with [Ru(H<sub>2</sub>)(CO)(PPh<sub>3</sub>)<sub>3</sub>] (2.3 mg, 0.0025 mmol, 1 mol%), isopropyltolylphos (1.63 mg, 0.0025 mmol, 1 mol%), and xylene (250 µL) added. The vial was sealed and the reaction mixture microwave irradiated for 15 min at 80 °C for complexation. Under an inert Ar atmosphere, benzyl alcohol substrate (26 µL, 0.25 mmol) was added, followed by crotonitrile (31 µL, 0.375 mmol). The reaction was microwave irradiated for a further 25 mins at 140 °C. The resultant yellow mixture was cooled, diluted with dichloromethane, and both solvents removed in vacuo, and the sample analysed by <sup>1</sup>H NMR using an internal standard.

### Representative procedure for the solvent-free microwave mediated oxidation of benzyl alcohol to benzaldehyde

A dry microwave vial under Ar gas was charged with [Ru(H<sub>2</sub>)(CO)(PPh<sub>3</sub>)<sub>3</sub>] (6.9 mg, 0.01 mmol, 1 mol%), isopropylxantTolylphos (4.89 mg, 0.01 mmol, 1 mol%), benzyl alcohol substrate (78 µL, 1 mmol), and crotonitrile (93 µL, 1.5 mmol). The resultant mixture was microwave irradiated for a total of 35 mins at the specified reaction temperature (100, 120, or 140 °C), and samples withdrawn every 5 mins and analysed by <sup>1</sup>H NMR using an internal standard.

## 4.5 References

- 1 Hamid, M. H. S. A.; Slatford, P. A.; Williams, J. M. J. *Adv. Synth. Catal.* **2007**, *349*, 1555-1575.
- 2 Dobereiner, G. E.; Crabtree, R. H. *Chem. Rev.* **2010**, *110*, 681-703.
- 3 Nixon, T. D.; Whittlesey, M. K.; Williams, J. M. J. *Dalton Trans.* **2009**, 753-762.
- 4 Seiple, I. B., Borrowing Hydrogen, *Baran Group Meeting Presentation*, **2010**. The Baran Laboratory at The Scripps Research Institute, <http://www.scripps.edu/chem/baran/html/meetingschedule.html> (accessed 12/12/2010).
- 5 Owston, N. A.; Parker, A. J.; Williams, J. M. J. *Chem. Commun.* **2008**, 624-625.
- 6 Bekiroglu, S.; Myrberg, O.; Östman, K.; Ek, M.; Arvidsson, T.; Rundlöf, T.; Hakkarainen, B. *J. Pharm. Biomed. Anal.* **2008**, *47*, 958-961.
- 7 Kappe, C.; Dallinger, D. *Mol. Divers.* **2009**, *13*, 71-193.
- 8 Tundel, R. E.; Anderson, K. W.; Buchwald, S. L. *J. Org. Chem.* **2006**, *71*, 430-433.
- 9 Petricci, E.; Mann, A.; Salvadori, J.; Taddei, M. *Tetrahedron Lett.* **2007**, *48*, 8501-8504.
- 10 Petricci, E.; Mann, A.; Schoenfelder, A.; Rota, A.; Taddei, M. *Org. Lett.* **2006**, *8*, 3725-3727.
- 11 Roberts, B. A.; Strauss, C. R. *Acc. Chem. Res.* **2005**, *38*, 653-661.
- 12 Asensio, G.; Cuenca, A. B.; Esteruelas, M. A.; Medio-Simón, M.; Oliván, M.; Valencia, M. *Inorg. Chem.* **2010**, *49*, 8665-8667.
- 13 Crabtree, R. H. *The organometallic chemistry of the transition metals*; John Wiley & Sons, Inc.: Hoboken, New Jersey, **2005**, p 24-25.
- 14 Crabtree, R. H. Iridium. In *The Handbook of Homogeneous Hydrogenation*; De Vries, J. G., Elsevier, C. J., Eds.; Wiley: Weinheim, **2007**, p 31-43.
- 15 Oro, L. A.; Carmona, D. Rhodium. In *The Handbook of Homogeneous Hydrogenation*; De Vries, J. G., Elsevier, C. J., Eds.; Wiley: Weinheim, **2007**, p 3-27.
- 16 Ledger, A. E. W.; Slatford, P. A.; Lowe, J. P.; Mahon, M. F.; Whittlesey, M. K.; Williams, J. M. J. *Dalton Trans.* **2009**, 716-722.
- 17 Kranenburg, M.; Vanderburgt, Y. E. M.; Kamer, P. C. J.; van Leeuwen, P. W. N. M.; Goubitz, K.; Fraanje, J. *Organometallics* **1995**, *14*, 3081-3089.

- 18 Dierkes, P.; van Leeuwen, P. W. N. M. *J. Chem. Soc., Dalton Trans.* **1999**, 1519-1529.
- 19 Freixa, Z.; van Leeuwen, P. W. N. M. *Dalton Trans.* **2003**, 1890-1901.
- 20 van Leeuwen, P. W. N. M.; Kamer, P. C. J.; Reek, J. N. H. *Pure Appl. Chem.* **1999**, 71, 1443-1452.
- 21 van Leeuwen, P. W. N. M.; Kamer, P. C. J.; Reek, J. N. H.; Dierkes, P. *Chem. Rev.* **2000**, 100, 2741-2769.
- 22 Satrio, J. A. B.; Doraiswamy, L. K. *Chem. Eng. J.* **2001**, 82, 43-56.
- 23 Slatford, P. A.; Whittlesey, M. K.; Williams, J. M. J. *Tetrahedron Lett.* **2006**, 47, 6787-6789.
- 24 Mispelaere-Canivet, C.; Spindler, J.-F.; Perrio, S.; Beslin, P. *Tetrahedron* **2005**, 61, 5253-5259.
- 25 Hayes, B. L. *Microwave Synthesis, Chemistry at the Speed of Light*; CEM Publishing: Matthews, **2002**, p 29-77.
- 26 Hayes, B. L. *Microwave Synthesis, Chemistry at the Speed of Light*; CEM Publishing: Matthews, **2002**, p 35.
- 27 Kerton, F. M. *Alternative Solvents for Green Chemistry*; The Royal Society of Chemistry Cambridge, **2009**, p 23-24.

## Chapter 5

# Microwave assisted transfer hydrogenation of ketones

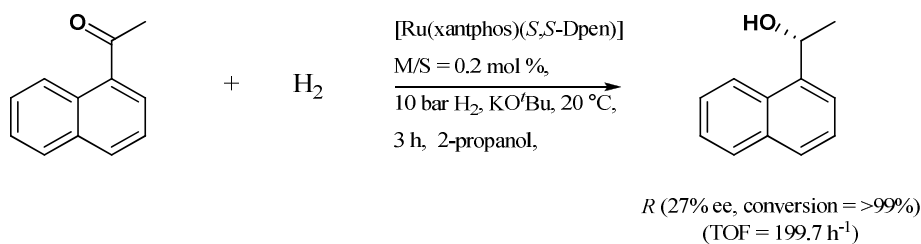
### 5.1 Introduction

To further the catalytic scope of the prepared xanthene family ligands, transfer hydrogenation via Meerwein-Ponndorf-Verly (MPV) type reactions [1-2] were investigated. This type of reaction involves the reduction of a carbonyl to an alcohol by transfer hydrogenation employing a small organic molecule as the hydrogen source. Such homogeneously catalysed reactions can provide access to a wide variety of valuable intermediates for academic and industrial application.

MPV type hydrogenation reactions avoid the use of molecular hydrogen which results in significantly lower reaction pressures. Moreover, the hydrogen source is usually the readily available alcohol 2-propanol [3], which is relatively inexpensive, is oxidised to acetone that can be easily removed, is used in excess which shifts the redox equilibrium towards the desired product, and can be simultaneously used as the solvent. Furthermore, 2-propanol is classified as a high absorbance microwave solvent [4] that is very efficient at coupling and transferring microwave energy. This suggests that an MPV type reaction using 2-propanol can be successfully adapted to microwave assisted conditions.

The reduction of ketones to secondary alcohols is a fundamental and widely employed reaction in synthetic chemistry [5]. Although diphosphines, for example BINAP, have been successfully and extensively applied to such reactions, extensive studies involving xantphos and xanthene family ligands are not common. To the best of our knowledge, there are only two reported studies using any of the xanthene related ligands discussed in Chapter 3.

In a comparative study on the effect of diphosphorus ligands on Ru catalysed asymmetric hydrogenation of 1-acetonaphthone, Subongkoj et al. [6] investigated a [Ru(xantphos)(*S,S*-Dpen)] catalyst, **Scheme 28**. It was proposed that the Dpen ligand would induce a chiral disposition of the phenyl rings at the phosphorus centre that would assist in enantiomeric selectivity for the alcohol. In addition to 2-propanol, the use of molecular hydrogen at elevated pressures (10 bar) was also reported to drive the reaction to completion. Xantphos was found to be as active as BINAP for the reaction (>99% conversion), however poor enantiomeric excess (ee), 27%, was observed. It was suggested the larger bite angle of xantphos relative to Dpen did not allow the chiral amine to efficiently induce chirality leading to the relatively poor ee value.



**Scheme 28.** Ru xantphos catalysed asymmetric hydrogenation of 1-acetonaphthone [6].

In a recent communication, Deb et al. [7] reported the preparation of stable dicarbonylruthenium(II) complexes containing xantphos and DPEphos, **Figure 34**. In a preliminary study, three substrates were screened for activity, and the reported complexes showed higher activity for the hydrogenation of benzaldehyde than for the ketones acetophenone and benzophenone. The [Ru(CO)<sub>2</sub>Cl<sub>2</sub>(DPEphos)] complex also showed slightly higher activity compared to xantphos. In a later work, the same authors reported the preparation of xantphos and DPEphos derivatised with sulphur donors via selective oxidation of one of the phosphorus atoms [8]. This resulted in a P $\searrow$ S heterobidentate ligand with tridentate coordination to both phosphorus atoms and the sulphur heteroatom. However, due to the extent of the derivatisation and the heterobidentate coordination, these ligands are not discussed further in this work.

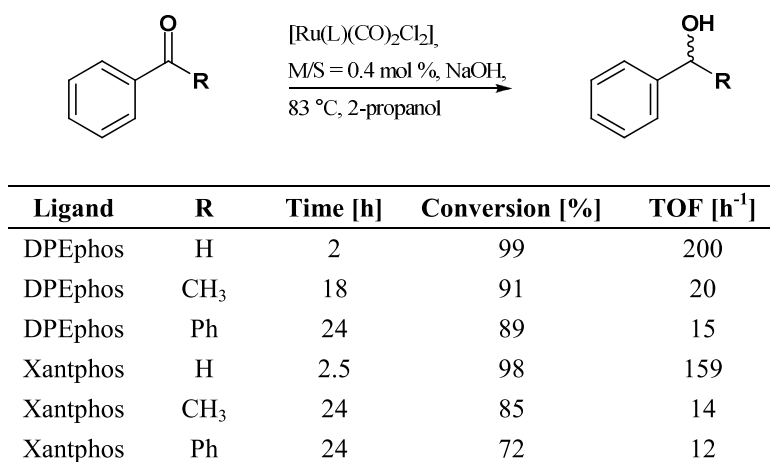


**Figure 34.** Ru catalysed hydrogenation of benzaldehyde, acetophenone, and benzophenone [7].

## 5.2 Results and Discussion

*All catalytic results are presented as an average of 2 or more runs. Turn over Frequency (TOF) = (amount of product [mmol] / amount of catalyst [mmol] / time [hour]). All products were quantified by  $^1\text{H}$  NMR using an internal standard (1,4-dimethoxybenzene, or 2,6-lutidine) and normal interpolation techniques [9]. Further details on the experimental conditions and procedures are presented at the end of this chapter.*

The development of the catalytic testing protocols necessitated a good basis or prototype reaction for subsequent modifications. The well established transfer hydrogenation reactions of Noyori [2] were used as a suitable starting point. Although the work of Noyori involves asymmetric hydrogenation reactions, this study is primarily interested in the activity, rather than enantiomeric selectivity, of xanthene family ligands for the reduction of ketones. Future work could include the use of the developed protocols for the catalytic testing of xanthene family ligands modified for chirality.

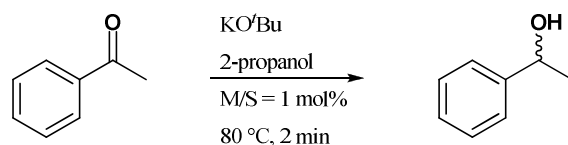
Similar to Noyori, a 2-propanol hydrogen source, strong base, and  $[\text{Ru}(p\text{-cymene})\text{Cl}_2]_2$  metal precursor were identified.  $[\text{Ru}(p\text{-cymene})\text{Cl}_2]_2$  has been extensively employed for hydrogen transfer reactions [10]. Moreover, most reported complexes have good solubility in 2-propanol [11-12], whereas other precursors sometimes require the addition of a co-solvent such as toluene, or benzene [13-14]. In contrast to Noyori's Ru catalysts [2], a secondary diamine ligand was not employed. The use of achiral complexes for the reduction of ketones results in a 50% ee of *R* and *S* enantiomers. Therefore, all results are presented with regards to total yield and TOF to the secondary alcohol to highlight the catalytic activity aspect of this study.

Initial investigative and validation studies were performed using various metal precursors, acetophenone substrate, a strong base, and xantphos. Due to the effective microwave solvent 2-propanol, all studies were immediately carried out via microwave irradiation. To the best of our knowledge, this study represents the first reported application of xantphos, and xanthene family complexes, in microwave assisted hydrogenation reactions. Although the Ru-*p*-cymene precursor was previously identified, analogous half-sandwich  $\pi$  donor Rh and Ir complexes, as well metal hydride complexes, were also screened, **Figure 35**. All precursors and ligands were used in a 1:3 ratio and complexed at 60 °C to ensure complete complexation and promote solubility, and all hydrogenation reactions ran at 80 °C.

Screening of the Ru and Rh metal complexes in **Entries 1** and **2** gave excellent results after 2 mins with high yield of the alcohol product (98 and 92% respectively), and good turn-over frequencies, **Figure 35**. The analogous Ir complex, **Entry 3**, was poorly activating after 2 mins. This reaction was allowed to run for 15 mins, and an alcohol yield of 22% obtained, with the TOF two orders of magnitude less than for the Ru and Rh complexes. These initial results compare favourably with literature. In comparison with results obtained with the  $[\text{Ru}(\text{xantphos})(\text{CO})_2\text{Cl}_2]$  catalyst of Deb et al. [7], **Figure 34**, the Ru-*p*-cymene xantphos complex was more reactive towards 1-phenylethanol at a significantly greater TOF (2916 vs. 159  $\text{h}^{-1}$ ). The reactivity of the reported DPEphos complex was similar to the Ru-*p*-cymene xantphos complex prepared in this work, however the TOF was also significantly lower. No meaningful comparison can be made with the reported



[Ru(xantphos)(*S,S*-Dpen)] catalyst of Subongkoj et al. [6] due to the use of only a single substrate and molecular hydrogen in the literature example.



Entry	Metal	Ligand	Yield [%]	TOF [h <sup>-1</sup> ]
<b>1<sup>a</sup></b>	[Ru( <i>p</i> -cymene)Cl <sub>2</sub> ] <sub>2</sub>	Xantphos	98	≥2916
<b>2<sup>a</sup></b>	[Rh(Cp*)Cl <sub>2</sub> ] <sub>2</sub>	Xantphos	92	≥2760
<b>3<sup>b</sup></b>	[Ir(Cp*)Cl <sub>2</sub> ] <sub>2</sub>	Xantphos	22	≥88
<b>4<sup>c</sup></b>	[Ru(H) <sub>2</sub> (CO)(PPh <sub>3</sub> ) <sub>3</sub> ]	Xantphos	NR	-
<b>5<sup>c</sup></b>	[Rh(H)(CO)(PPh <sub>3</sub> ) <sub>3</sub> ]	Xantphos	NR	-
<b>6<sup>c</sup></b>	[Ir(H)(CO)(PPh <sub>3</sub> ) <sub>2</sub> ]	Xantphos	NR	-
<b>7<sup>a</sup></b>	[Ru- <i>p</i> -cymeneCl <sub>2</sub> ] <sub>2</sub>	-	4	≥119
<b>8<sup>a</sup></b>	[Rh(Cp*)Cl <sub>2</sub> ] <sub>2</sub>	-	12	≥360
<b>9<sup>a</sup></b>		Xantphos	NR	-
<b>10<sup>a</sup></b>	-	-	NR	-

*Complexation of metal precursor and ligand = 5 min at 60 °C,*

*<sup>a</sup>Reaction = 2 min at 80 °C,*

*<sup>b</sup>Reaction = 15 min at 80 °C*

*<sup>c</sup>Reaction = 15 min at 80 °C, No base*

**Figure 35. Validation and metal optimisation studies for the microwave assisted hydrogenation of acetophenone.**

The reactions involving the metal hydride complexes, **Entries 4–6, Figure 35**, were run in the absence of a base as the required acidic hydrogen is incorporated in the metal complex. In all instances, no observable reaction was evident after 15 mins. It has been previously reported [15-16] that certain metal hydride complexes are either poorly active or inactive in the absence of a specialised additive. Four blank experiments were performed to determine the validity of the organometallic catalysis, **Entries 7-10**. The experiments with the metal precursors, **Entries 7-8**, showed minimal conversion. The reaction with the ligand only, **Entry 9**, showed no observable reaction, while **Entry 10** eliminates the possibility of acetophenone degradation or polymerisation in the presence of the strong base [17]. Due to the increased activity, TOF, and economic considerations, Ru-*p*-cymene complexes were used for all further studies.

The presence of a strong base is usually a necessary requirement for this catalytic system. It has been proposed that the purpose of the base is to generate the catalytically active hydride species by the abstraction of the Cl from the metal [15]. In all initial hydrogenation reactions, the strong base KOtBu was employed. The effect of different bases of varying strength on the hydrogenation reaction was also investigated, **Figure 36**. It was found

that the reaction only occurred in the presence of a strong base, **Entries 1** and **3**. In the absence of the base, no reaction was observed, **Entry 5**. To investigate the effect of no base and an alternate hydrogen source, a hydrogenation reaction was attempted in water with sodium formate, **Entry 6**. No reaction was observed, possibly due to insolubility of the ligand. The hydrogenation was also unsuccessful when a mixture of triethylamine and formic acid (TEAF) [18] was used as the hydrogen source **Entry 7**. All further hydrogenation reactions were therefore carried out using a strong base, KO<sup>t</sup>Bu, and the previously identified hydrogen source 2-propanol.

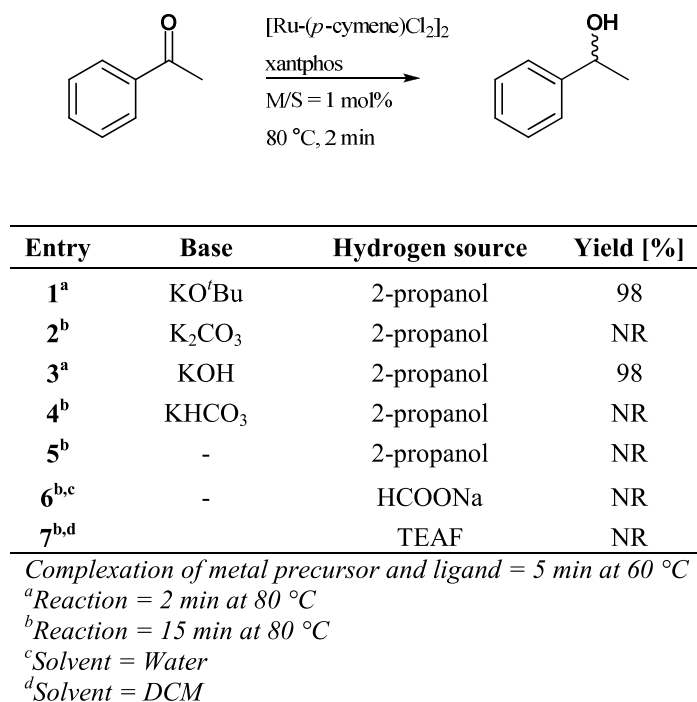
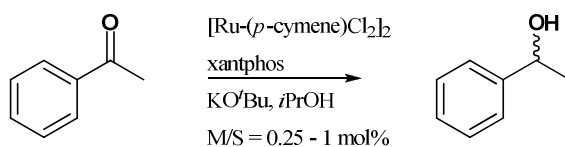


**Figure 36. Investigation of the alternative bases for the hydrogenation of acetophenone.**

The effect of catalyst loading on the hydrogenation of acetophenone was investigated, **Figure 37**. At the preliminary conditions of 1 mol% and 80 °C, a high yield of the secondary alcohol and high TOF were observed, **Entry 1**. The reaction temperature was decreased by 20 °C with the catalyst loading kept constant, **Entry 2**. Encouraged by the negligible difference in yield and TOF at the lower, ‘greener’ temperature, the catalyst loading was then halved, **Entry 3**. After 2 mins, a yield of 70% 1-phenylethanol was obtained, however the high TOF prompted an increase in the reaction time to 5 mins at this lower loading. A high product yield (98%) and TOF still comparable to **Entries 1** and **2** were obtained at the new conditions, **Entry 4**. In a final reaction, the loading was further decreased to 0.25 mol%, and a 50% yield, and significantly lower TOF were obtained after 10 mins. As a result of this decreased activity, a loading of 0.5 mol% was used for all further studies.



Entry	Loading [mol%]	Temperature [°C]	Time[min]	Yield [%]	TOF [h <sup>-1</sup> ]
1	1	80	2	98	≥2922
2	1	60	2	97	≥2892
3	0.5	60	2	70	≥4174
4	0.5	60	5	98	≥2337
5	0.25	60	10	50	≥1196

*Complexation of metal precursor and ligand = 5 min at 60 °C*

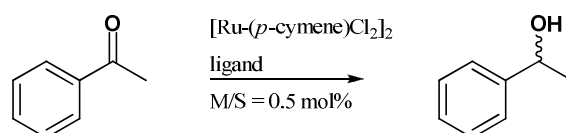
**Figure 37. Optimisation of catalyst loading for the hydrogenation of acetophenone.**

Selected bidentate ligands prepared in Chapter 3 were screened for activity for the Ru catalysed hydrogenation of acetophenone. Two sets of screenings at different reaction conditions were performed, viz. **Condition a**, and **Condition b**. The results are presented numerically in **Figure 38**, and the reactivity at the two conditions are compared graphically in **Figure 39**.

The reaction conditions for **Condition a** were obtained from the previous optimisation study, **Figure 37**. At these conditions, 0.5 mol% loading and 60° C, no obvious trend between the reactivity and natural bite angle can be observed, **Figure 38**. A similar result was obtained in the catalytic oxidation study, Chapter 4. In general, the xanthene family ligands gave good yields of the secondary alcohol with high TOFs, **Entries 4-9**. Notable exceptions are isopropoxantButylphos, **Entry 11**, and phosxantphos, **Entry 2**. The observed low reactivity in **Entry 11** is possibly due to the steric bulk of the butyl groups on the phosphine moieties and the wide natural bite angle. The significantly poorer activity of phosxantphos, relative to the other xanthene family ligands, was unexpected. It is speculated that in the presence of a strong base, the phosphorus in the ring is more susceptible to nucleophilic attack that can significantly alter the electronic properties of the system. The xanthene related ligands, **Entries 1, 3**, and **10**, showed poor activity relative to the xanthene family ligands, highlighting the effect of the core xanthene structure or backbone. This poorer activity relative to the xanthene family was also observed in the previous oxidation study. These results contrast those reported by Deb et al. [7], where DPEphos is shown to be relatively more active than xantphos for the hydrogenation of acetophenone and benzaphenone, **Figure 34**. Although no definitive reason was reported by the authors, the observed activity could possibly be due to the unusual polymeric metal precursor  $[\text{Ru}(\text{CO})_2(\text{Cl}_2)]_n$  which results in strongly hexa-coordinated complexes.

To further optimise the reaction and in particular the TOF, the hydrogenation was performed at **Condition b** for all ligands. The reaction time was lowered to 4 mins, however this was compensated by increasing the

complexation and reaction temperatures to 80 °C. Although lower operating temperatures are considered ‘greener’, a reaction temperature of 80 °C still compares favourably to other reported transfer hydrogenation studies [19]. In general, the reactivity towards the secondary alcohol increased for all ligands, **Figure 38**. This is more clearly illustrated in **Figure 39**. Similar trends in reactivity (or lack thereof) were observed at **Condition b** for all ligands. The xantphos family ligands showed similarly good alcohol yields (> 99%) and high TOFs at the new reaction conditions. The most significant increase in reactivity for the family ligands was thixantphos, **Entry 5**, where a 19% increase in 1-phenylethanol yield was observed. **Entries 2** and **11** also exhibited a significant increase in alcohol yield, however the reactivity was still considerably lower than that of the other family ligands. The xanthene related ligands, **Entries 1, 3, and 10**, showed increases in reactivity of the same or similar magnitude to the xanthene family ligands in **Entries 2** and **11**. Although the xanthene family ligands, **Entries 4-9**, gave similarly good reactivity, the parent ligand xantphos was used as representative for all further studies.



Entry	Ligand	Bite angle [βn]	Condition a		Condition b	
			Yield [%]	TOF [h <sup>-1</sup> ]	Yield [%]	TOF [h <sup>-1</sup> ]
<b>1</b>	DPEphos	102.2	33	786	53	≥1580
<b>2</b>	Phosxantphos	108.0	22	525	39	≥1163
<b>3</b>	PTEphos	107.9	59	1407	77	≥2296
<b>4</b>	Sixantphos	108.5	98	2338	> 99	≥2982
<b>5</b>	Thixantphos	109.6	78	1860	97	≥2892
<b>6</b>	Xantphos	111.4	98	2338	> 99	≥2982
<b>7</b>	Isopropxantphos	113.2	97	2313	> 99	≥2982
<b>8</b>	Nixantphos	114.1	98	2338	> 99	≥2982
<b>9</b>	Hexantphos	116.0	98	2338	> 99	≥2982
<b>10</b>	DBFphos	131.1	8	191	19	≥567
<b>11</b>	IsopropxantButylphos	137.9	5	119	24	≥716

<sup>a</sup>Complexation of metal precursor and ligand = 5 min at 60 °C, Reaction time = 5 mins at 60 °C

<sup>b</sup>Complexation of metal precursor and ligand = 5 min at 80 °C, Reaction time = 4 mins at 80 °C

**Figure 38. Optimisation of ligands for the Ru catalysed hydrogenation of acetophenone. Please refer to Chapter 2, Table 2a-b for ligand structures.**

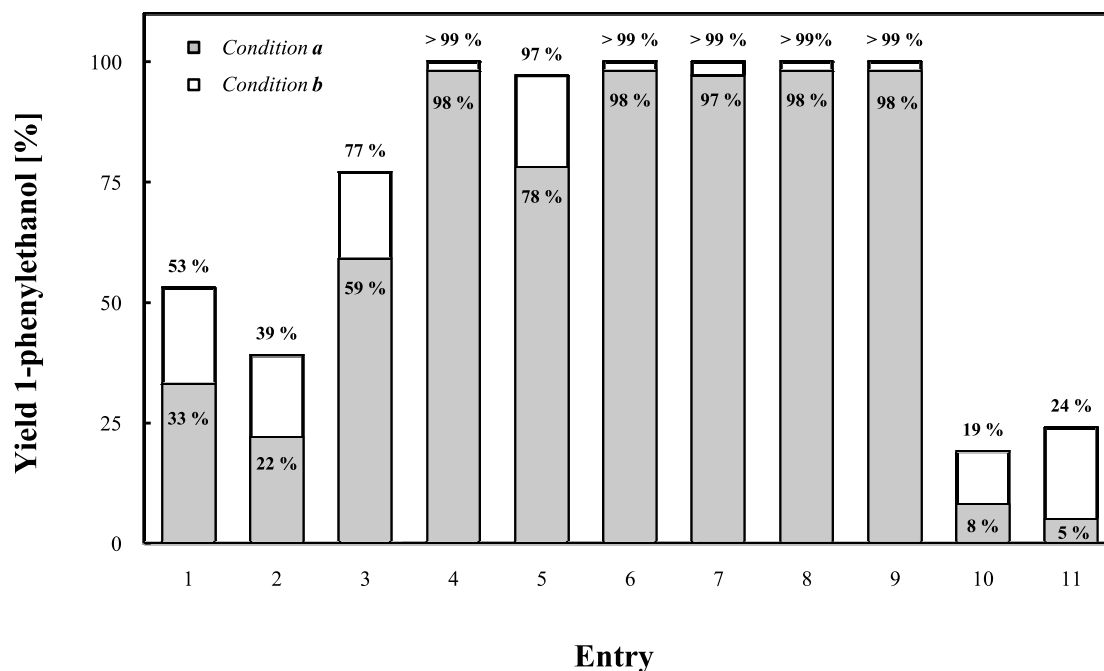
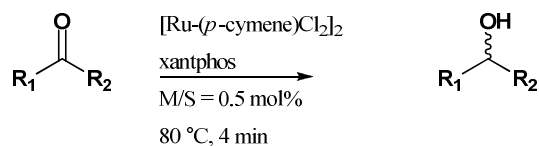


**Figure 39. Comparison of reactivity at different reaction conditions for the Ru catalysed hydrogenation of acetophenone with different bidentate ligands.**

The catalytic testing study was extended to additional ketone substrates to determine the efficacy and scope of the Ru-*p*-cymene xantphos complex, **Figure 40a-b**. A selection of aryl substituted acetophenone derivatives, **Entries 1–11**, and aromatic ketones, **Entries 12–14**, were tested. Acetophenone, **Entry 1**, is used as the benchmark and all results are discussed relative to this substrate. The results for **Entry 1** have been presented previously and are collated here for ease of reference.

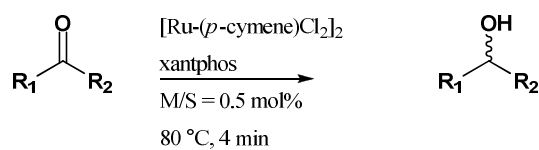
**Entries 2–6** represent acetophenone derivatives modified at the 4' position. No reaction was observed in **Entry 2**. This is presumably due to the strong electron withdrawing nature of the nitro substituent that renders the Ru hydride species more basic, thus inhibiting the catalysis. Similar poor results were obtained for strong electron withdrawing substrates for the oxidation of primary alcohols using a Ru hydride isopropoxantphos complex, **Chapter 4**. This similarity suggests that the reactivity of the xanthene family ligands in the presence of such substrates is somewhat diminished. Therefore, favourable yields were expected for the relatively weaker electron deficient substrates, **Entries 3–4**. The Cl containing substrate, **Entry 4**, exhibited high yield and TOFs towards the secondary alcohol product. However, the yield for the bromo substrate, **Entry 3**, was significantly reduced. This observed low yield was due to limited solubility of 4'-bromoacetophenone, a solid at room temperature, that when added to the reaction mixture afforded a turbid, milky solution. The good electron donating substrates, **Entries 5–6**, were efficiently catalysed to the corresponding alcohols. Complete conversion was observed, with good selectivity and rate.

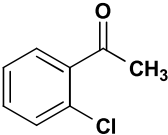
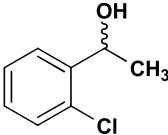
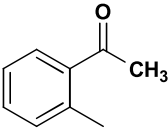
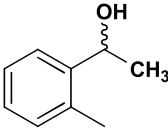
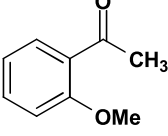
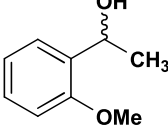
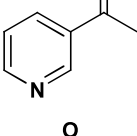
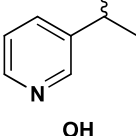
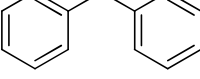
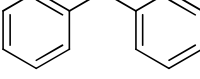
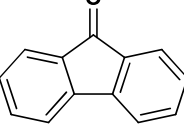
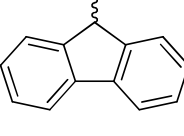
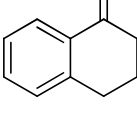
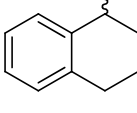


Entry	Ketone	Alcohol	Yield [%]	TOF [h <sup>-1</sup> ]
1			>99	≥2982
2			NR	-
3			48	≥1431
4			93	≥2773
5			>99	≥2982
6			>99	≥2982
7			NR	-

Complexation of metal precursor and ligand = 5 min at 80 °C,  
Reaction time = 4 mins at 80 °C

Figure 40a. Ru catalysed hydrogenation of ketones.



Entry	Ketone	Alcohol	Yield [%]	TOF [h <sup>-1</sup> ]
8			64	≥1908
9			98	≥2922
10			>99	≥2982
11			NR	-
12			>99	≥2982
13			>99	≥2982
14			>99	≥2982

Complexation of metal precursor and ligand = 5 min at 80 °C,  
Reaction time = 4 mins at 80 °C

Figure 40b. Ru catalysed hydrogenation of ketones.

**Entries 7-10** represent acetophenone derivatives modified at the 2' position. **Entry 7**, analogous to **Entry 2**, was similarly unreactive. Similar good reactivity was observed for the substrates in **Entries 9-10**, analogous to the related substrates **Entries 5-6**. Although this suggests that the position of the functional group, either *para* or *ortho*, has no effect on the conversion and yield, a contradictory result was observed in **Entry 8**. The yield for the reduction of 2'-chloroacetophenone was significantly reduced compared to the analogue, **Entry 4**. No reaction was observed in **Entry 11**, possibly due to transient coordination of the sp<sup>2</sup> nitrogen to the metal centre inhibiting the catalytic cycle.

The aromatic ketone substrates, **Entries 12-14**, were efficiently catalysed to the secondary alcohol products in good yield. The reduction of **Entry 12** was previously reported by Deb et al. [7] where a lower conversion (72%) and TOF were reported with a Ru xantphos complex. It was concluded by the authors that the reactivity of the xantphos complex decreased with an increase in the steric bulk of the substrates, **Figure 34**. However, only two ketone substrates were tested in the literature. Due to the limited substrate scope, no meaningful conclusion regarding this trend can be drawn from the reported catalytic testing [7]. From the results obtained in this work, there was no obvious correlation between the reactivity of the Ru-*p*-cymene xantphos complex for the 'bulky' aromatic or aryl substituted ketones. Most substrates, with the exception of those containing strongly electron withdrawing or nitrogen donors, gave good yields and good TOFs towards the desired secondary alcohol.

### 5.3 Conclusions

The transition metal catalysed transfer hydrogenation of ketones in the presence of a base and hydrogen source was investigated. Reported catalytic methods were adapted from literature for the reduction of acetophenone and successfully extended to the microwave assisted reduction of acetophenone and other ketone substrates. In comparison to Ru, Rh, and Ir metal hydrides, the Ru and Rh half-sandwich  $\pi$  donor xantphos analogues were found to efficiently catalyse the transfer hydrogenation of acetophenone to 1-phenylethanol. A Ru-*p*-cymene xanthene complex was therefore used for all further testing. Strong bases were found to promote the reaction, while weak or base free reactions were inactive. The base KO<sup>t</sup>Bu and 2-propanol as the hydrogen source were used for all further studies. The effect of catalyst loading for the reduction of acetophenone was also investigated. The xanthene family ligands were applied to the hydrogenation of acetophenone at 2 conditions. No obvious correlation between the bite angle and reactivity was observed. However, most xanthene family ligands were found active giving good yields of the desired alcohol product. The xantphos family ligands gave similar good activity, therefore the parent ligand xantphos was used as representative for all further studies. A total of fourteen ketone substrates were investigated. Good yields and good TOFs were observed, between 48-99% and  $\geq 1431$ -2982 h<sup>-1</sup> respectively, for substrates containing electron donating and weakly electron withdrawing groups. The protocols developed in this study can be successfully applied for the reduction of aryl and aromatic substituted ketones. Based on these studies future work could include the use of these protocols with xanthene modified ligands containing chiral centres for asymmetric transfer hydrogenation reactions.



## 5.4 Experimental

### 5.4.1 General

The metal precursors  $[\text{Ru}(p\text{-cymene})\text{Cl}_2]_2$ ,  $[\text{Rh}(\text{Cp}^*)\text{Cl}_2]_2$ , and  $[\text{Ir}(\text{Cp}^*)\text{Cl}_2]_2$  were Aldrich grade (> 97%). All other metal precursors were prepared as described in Chapter 3. All solvents, ketone substrates, and secondary alcohols (for calibration purposes), were purchased from Aldrich, Merck, and Fluka unless stated otherwise.

A calibration curve for each substrate-product combination was generated. This involved the  $^1\text{H}$  NMR analysis of a mixture of varying concentrations of a ketone and its respective reduced product in  $\text{CDCl}_3$  (250  $\mu\text{L}$ ). An internal standard was used for each run at constant concentration (2.5 mg) and set as the reference peak (integration value of 1). Relevant proton peaks of the substrate and product were integrated at the current concentration and a curve of integration area versus concentration (minimum 4 points) was generated. Least squares regression yielded the calibration equation which was used for all catalytic testing, with normal interpolation techniques used when necessary. For further details see Bekiroglu et al. [9].

#### Microwave Instrument/Methods

All microwave mediated reactions were conducted using a CEM Discover microwave. Temperature measurements were conducted using an infrared temperature sensor situated below the reaction vessel. Reaction times refer to the total hold time at the indicated temperature with the ramp times ranging from 1 to 2 minutes. While there was some variation in the ramp time for each experiment, all reported examples were reproducible using the indicated hold time/temperature. The microwave was calibrated for power and temperature by the distributor prior to all experiments.

#### Representative procedure for the reduction of acetophenone to 1-phenylethanol in 2-propanol

A dry microwave vial under Ar gas was charged with the metal precursor (0.0025 mmol, 1 mol%), xantphos (4.23 mg, 0.0075 mmol, 3 equivalents to metal), and freshly distilled 2-propanol (4 mL) was added. The vial was sealed and the reaction mixture microwave irradiated for 5 min at 60 °C for complexation. The mixture was allowed to cool for 2 mins. Under an inert Ar atmosphere, acetophenone (58  $\mu\text{L}$ , 0.49 mmol) was added, followed by freshly prepared 0.1 M KO<sup>t</sup>Bu (2 equivalents to metal) in 2-propanol. The reaction mixture was microwave irradiated for 2 mins at 80 °C. The resultant yellow-brown mixture was cooled, 2 mL of sample withdrawn, passed through a small plug of silica gel to remove any catalyst, 2-propanol removed in vacuo, and the sample analysed by  $^1\text{H}$  NMR using an internal standard.

For the investigations using different bases, the reaction was carried out as reported above using the base in equivalents to the metal. For the case of potassium hydroxide, a stock solution of potassium hydroxide (100 mg) in 2-propanol (5 mL) was first prepared. The Ru xantphos arene catalyst was not isolated and were generated in situ in all reactions carried out. A six decimal point analytical balance was used to weigh the

catalyst amounts in a closed room. The Ru metal precursor is very expensive and it was therefore used in moderation. Similar small amounts of catalyst are reported for microwaved assisted transfer hydrogenation reactions [11,20-21]. As a result scale up reactions were not carried out.

#### **Representative procedure for the reduction of acetophenone to 1-phenylethanol using formate as hydrogen source**

A dry microwave vial under Ar gas was charged with  $[\text{Ru}(p\text{-cymene})\text{Cl}_2]_2$  (1.5 mg, 0.0025 mmol, 1 mol%), xantphos (4.23 mg, 0.0075 mmol, 3 equivalents to metal), and water (2 mL) was added. The vial was sealed and the reaction mixture microwave irradiated for 5 min at 60 °C for complexation. The mixture was allowed to cool for 2 mins, followed by the addition of sodium formate (340 mg). Under an inert Ar atmosphere, acetophenone (58  $\mu\text{L}$ , 0.49 mmol) was added. The reaction mixture was microwave irradiated for 15 mins at 80 °C. The resultant orange-yellow mixture was cooled, ethyl acetate (2 mL) added, the organic layer separated, dried over anhydrous magnesium sulphate, filtered, the solvent removed in vacuo, and the sample analysed by  $^1\text{H}$  NMR using an internal standard.

#### **Representative procedure for the reduction of acetophenone to 1-phenylethanol using TEAF**

The TEAF was prepared according to literature methods [18]. A dry microwave vial under Ar gas was charged with  $[\text{Ru}(p\text{-cymene})\text{Cl}_2]_2$  (1.5 mg, 0.0025 mmol, 1 mol%), xantphos (4.23 mg, 0.0075 mmol, 3 equivalents to metal), and DCM (2 mL) was added. The vial was sealed and the reaction mixture microwave irradiated for 5 min at 50 °C for complexation. The mixture was allowed to cool for 2 mins. Under an inert Ar atmosphere, acetophenone (58  $\mu\text{L}$ , 0.49 mmol) was added, followed by the addition of TEAF (2 equivalents to metal). The reaction mixture was microwave irradiated for 15 mins at 50 °C. The resultant mixture was cooled, the organic layer separated, the solvent removed in vacuo, and the sample analysed by  $^1\text{H}$  NMR using an internal standard.

#### **Representative procedure for the reduction of ketone substrates to secondary alcohols in 2-propanol for reaction condition *b***

A dry microwave vial under Ar gas was charged with  $[\text{Ru}(p\text{-cymene})\text{Cl}_2]_2$  (1.5 mg, 0.0025 mmol, 0.5 mol%), ligand (0.0075 mmol, 3 equivalents to metal), and freshly distilled 2-propanol (4 mL) was added. The vial was sealed and the reaction mixture microwave irradiated for 5 min at 80 °C for complexation. The mixture was allowed to cool for 2 mins. Under an inert Ar atmosphere, the ketone substrate (0.97 mmol) was added, followed by freshly prepared 0.1 M KO<sup>t</sup>Bu (2 equivalents to metal) in 2-propanol. The reaction mixture was microwave irradiated for 4 mins at 80 °C. The resultant mixture was cooled, 2 mL of sample withdrawn, passed through a small plug of silica gel to remove any catalyst, 2-propanol removed in vacuo, and the sample analysed by  $^1\text{H}$  NMR using an internal standard.

## 5.5 References

- 1 Klomp, D.; Hanefeld, U.; Peters, J. A. Transfer Hydrogenation Including the Meerwein-Ponndorf-Verley Reduction. In *The Handbook of Homogeneous Hydrogenation*; De Vries, J. G., Elsevier, C. J., Eds.; Wiley: Weinheim, **2007**, p 585-630.
- 2 Noyori, R.; Hashiguchi, S. *Acc. Chem. Res.* **1997**, *30*, 97-102.
- 3 Klomp, D.; Hanefeld, U.; Peters, J. A. Transfer Hydrogenation Including the Meerwein-Ponndorf-Verley Reduction. In *The Handbook of Homogeneous Hydrogenation*; De Vries, J. G., Elsevier, C. J., Eds.; Wiley: Weinheim, **2007**, p 598.
- 4 Hayes, B. L. *Microwave Synthesis, Chemistry at the Speed of Light*; CEM Publishing: Matthews, **2002**, p 70.
- 5 Clarke, M. L.; Roff, G. J. Homogeneous Hydrogenation of Aldehydes, Ketones, Imines and Carboxylic Acid Derivatives: Chemoselectivity and Catalytic Activity. In *The Handbook of Homogeneous Hydrogenation*; De Vries, J. G., Elsevier, C. J., Eds.; Wiley: Weinheim, **2007**, p 413.
- 6 Subongkoj, S.; Lange, S.; Chen, W.; Xiao, J. J. *Mol. Catal. A: Chem.* **2003**, *196*, 125-129.
- 7 Deb, B.; Borah, B. J.; Sarmah, B. J.; Das, B.; Dutta, D. K. *Inorg. Chem. Commun.* **2009**, *12*, 868-871.
- 8 Deb, B.; Sarmah, P. P.; Dutta, D. K. *Eur. J. Inorg. Chem.* **2010**, 1710-1716.
- 9 Bekiroglu, S.; Myrberg, O.; Östman, K.; Ek, M.; Arvidsson, T.; Rundlöf, T.; Hakkarainen, B. J. *Pharm. Biomed. Anal.* **2008**, *47*, 958-961.
- 10 Samec, J. S. M.; Backvall, J.-E.; Andersson, P. G.; Brandt, P. *Chem. Soc. Rev.* **2006**, *35*, 237-248.
- 11 Lutsenko, S.; Moberg, C. *Tetrahedron: Asymmetry* **2001**, *12*, 2529-2532.
- 12 Hashiguchi, S.; Fujii, A.; Takehara, J.; Ikariya, T.; Noyori, R. *J. Am. Chem. Soc.* **1995**, *117*, 7562-7563.
- 13 Leijondahl, K.; Fransson, A.-B. L.; Bäckvall, J.-E. *J. Org. Chem.* **2006**, *71*, 8622-8625.
- 14 Naud, F.; Malan, C.; Spindler, F.; Rüggeberg, C.; Schmidt, A. T.; Blaser, H.-U. *Adv. Synth. Catal.* **2006**, *348*, 47-50.
- 15 Carrión, M. C.; Sepúlveda, F.; Jalón, F. I. A.; Manzano, B. R.; Rodríguez, A. M. *Organometallics* **2009**, *28*, 3822-3833.
- 16 Dong, Z.-R.; Li, Y.-Y.; Chen, J.-S.; Li, B.-Z.; Xing, Y.; Gao, J.-X. *Org. Lett.* **2005**, *7*, 1043-1045.
- 17 Ohkuma, T.; Koizumi, M.; Muñoz, K.; Hilt, G.; Kabuto, C.; Noyori, R. *J. Am. Chem. Soc.* **2002**, *124*, 6508-6509.
- 18 Fujii, A.; Hashiguchi, S.; Uematsu, N.; Ikariya, T.; Noyori, R. *J. Am. Chem. Soc.* **1996**, *118*, 2521-2522.
- 19 Klomp, D.; Hanefeld, U.; Peters, J. A. Transfer Hydrogenation Including the Meerwein-Ponndorf-Verley Reduction. In *The Handbook of Homogeneous Hydrogenation*; De Vries, J. G., Elsevier, C. J., Eds.; Wiley: Weinheim, **2007**, p 604-607.
- 20 Samec, J. S. M.; Mony, L.; Bäckvall, J.-E. *Canadian Journal of Chemistry* **2005**, *83*, 909-916.
- 21 Díaz-Valenzuela, M. B.; Phillips, S. D.; France, M. B.; Gunn, M. E.; Clarke, M. L. *Chem.--Eur. J.* **2009**, *15*, 1227-1232.

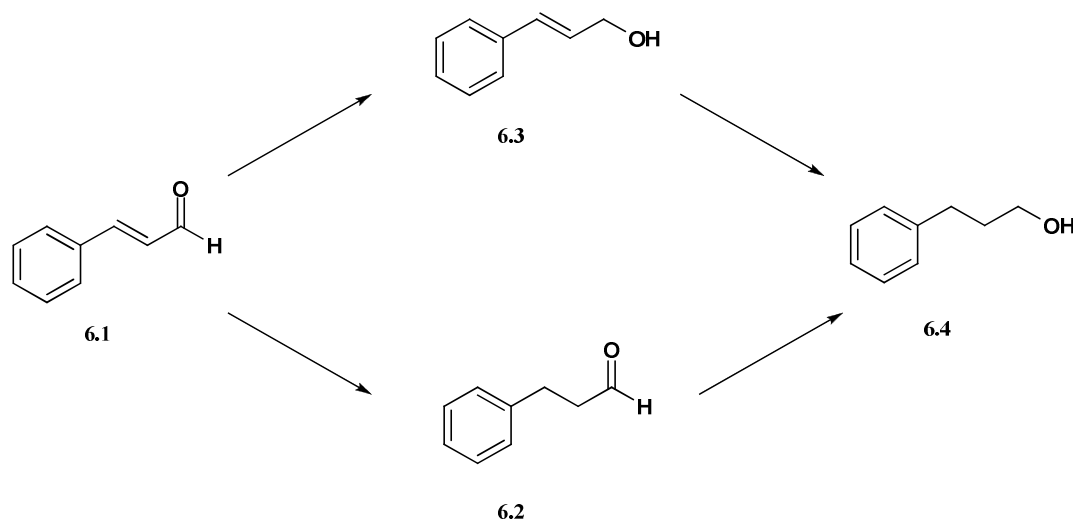
# Chapter 6

## An investigation into the selective hydrogenation of $\alpha,\beta$ -unsaturated carbonyls

### 6.1 Introduction

In the preceding chapter, the hydrogenation of aryl and aromatic substituted ketones via transfer hydrogenation was investigated. The favourable catalytic results prompted the application of the prepared xanthene family ligands to further hydrogenation reactions. To differentiate this study and examine the versatility of the ligands under different operating conditions, hydrogenation reactions using molecular hydrogen were identified. Although the operating pressures for such reactions are greatly increased relative to transfer hydrogenation, this is partially offset by the increased atom economy. To further differentiate this study and examine the substrate scope and selectivity for relatively more complex substrates, the reduction of  $\alpha,\beta$ -unsaturated carbonyls was investigated.

$\alpha,\beta$ -Unsaturated aldehydes and ketones are important starting materials for many products in the fine chemicals, pharmaceutical, and polymers industry [1-3]. Homogeneous catalysis contributes to 15% of industrial selective hydrogenations of  $\alpha,\beta$ -unsaturated aldehydes [4]. Therefore the use of molecular hydrogen is seen as a cost effective and economic alternative to stoichiometric reduction agents [5]. In keeping with the previous catalytic testing strategies, a model compound, cinnamaldehyde **6.1**, was identified as representative of such substrates, and used in initial investigative experiments. The typical hydrogenation pathway for cinnamaldehyde is shown in **Scheme 29** [6-9].



**Scheme 29.** Hydrogenation pathway of cinnamaldehyde **6.1** [6-9].

The unsaturated aldehyde **6.1** can be partially reduced to either a saturated aldehyde, 3-phenyl propanal **6.2**, or an unsaturated alcohol, cinnamyl alcohol **6.3**. Further reduction of **6.2** and **6.3** affords the fully reduced compound 3-phenyl propanol **6.4**. The transition metal catalysed hydrogenation of **6.1** has been extensively studied [10], however selectivity to either of the partial reduction products remains an important consideration [1,7]. Although **6.3** is the relatively more valuable product [11], **6.2** is also desirable as it is an important intermediate in HIV treatment pharmaceuticals [2,12]. In such applications, **6.2** is used for the preparation of hydrocinnamic acid, and the preparation thereof can be contaminated by incomplete oxidation of **6.3**, if present. Therefore, catalysts that are selective for the reduction to the saturated aldehyde would be beneficial for such applications.

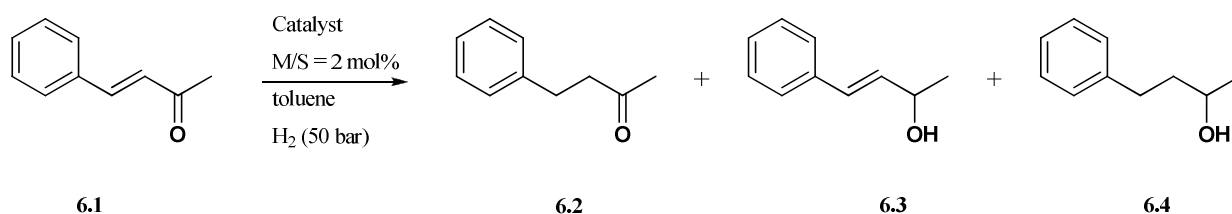
Transition metal complexes involving numerous and varied classes of ligands have been applied to the hydrogenation of  $\alpha,\beta$ -unsaturated carbonyls, for example diphosphines [13-16], phosphorus-nitrogen hemilabile ligands [11], phosphanoborates [6], trianisylphosphines [17], and hydro(pyrazolyl)borates [8]. However, to the best of knowledge, there have been no reported applications of xantphos or family ligands for these reactions. Xantphos ligated to Rh is well known as a hydroformylation catalyst that can efficiently attack C=C bonds to selectively give linear aldehydes with minimal isomerisation and hydrogenation [18]. The use of transition metal complexes containing diphosphorus ligands, for example dppp and dppb with 1,5-cyclooctadiene precursors, have been reported to give good selectivity towards the saturated aldehyde product **6.2**, **Scheme 29** [13-14]. Furthermore, Rh complexes are known to more easily affect the alkene bond hydrogenation, relative to Ir and Ru complexes which are more selective towards C=O bond hydrogenation [11,19]. It was therefore speculated that the combination of a Rh cod metal precursor and xantphos ligand would afford a catalyst that showed good selectivity towards the formation of the saturated aldehyde. To facilitate the use of a molecular hydrogen source, hydrogenation reactions were performed under pressure (50 bar) in a mini reactor (100 mL) equipped with a mass flow meter for H<sub>2</sub> regulation and control.

## 6.2 Results and Discussion

*Catalytic results are presented as an average of 2 runs. All products were quantified by <sup>1</sup>H NMR using an internal standard (1,4-dimethoxybenzene, or 1,4-lutadiene) and normal interpolation techniques [20]. Further details on the experimental conditions and procedures are presented at the end of this chapter.*

For this investigative study the parent ligand xantphos was used as representative of the family of ligands for all reactions. As no previous studies involving xantphos have been reported for this application, catalytic testing protocols were developed for the model substrate cinnamaldehyde. From the previous catalytic testing studies, Chapter 4 and Chapter 5, the metal complexes were generally found to be active in loadings of 0.5–1 mol%. However, to eliminate possible bottlenecks, a catalyst loading of 2 mol% and a long reaction time (12 hours) were used for the initial investigations. The reaction temperature was also set to 60 °C to mimic that of the transfer hydrogenation reactions. The catalyst was prepared beforehand, and the reactor charged with toluene, catalyst, and substrate, purged repeatedly with H<sub>2</sub>, the operating pressure set, and the reaction brought up to temperature. Molecular H<sub>2</sub> at 50 bar was used, a value typically employed in such studies [21-23]. At these

initial conditions, analysis of the reaction mixture revealed 100% conversion of the substrate, **Entry 1, Figure 41**. No conversion towards the unsaturated alcohol **6.3** was observed, with the reaction mixture comprised of 57% saturated aldehyde **6.2**, and 43% completely reduced alcohol **6.4**. The [Rh(xantphos)(cod)(Cl)] complex was highly active at these initial conditions, with the possibility that the saturated aldehyde **6.2** was hydrogenated to the fully reduced product **6.4** at high or complete conversion of the substrate.



Entry	Catalyst	Time [h]	Temperature [°C]	Conversion [%]	Selectivity [%]		
					6.2	6.3	6.4
1	[Rh(xantphos)(cod)Cl]	12	60	100	57	-	43
2	[Rh(xantphos)(cod)Cl]	3	60	100	79	-	21
3	[Rh(xantphos)(cod)Cl]	3	25	92	98	-	2
4	[Rh(cod)(Cl)] <sub>2</sub>	4	25	NR	-	-	-
5	[Ir(xantphos)(cod)Cl]	12	60	61	59	18	23
6	[Ir(xantphos)(cod)Cl]	4	25	NR	-	-	-

**Figure 41. Hydrogenation of cinnamaldehyde 6.1.**

At the same conditions, the reaction time was limited to 3 hours, **Entry 2, Figure 41**. Complete conversion of the substrate was observed, with the selectivity towards **6.2** greatly improved. Encouraged by the activity of the complex, the reaction temperature was lowered to room temperature (ca. 25 °C) and the reaction run for 3 hours, **Entry 3**. At these relatively milder conditions, high conversion of the substrate was once again observed (92%) with further improvements in the selectivity towards **6.2**. This improved selectivity at the shorter reaction time supported the assumption of the concomitant hydrogenation of **6.2** at low or diminished substrate **6.1** concentrations. To further investigate this, a study of the substrate conversion and product distribution as a function of time was undertaken. The hydrogenation reaction was run at the conditions in **Entry 3** and the reaction mixture periodically sampled and analysed. The time dependant conversion and yield profiles are presented graphically in **Figure 42**. Similar good selectivity of 93.9% and 95.1% of **6.3** was reported by Li et al. for the catalysts [Ru(H)Cl(CO)(PPh<sub>3</sub>)(BDNA)] and [Ru(H<sub>2</sub>)(CO)(PPh<sub>3</sub>)(BDNA)] respectively [23]. The conversion reported was 86.4% and 61.5 % for the respective catalyst. In a related study [24] the complex [Ru(H<sub>2</sub>)(CO)(PPh<sub>3</sub>)(BISBI)] was observed to give 88% selectivity towards **6.3** but with poor conversion of 11%. Among the different metal precursors screened in both studies it was concluded that the selectivity of the catalyst was due to both the geometric and electronic environment of the metal centre induced by the diphosphine ligands.

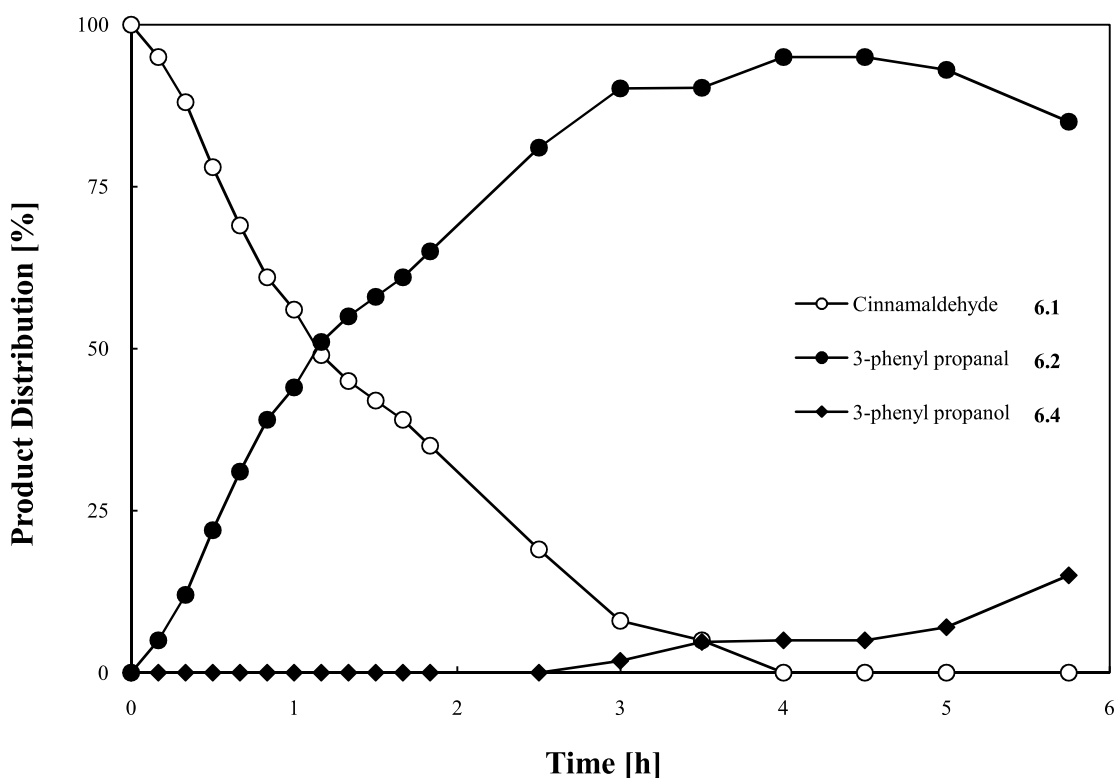
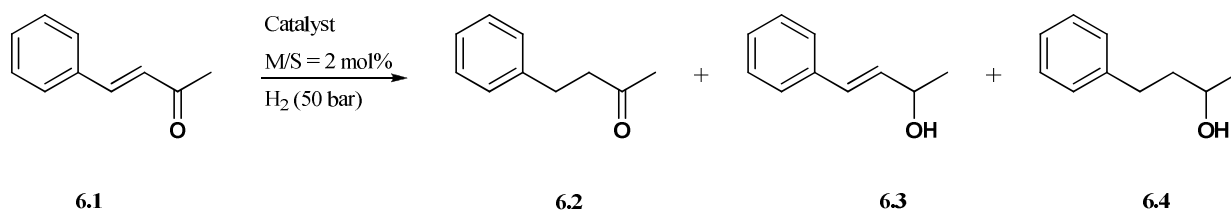


**Figure 42.** Product distribution as a function of time at 2 mol% loading and 50 bar H<sub>2</sub>, in toluene.

At the specified conditions, complete conversion of **6.1** occurs after approximately 4 hours, **Figure 42**, while hydrogenation of **6.2** to **6.4** is initiated at approximately 2.5 hours. From the slopes of the appropriate curves, it is evident that the second hydrogenation step is significantly slower. This implies that the reaction first occurs preferentially at the alkene bonds giving **6.2** as the major product until **6.1** is significantly consumed ( $> \pm 80\%$ ), after which time **6.4** is generated at a significantly slower rate. To validate the favourable results obtained in **Entry 3**, **Figure 41**, a blank run with only the cod metal precursor was investigated. The [Rh(cod)Cl]<sub>2</sub> precursor was found to be inactive for this reaction in the absence of the ligand, **Entry 4**, **Figure 41**.

Ir complexes have been shown to be selective, albeit not as active, for the formation of the unsaturated alcohol **6.3** [22]. An [Ir(xantphos)(cod)Cl] complex was prepared and applied to the reduction of cinnamaldehyde. At 2 mol% loading and 60 °C, 61% conversion of the substrate was observed, **Entry 5**, **Figure 41**. A mixture of three products was obtained with **6.2** as the major (59% selectivity), and **6.3** as the minor (18% selectivity). The reaction temperature was lowered to 25 °C, **Entry 6**, however, no reaction was observed after 4 hours. The poor activity of the Ir xantphos complex at 60 °C and the lack of activity of 25 °C suggest that this complex would require elevated reaction temperatures and longer reactions times to achieve comparable substrate conversion rates to the Rh cod xantphos complex. As a result, these complexes were not used for any further studies.

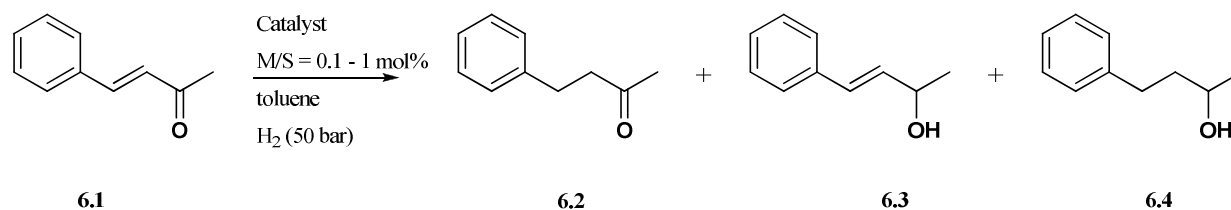


Entry	Solvent	Time [h]	Conversion [%]	Selectivity [%]	
				6.2	6.4
1	Toluene	2	71	100	-
2	Toluene	4	100	95	5
3	Et <sub>2</sub> O	2	82	96	4
4	CH <sub>3</sub> CN	5	< 1	-	-
5	DCM	5	45	93	7
6	THF	5	71	94	6
7	MeOH	5	97	92	8
8	H <sub>2</sub> O	5	92	80	20

**Figure 43.** Hydrogenation of cinnamaldehyde **6.1** in different solvents.

The choice of solvent is known to have a dramatic and sometimes unpredictable effect on catalysis [25-26]. The model hydrogenation reaction was run in different solvents to determine the effect on the rate and selectivity, **Figure 43**. Three broad classes of solvents were investigated, non polar (**Entries 1–3**), polar aprotic (**Entries 4–6**), and polar protic (**Entries 7–8**). The ubiquitous laboratory solvent toluene was used in the initial studies, discussed previously. At 2 hours favourable conversion of **6.1** and selectivity towards the desired product **6.2** was obtained, **Entry 1**. After 4 hours complete conversion of the substrate and good selectivity to **6.2** was also observed, **Entry 2**. The more volatile solvent diethyl ether resulted in a somewhat higher reaction rate than toluene, **Entry 3**. However the increased volatility results in operational difficulties at the high reaction pressures. Low (< 1% **Entry 4**) and mediocre (45% **Entry 5**) conversions were observed for the strong donor solvents [27] CH<sub>3</sub>CN and DCM. The strong donor solvent THF promoted good conversion, **Entry 6**, at the expense of increased reaction time (5 hours). The use of the polar protic solvents, **Entries 7–8**, resulted in high conversions comparable to **Entries 1–3**, at a slightly increased reaction time. The reaction was catalysed in the presence of water as a solvent, **Entry 8**. However, at the end of the reaction 2 immiscible phases (oily-solid catalyst and reaction mixture) were observed that made sample withdrawal over time difficult. It has been previously reported by Malmström et al. [28] that hydrogenation reactions are catalysed in water with the same mechanism as organic solvents. This allows the possibility of the extension of this reaction system to phase transfer catalysis applications that could aid in catalyst recycling and separation. The metal complexes were insoluble in hexane at the reaction temperature therefore it was not used as a solvent. Therefore due to the favourable reactivity of the system in toluene and further operational considerations, this solvent was used in all subsequent studies.





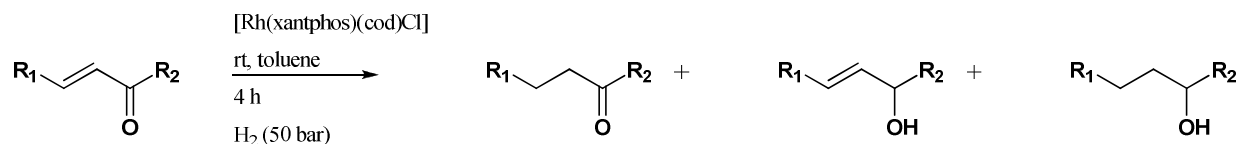
Entry	Loading [mol%]	Time [h]	Conversion [%]	Selectivity [%]	
				6.2	6.4
1	2	4	100	95	5
2	1	9	93	98	2
3	0.4	20.5	88	100	-
4	0.2	20.5	63	100	-
5	0.1	20.5	8	100	-

**Figure 44. Hydrogenation of cinnamaldehyde 6.1 at different catalyst loadings.**

In the preceding studies, a catalyst loading of 2 mol% was employed to ensure catalytic activity at the initial testing conditions. This loading was thereafter varied to determine the effect on substrate conversion and selectivity, **Figure 44**. **Entry 1** has been discussed previously and is presented here for ease of reference. The loading was first halved and periodical analysis of the reaction mixture revealed 93% conversion of **6.1** after 9 hours with a selectivity of 98% towards **6.2**, **Entry 2**. The loading was further decreased to 0.4 mol%, **Entry 3**, where it was found that it was necessary to run the reaction for at least 20 hours to obtain good substrate conversion, albeit with excellent selectivity. Similar reduction in the loading, (0.2 and 0.1 mol% in **Entries 4** and **5** respectively) resulted in not unexpected diminished reactivity, however the good selectivity was maintained. Due to the significantly shorter reaction times and favourable catalytic activity, 2 mol% loading was used for all further studies.

The favourable catalytic results obtained for the hydrogenation of **6.1** prompted the investigation of other  $\alpha,\beta$ -unsaturated aldehydes and ketones, **Figure 45**. Two unsaturated aldehyde substrates differing in electronic nature were investigated. A relatively low conversion of the aldehyde substrate was observed after 4 hours in **Entry 1**, presumably due to the strong electron withdrawing nature of the  $\text{NO}_2$  functionality that makes the alkene bond relatively more difficult to reduce than **6.1**. In contrast, the strong electron donating OMe group of the substrate in **Entry 2** presumably makes the  $\text{C}=\text{C}$  more electron rich and easier to hydrogenate relative to **Entry 1**, leading to the observed good activity and selectivity. The catalytic testing conditions used for the aldehydes were extended to two  $\alpha,\beta$ -unsaturated ketone substrates. Excellent activity and selectivity were observed for both substrates, **Entries 3-4**. It is interesting to note that although 100% conversion was achieved for both unsaturated ketones, no further hydrogenation of the saturated ketone to the fully reduced alcohol was observed. From the available substrate testing data it is difficult to draw any definite conclusions, however it is speculated that the absence of the fully reduced alcohol is due to the more difficult or slower hydrogenation of

the saturated ketone relative to the saturated aldehyde in **Entry 2**. This is consistent with the work of Burk et al. [29] where it was found that it was relatively more difficult to hydrogenate a ketone than an aldehyde with a diphosphorus Rh cod complex.



Entry	Substrate	Conversion [%]	Selectivity [%]	
			6.2	6.4
1		69	100	-
2		100	95	5
3		100	100	-
4		100	100	-

**Figure 45. Hydrogenation of  $\alpha,\beta$ -unsaturated carbonyls.**

### 6.3 Conclusions and Future Perspectives

A preliminary study of the hydrogenation ability of a [Rh(xantphos)(cod)Cl] complex for  $\alpha,\beta$ -unsaturated carbonyls has been investigated. To the best of our knowledge, this is the first reported application of xantphos for this reaction. The hydrogenation of cinnamaldehyde was identified as the prototype reaction. The hydrogenation experiments were run with molecular hydrogen at 50 bar in a mini reactor (100 mL) and a [Rh(xantphos)(cod)Cl] complex was found to be active at 60 °C with good selectivity towards the saturated aldehyde product. This reaction was also found to proceed efficiently at 25 °C and this temperature was used for all further investigations. No selectivity towards the unsaturated alcohol product was observed at any

conditions studied for the Rh complex. An analogous [Ir(xantphos)(cod)Cl] complex was found to be poorly active at 60 °C and inactive at 25 °C and was not used in any further investigations.

From a study of the product distribution over time it was found that hydrogenation of the saturated aldehyde to the fully reduced alcohol occurred at low substrate concentrations at a much slower rate than the initial hydrogenation. The reduction of cinnamaldehyde was found to proceed best in the presence of non-polar solvents such as toluene, although polar protic solvents could be equally used. The testing conditions were extended to two further aldehyde substrates. A strong electron withdrawing substrate showed poorer conversion relative to a strong electron donating substrate. The hydrogenation of two unsaturated ketones showed complete conversion and 100% selectivity towards the saturated aldehyde product.

The results obtained in this preliminary investigation can be used as a basis for future studies involving xantphos family complexes and a more rigorous investigation of the substrate scope for unsaturated carbonyls. Furthermore, in-depth studies on the parameters influencing the catalytic activities, for example molecular hydrogen pressure, reaction time, and temperature, could lead to the preparation of tailor-made xanthene based catalysts for this reaction.

## 6.4 Experimental

### 6.4.1 General

All solvents, reagents, and miscellaneous chemicals were sourced from Aldrich, Fluka, or Merck unless otherwise stated. All solvents were dried using standard methods. Reactions were carried out using UHP grade hydrogen, and the transition metal catalysts prepared as described previously, **Chapter 3**.

A 100 mL, stainless steel mini reactor purchased from Autoclave Engineers based in the USA, equipped with a stirrer, Teflon liner, thermal couple, and sample withdrawal port, was employed for all testing reactions. The reactor was fitted to a mass flow meter (Siemens, Sitrans FC Massflo® Mass 6000), calibrated by the supplier for low flow rates (0-0.5 kg/h), and equipped with a remote unit for hydrogen flow regulation. A gas sensor/alarm unit (Oldham) was installed to detect hydrogen leakage during the high pressure reactions.

A calibration curve for each substrate-product combination was generated. This involved the <sup>1</sup>H NMR analysis of a mixture of varying concentrations of an α,β-unsaturated carbonyl and its respective reduced product in CDCl<sub>3</sub> (250 μL). An internal standard was used for each run at constant concentration (2.5 mg) and set as the reference peak (integration value of 1). Relevant proton peaks of the substrate and product were integrated at the current concentration and a curve of integration area versus concentration (minimum 4 points) was generated. Least squares regression yielded the calibration equation which was used for all catalytic testing, with normal interpolation techniques used when necessary. For further details see Bekiroglu et al. [20]. In some cases GC-MS was used as a supplementary analysis tool.

### Representative procedure for the hydrogenation of cinnamaldehyde at 60 °C and 50 bar H<sub>2</sub>

The reactor was charged with dry toluene (12 mL), catalyst (0.0146 mmol, 2 mol%), and cinnamaldehyde (93 µL, 0.74 mmol). The autoclave was first purged several times with hydrogen, and then filled with hydrogen at 50 bar. The reaction mixture was heated to 60 °C, stirred, and the reaction time monitored. Sample analysis involved the withdrawal of an aliquot, dilution with wet DCM, removal of toluene in vacuo, and analysis by <sup>1</sup>H NMR in the presence of an internal standard. When the reaction was complete, it was cooled by immersion in an ice-bath, and analysis of the reaction mixture repeated. For the investigations using different solvents and catalytic loadings, the reaction was carried out as reported above.

### Representative procedure for the hydrogenation of α,β-unsaturated carbonyl substrates at ambient temperature and 50 bar H<sub>2</sub>

The reactor was charged with dry toluene (12 mL), catalyst (12 mg, 0.0146 mmol, 2 mol%), and substrate (0.74 mmol). The autoclave was first purged several times with hydrogen, and then filled with hydrogen at 50 bar. The reaction mixture was stirred and the reaction time monitored. Sample analysis involved the withdrawal of an aliquot, dilution with wet DCM, removal of toluene in vacuo, and analysis by <sup>1</sup>H NMR in the presence of an internal standard.

## 6.5 References

- 1 Grosselin, J. M.; Mercier, C.; Allmang, G.; Grass, F. *Organometallics* **1991**, *10*, 2126-2133.
- 2 Muller, A. J.; Bowers, J. S.; Eubanks, J. R. I.; Geiger, C. C.; Santobianco, J. G., U.S. Patent, 5,939,581, Aug. 17, 1999.
- 3 Bianchini, C.; Peruzzini, M.; Farnetti, E.; Kašpar, J.; Graziani, M. *J. Organomet. Chem.* **1995**, *488*, 91-97.
- 4 Joubert, J.; Delbecq, F. *Organometallics* **2006**, *25*, 854-861.
- 5 Klomp, D.; Hanefeld, U.; Peters, J. A. Transfer Hydrogenation Including the Meerwein-Ponndorf-Verley Reduction. In *The Handbook of Homogeneous Hydrogenation*; De Vries, J. G., Elsevier, C. J., Eds.; Wiley: Weinheim, **2007**, p 413-414.
- 6 Jiménez, S.; López, J. A.; Ciriano, M. A.; Tejel, C.; Martínez, A.; Sánchez-Delgado, R. A. *Organometallics* **2009**, *28*, 3193-3202.
- 7 Lashdaf, M.; Krause, A. O. I.; Lindblad, M.; Tiitta, M.; Venäläinen, T. *Appl. Catal. A: Gen.* **2003**, *241*, 65-75.
- 8 López-Linares, F.; Agrifoglio, G.; Labrador, Á.; Karam, A. *J. Mol. Catal. A: Chem.* **2004**, *207*, 117-122.
- 9 Nuithitikul, K.; Winterbottom, M. *Chem. Eng. Sci.* **2004**, *59*, 5439-5447.
- 10 Gallezot, P.; Richard, D. *Catalysis Reviews* **1998**, *40*, 81-126.
- 11 Kostas, I. D. *J. Organomet. Chem.* **2001**, *634*, 90-98.
- 12 Muller, A. J.; Bowers, J. S.; Eubanks, J. R. I.; Geiger, C. C.; Santobianco, J. G., World Intellectual Property Organisation (WIPO), WO 99/08989, Feb. 25, 1999.
- 13 Sakaguchi, S.; Yamaga, T.; Ishii, Y. *J. Org. Chem.* **2001**, *66*, 4710-4712.
- 14 Spogliarich, R.; Farnetti, E.; Kaspar, J.; Graziani, M.; Cesarotti, E. *J. Mol. Catal.* **1989**, *50*, 19-29.
- 15 Visintin, M.; Spogliarich, R.; Kaspar, J.; Graziani, M. *J. Mol. Catal.* **1984**, *24*, 277-280.
- 16 Farnetti, E.; Kaspar, J.; Graziani, M. *J. Mol. Catal.* **1990**, *63*, 5-13.
- 17 Landaeta, V. R.; López-Linares, F.; Sánchez-Delgado, R.; Bianchini, C.; Zanobini, F.; Peruzzini, M. *J. Mol. Catal. A: Chem.* **2009**, *301*, 1-10.
- 18 van Leeuwen, P. W. N. M. *Homogeneous Catalysis: Understanding the Art*; Kluwer Academic Publishers: Dordrecht, **2004**, p 155-160.

- 19 Sánchez-Delgado, R. A.; Andriollo, A.; Valencia, N. *J. Mol. Catal.* **1984**, *24*, 217-220.
- 20 Bekiroglu, S.; Myrberg, O.; Östman, K.; Ek, M.; Arvidsson, T.; Rundlöf, T.; Hakkarainen, B. *J. Pharm. Biomed. Anal.* **2008**, *47*, 958-961.
- 21 Hotta, K. *J. Mol. Catal.* **1985**, *29*, 105-107.
- 22 Li, R.-X.; Li, X.-J.; Wong, N.-B.; Tin, K.-C.; Zhou, Z.-Y.; Mak, T. C. W. *J. Mol. Catal. A: Chem.* **2002**, *178*, 181-190.
- 23 Li, R.-X.; Wong, N.-B.; Li, X.-J.; Mak, T. C. W.; Yang, Q.-C.; Tin, K.-C. *J. Organomet. Chem.* **1998**, *571*, 223-229.
- 24 Li, R.-X.; Tin, K.-C.; Wong, N.-B.; Mak, T. C. W.; Zhang, Z.-Y.; Li, X.-J. *J. Organomet. Chem.* **1998**, *557*, 207-212.
- 25 Burk, M. J.; Kalberg, C. S.; Pizzano, A. *J. Am. Chem. Soc.* **1998**, *120*, 4345-4353.
- 26 Rajadhyaksha, R. A.; Karwa, S. L. *Chem. Eng. Sci.* **1986**, *41*, 1765-1770.
- 27 Herrmann, W. A.; Frey, G. D.; Herdtweck, E.; Steinbeck, M. *Adv. Synth. Catal.* **2007**, *349*, 1677-1691.
- 28 Malmstrom, T.; F. Wendt, O.; Andersson, C. *J. Chem. Soc., Dalton Trans.* **1999**, 2871-2875.
- 29 Burk, M. J.; Harper, T. G. P.; Lee, J. R.; Kalberg, C. *Tetrahedron Lett.* **1994**, *35*, 4963-4966.

# Chapter 7

## Towards the preparation of tridentate xanthene family ligands and catalysts

### 7.1 Introduction

The upgrading of relatively inert substrates to more active intermediates is a good way to monetise otherwise ineffective feed-stocks. An example of this, briefly discussed in Chapter 4, is alcohol activation via borrowing hydrogen. A more appropriate example in a South African industrial context is C-H bond activation [1], in particular the conversion of alkanes to alkenes. The archetypal C-H activation catalysts are the tridentate Ir PCP pincer complexes that are known to be highly efficient for the dehydrogenation of linear and cycloalkanes [2-9]. A generalised structure is shown in **Figure 46**, where coordination of the phosphorus donors ( $P^{\wedge}P$ ) and ortho-metallation of the third donor (C) results in active and stable catalysts with relatively planar backbones.

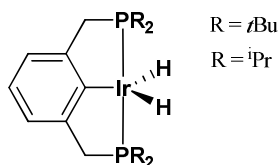
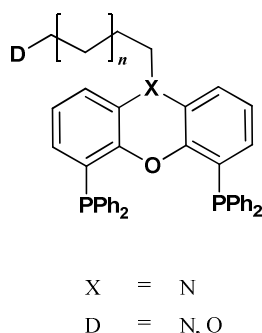


**Figure 46.** Generalised structure of an Ir PCP complex.

Although highly active, the selectivity of Ir PCP complexes towards the linear alkene is hindered by the isomerisation of the terminal alkene bond to internal olefins. There has therefore been much investigation into the modification of these types of ligands resulting in a new class of chemistry termed pincer chemistry [10]. Despite extensive derivatisation, the most selective alkane dehydrogenation pincer complexes essentially possess the same core structure, with the phosphorus moieties altered to induce varying steric and electronic effects [11-13].

It was therefore speculated that a tridentate ligand that can form stable metal complexes, and whose reactivity is amenable to electronic and steric changes in the ligand environment could possibly be applied to similar C-H activation reactions. Therefore, the development of tridentate ligands based on the xanthene backbone was investigated, **Figure 47**. The diphenylphosphine donors of the proposed ligands were kept constant, with the third donor (D) varied with contrasting hard and soft atoms, for example N and O. An alternate coordination mode for the third donor was also proposed. As an alternative to ortho-metallation, *fac* coordination via a donor-linker tail that originates from the backbone and comes over the plane formed by the backbone and phosphorus donors to chelate to the metal centre, was desired. It was postulated that tridentate coordination in

such a manner would not only increase the stability of a xanthene based catalyst, but also block an active site and introduce additional steric hindrance that could possibly prevent the formation or coordination of the isomerised product. A similar coordination mode is enforced in scorpionate type ligands, the classical examples of which are the trispyrazoleborates of Trofimenko et al. [14-15]. However, application of these ligands to C-H activation reactions has been mostly unsuccessful, primarily due to de-chelation during catalysis [16]. An Ir metal centre with a cod counter ligand was identified due to its ubiquitous and successful use in pincer chemistry applications.

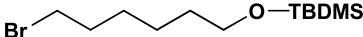
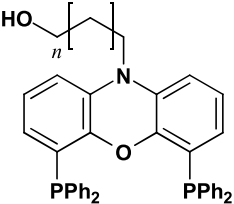
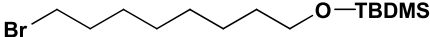
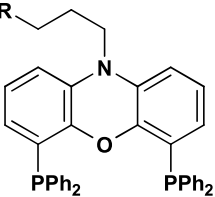
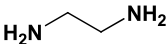
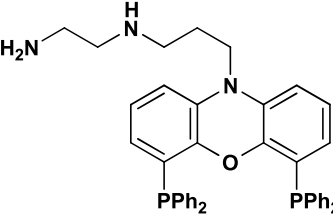


**Figure 47. Generalised structure of the proposed tridentate ligands.**

In a recent publication, Asensio et al. [17] have reported the preparation of a tridentate Os xantphos complex via ortho-metallation of the ether linkage in the backbone. However, to the best of our knowledge, there have been no reports on the preparation of *fac* coordinating tridentate xantphos or xanthene family complexes. The preparation of nixantphos type ligands functionalised with a third donor for supported catalysis applications have been previously reported [18-20], but no reports on successful chelation of the third donor to the metal centre exist. To facilitate functionalisation of the linker tail for this work, nixantphos,  $X = N$ , **Figure 47**, has been employed as the bidentate ligand basis for modifications.

## 7.2 Results and Discussion

**Table 11** presents a summary of the tridentate ligands prepared in this work, along with the corresponding linker tail and bidentate precursor. The preparation of the ligand backbone, 10-(*t*-butyldimethylsilyl) phenoxazine, and the bidentate precursor nixanpthos, have been previously described, Chapter 3.

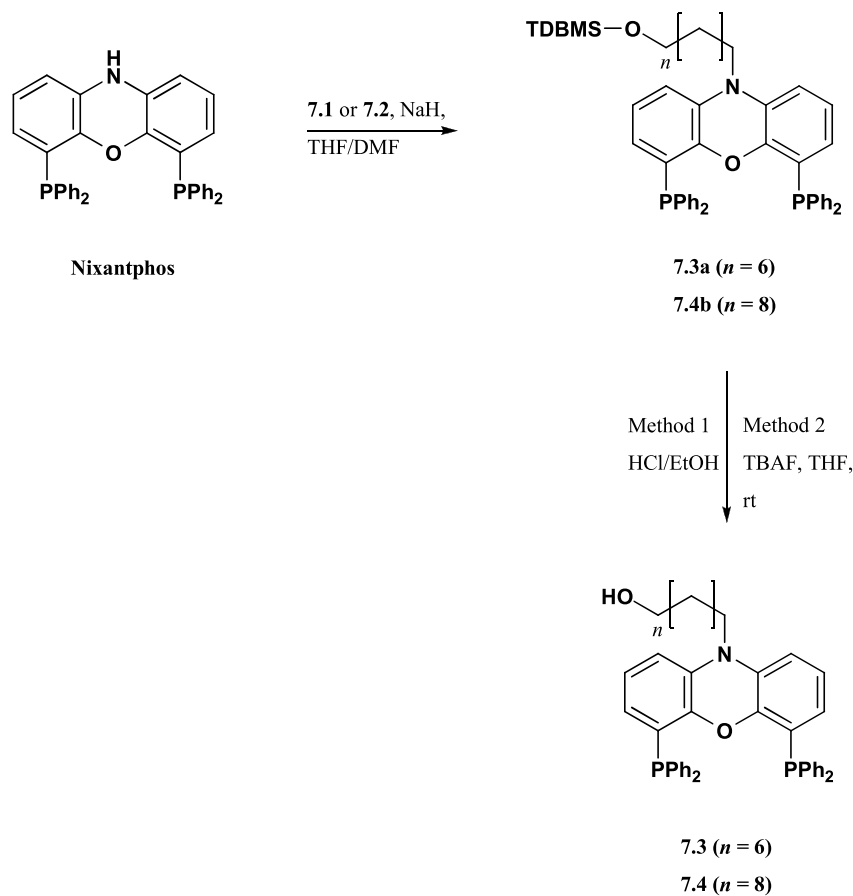
Bidentate Precursor	Linker Tail	Tridentate Ligand
Nixantphos	 <p>7.1</p>	 <p>7.3 (<math>n = 6</math>)</p> <p>7.4 (<math>n = 8</math>)</p>
Nixantphos	 <p>7.2</p>	 <p>7.6 (<math>R = 0.73 + 0.27 \text{ Br}</math>)</p>
7.6	 <p>7.7</p>	 <p>7.8</p>

**Table 11. Summary of the prepared tridentate ligands and corresponding linker tails.**

The strategy for the preparation of the tridentate ligands involved functionalisation of the previously prepared bidentate precursor with the linker tail. The linker functionality was not consolidated or incorporated into the synthesis of the backbone due to the possibility of attack during the lithiation step for the addition of the diphenylphosphine moieties. In terms of preparation, protection/de-protection and chelation considerations, an O donor ligand was identified as a good synthetic starting point. It was further expected that a hydroxyl group would readily displace the cod counter ligand and undergo oxidative addition to the Ir metal centre upon complexation. Alkyl linker tails were chosen for flexibility considerations, and two hard O donor tridentate



ligands of differing tail lengths were successfully prepared, **7.3**, **7.4**, **Table 11**. The preparation thereof is illustrated in **Scheme 30**.



**Scheme 30. Preparation of tridentate ligands 7.3 and 7.4.**

The tail precursors were prepared in the protected form. The six carbon length linker, bromohexylsilylether **7.1**, was purchased and used as is. Bromooctanol was protected to afford bromooctylsilylether **7.2** in 85% yield [21]. For each tridentate ligand, the tail precursor was added to a solution of nixantphos in NaH. Repeated synthesis showed that either an aprotic solvent (DMF), or an easily distilled solvent (THF), were equally applicable. Two possibilities were investigated for the deprotection of the resulting compounds: (1) an ethanolic solution of HCl was added immediately to the crude reaction mixture and allowed to stir, or (2) the reaction mixture was purified by column chromatography and deprotected by TBAF in THF. However, both methods afforded low yields of the desired product (< 25%). Subsequent aqueous work up was carried out, and the tridentate ligands **7.3** and **7.4** were purified by column chromatography. A good quality single crystal of **7.3** was obtained by slow diffusion at room temperature over several days from a solution of DCM/EtOH (1/1, v/v). An ORTEP representation of ligand **7.3** is presented in **Figure 48**, where the thermal ellipsoids are shown at 50% probability, with the hydrogen atoms omitted for clarity. A full listing of crystal data and further supplementary information are presented in **Appendix B** of this dissertation.

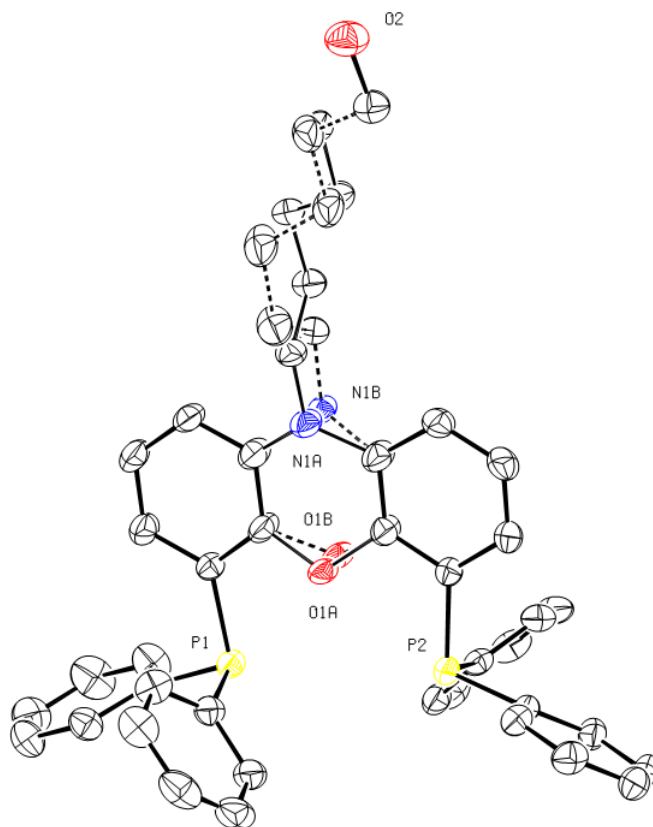
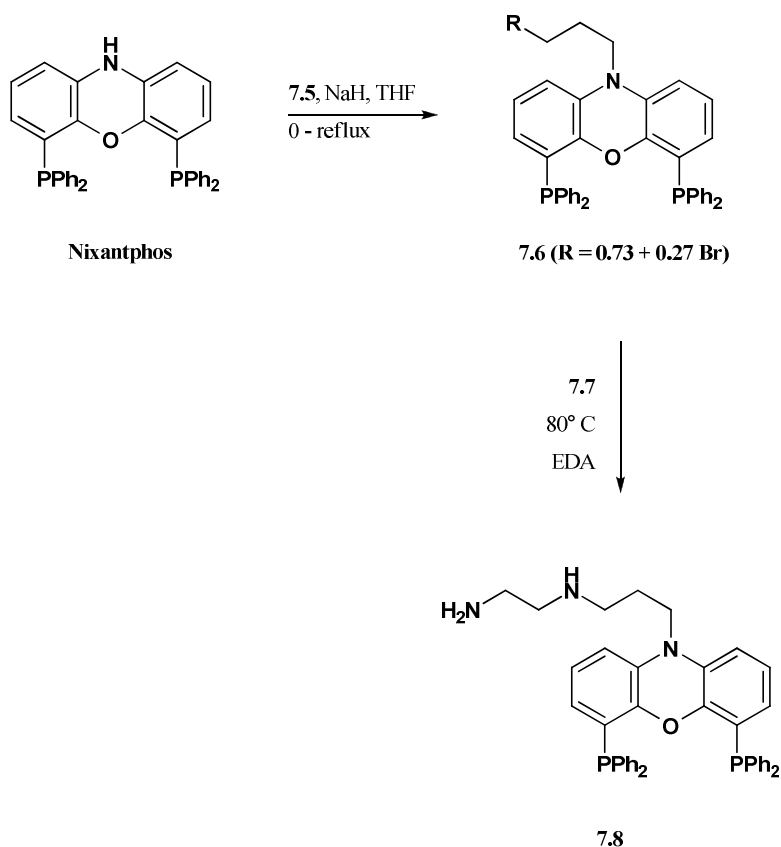


**Figure 48.** Crystal structure of tridentate ligand **7.3**.

In comparison to the bidentate precursor nixantphos, the novel crystal structure of **7.3** is similarly planar, dihedral angle of  $3.12^\circ$  (2), with an essentially identical intramolecular P...P distance, 4.255 (2) Å and 4.253 (2) Å respectively. The angles involving the phosphorus atoms for **7.3** range from  $100.21^\circ$  (7) to  $104.89^\circ$  (7). The *N*-hexanol group was found to be disordered and refined over two positions with final occupancies of 0.683 (3) and 0.317 (3), which affected the C-O and C-N bond lengths. The C-O bond lengths range from 1.402 (2) to 1.415 (2) Å, and for C-N from 1.410 (2) to 1.448 (3) Å for the major disorder component. The corresponding ranges for the minor disorder component are 1.408 (3) to 1.429 (3), and 1.474 (3) to 1.474 (4) Å respectively. In comparison, the C-O bond lengths (1.388 (2) to 1.392 (2) Å) and C-N bond lengths (1.398 (3) to 1.403 (3) Å) for the crystal structure of nixantphos are relatively shorter. It is speculated that the cause of the disorder for the *N*-hexanol group is due to the nature of the atoms and bonds involved, i.e. the  $sp^2$  carbon bonded to similar  $sp^2$  carbons. This promotes the free movement of the straight long alkyl chain that could possibly result in the observed positional disorder. If the nixantphos moiety in **7.3** is considered as the head of the compound and the hexanol chain as the tail, then the crystal structure packing can be described as stacked in a head to tail arrangement. Due to this arrangement several intermolecular interactions, especially of the type O2-H...O1 are observed between the heads and tails of adjacent molecules. The H...O1 interatomic lengths range from 2.733 to 3.346 Å. Although these are unusually long for classical hydrogen bonding [22-23], these interactions are significant in maintaining the integrity of the disordered crystal structure.



**Scheme 31. Preparation of tridentate precursor 7.6 and tridentate ligand 7.8.**

Encouraged by the successful preparation of the hard O donor ligands, the preparation of the counterpart soft N donor ligands were also investigated, **Scheme 31**. The synthetic strategy was slightly modified from that of ligands **7.3** and **7.4**. The direct functionalisation of the backbone with the desired donor-linker combination was avoided, and the preparation of a tridentate precursor ligand with a good leaving group to be used as a basis for the addition of further linkers was investigated. This precursor ligand, **7.6**, was prepared by the addition of 1-bromo-3-chloropropane **7.5**, to a mixture of nixantphos in NaH and THF. Recrystallisation from DCM/EtOH afforded a white solid in 74% yield. An X-ray quality single crystal of **7.6** was grown, and an ORTEP representation is presented in **Figure 49**, where the thermal ellipsoids are shown at 50% probability, with the hydrogen atoms omitted for clarity. A substitution reaction [24] of **7.6** with ethylene diamine (EDA) **7.7** afforded tridentate ligand **7.8** as an off-white solid in 53% yield.

The novel crystal structure of **7.6** exhibits chloro/bromo substitutional disorder in a 3:1 ratio. The source of the disorder is the sodium hydride induced alkylation using the tail precursor 1-bromo-3-chloropropane **7.5**. The precursor **7.5** is symmetrical with a chloride and bromide functionality on either side of the propyl chain, hence a competitive substitution reaction between the 2 leaving groups. The model of the disordered halide site is in agreement with Br as the more basic and better leaving group relative to Cl. Other cases of halide substitutional disorder have also been reported with Cl/Br disorder in a 3:1 ratio [25-27]. The MS data for **7.6** is consistent with the crystal structure showing two m/z fragments with isotopic patterns typical of halogen containing

compounds. For the Cl containing compound  $C_{39}H_{33}ClNOP_2$  under electron spray ionisation (ESI) conditions, an ion  $[M+H]^+$  at  $m/z$  628.1720 was observed, and for the Br containing compound  $C_{39}H_{33}BrNOP_2$  an ion  $[M+H]^+$  at  $m/z$  672.1209 was observed. The backbone of **7.6** is essentially planar, dihedral angle of  $4.66^\circ$  (2), with an intramolecular P...P distance of 4.263 (2) Å, that compares favourably to both the bidentate precursor nixantphos and the related O donor ligand **7.3**. The C-O bond lengths range from 1.380 (2) to 1.384 (2) Å, and for C-N from 1.398 (2) to 1.402 (2) Å. This compares favourably to nixantphos, and by extension are therefore also shorter than those measured for the crystal structure of **7.3**.

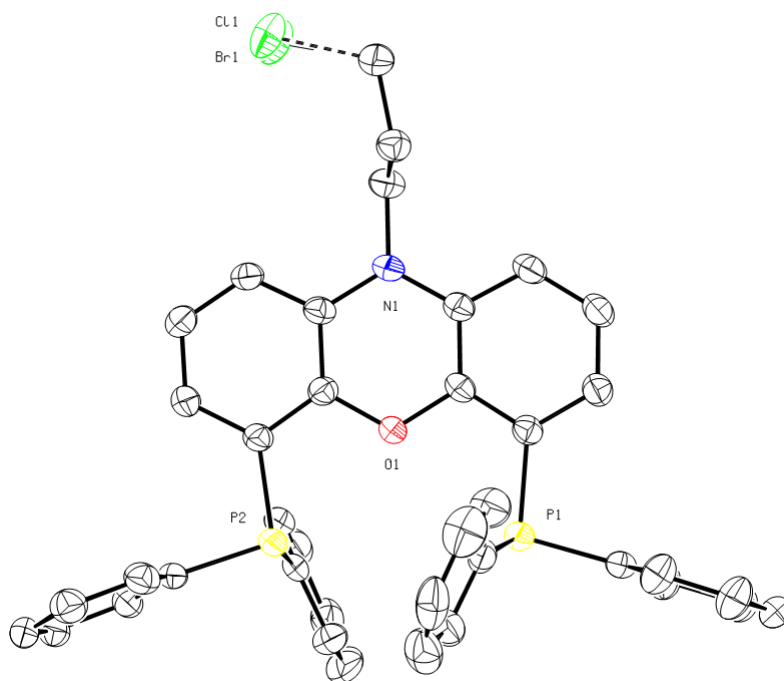
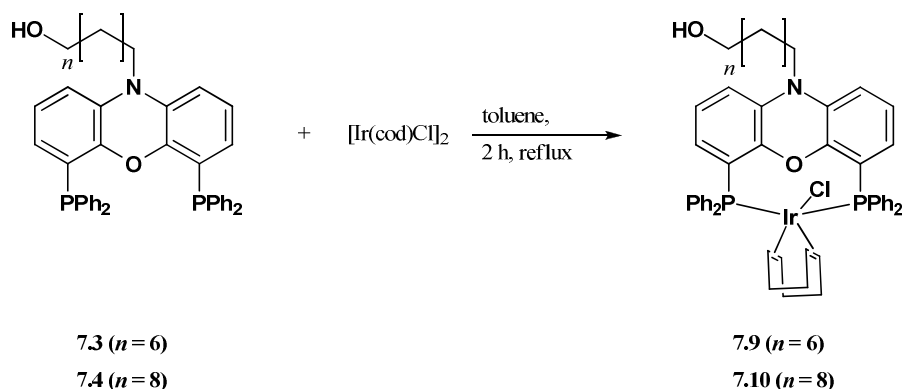
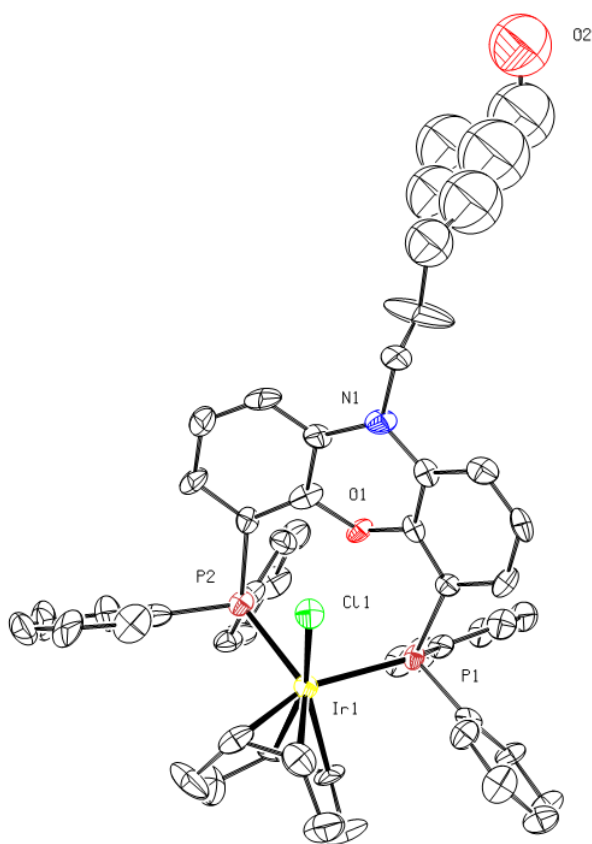


Figure 49. Crystal structure of tridentate precursor **7.6**.



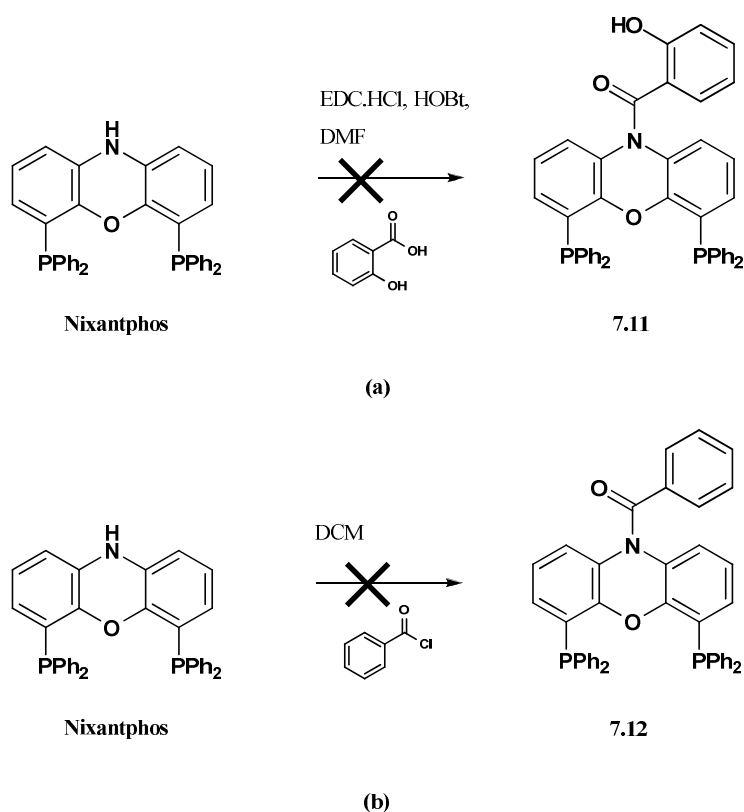
Scheme 32. Complexation of tridentate ligands **7.3** and **7.4**.

The O donor ligands, **7.3** and **7.4** were complexed to  $[\text{Ir}(\text{cod})\text{Cl}]_2$  in toluene under reflux conditions, **Scheme 32**. The reaction was carried out by the addition of 1 equivalent of ligand to 0.5 equivalent of precursor dissolved in dry degassed solvent, and refluxed overnight. A pale yellow precipitate was obtained in both instances, washed with hexane, and dried *in vacuo*. Characterisation of the resulting complexes, **7.9** and **7.10**, by NMR, IR, and MS, revealed that only bidentate coordination of the phosphorus donors had occurred in both instances. It was speculated that despite the bending of the xanthene backbone about the C-O axis to facilitate coordination of the phosphines, the backbone was too rigid or constrained to facilitate the positioning and coordination of the six and eight carbon length alkyl chains. A single crystal of **7.10** was grown, and the ORTEP representation is presented in **Figure 50**. Repeated attempts at the refinement of the novel crystal structure were unable to yield satisfactory results. Therefore this crystal structure is not discussed further, but is merely presented to qualitatively illustrate the bidentate chelation and uncoordinated hydroxyl group of ligand **7.4**.

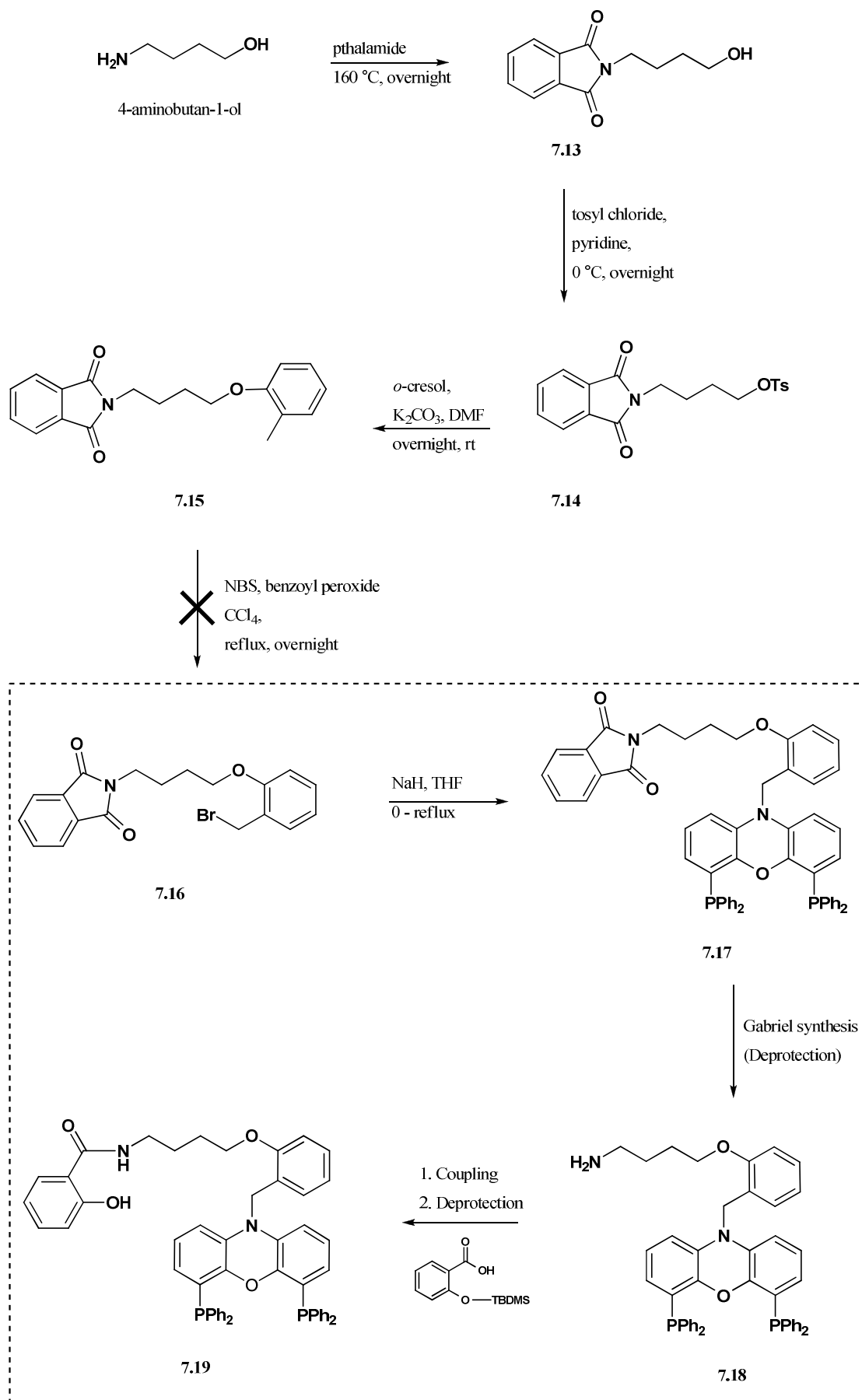


**Figure 50.** Crystal structure of complex **7.10**.

It was speculated that to enforce tridentate chelation, a longer alkyl chain or the introduction of a ‘kink’ was required. The ‘kinked’ ligand involves the introduction of a heteroatom or functional group into the linker tail to facilitate hinge like movement to assist positioning and *fac* coordination of the third donor. The introduction of such kinks for terpyridine-catechol linked ligands has been reported to be relatively successful, resulting in pentadentate coordination [28]. Therefore, this approach was investigated in this work. Furthermore, the use of bulky functional groups was investigated in the hope of inducing a Thorpe-Ingold effect [29]. As a preliminary investigation, the one step coupling of salicylic acid to nixantphos was attempted using standard organic coupling reagents **Scheme 33a**. However, functionalisation using this direct coupling method failed to give any desired product, possibly due to the stabilisation of the amine in the backbone which renders it relatively unreactive [19]. A further coupling reaction using benzoyl chloride was attempted, **Scheme 33b**, however this reaction was also unsuccessful. It was therefore concluded that introduction of the kink directly onto the nixantphos backbone was not feasible, thereby necessitating the preparation of the linker chain including the kink, prior to functionalisation.



**Scheme 33.** Attempted one step coupling of (a) salicylic acid, and (b) benzoyl chloride, to nixantphos.



Scheme 34. Proposed synthetic route to a tridentate xanthene ligand containing a kinked linker.

The proposed synthetic route towards a tridentate xanthene ligand containing a kinked linker is shown in **Scheme 34**. The reactions enclosed in the dashed box in the scheme were precluded due to the unsuccessful preparation of **7.16**, and are only presented for illustrative purposes. The proposed synthetic strategy involved the preparation of a single kink N donor ligand, **7.18**, that could be further functionalised with a second kink to afford **7.19**, if required. The nitrogen donor in 4-aminobutan-1-ol was protected with pthalamide to afford compound **7.13**. To promote functionalisation of the first kink, the hydroxyl group of **7.13** was reacted with tosyl chloride and pyridine at 0 °C overnight to give **7.14**. The first kink was introduced into the linker tail via base induced alkylation of *o*-cresol to yield compound **7.15**. The subsequent step in the reaction sequence involved the bromination of the cresol moiety to facilitate functionalisation to the xanthene backbone. However, despite numerous repeated attempts at the preparation of **7.16**, low yields of the desired product were obtained (< 15 %). This resulted in a reaction mixture comprising the unreacted starting material, desired product, decomposition products, and organic reagents, that could not be purified any further. As a result, the preparation of **7.16** and the further compounds described in **Scheme 34** was therefore precluded. Moreover, due to the unsuccessful chelation of complexes **7.9** and **7.10**, and the tedious, unsuccessful synthesis of the kinked tail tridentate ligand, no further investigations involving a xanthene backbone were carried out.

### 7.3 Conclusions

An investigation into the preparation of *fac* coordinating tridentate xanthene based ligands and metal complexes was undertaken. The bidentate ligand nixantphos was used as the basis for modification via functionalisation of a donor-linker tail assembly. Two hard O donor tridentate ligands were successfully prepared with alkyl linker units of differing length (six and eight carbon atoms). Counterpart soft N donor ligands were also investigated. A tridentate ligand with a halide leaving group was successfully prepared as a precursor to other ligands via functionalisation with the desired donor. A tridentate N donor ligand was successfully prepared from the tridentate precursor. Single crystals suitable for X-ray analysis were obtained for the six carbon length alkyl linker O donor, and the tridentate precursor. The O donor crystal exhibited positional disorder in the linker tail, while Cl/Br substitutional disorder was observed in the tridentate precursor crystal. The two O donor ligands were complexed with an Ir cod metal precursor, however only bidentate coordination of the diphenylphosphine moieties was observed with the hydroxyl group remaining unattached. A kinked linker tail tridentate ligand based on nixantphos was proposed, but the preparation thereof was unsuccessful. Although tridentate coordination of the prepared ligands was not achieved, the synthetic protocols developed for the tridentate ligands are useful for supported catalysis applications, or for the investigation of possible tridentate coordination with different metal centres, for example Os. Furthermore, the crystal structure data of the free ligands are beneficial for molecular modelling applications.



## 7.4 Experimental

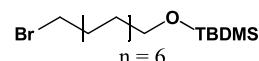
### 7.4.1 General

Pyridine and dimethylformaldehyde (DMF) was distilled before use. DMF was distilled under high vacuum and stored under inert Ar atmosphere. THF, DCM, toluene, Et<sub>2</sub>O, and alcohol solvents were dried using standard methods. Dibromooctane (98%), sodium hydride (NaH, 60% dispersed in mineral oil), (6-bromohexyloxy)(*t*-butyl)dimethylsilane **7.1** (99%), 4-amino-1-butanol (98%), and 1-bromo-3-chloropropane **7.5** (98%) were purchased from Sigma-Aldrich. Imidazole (99%), 1-bromo-8-octanol (95%), and 1,4-dibromobutane (98%) were purchased from Fluka. Ethylene diamine **7.7**, *o*-cresol, salicylic acid, benzoyl peroxide, 4-toluenesulfonyl chloride, phthalic anhydride, 1-Ethyl-3-(3-dimethylaminopropyl)carbodiimide hydrochloride (EDC.HCl), hydroxybenzotriazole hydrate (HOBt.H<sub>2</sub>O), and *N*-bromosuccinimide (NBS) were of reagent grade. 4-Toluenesulfonyl chloride and benzoyl peroxide were recrystallised before use.

### 7.4.2 Experimental Methods

#### (8-bromooctyloxy)(*t*-butyl)dimethylsilane (**7.2**)

The synthesis of **7.2** was adapted from literature [21]. To a solution of 8-Bromo-1-octanol (0.10 g, 0.5 mmol) in DMF (2.0 mL), *t*-butyldimethylsilylchloride (0.90 g, 6 mmol), and imidazole (0.85g, 12.5 mmol) were added, and the reaction mixture stirred at room temperature overnight. The extremely viscous mixture was diluted with 8 mL of diethyl ether and the organic phase washed with brine, dried, and the solvent removed in vacuo. The resulting viscous liquid was filtered through a short plug of silica gel with hexane to give the pure compound **7.2**.



Yield: 86% (38 mg oil)

TLC: *R<sub>f</sub>* 0.4 (hexane/EtOAc 25/75)

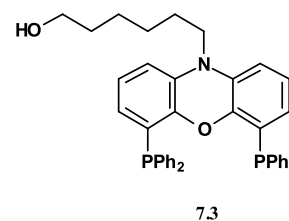
<sup>1</sup>H NMR (400 MHz, CDCl<sub>3</sub>, δ): 3.57 (t, *J* = 6.6 Hz, 2H), 3.38 (t, *J* = 6.8 Hz, 2H), 1.89 – 1.75 (m, 2H), 1.56 (m, 4H), 1.29 (m, 6H), 0.87 (9H,  $-(CH_3)_3CSi$ ), 0.02 (6H,  $-(CH_3)_2Si$ ).

<sup>13</sup>C NMR (101 MHz, CDCl<sub>3</sub>, δ): 63.3 ( $-CH_2OH$ ), 34.1 ( $-CH_2Br$ ), 32.8 (CH<sub>2</sub>), 29.2 (CH<sub>2</sub>), 28.8 (CH<sub>2</sub>), 28.1 (CH<sub>2</sub>), 26.0 (CH<sub>2</sub>), 25.7  $-(CH_3)_3CSi$ , 18.4 (C), -5.25  $-(CH_3)_2Si$ .

#### 6-(4,6-bis(diphenylphosphino)-10H-phenoxazin-10-yl)hexan-1-ol (**7.3**)

Nixantphos (200 mg, 0.36 mmols) was dissolved in DMF (4 mL). To the orange reaction mixture, NaH (400 mg, 0.72 mmol) was added. Reagent **7.1** (180 mg, 0.63 mmol) was slowly added, and the mixture stirred at 100 °C overnight. The reaction was worked up by the addition of water (10 mL) and the organic phase extracted with 4 x 10 mL EtOAc. The collective fractions were dried over sodium sulphate and chromatographed with 10 % hexane/ EtOAc. The resulting oil was dissolved in 25 mL THF, and TBAF added. The solution turned

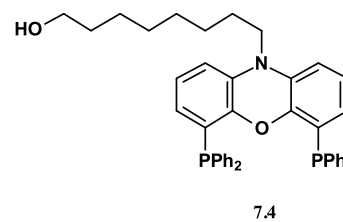
yellow and was left to stir overnight at room temperature. Thereafter, similar aqueous work-up was carried out. The crude product was chromatographed with 20% EtOAc /hexane. Ligand **7.3** was recrystallised from DCM/EtOH in a (1/1) ratio.



Yield:	30% (70 mg white solid)
mp:	167-168 °C
TLC:	$R_f$ 0.3 (hexane/EtOAc 70/30)
$^1\text{H}$ NMR (400 MHz, $\text{CDCl}_3$ , $\delta$ ):	7.22 – 7.00 (m, 20H), 6.64 (t, $^3J(\text{H,H}) = 7.9$ Hz, 2H), 6.41 (d, $^3J(\text{H,H}) = 7.8$ Hz, 2H), 5.97 (d, $^3J(\text{H,H}) = 7.8$ Hz, 2H), 3.65 (t, $J = 6.4$ Hz, 2H), 3.49 (d, $J = 24.6$ Hz, 2H), 1.44-1.68 (m, 8H).
$^{13}\text{C}$ NMR (101 MHz, $\text{CDCl}_3$ , $\delta$ ):	147.1 (t, $J(\text{P,C}) = 20.9$ Hz, CO), 137.0 (t, $J(\text{P,C}) = 12.4$ Hz, phenyl C- <i>ipso</i> , PC), 133.8 (t, $J(\text{P,C}) = 20.6$ Hz, CH phenyl), 133.1 (C), 128.2 (CH), 128.1 (t, $J(\text{P,C}) = 3.3$ Hz, CH), 125.1 (CH), 124.7 (dd, $J(\text{P,C}) = 11.4, 7.5$ Hz, PC), 123.6 (CH), 111.7 (CH), 62.9 ( $\text{CH}_2\text{OH}$ ), 44.6 ( $\text{NCH}_2$ ), 32.7 ( $\text{CH}_2$ ), 26.8 ( $\text{CH}_2$ ), 25.6 ( $\text{CH}_2$ ), 24.7 ( $\text{CH}_2$ ).
$^{31}\text{P}$ NMR (243 MHz, $\text{CDCl}_3$ ) $\delta$ :	-19.2
IR $\nu_{\text{max}}$ ( $\text{cm}^{-1}$ ):	3365(m), 3054(m), 2926(m), 2854(w), 1722(m), 1554(m), 1462(s), 1433(s), 1378(s), 1272(m), 1219(m), 742(s), 693(s).
HRESIMS (m/z):	$[\text{M}+\text{H}]^+$ calcd for $\text{C}_{42}\text{H}_{40}\text{NO}_2\text{P}_2$ , 652.2529; found, 652.2528

#### 8-(4,6-bis(diphenylphosphino)-10H-phenoxazin-10-yl)octan-1-ol (**7.4**)

Ligand **7.4** was prepared analogously to ligand **7.3** using nixantphos (200 mg, 0.36 mmols) in DMF (4 mL), NaH (400 mg, 6.6 mmol), and **7.2** (180 mg, 0.63 mmol).

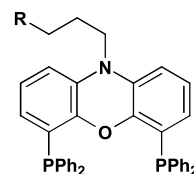


Yield:	28% (38 mg oil)
TLC:	$R_f$ 0.4 (hexane/EtOAc 75/25).
$^1\text{H}$ NMR (400 MHz, $\text{CDCl}_3$ , $\delta$ ):	7.23 – 7.11 (m, 20H), 6.63 (t, $^3J(\text{H,H}) = 7.8$ Hz, 2H), 6.40 (d, $^3J(\text{H,H}) = 7.8$ Hz, 2H), 5.96 (d, $^3J(\text{H,H}) = 7.8$ Hz, 2H), $\delta$ 3.63 (t, $J = 6.5$ Hz, 1H), 3.48 – 3.41 (m, 1H), 1.62 – 1.26 (m, 12H).
$^{13}\text{C}$ NMR (101 MHz, $\text{CDCl}_3$ , $\delta$ ):	147.1 (m), 137.0 (t, $J(\text{P,C}) = 12.4$ Hz, phenyl C- <i>ipso</i> , PC), 133.8 (t, $J(\text{P,C}) = 20.7$ Hz), 133.2 (C), 128.2 (s), 128.1 (t, $J(\text{P,C}) = 3.4$ Hz, PC), 125.1 (CH), 123.6 (CH), 111.7 (CH), 63.0 ( $\text{CH}_2\text{OH}$ ), 44.7 ( $\text{NCH}_2$ ), 32.7 ( $\text{CH}_2$ ), 29.4 ( $\text{CH}_2$ ), 29.4 ( $\text{CH}_2$ ), 26.9 ( $\text{CH}_2$ ), 25.7 ( $\text{CH}_2$ ), 24.7 ( $\text{CH}_2$ ).
$^{31}\text{P}$ NMR (162 MHz, $\text{CDCl}_3$ ) $\delta$ :	-19.1

IR $\nu_{\max}$ ( $\text{cm}^{-1}$ ):	3343(m), 3053(m), 2924(m), 2853(m), 1726(m), 1462(s), 1435(s), 1412(s), 1276(m), 1222(m), 743(s), 693(s).
HRESIMS (m/z):	$[\text{M}+\text{H}]^+$ calcd for $\text{C}_{44}\text{H}_{44}\text{NO}_2\text{P}_2$ , 680.2842; found, 680.2843

### 10-(3-chloropropyl)-4,6-bis(diphenylphosphino)-10H-phenoxazine (7.6)

The preparation of **7.6** was adapted from literature [30]. Sodium hydride (8.1 mg, 0.14 mmol) was added to a cooled solution of nixantphos (50 mg, 0.09 mmol) dissolved in THF (25 mL). The reaction contents were allowed to warm to room temperature and refluxed for 1 h. Thereafter the reaction was cooled to room temperature, and **7.5** (0.54 mL, 0.54 mmol) was quickly added and the mixture refluxed overnight. The solution was cooled and the solvent removed in vacuo to afford a pale yellow residue. The yellow solid was dissolved in DCM and filtered through a glass sintered funnel. Thereafter the solvent was removed in vacuo and the solid recrystallised from DCM/MeOH to afford **7.6**.

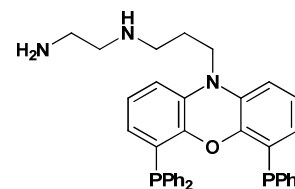


**7.6** ( $\text{R} = 0.73 \text{ Cl} + 0.27 \text{ Br}$ )

Yield:	75% (42.5 mg white solid)
mp:	220 °C
$^1\text{H}$ NMR (400 MHz, $\text{CDCl}_3$ , $\delta$ ):	7.45 – 6.92 (m, 20H), 6.65 (t, $^3J(\text{H,H}) = 7.8$ Hz, 2H), 6.50 (d, $^3J(\text{H,H}) = 7.9$ Hz, 2H), 6.00 (d, $^3J(\text{H,H}) = 7.4$ Hz, 2H), 3.73 – 3.64 (m, 2H), 3.52 (t, $J = 5.9$ Hz, 2H), 2.29 – 2.19 (m, 2H), 2.19 – 2.09 (m, 2H).
$^{13}\text{C}$ NMR (101 MHz, $\text{CDCl}_3$ , $\delta$ ):	147.0 (t, $J(\text{P,C}) = 20.6$ Hz, CO), 137.0 (t, $J(\text{P,C}) = 12.3$ Hz), 134.0 (t, $J(\text{P,C}) = 20.6$ Hz, CH), 132.8 (C), 128.2 (CH), 128.1 (t, $J(\text{P,C}) = 3.4$ Hz), 125.5(CH), 123.7 (CH), 111.7 (CH), 42.9 ( $-\text{CH}_2\text{CH}_2\text{Br}$ ), 42.7 ( $-\text{CH}_2\text{CH}_2\text{Cl}$ ), 41.8 ( $\text{NCH}_2$ ), 30.8 ( $-\text{CH}_2\text{CH}_2\text{Br}$ ), 27.5 ( $-\text{CH}_2\text{CH}_2\text{Cl}$ ).
$^{31}\text{P}$ NMR (162 MHz, $\text{CDCl}_3$ ) $\delta$	-19.1
IR $\nu_{\max}$ ( $\text{cm}^{-1}$ ):	3053(w), 1552(m), 1433(m), 1462(m), 1418(s), 1380(s), 1274(s), 1231(m), 795(m), 722(m), 745(s), 697(s), 516(m).
HRESIMS (m/z):	$[\text{M}+\text{H}]^+$ calcd for $\text{C}_{39}\text{H}_{33}\text{ClNOP}_2$ , 628.1720; found, 628.1720 and $[\text{M}+\text{H}]^+$ calcd for $\text{C}_{39}\text{H}_{33}\text{BrNOP}_2$ , 672.1215; found, 672.1209

### $\text{N}^1$ -(3-(4,6-bis(diphenylphosphino)-10H-phenoxazin-10-yl)propyl)ethane-1,2-diamine (7.8)

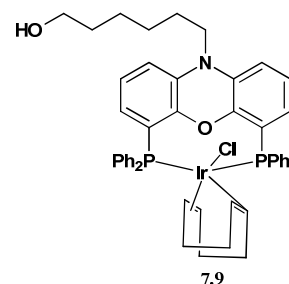
Compound **7.6** (100 mg, 0.16 mmol) was dissolved in **7.7** (6 mL) and the solution left to stir overnight at 80 °C. Thereafter  $\text{H}_2\text{O}$  (10 mL) was added to afford a cream precipitate that was further washed with  $\text{H}_2\text{O}$  (3 x 10 mL) and dried under vacuo overnight.



Yield:	53% (55 mg off-white solid)
mp:	156-158 °C
$^1\text{H}$ NMR (400 MHz, $\text{C}_6\text{D}_6$ , $\delta$ ):	7.44 (m), 7.03 (m), 6.52 (m), 3.19 (m, $\text{CH}_2$ ), 2.25 (m, $\text{CH}_2$ ), 2.21 (m, $\text{CH}_2$ ), 1.34 (m, $\text{CH}_2$ ).
$^{13}\text{C}$ NMR (101 MHz, $\text{C}_6\text{D}_6$ , $\delta$ ):	137.9(C), 134.5 (t, $J(\text{P},\text{C}) = 20.6$ Hz, CH), 133.7 (C), 128.4 (m, CH), 128.5, (C), 127.8 (CH), 125.6 (CH), 124.1 (CH), 112.3 (CH), 52.3 ( $\text{CH}_2$ ), 46.8 ( $\text{CH}_2$ ), 42.4 ( $\text{CH}_2$ ), 41.7 ( $\text{CH}_2$ ), 25.6 ( $\text{CH}_2$ ).
$^{31}\text{P}$ NMR (162 MHz, $\text{CDCl}_3$ ) $\delta$	-19.2
IR $\nu_{\text{max}}$ ( $\text{cm}^{-1}$ ):	1938(s), 2920(m), 1585(m), 1489(s).
HRESIMS (m/z):	$[\text{M}^+]$ calcd for $\text{C}_{41}\text{H}_{40}\text{N}_3\text{OP}_2$ , 652.2641; found, 652.2633

### Complex 7.9

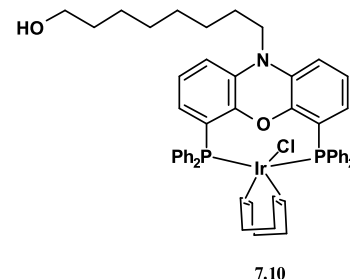
Ligand **7.3** (30 mg, 0.05 mmol) was added to  $[\text{Ir}(\text{cod})\text{Cl}]_2$  (16.8 mg, 0.03 mmol) in THF (6 mL) under an inert argon atmosphere at room temperature. Immediate discoloration was observed, and the mixture was allowed to stir overnight. The THF solvent was removed in vacuo and the resulting precipitate was washed with hexane (3 x 6 mL), and extracted with DCM (2 x 6 mL). The DCM solvent was removed in vacuo and the yellow complex **7.9** dried under high vacuum overnight.



Yield:	52% (31 mg yellow powder)
mp:	226 °C
$^1\text{H}$ NMR (400 MHz, $\text{CDCl}_3$ , $\delta$ ):	$\delta$ 7.65 – 7.17 (m), 7.05 (s), $\delta$ 6.79 (t, $^3J(\text{H},\text{H}) = 7.9$ Hz, 2H), 6.60 (d, $^3J(\text{H},\text{H}) = 7.8$ Hz, 2H), 6.79 (t, $^3J(\text{H},\text{H}) = 7.7$ Hz, 2H), 3.61 (t, $J = 6.5$ Hz, 2H), 3.59 – 3.54 (m, 2H), 3.38 (m, 4H), 1.86 – 0.99 (m, 16H).
$^{13}\text{C}$ NMR (151 MHz, $\text{CDCl}_3$ ) $\delta$	147.9 (t, $J(\text{P},\text{C}) = 9.7$ Hz, CO), 137.7 (d, $J(\text{P},\text{C}) = 47.2$ Hz, <i>Cipso</i> phenyl, PC), 134.4 (t, $J(\text{P},\text{C}) = 5.4$ Hz, C), 133.9 (t, $J(\text{P},\text{C}) = 10.5$ Hz CH), 132.8 (m, C), 132.7 (CH), 129.0 (CH), 128.8 (CH), 125.1 (CH), 120.8 (dd, $J(\text{P},\text{C}) = 5.3, 37.4$ Hz P-CCHCH), 112.6 (CH), 63.2 (“dt”, $J = 14.6, 8.2$ Hz, CH, olefinic C, cod), 62.8 ( $-\text{CH}_2\text{OH}$ ), 44.1 ( $\text{CH}_2$ ), 32.7 ( $\text{CH}_2$ ), 26.9 ( $\text{CH}_2$ ), 25.5 ( $\text{CH}_2$ ), 24.6 ( $\text{CH}_2$ ).
$^{31}\text{P}$ NMR (243 MHz, $\text{CDCl}_3$ ) $\delta$	-17.6
IR $\nu_{\text{max}}$ ( $\text{cm}^{-1}$ ):	1938(s), 2920(m), 1585(m), 1489(s).
HRESIMS (m/z):	$[\text{M}]^+ - \text{Cl}$ calcd for $\text{C}_{50}\text{H}_{51}\text{IrNO}_2\text{P}_2$ , 952.3019; found, 952.3019
EA:	Calculated for $\text{C}_{50}\text{H}_{51}\text{ClIrNO}_2\text{P}_2$ : C, 60.8; H, 5.2; N, 1.4. Found: C, 60.2; H, 4.8; N, 1.3

### Complex 7.10

Complex **7.10** was prepared analogously to complex **7.9** using ligand **7.4** (30 mg, 0.04 mmol),  $[\text{Ir}(\text{cod})\text{Cl}]_2$  (13.4 mg, 0.02 mmol) and THF (6 mL).



Yield:	52% (21 mg yellow powder)
mp:	231 °C
$^1\text{H}$ NMR (400 MHz, $\text{CDCl}_3$ ) $\delta$	7.60 – 6.90 (m, 20H), 6.79 (t, $^3J(\text{H,H}) = 7.9$ Hz, 2H), 6.60 (d, $^3J(\text{H,H}) = 7.8$ Hz, 2H), 6.25 (d, $^3J(\text{H,H}) = 6.1$ Hz, 2H), 4.15 – 3.50 (m, 4H), 3.39 (s, 4H), 2.13 – 1.00 (m, 20H).
$^{13}\text{C}$ NMR (151 MHz, $\text{CDCl}_3$ ) $\delta$	147.8 (t, $J(\text{P,C}) = 9\text{Hz}$ , CO), 138.4 – 137.0 (m, <i>Cipso</i> phenyl, PC), 134.4 (t, $J(\text{P,C}) = 5.6\text{Hz}$ , C), 133.9 – 133.7 (m), 132.8 (dt, $J(\text{P,C}) = 13.4, 5.6$ Hz), 128.9 (d, $J = 24.4$ Hz), 128.1 (t, $J(\text{P,C}) = 8$ Hz, CH), 125.0 (CH), 123.5 (CH), 120.7 (dd, $J(\text{P,C}) = 37.4, 5.3$ Hz), 112.6 (CH), 63.1, (dt, olefinic C, cod), 63.0 ( $\text{CH}_2\text{OH}$ ) 44.2 ( $\text{CH}_2$ ), 32.7 ( $\text{CH}_2$ ), 29.3 (d, $J = 4.6$ Hz, aliphatic C, cod), 27.0 ( $\text{CH}_2$ ), 25.6 ( $\text{CH}_2$ ), 25.5 ( $\text{CH}_2$ ), 24.5 ( $\text{CH}_2$ ).
$^{31}\text{P}$ NMR (243 MHz, $\text{CDCl}_3$ ) $\delta$	-18.1
IR $\nu_{\text{max}}$ ( $\text{cm}^{-1}$ ):	1938(s), 2920(m), 1585(m), 1489(s).
HRESIMS (m/z):	$[\text{M}]^+ - \text{Cl}$ calcd for $\text{C}_{52}\text{H}_{55}\text{IrNO}_2\text{P}_2$ , 980.3332; found, 980.3333
EA:	Calculated for $\text{C}_{52}\text{H}_{55}\text{ClIrNO}_2\text{P}_2$ : C, 61.5; H, 5.5, N;1.4. Found: C, 61.0; H, 5.2; N, 1.3

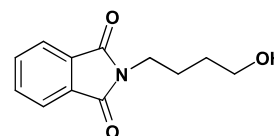
### General procedure for the attempted synthesis of **7.11** and **7.12**

Salicylic acid (50 mg, 0.36 mmol) was added to a round bottom flask, followed by the addition of DMF (1.3 mL), HOBT (72 mg, 0.047 mmol), and EDC.HCl (90 mg, 0.047 mmol). The reaction was allowed to stir for 30 mins at room temperature. Nixantphos (200 mg, 0.36 mmol) dissolved in DMF (0.7 mL) was then added to the reaction mixture and left to stir overnight. The reaction mixture was poured into chilled water (12 mL), followed by the addition of ethyl acetate (10 mL), and allowed to stir for 15 mins. The organic layer was separated and the aqueous layer extracted with ethyl acetate (1 x 15 mL, followed by extraction with DCM (1 x 15 mL). The organic fractions were combined and evaporated until nearly dry, followed by dilution with ethyl acetate (15 mL), and washed with 10% HCl solution (2 x 5 mL) to remove the urea formed from the EDC reagent. The organic layer was separated once more, dried over anhydrous magnesium sulphate and concentrated to dryness on a rotary evaporator. The crude residue was left under high vacuum to remove the remaining DMF for 4 h. The crude mixture was analysed by TLC as coupling reactions are not very clean. However no conversion to the coupled product **7.11** was observed. The  $^{31}\text{P}$  NMR spectrum revealed only the

nixantphos starting material. In a second attempt, nixantphos (200 mg, 0.36 mmol) was dissolved in DCM (6 mL), followed by the addition of benzoyl chloride (0.5 mL, 3.96 mmol). The reaction was left to stir overnight, followed by aqueous work up. Analysis of the crude did not reveal the coupled product **7.12**.

### 2-(4-hydroxybutyl)isoindoline-1,3-dione (**7.13**)

The preparation of **7.13** was reproduced from literature [28]. 4-Amino-1-butanol (0.5 mL, 4.8 mmol), phthalic anhydride (0.72 g, 4.8 mmol), and pyridine (0.6 mL) were melted at 160 °C for 15 min. The reaction mixture was evacuated under high vacuum for 15 minutes to remove the water formed. The mixture was cooled to room temperature and diluted with DCM (15 mL). The solution was acid washed (0.5 M HCl solution), followed by a base wash with saturated sodium hydrogen carbonate (NaHCO<sub>3</sub>). The combined organic layers were dried over anhydrous magnesium sulphate and evaporated to dryness. The desired product **7.13** solidified at room temperature.

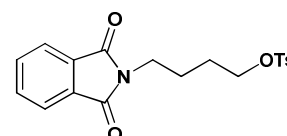


**7.13**

Yield: 75% (0.79 g white solid)  
 mp: 55 °C (lit. [28] mp 54-55 °C dec)  
<sup>1</sup>H NMR (400 MHz, CDCl<sub>3</sub>, δ): 7.81 (dd, *J* = 5.4, 3.0 Hz, 2H), 7.68 (dd, *J* = 5.4, 3.1 Hz, 2H), 3.71 (t, *J* = 7.1 Hz, 2H), 3.66 (t, *J* = 6.4 Hz, 2H), 2.20 – 1.72 (m, 2H), 1.68 – 0.78 (m, 2H).  
<sup>13</sup>C NMR (101 MHz, CDCl<sub>3</sub>, δ): 168.5 (C=O), 134.0 (CH), 132.1 (C), 123.2 (CH), 62.4 (CH<sub>2</sub>), 37.7 (CH<sub>2</sub>), 29.8 (CH<sub>2</sub>), 25.1 (CH<sub>2</sub>).  
 IR ν<sub>max</sub> (cm<sup>-1</sup>): 3405(s), 2930(w), 2855(w), 1489(s), 3405(s), 1722(s), 1689(s), 1489(vs), 1068(m), 1071(s), 716(s), 871(s).

### 4-(1,3-dioxisoindolin-2-yl)butyl 4-methylbenzenesulfonate (**7.14**)

Compound **7.14** was prepared from literature methods [28]. Compound **7.13** (0.4 g, 1.8 mmol) in dry pyridine (0.5 mL), and 4-toluenesulfonyl chloride (0.35 g, 1.8 mmol) in pyridine (0.5 mL), were combined at 0 °C. The mixture was left to stir overnight between 0 – 4 °C during which time the pyridinium salts precipitated out. The reaction mixture was poured into a 1M HCl (30 mL) solution containing ice (10 g). The product formed as an oily layer that slowly solidified on continuous cooling. The white solid was collected by vacuum filtration, washed with water (2 x 10 mL), extracted with DCM (3 x 10 mL), dried over anhydrous magnesium sulphate, filtered, and the solvent removed in vacuo. The product **7.14** solidified upon drying at high vacuum.



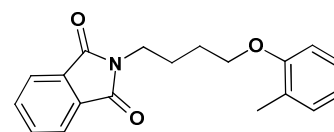
**7.14**

Yield: 30% (0.2 g white solid)

mp:	106 °C (lit. [28] mp 109-110 °C dec)
<sup>1</sup> TLC:	<i>R<sub>f</sub></i> 0.3 (hexane/EtOAc 2.5%).
<sup>1</sup> H NMR (400 MHz, CDCl <sub>3</sub> , δ):	δ 7.83 (dd, <sup>3</sup> <i>J</i> (H,H) = 5.5, 3.0 Hz, 2H), 7.78 (d, <sup>3</sup> <i>J</i> (H,H) = 8.2 Hz, 2H), 7.72 (dd, <sup>3</sup> <i>J</i> (H,H) = 5.4, 3.1 Hz, 2H), 7.34 (d, <sup>3</sup> <i>J</i> (H,H) = 8.1 Hz, 2H), 4.06 (t, <i>J</i> = 5.6 Hz, 2H), 3.65 (t, <i>J</i> = 6.4 Hz, 2H), 2.44 (CH <sub>3</sub> , 3H), 1.90 – 1.80 (m, 2H), 1.70 (m, 2H).
<sup>13</sup> C NMR (101 MHz, CDCl <sub>3</sub> ) δ	168.3 (C=O), 144.8 (C), 134.0 (CH), 133.0 (C), 132.0 (C), 129.9 (CH), 127.9 (CH), 123.3 (CH), 69.7 (CH <sub>2</sub> ), 44.2 (CH <sub>2</sub> ), 26.2 (CH <sub>2</sub> ), 24.7 (CH <sub>2</sub> ), 21.6 (CH <sub>3</sub> ).
IR ν <sub>max</sub> (cm <sup>-1</sup> ):	1938(s), 2920(m), 1585(m), 1489(s).

### 2-(4-(*o*-tolxyloxy)butyl)isoindoline-1,3-dione (7.15)

Compound **7.14** (0.67 g, 1.8 mmol), *o*-cresol (0.16 g, 1.5 mmol), and potassium carbonate (K<sub>2</sub>CO<sub>3</sub>) (0.83 g, 6 mmol) in DMF (7 mL), were combined and stirred overnight. The DMF solvent was removed under high vacuum, followed by the addition of water (10 mL), and the organic layer extracted with DCM (3 x 15 mL). The combined fractions were dried over anhydrous magnesium sulphate, filtered, and the solvent removed to dryness. The product **7.15** was purified by column chromatography using 10 % EtOAc/hexane elution.



**7.15**

Yield:	43% (0.2 g white solid)
mp:	97 °C
TLC:	<i>R<sub>f</sub></i> 0.6 (hexane/EtOAc 90/10)
<sup>1</sup> H NMR (400 MHz, CDCl <sub>3</sub> , δ):	7.83 (dd, <i>J</i> = 5.4, 3.1 Hz, 2H), 7.69 (dd, <i>J</i> = 5.4, 3.0 Hz, 2H), 7.10 (t, <i>J</i> = 7.4 Hz, 2H), 6.94 – 6.39 (m, 2H), 3.93 (dd, <i>J</i> = 45.2, 39.5 Hz, 2H), 3.76 (t, <i>J</i> = 6.8 Hz, 2H), 2.19 (s, 2H), 2.03 – 1.77 (m, 4H).
<sup>13</sup> C NMR (101 MHz, CDCl <sub>3</sub> , δ):	168.5 (C=O), 157.0 (CO), 134.0 (C), 132.1 (CH), 130.6 (CH), 126.7 (CH), 123.2 (CH), 120.2 (CH), 110.9 (CH), 67.0 (CH <sub>2</sub> ), 37.7 (CH <sub>2</sub> ), 26.8 (CH <sub>2</sub> ), 25.4 (CH <sub>2</sub> ), 16.3 (CH <sub>3</sub> ).
IR ν <sub>max</sub> (cm <sup>-1</sup> ):	1938(s), 2920(m), 1585(m), 1489(s).

### Attempted synthesis of 2-(4-(2-(bromomethyl)phenoxy)butyl)isoindoline-1,3-dione (7.16)

The attempted synthesis of **7.16** was adapted from literature [31]. Compound **7.15** (0.2 g, 0.72 mmol) in 23 mL carbon tetrachloride (CCl<sub>4</sub>), was added to NBS (0.26 g, 1.4 mmol). The solution was heated to 50 °C and a catalytic amount of benzoyl peroxide added. The reaction was heated and refluxed overnight. Thereafter, the

reaction was filtered, and washed with CCl<sub>4</sub> (2 x 10 mL). The CCl<sub>4</sub> was carefully removed under vacuum to give a brown-orange residue. The crude product was purified by column chromatography with 20% EtOAc/hexane elution. However, the yield of the desired product **7.16** was very low (< 15%) and repeated attempts to isolate the product were unsuccessful.

## 7.5 References

- 1 Crabtree, R. H. *J. Chem. Soc. Dalton Trans.* **2001**, 2437-2450.
- 2 Gupta, M.; Hagen, C.; Kaska, W. C.; Cramer, R. E.; Jensen, C. M. *J. Am. Chem. Soc.* **1997**, *119*, 840-841.
- 3 Jensen, C. M. *Chem. Commun.* **1999**, 2443-2449.
- 4 Liu, F.; Pak, E. B.; Singh, B.; Jensen, C. M.; Goldman, A. S. *J. Am. Chem. Soc.* **1999**, *121*, 4086-4087.
- 5 Göttker-Schnetmann, I.; Brookhart, M. *J. Am. Chem. Soc.* **2004**, *126*, 9330-9338.
- 6 Goldman, A. S.; Goldberg, K. I. Organometallic C-H Bond Activation: An Introduction. In *Activation and Functionalisation of C-H Bonds, ACS Symposium Series 885*; Goldberg, K. I., Goldman, A. S., Eds.; American Chemical Society: **2004**, p 27.
- 7 Zhu, K.; Achord, P. D.; Zhang, X.; Krogh-Jespersen, K.; Goldman, A. S. *J. Am. Chem. Soc.* **2004**, *126*, 13044-13053.
- 8 Rybtchinski, B.; Crabtree, R. H. Pincer systems as models for the activation of strong bonds: scope and mechanism. In *The Chemistry of Pincer Compounds*; Morales-Morales, D., Jensen, C. M., Eds.; Elsevier: Amsterdam, **2007**, p 87-103.
- 9 Kundu, S.; Choliy, Y.; Zhuo, G.; Ahuja, R.; Emge, T. J.; Warmuth, R.; Brookhart, M.; Krogh-Jespersen, K.; Goldman, A. S. *Organometallics* **2009**, *28*, 5432-5444.
- 10 Morales-Morales, D.; Jensen, C. M. *The chemistry of pincer complexes*; Elsevier: Amsterdam, **2007**, p 445.
- 11 Morales-Morales, D. *Rev. Soc. Quim. Mex.* **2004**, *48*, 338-346.
- 12 Liu, F. C.; Goldman, A. S. *Chem. Commun.* **1999**, 655-656.
- 13 Choi, J.; MacArthur, A. H. R.; Brookhart, M.; Goldman, A. S. *Chem. Rev.* **2011**, *111*, 1761-1779.
- 14 Trofimenko, S. *Chem. Rev.* **1972**, *72*, 497-509.
- 15 Trofimenko, S. *Chem. Rev.* **1993**, *93*, 943-980.
- 16 Bromberg, S. E.; Yang, H.; Asplund, M. C.; Lian, T.; McNamara, B. K.; Kotz, K. T.; Yeston, J. S.; Wilkens, M.; Frei, H.; Bergman, R. G.; Harris, C. B. *Science* **1997**, *278*, 260-263.
- 17 Asensio, G.; Cuenca, A. B.; Esteruelas, M. A.; Medio-Simón, M.; Oliván, M.; Valencia, M. *Inorg. Chem.* **2010**, *49*, 8665-8667.
- 18 Deprele, S.; Montchamp, J. L. *Org. Lett.* **2004**, *6*, 3805-3808.
- 19 Ricken, S.; Osinski, P. W.; Eilbracht, P.; Haag, R. *J. Mol. Catal. A: Chem.* **2006**, *257*, 78-88.
- 20 Sandee, A. J.; Reek, J. N. H.; Kamer, P. C. J.; van Leeuwen, P. W. N. M. *J. Am. Chem. Soc.* **2001**, *123*, 8468-8476.
- 21 Gadwood, R. C.; Mallick, I. M.; Dewinter, A. J. *J. Org. Chem.* **1987**, *52*, 774-782.
- 22 Chen, L.; Craven, B. M. *Acta. Crystallogr., Sect. B* **1995**, *51*, 1081-1097.
- 23 Monge, A.; Martínez-Ripoll, M.; García-Blanco, S. *Acta. Crystallogr., Sect. B* **1978**, *34*, 2847-2850.
- 24 Klein, G.; Kaufmann, D.; Schurch, S.; Reymond, J. L. *Chem. Commun.* **2001**, 561-562.
- 25 Laungani, A. C.; Keller, M.; Breit, B. *Acta. Crystallogr., Sect. E: Struct. Rep. Online* **2008**, *64*, m24-m25.
- 26 Norman, N. C.; Orpen, A. G.; Quayle, M. J.; Robins, E. G. *Acta. Crystallogr., Sect. E: Crystal Structure Commun.* **2000**, *56*, 50-52.
- 27 Rotar, A.; Varga, R. A.; Silvestru, C. *Acta. Crystallogr., Sect. E: Struct. Rep. Online* **2008**, *64*, m45.
- 28 Nagata, T.; Tanaka, K. *Inorg. Chem.* **2000**, *39*, 3515-3521.
- 29 Beesley, R. M.; Ingold, C. K.; Thorpe, J. F. *J. Chem. Soc., Trans.* **1915**, 1080-1106.
- 30 Webb, P. B.; Kunene, T. E.; Cole-Hamilton, D. J. *Green Chem.* **2005**, *7*, 373-379.
- 31 Sorrell, T. N.; Pigge, F. C. *J. Org. Chem.* **1993**, *58*, 784-785.



## Summary and Future Perspectives

### Bidentate ligands

- The aim with regard to preparing a series of bidentate ligands of varying bite angle was successful.
- Full characterisation of all ligands and metal complexes has been presented and, where possible, ligands and their metal complexes were characterised by X-ray crystallography.
- The natural bite angle was correlated to the metal preferred bite angle using molecular modelling.
- A complementary analysis of the other molecular descriptors could be beneficial to this study.

### Tridentate ligands

- The synthesis of tridentate mixed donor ligands was attempted. Due to the rigid xanthene backbone successful coordination of the third donor was not observed.
- The scope of the ligands was then extended to the introduction of “kinked” functional groups on to the xanthene backbone.
- Although, several synthetic avenues were tried, the target ligand was not prepared.
- Nonetheless, modification of these ligands to become soluble in non-polar solvents and the application thereof to C-H activation reactions might be worthwhile.
- Additionally, the uncoordinated donor on the alkyl tail can be anchored onto an organic support. This could result in the immobilisation of the catalyst and offers great potential for recovery of the expensive transition metal catalysts.

### Microwave assisted Hydrogen Transfer Reactions

- Oxidation of primary alcohols was successfully carried out using improved reaction protocols.
- Among the transitional metal precursors screened, the Ru catalyst gave the highest yields towards oxidation of benzyl alcohol to benzaldehyde.
- At the optimised reaction conditions; 1 mol% of  $[\text{Ru}(\text{H})_2(\text{CO})(\text{isopropxantphos})(\text{PPh}_3)]$  was microwave irradiated at 120 °C for 25 min to yield 92 % of benzaldehyde.
- The reactivity of the transition metal catalysts was found to be sensitive to the electronic nature of the substrate. IsopropxantTolylphos showed improved reactivity for both electron withdrawing and donating substrates.
- Sterically bulky isopropxantTolylphos on Ru was a poor oxidation catalyst. Future work would involve growing a single X-ray quality crystal of the metal complex and this data will be used to calculate steric parameters discussed in Chapter 2. These parameters, together with the bite angle, will help understand the steric effects of the ligand and its influence on the metal centre.
- Solvent-free conditions were found to give similar, if not better, reactivity for the oxidation of benzyl alcohol at all three reaction temperatures tested.

- The transfer hydrogenation of ketones to alcohols was also successfully demonstrated by Ru(xantphos)arene catalysts using 2-propanol in the presence of a strong base.
- Many metal precursors were screened for activity, but only Ru and Rh were found to be active.
- The xanthene family ligands were applied to the hydrogenation of acetophenone at two conditions.
- No obvious correlation between the bite angle and reactivity was observed.
- Good TOFs were observed,  $\geq 1431\text{--}2982\text{ h}^{-1}$ , for acetophenone derivatives and bulky ketones.
- Extension of this reaction scope to asymmetric transfer hydrogenation using chiral xanthene based ligands would be a useful study.

### Chemo-selective Hydrogenation with Molecular Hydrogen

- In this preliminary study it was shown that the [Rh(cod)(xantphos)Cl] preferentially catalysed C=O over the C=C functional group.
- When Ir was used as the metal centre with the same ligand, the selectivity was lower towards the allylic alcohol. There was no clear preference for the hydrogenation of C=O or C=C.
- The catalyst loading, reaction temperature and solvent were optimised using cinnamaldehyde as the benchmark substrate.
- The study of yields over reaction time was carried out.
- This optimised time was used for the hydrogenation of various  $\alpha,\beta$ -unsaturated aldehydes and ketones.
- These observations have set the premise for future investigations that could include the monitoring of hydrogen consumption and extending the substrate scope.

### Overall conclusions

- The use of microwave energy significantly improved reaction yields and shortened reaction times. The use of the laboratory modified microwave was easily adapted to solvent-free conditions. Future work would be to fully investigate the scope of solvent free reactions with regard to catalyst recycling using supported ligands.
- Xanthene diphosphorus ligands played an important role in directing coordination, giving stability, imparting solubility and hence influencing the reactivity of the metal complex. These functions cannot be isolated, as it is rather a combination of the ligand properties and inherent metal activity that contribute to the overall reactivity of the catalyst.
- The use of the natural bite angle alone cannot be used to understand these complex roles. However, this study forms the basis for future work where other equally diagnostic molecular descriptors can be included with the help of mechanistic studies.
- Although a combination of electronic, geometric and steric effects contribute to the reactivity of the metal centre, fine tuning of the ligands was carried out for isopropylbutylphos.
- Steric effects were demonstrated by the bulky isopropylbutylphos which was unsuccessful on Ru for both hydrogen transfer reactions examined. It would be interesting to apply this ligand to chemo-selective hydrogenation of carbonyl compounds.

- Sensitivity of the electronic environment of the metal centres was best illustrated by the relatively large electron rich and electron deficient substrate scope tested.
- Structural effects were demonstrated by the xanthene related ligands DPEphos, PTEphos and DBFphos. These ligands performed poorly as compared to the xanthene based ligands in both hydrogen transfer reactions. There is a subtle interplay between the degree of flexibility and rigidity that was found to be balanced for the xanthene diphosphorus ligands.
- Xanthene diphosphorus ligands have demonstrated both high selectivity and good activity at mild reaction conditions and thus have great potential for industrial use for the synthesis of fine chemicals.